Final Report

LastHope - A Drone to Call for Help

DSE 2021 Group 02

TUDelft

Final Report

LastHope - A Drone to Call for Help

by

DSE 2021 Group 02

Student Name	Student Number
Alex van Roon	4643453
Michele Bianconi	4857771
Florian Schimmel	4649656
Julio Wu Qiu	4656946
Mark Kalsbeek	4546393
Ruben Overwater	4832205
Gijs Feenstra	4657578
Vincent Lechner	4785940
Remco Roelofs	4820479
Edward Neate	4647572

TUDelft

Executive Overview

DSE Group 2 is tasked with designing a drone to call for help in situations where other means of communication are not available. The areas where hikers most like to go are also often the areas with the poorest connectivity. The Last Hope drone will be able to fly up and out of reach of any obstacles and call for help in situations current technologies cannot. This would improve the safety of outdoor adventurers in the most critical situations.

The Last Hope drone will autonomously find a clear path into the sky from the ground and ascend to an altitude of up to two thousand meters. Within 20 minutes it transmits a call for help with exact location information to rescue operators via the Iridium satellite network. If available, a 2G cellular connection is used instead. Once the message has been received the drone will return to the user, to be used again and again in the future. Almost all of the non-electronic components are made out of recyclable materials in order to reduce the environmental impact of the product at the end of its life-cycle as much as it possible. A detailed design has been made of this drone. It was found that it is possible to make a design that fulfils the design mission.

Autonomous flight is realised by a commercial flight computer, however due to the computational load path planning and navigation tasks are off-boarded to a companion computer. Due to the implementation of a detailed dynamical model and optical ground tracking the drone will be able to navigate even when GNSS signals are unavailable. Several path-finding algorithms were evaluated but further research is needed in order to draw firm conclusions about their feasibility in a real world environment.

To optimise propulsive efficiency and save battery mass, a propeller is designed to suit the mission profile. This propeller saves a considerable amount of energy compared to the available commercial standard. The propeller is coupled with an electric motor selected out of a database of over a thousand motors for highest efficiency. It is coupled with an electronic speed controller that is cheap, light and readily available.

Due to the increased efficiency of the propeller, a lower peak power draw is required. This enables the selection of a lithium ion battery, instead of the heavier lithium polymer batteries that are the industry standard. The battery is protected from over- and under-charging by a battery management system. This prevents user error from causing accidents, improves the drone safety during operation and helps ensure the longevity of the product. A power distribution board is used to power each system in the drone at the correct voltage.

All the components are housed and protected by the frame of the drone. All the components of the frame are made out of non-toxic and recyclable materials. All components are designed with either a safe-life or fail-safe approach where applicable. The frame is tailored to achieve a balance between aerodynamic efficiency, mass, structural performance and reliability. It is designed to fold into a small space in order to make it as convenient as possible for the user to bring along on their adventures.

In order to keep the drone safe and fully operational during transport, a container is designed. It is made mostly out of bio-based and recyclable materials and is designed for users to be able to retrieve the drone even in situations where they are injured and only have one functional limb. It is water and dust proof and can keep the drone fully charged for at least one month. The case also features a secondary user interface that can be used to give the drone more detailed instructions and information to pas along to rescue services.

The primary user interface is located on the drone itself and enables the user to deploy the drone in one step. It also features a set of LED indicators to report status and diagnostic information to the user. While ascending, the drone will record video of the user and their environment in order to reduce the time the rescue workers will need to spend in order to find the user. During the mission, a warning system consisting of lights, buzzers, fluorescent paint and reflective strips serves to alert bystanders to the presence of the drone. It also aids in recovery of the drone in the event of a crash or forced landing away from the user.

A number of uncertainties remain. Firstly, the given constraint of a maximum mass of 500 grams proved infeasible in this analysis. Secondly, with the current means available, it is not possible to evaluate whether dynamic obstacle avoidance is possible, and static obstacle avoidance is still hard, if not impossible, to guarantee. This is because the scope of the sensor array is severely constrained by the cost and mass budgets. It is also expected that further development costs will exceed the cost budget. Given the constraints, the most feasible option is an array consisting of five ultrasonic sensors, but these can only determine the distance to an obstacle, and not its exact relative position. Lastly, the market return on investment analysis revealed that there is no sound basis for investing in this as a consumer product due to the low expected returns and the inherent risk in marketing a product that is not yet legally permissible.

Contents

Nomenclature

Abbreviations

ACAI   Available Control Authority Index

ADS-B Automatic Dependent Surveillance-Broadcast

AHP   Analytical Hierarchy Process

BDS   BeiDou Navigation Satellite System

BEC   Battery Eliminator Circuit

BEMT Blade Element Momentum Theory

BMS   Battery Management System

CAGR Compound Annual Growth Rate

CAS   Collision Avoidance System

CFD   Computational Fluid Dynamics

CFRP Carbon Fibre Reinforced Polymers

COTS Commercial off-the-shelf

CR   Consistency Ratio

DC   Direct Current

DSE   Design Synthesis Exercise

EKF   Extended Kahlman Filter

EPS   Electrical Power System

ESC   Electronic Speed Controller

FBS   Functional Breakdown Structure

FEM   Finite Element Method

FFBD Functional Flow Block Diagram

GNSS Global Navigation Satellite System

GPS   Global Positioning System

IMU   Inertial Measurement Unit

IP   Ingress Protection

ISA   International Standard Atmosphere

LDR   Light Dependant Resister

LiPo   Lithium Polymer

MTBF Mean Time Between Failure

NATO North Atlantic Treaty Organization

NiMH Nickel-metal-hydride

PC   Polycarbonate

PDB   Power Distribution Board

PID   Proportional Integral Derivative

PLA   Polylastic Acid

PLB   Personal Locator Beacon

RAMS Reliabilty, Availability, Maintainability & Safety

RGB   Red green blue

RIT   Relative Importance Table

ROHS Restriction of Hazardous Substances

RPM   Revolutions Per Minute

SAR	Search and Rescue	C_D	Drag coefficient
SBD	Short Burst Data	C_L	Lift coefficient
SD	Secure Digital	d_{cg-rp}	Horizontal distance from rotor center to center line
SD	Standard Deviation		
SLS	Selective Laser Sintering	E_{elec}	Electrical energy
SMS	Short Message Service	P_{elec}	Electrical power
SOS	Save Our Souls	P_{shaft}	Shaft power
TBD	To Be Decided	Q	Torque
TPU	Thermoplastic Polyurethane	r	Radius to propeller section
TTFF	Time To First Fix	R_m	Internal resistance of the copper winding in the motor
UAV	Unmanned Aerial Vehicle		
UD	User Defined	U	Actual inflow velocity
UI	User Interface	v	Actual axial inflow velocity
UV	Ultraviolet	v'	Actual tangential inflow velocity
VHF	Very High Frequency	V_∞	Axial incoming flow velocity
WBS	Work Breakdown Structure	V_Ω	Tangential incoming flow velocity
WFD	Work Flow Diagram	A	Aspect ratio

Symbols

α	Angle of Attack	a	Acceleration
Δr	Width of propeller section	c	Crumple zone distance
δ	Deflection	D	Drag
μ	Dynamic viscosity	E	Young's Modulus
μ	Mean	g	Gravitational constant
Ω	Rotational velocity	I	Area moment of inertia
ϕ	Inflow angle	I	Current
ρ	Density	J	Principal moment of inertia
σ	Rotor solidity	M	Moment
σ	Standard deviation	m	Mass
τ	Shear stress	Q	First moment of area
a	Axial induction factor	R	Radius
a'	Tangential induction factor	Re	Reynolds Number
B	Number of blades on propeller	S	Area
c	Chord length	T	Thrust
C_Q	Torque coefficient	V	Velocity
C_T	Thrust coefficient	V	Voltage
		W	Weight

1. Introduction

Analysis on visitor trends within European natural parks has shown a continual increase in recent years, with an even larger increase during the pandemic. Correspondingly, the number of incidents of people getting lost or injured has followed suit, with some areas seeing a 40% increase since the start of the pandemic[1]. Although there are numerous satellite-based options available, these options are not always reliable as the line-of-sight with the satellite is obstructed in certain cases. In addition to this, most hikers still rely on their phones, even though the remote areas which they travel to frequently have the worst connectivity.

To combat this trend and provide a more reliable option, DSE Group 2 has been tasked with designing a drone called LastHope "that utilises autonomous decision making to secure a connection in remote areas and transmit a message to emergency services[1]." The LastHope quadcopter, shown in figure 1.1, will be able to fly up and out of reach of any obstacles and call for help in situations where the user cannot reach an area with unobstructed satellite connectivity. The LastHope drone will do this by autonomously finding a clear path into the sky from the ground and ascending to an altitude of up to two thousand meters, a point where no obstacles in Europe can obstruct it. Here it transmits a call for help with exact location information to rescue operators via the Iridium satellite network, loitering for up to 20 minutes depending on the proximity of satellites. If available, a 2g cellular connection is used instead. Once the message has been transmitted, it will return to the user to be used again in the future if needed. This would improve the safety of outdoor adventurers in the most critical situations.

This report consists of an overview of the final design of the drone and its various subsystems, the methods used to reach this, and future recommendations. Previous phases of the design worked on establishing the governing requirements, narrowing down the most influential design aspects, and performing initial sizing of the quadcopter. In this report, chapters 2-6 consist of overviews on the drone as a whole, the strategy and process used to design it, the environments it can be used in and a functional analysis. Chapters 7-12 detail the six subsystems of the drone, how they were designed and what led to certain design choices being made. Chapters 14-16 consist of an overview of the technical budgets, the risk associated with the drone and the RAMS Characteristics. Chapter 17 goes over the future development of the drone through its operations logic, a Gantt chart for the upcoming phases, and a review of the drone's effectiveness in the market via a market analysis and return on investment. Chapters 18-19 go over the production plan for the current version of the drone and an overview on the sustainability approach taken in this phase and an outlook for its implementation in future phases.
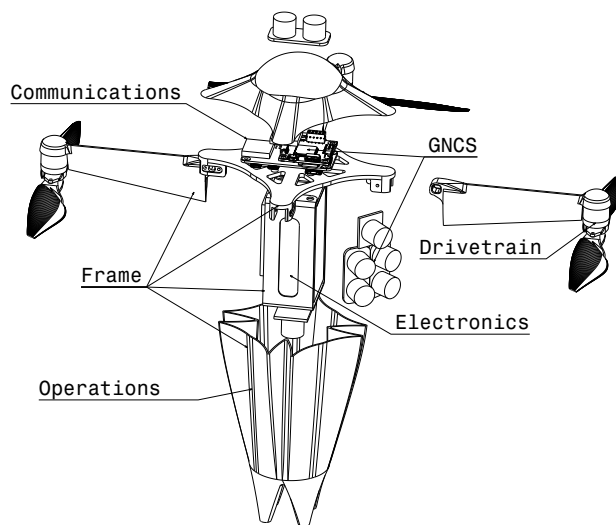
Figure 1.1: LastHope Drone Exploded View

[1]Lake District Incidents `https://www.grough.co.uk/magazine/2020/12/12/new-lake-district-visitors-push-rescuers-avoidable-incidents` [accessed on 29.06.21]

2.   Current Design

This chapter presents the current design of the LastHope drone. A brief overview of the key concepts of the drone and its specifications is shown followed by a compliance matrix of the system requirements.

2.1. Design Specifications

After evaluating numerous flight concepts, a quadcopter has been chosen and developed to perform the mission. It features an optimised propeller-motor combination to aid in its ascent to its loiter altitude of 2km. The quadcopter uses a Lithium Ion battery to power its onboard sensors and flight computers which allow the drone to autonomously search for connection. A warning system using LEDs and a buzzer were included to help protect the user before it takes off and to aid in its recovery after landing. A folding system is used for the arms and propellers to help decrease the storage space needed. Recyclable materials such as PETG, PA12 Nylon, and alumninium have been chosen for the main components of the drone's frame. The main specifications of the quadcopter are compiled in Table 2.1. The main dimensions can be seen in figure 2.1 for the unfolded quadcopter and in figure 2.2 the folded version sizes can be seen.

Table 2.1: Main specifications of the quadcopter are specified here

Mass:	586 grams	Climb Time:	1 min 48 seconds	Operational Zone:	Europe
Cost:	646 euros	Comms Systems:	Sattelite + 2G	Dimensions Extended:	367x367x191mm
Climb Speed:	18.4 m/s	Battery Capacity:	3000mAh 3S	Dimensions Folded:	100x100x191mm
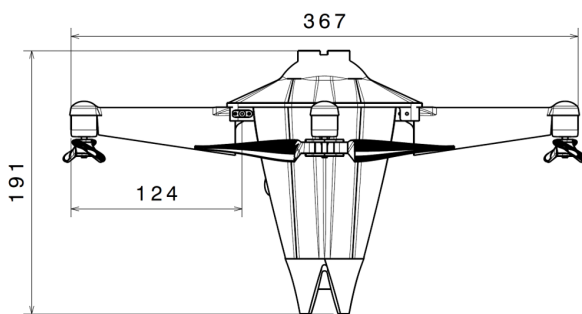
Figure 2.1: Unfolded drone sizes
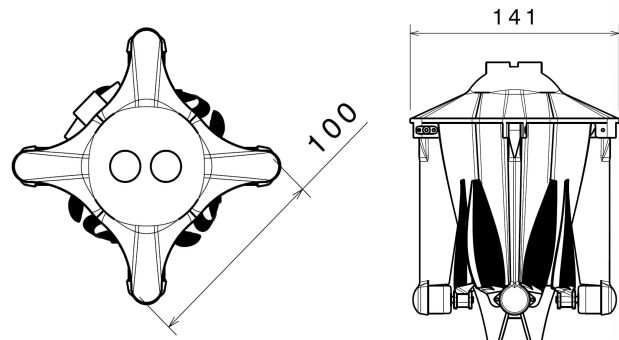
Figure 2.2: Folded drone sizes

2.2. Compliance Matrix on System Level

With the final specifications of the drone presented, the system can now be checked for compliance against the system requirements set down in[1]. This is found in Table 2.2. To validate the requirements, the following methods (and abbreviations) are used:

- Testing: Test
- Analysis: Ana
- Simulation: Sim
- Review of Design: RoD
- Comparability: Comp

When requirements aren't met, a comment is made, which can be found after Table 2.2.

Table 2.2: Compliance matrix of system

Identifier	Requirement	Compliant?	Comment	Validated by:
STAK-GENR-01	The drone shall be able to operate in Europe and in coastal zones	✓		Ana
STAK-GENR-02	The drone should be able to operate worldwide		[a]	Ana
STAK-GENR-03	The drone shall not have exposed electronics	✓		RoD
STAK-GENR-07	The drone or its element(s) shall stay on the water surface for at least 72 hours	✓		Test
SYST-GENR-07-A	The drone or some indication mark shall have positive buoyancy	✓		Ana
SYST-GENR-08-A	The drone shall be visible from 200 m under normal weather conditions	✓		Test
STAK-GENR-08	The drone shall be able to operate at night	✓		Test
SYST-GENR-08-A	The drone shall be able to operate in illuminance greater than 0.0001 lux	✓		Test
SYST-GENR-09	The drone shall be able to operate with rain up to 10 mm/hour	✓		Test
SYST-GENR-10	The drone shall be able to operate in snow	✓		Test
STAK-GENR-11	The drone shall be able to operate in fog	✓		Test
STAK-GENR-12	The drone shall be able to operate in smoke	✓		Test
SYST-GENR-01	The weight of the drone shall not exceed 500 grams		[b]	RoD
SYST-GENR-02	The weight of the drone should not exceed 250 grams		[b]	RoD
SYST-GENR-03	The maximum dimensions of the drone in storage mode shall not exceed 200 x 100 x 100 mm (length, width, height)	✓		RoD
SYST-GENR-04	The non-return flight distance of the drone should be 5 km	✓		Test
SYST-GENR-13	In flight mode, the drone shall fit through an opening with minimum dimensions of 40x40 cm	✓		RoD
PROJ-PER-16	The drone shall be able to achieve an altitude of 2000 m	✓		Test
PROJ-PER-17	The drone shall be able to loiter at 2000 m for 20 minutes	✓		Test
PROJ-PER-18	The drone shall be able to operate at a height of 4500 m above sea level	✓		Test
STAK-COST-01	The cost of the drone for the end-user shall not exceed EUR 700		[c]	Ana
STAK-COST-03	The subscription costs of the additional service shall not exceed EUR 15 per month	✓		Ana
STAK-SUST-01	The drone shall be able to be repaired in a modular fashion	✓		Test
SYST-SUST-02-A	The drone shall be electrically powered	✓		RoD
SYST-SUST-02-B	The drone shall not be manufactured out of toxic materials	✓		RoD
SYST-SUST-03	The drone shall not be a fire hazard in case of malfunction or during landing	✓		Test
SYST-SUST-04	The drone shall not use a material which has a high hazard rating with high confidence for all Group I human hazards	✓		RoD
SYST-SUST-05	The drone shall not use a material which has a high hazard rating with high confidence for Acute Aquatic Toxicity	✓		RoD
SYST-SUST-06	The drone shall not use a material which has a high hazard rating with high confidence for Chronic Aquatic Toxicity	✓		RoD
SYST-SUST-07	The drone shall not use a material which has a high hazard rating with high confidence for Terrestrial Ecotoxicity	✓		RoD
SYST-SUST-08	The drone shall not use a material which has a high hazard rating with high confidence for Bioaccumulation	✓		RoD

SYST-SUST-09	The drone shall not use a material which the user would have direct contact with which has a high hazard rating with high confidence for all Group II human hazards	✓	RoD
SYST-SUST-10	The structure surrounding possibly flammable materials shall not be made of a material which has a high hazard rating with high confidence for flammability	✓	RoD
SYST-SUST-12	Each material in the drone shall use a recyclable material if it does not directly compromise performance requirements	✓	RoD
STAK-COMM-01	The drone shall have at least 2 different means of communication with emergency services	✓	RoD
STAK-COMM-02	The drone shall be able to communicate with emergency services at areas with cellular reception	✓	Test
STAK-COMM-03	The drone shall communicate the user location to the emergency services	✓	Test
STAK-COMM-04	The drone shall communicate user data to the emergency services	✓	Test
STAK-COMM-06	The drone should transmit its live location to the user	[d]	-
SYST-COMM-01	The drone shall have at least one mean of communication, between drone and emergency services, that is "two-way"	✓	RoD
SYST-COMM-02	The drone should have at least one mean of communication, between drone and user, that is "two-way"	[e]	-
SYST-DFPP-01	The flight parameters of the drone shall be valid after 1-month storage after full charging	✓	Ana
STAK-DFPP-02-A	The drone shall be able to operate at wind with an average speed up to 15 m/s	✓	Sim
STAK-DFPP-02-B	The drone shall be able to operate at wind gusts up to 20 m/s	✓	Sim
STAK-ELEC-01	The drone shall be able to be charged in a field environment	✓	RoD
STAK-ELEC-02	The drone shall be able to be charged in a sea environment	✓	RoD
STAK-GNCS-01	The drone shall store the first known location for easy transfer to the rescue team	✓	Test
STAK-GNCS-02	The drone shall be able to operate without user input	✓	Test
SYST-GNCS-02-A	The drone shall be able to autonomously plan the flight path	✓	Sim
SYST-GNCS-02-B	The drone shall be able to autonomously select its altitude	✓	Sim
SYST-GNCS-02-C	The drone shall be able to autonomously navigate towards the most probable location where contact with emergency services is possible	✓	Sim
SYST-GNCS-02-D	The drone shall be able to autonomously make critical decisions during the mission	✓	Sim
SYST-GNCS-02-E	The drone shall be able to autonomously select the place to land	✓	Sim
SYST-GNCS-02-F	The drone shall be able to autonomously land	✓	Test
SYST-GNCS-02-G	The drone shall be able, after establishing two way communication with emergency services, to decide if return flight is possible	✓	Sim
STAK-GNCS-03	The drone shall have a collision avoidance system	✓	RoD
STAK-OPER-01	The user interface shall be intuitive to use to a range of users	✓	Test
STAK-STOR-01	The drone shall have a protective casing for travel	✓	RoD
STAK-STRC-01	The drone shall be able to be reused after a non-destructive landing	✓	Test
SYST-THER-01	The drone shall be able to operate in a temperature range from -20 to +40 °	✓	Test
SYST-THER-02	The drone should be able to operate in a temperature range from -30 to +50 °	✓	Test

SYST-RISK-01	The guidance sensor shall be inoperable with multiple GNSS systems	✓		RoD
SYST-RISK-04	The propellers shall be foldable	✓		RoD
SYST-RISK-08	The flight computer shall be able to recognise faulty states of the autopilot routine	✓		Sim
SYST-RISK-09	The flight computer shall be able to restart the autopilot routine when faulty states are detected	✓		Sim
SYST-RISK-10	The drone shall be IP rated to at least IP 55	✓		Test
SYST-RISK-11	The storage case shall be IP rated to at least IP 57	✓		Test

a : The region of operation was narrowed to Europe based on the operating environments.

b : The mass of the current design is 586 grams.

c : The cost of the current design is EUR 646. This only includes the cost for the production or buying the components that make up the drone. It is expected that the cost for the end-user will be above € 700.

d : This additional feature was considered, but was found to be too expensive.

e : This additional feature was considered, but was found to be too expensive and energy demanding.

3. Design Strategy

This chapter deals with the formulation of the design strategy for the detailed design phase. In order to find an effective distribution of man-hours each necessary component is identified. For each of the components an analysis is made in order to establish whether it is justifiable to make a novel design instead of buying a commercial off the shelf component. The analysis consists of a match between the market availability and suitability of the component and the skills and interests of the design team. The results of this analysis is presented in Table 3.1.

Table 3.1: Final report design approach for each component

	Component	**Approach**
Sensors	GNSS Module	COTS
	Ultrasonic	Adapt existing
	Lidar	Adapt existing
	Camera	Adapt existing
Comms	Iridium Module	COTS
	GSM Module	COTS
Flight computer	Autopilot	COTS
	Flight software	Adapt existing
EPS	PDB	COTS
	BMS	COTS
	Battery	Adapt existing
	Wring Harness	Design from scratch
	Connectors	COTS
Propulsion	Motors	Design from scratch
	ESC	COTS
	Propeller	Design from scratch
Structure	Quadcopter Frame	Design from scratch
	Lights	COTS
Storage Container	Hardshell case	Design from scratch
	Charging module	Adapt existing

- **Lidar Ranging Modules**: In the market analysis, it was seen that there are many options available but there is a lack of options which can move on their own which are also affordable. There is only a bit of

expertise available to help with designing a new version which results in a significant time investment associated with designing it. It does not drive the design, but it does add quite a lot of value to design a cheaper version which can move to cut down on costs for the drone.

- **Camera:** A camera module would have to be adjusted such that the video storage goes straight to the black box and not to the video storage card with the camera. While there is a lack of expertise and unfeasible time investment associated with designing a new camera from scratch, the group can modify existing solutions to meet the black box requirements.

- **Flight Software:** Flight software is an important part of the drone, but the expertise to write full flight code is not available or easy to develop in a short time-span. However, there are viable alternatives on the market that are open source and fulfil most of the functions that the autopilot needs to fulfil. The choice is made to build a functional description of the software around the routines available.

- **Battery:** The battery could have a massive effect on the final design of the drone as it is the component which dominates the total mass the most. There are many options available on the market, yet many are either going to be a bit more or a bit less than what the drone needs exactly. A battery could be sized which fits the needs of the drone more accurately. Yet, the team does not have the expertise needed to design a new battery and a large time investment would be required to do so. As it drives the design greatly and its improvement would have a large influence, it is decided to look into designing a new battery for the drone.

- **Wiring harness** As the harness is dependent on the final layout of the drone and solutions which match the drone do not exist on the market, one will have to be designed. The team has the expertise to design a harness and it would require an acceptable time investment for the group to complete.

- **Motors** Since the propulsive efficiency is important to the mission success, it could be valuable to make a new motor design. However, the depth to which this can be performed by the team is limited by the available expertise in brushless DC motor design. It is recommended an attempt it made to make this design, but if the department finds out during the literature review that this does not fit the available resources it can be swapped out for a commercial option.

- **Propeller** Due to the knowledge in aerodynamics thanks to the team's experience in aerospace engineering it was deemed appropriate for the team to design the propeller for the drone. Propellers for quadcopters specifically designed for loitering and hovering are not strictly available hence this is a great component that the team could optimise to obtain a more efficient design.

- **Frame** With the experience of aerospace engineering students, it is safe to say that enough knowledge is available to design a structure able to tolerate the maximum loads experienced by the drone. The requirements placed for this project aims for some ambitious goals, hence it is best if the design of the frame is well controlled by the team rather than taken off the shelf as testing is not an option within the scope of the project. The configuration of the drone is also quite unconventional hence the frame of the drone will be heavily tailored. Moreover, this presents an opportunity to develop a frame made out of more sustainable materials than is the current market standard.

- **Hardshell case** The case is where the drone will live as long as it is not in operation or being reviewed. This means that the case has to be tailored specifically for all possible conditions that the user might encounter, meaning it should be water proof, crush proof, insulated, light and compact. This also enables integration of other components such as the charging module which is explained in the next point.

- **Charging module** An integrated charging module will provide the user with some peace of mind regarding the charge of the drone if the situation arises that they need to use it. This increases the practicality and the user experience hence it is deemed as quite valuable. Moreover, there are no standard charging modules that exist in the market which can be easily integrated to a personalised case.

From this analysis, it was found that there are components which may already exist on the market, but would provide a large benefit to the overall design if resources are allocated to design options tailored to the Last Hope Mission. There are also Commercial Off The Shelf (COTS) options available for a number of components that satisfy the project needs. Lastly, there are also components where no solutions exist on the market which will need to be designed by the group independently. Overall, this analysis has helped narrow down where the team's resources will be applied during the detailed design phase to get the most effective design at its end.

4. Design Process

This chapter gives an overview of system engineering tools used in the detailed design process. First the trade-off method that is consistently used during the design phase is described. After that the usage of the technical budgets is discussed.

4.1. Trade-off Process

Here the processes used in the final design phase will be described. First the Analytical Hierarchy Process (AHP) will be explained and the scoring methods used.

AHP Explanation

To come up with the weights of the criteria in these trade-offs the AHP has been used [24]. This process uses the relative importance of the criteria versus each other to come up with each respective weight. To do this a relative importance table is setup where the trade-off criteria get compared using the scale that can be seen in Table 4.1.

Table 4.1: Relative importance scale used [24]

Scale	Degree of importance	Reciprocal (decimal)
1	Equally important	1
2	Equally to moderately important	1/2 (0.500)
3	Moderately important	1/3 (0.333)
4	Moderately to strongly important	1/4 (0.250)
5	Strongly important	1/5 (0.200)
6	Strongly to very strongly important	1/6 (0.167)
7	Very strongly important	1/7 (0.143)
8	Very strongly to extremely important	1/8 (0.125)

Table 4.2: Relative importance table (RIT) example with a CR of 0.02

RIT:	A	B	C	D
A	1.0	0.3	0.3	1.0
B	3.0	1.0	0.5	3.0
C	3.0	2.0	1.0	3.0
D	1.0	0.3	0.3	1.0

RIT normalised:				Average:	Consistancy:
A	0.13	0.09	0.15	0.13	0.12	4.03
B	0.38	0.27	0.23	0.38	0.31	4.07
C	0.38	0.55	0.46	0.38	0.44	4.12
D	0.13	0.09	0.15	0.13	0.12	4.03

An example of a relative importance table can be seen in Table 4.2. The criteria of the row is compared to the criteria of the column. If criteria B is for example moderately more important than criteria A it is given a score of three in the Relative Importance Table (RIT). This comparison will be done for every criteria, and the reciprocal will be used when the criteria being compared is less important than the other.

This relative importance matrix will be normalised and from there the average of the comparisons will add up to the total weight of the criteria. To make sure this weight is properly motivated a consistency check is performed. If one rates both criteria B and C strongly more important than criteria A, it is implied that criteria B and C are of equal importance. However, if in the comparison between criteria B and D C is given a value of two instead of being equal the consistency of the ratings goes down. This check calculates the Consistency Ratio (CR), by multiplying the row in the relative importance table with the resulted weight. This value is called the Consistency Index (CI), this value is then divided by the Random Consistency Index (RI) to get the Consistency Ratio (CR). A value of less than 0.1 is considered acceptable.

Scoring Methods

As the design moves into the subsystem level, the increasingly diverse trade-offs will requires differing scoring methods. A short overview of the scoring methods is given here.

Statistical Method

When scoring quantitative parameters, for example mass, a statistical method can be used based on the Standard Deviations (SD). This provides a more objective scoring. The mean (μ) and SD (σ) of the candidates are calculated. The scoring scale of 0 - 3 is then assigned based on the number of SD away from the mean. If the parameter is to be minimised, then an example scoring is shown in Table 4.3

Table 4.3: Statistical scoring method

	Score
0	$\sigma \leq x$
1	$\mu \leq x < \sigma$
2	$\sigma \leq x < \mu$
3	$x \leq \sigma$

4.2. Technical Budgets

The technical budgets taken into account during the detailed design phase are the mass, cost, power and battery capacity budget. As there are no requirements for the power and battery capacity, these budgets will be discussed in chapter 11. These budgets depend on the selected battery and Power Distribution Board. At the start of the detailed design a cost and mass budget was allocated to every department. These budgets were based on the technical budgets from the midterm report [2]. As the departments and their responsibilities changed between the midterm and the final phase the budgets had to be adjusted. Also the margins for both budgets are spread out proportionally over the departments. For every department the components that add up to the mass or cost were specified. For example, for the mass budget the operations department should only note down the mass of the warning system and the user interface. In the cost budget the operations department should also note down the cost for the case. These technical budget will be updated after an iteration of the design is finished. After every iteration the allocated budgets for the departments will be re-evaluated.

5. Operational Environments

To better guide the design of certain subsystems, operating details of the system will now be defined in more detail. Previously, a number of user cases were identified[2], from which several requirements were derived. However, it is now necessary to also consider the operational environment (section 5.1) and operational situations (section 5.2). Operational environment refers to the types of geographical locations the drone will operate in, for example forests, whereas operational situations refers to the situation at the time of use, for example weather conditions. The aim of this section is to explore any new requirements and define the limits on the operational environments.

5.1. Operational Environment Definitions

Though the operating region of the drone has already been narrowed to Europe, a large variety of geographical topographies still exist. Therefore, the following environments are considered, with their chance of mission success given in brackets. These chances are explained later in this chapter.

- Cave (Likely)
- Crevasse (Even)
- Sparse Forest (Likely)

- Dense Forest (Very unlikely)
- Open sky (Very likely)

- Urban setting (Very unlikely)
- Body of water (Likely)

These environments are visualised in figure 5.1.

Cave: As can be seen in figure 5.1a, the cave environment where the drone should be able to operate is limited to the parts of the cave where the opening of the cave is still visible by the user. The exit of the cave can either be above the user or next to the user. A new requirement was identified while defining the cave environment. This requirement specifies the minimum outer dimensions of a gap where the drone shall fly through when it is in 'flight mode'. **SYST-GENR-13**: In flight mode, the drone shall fit through an opening with minimum dimensions of 40x40 cm. These dimensions are based on the dimensions of an average human

(a) Cave

(b) Crevasse

(c) Sparsely-populated Forest

(d) Densely-populated Forest

(e) Open Sky

(f) Body of Water

Figure 5.1: Collages of different environments that are considered

being[1]. This is because in a situation that a hiker falls into a small hole that leads to a cave, the drone should be able to leave this cave through the same hole again to be able to call for help. As the drone does not have an extremely advanced sensor package on board, the drone might not find the exit of the cave. Therefore the chance of mission success is dependent on how far in the cave the user is, which is considered likely for the pictures shown.

Crevasse: As can be seen in figure 5.1b a crevasse is a deep crack in an ice sheet. It is possible for a hiker to fall into a crevasse while hiking as most crevasses are covered by a small layer of snow such that they are almost invisible to see at the surface. As for the cave environment SYST-GENR-13 is also applicable to the crevasse environment. The drone should be able to fly out of the crevasse to be able to call for help. In general, crevasses are more narrow compared to caves. Therefore the chance of mission success is even.

Forest: While identifying the forest environment two main types of forest were identified , sparse and dense forests. As can be seen in figure 5.1c a sparse forest is an environment where the tree canopy coverage is discontinuous. A sparse forest also has a lower count of obstacles for the drone to avoid compared to the obstacles present in a dense forest. Therefore the chance of mission success is likely. Examples of a dense forest can be found in figure 5.1d. Given the limited resources and available expertise, though the drone *can* fly in this environment, there is a very unlikely chance for the drone to succeed the mission. A navigation strategy will need to be derived that can decide when the environment is too obstacle-rich. Further analysis should be performed on this operational environment post-DSE to aid the navigation strategy.

Open sky: As can be seen in figure 5.1e is defined as a place where there are little to no obstacles for the drone present in the landscape. Examples of open sky environments are desert, tundras and grasslands. The drone has to be able to operate in this environment with a very likely chance to perform the mission successfully.

Urban environment: The urban environment is an environment where buildings are present and people are living. The urban environment is characterised by a lot of dynamic obstacles and the possibilities to have easy access to the emergency services. Because of the dynamic obstacles, it is very unlikely that the drone will succeed its mission.

Body of Water: As can be seen in figure 5.1f there is a wide range in bodies of water. Some bodies of water flow. The drone has to be able to be launched while the user is in a body of water. In most cases when the drone is successfully deployed from the body of water the environment will look similar to the one from the

[1]Metric data 01 average dimensions of person standing, `https://www.firstinarchitecture.co.uk/metric-data-01-average-dimensions-of-person-standing/`, [accessed on 27.6.2021]

open sky environment as there are little to no obstacles present above a body of water. The only difference between the open sky environment and the body of water environment is the deployment phase of the drone. In a body of water this might be more difficult and therefore the chance of mission success in a body of water is not very likely, but likely.

As can be seen, several of the environments are in some way restricted for the operation of the drone. Caves are only considered when the user can see the opening, as the drone is unlikely to contain a navigation suite complex enough to find the exit autonomously. As a crevasse is more narrow than a cave the chance of mission success is lower. Two types of forests are identified, when the user gets in trouble in a sparse forest the user is more likely to be saved than in a dense forest. The mission success chance in an open sky is very likely. The user finding itself in a body of water might have troubles deploying the drone which decreases the mission success chance.

5.2. Operational Situation Definitions

Now the operational situations, cases when the drone will fly, are considered. Similar to the operational environments, though the The other aspect to now consider is the operational situations the drone will have to fly in. The following operational situations are considered, again with the chance of mission success.

- Fair Weather (Very Likely)
- Light Rain (Very Likely)
- Heavy Rain (Unlikely)
- Strong Winds (Likely)
- Hail (Unlikely)
- Snow (Likely)
- Forest Fires (Likely)
- Sandstorm (Unlikely)
- Volcanic Eruption (Very Unlikely)
- Hot Weather (Likely)
- Cold Weather (Likely)

These situations are now explained in more detail.

Fair Weather: The baseline operation situation; there are no problematic weather conditions that affect the drone's mission. This is why the chance of mission success is very likely, as this is the design point.

Light Rain: Requirement **SYST-GENR-09-A** states, "The drone shall be able to operate with rain up to 10 mm/hour" and as such 10mm/hour is taken as the boundary between light and heavy rain. The drone should be able to operate in this condition, therefore the chance of mission success is highly likely.

Heavy Rain: As mentioned in light rain, heavy rain outside the scope set by the requirement **SYST-GENR-09-A**, hence why the drone can *attempt* to fly heavy rain, the chance of mission success is downgraded to unlikely.

Strong Winds: Two requirements are of interest here, **STAK-DFPP-02-A**, which states, "The drone shall be able to operate at wind with an average speed up to 15 m/s" and **STAK-DFPP-02-B**, which states, "The drone shall be able to operate at wind gusts up to 20 m/s". Wind has implications for the control and stability of the drone, though is elaborated more in section 10.5 and section 10.4. As the design included this requirement, the chance of mission success is likely.

Hail: If the drone can perform its mission successfully in this weather condition depends on the size of the hailstones. A hit from a big hailstone can damage the drone or make it uncontrollable. As a result, the chance that the drone can perform its mission in this weather type is considered unlikely.

Snow: Whereas light snow poses the same problem as light rain, heavy snow means an unlikely mission success in the same way as heavy rain.

Forest Fires: Requirement **STAKGENR12**, "The drone shall be able to operate in smoke", the drone should be able to fly through smoke. However, forest fires are often associated with high temperatures, so as long as the drone does not fly through the fire itself, the chance of mission success is likely.

Sandstorm: These weather conditions are extreme as sandstorms will blow small high velocity particles onto the drone. Therefore, it is considered unlikely that the drone can successfully perform the mission.

Volcanic Eruption: These weather conditions are very extreme as ash clouds are electrically charged and reach very high up into the sky[2]. As a result, it is very unlikely that the drone can successfully perform the mission. There still has to be done more research into the influence of these ash clouds on the performance of the drone in the post-DSE phase.

Hot Weather: Requirement **SYST-THER-01** states, "The drone shall be able to operate in a temperature range from -20 to +40 ° " so the drone is designed to operate in temperatures up to +40 °. Beyond that

---

[2]Eruption column, `https://en.wikipedia.org/wiki/Eruption_column`, [accessed 27.6.2021]

temperature the performance of the drone might degrade. This means that with hot weather the drone is still likely to perform the mission.

Cold Weather: As stated in the previous weather condition, the drone shall be able to operate at a temperature of -20 °. This is the temperature on ground level. As the drone would fly up the temperature would even decrease further. The drone has to be designed to withstand these extreme cold temperatures. As a result, it is likely that the drone performs its mission in these weather conditions.

6. Functional Flow Diagrams

Now that the final concept has been chosen, the Functional Flow Block Diagram (FFBD) and Functional Breakdown Structure (FBS) can be updated. Furthermore, since the first iteration of the FFBD and FBS, the range requirement has been dropped in favour of the altitude requirement. These diagrams are used as design tools for the detailed design phase.

Functional Flow Block Diagram

The FFBD describes the sequential order the functions must be completed in. There are several points of interest: First is the exit conditions during flight. There are two exit conditions for system; if the available energy becomes too low or if the system successfully communicates. These are being continually checked (for example, the battery by block 5.0) and if either condition is triggered, the drone will move to the landing function. Another point is that this diagram considers the *functions* the drone must perform. For example, block 3.7.2, "Determine obstacle avoidance route closest to flight path", is elaborated on in section 10.8.

Functional Breakdown Structure

The FBS considers the functions identified in the FFBD and sorts them into functional groups to aid the subsystem division. It should be noted that where functions straddle several departments, they are grouped into the more relevant department. For example, block 7.1, "Find potential landing site" leans more on the GNCS department than the landing support. Each block from the FFBD is grouped, so repeating blocks appear together.

Functional Flow Block Diagram Legend (1 / 2)

Legend:
- Top level function — Identifier
- Sub level function — Identifier
- Sub sub level function — Identifier
- IF — If statement block, outputs are go and no-go
- G — Positive outcome of if statement (go)
- G̅ — Negative outcome of if statement (no-go)
- AND — AND block, indicates both branches need to be completed
- OR — OR block, indicates only one branch needs to be completed

Top level flow:

Store drone (1) → Deploy drone (2) → AND → Drone climbs (3) → Drone hovers (4) → Drone traces back to user (6) → Drone lands (7) → Recover drone (8) → OR → End of life (9)

Drone performs battery check (5)

Store drone breakdown:
REF Store drone (1.0) → Charge drone (1.1) → Provide drone with necessary data (1.2) → Drone and operator perform systems check (1.3) → Package drone (1.4) → REF Deploy drone (2.0)

Provide drone with necessary data:
REF Provide drone with necessary data (1.2.0) → Update necessary software (1.2.1) → AND → Provide drone with height map of area of interest (1.2.2) / Update airspace restrictions (1.2.3) / Update country specific emergency information (1.2.4) → REF Drone and operator perform systems check (1.3.0)

Drone and operator perform systems check:
REF Drone and operator perform systems check (1.3.0) → Perform visual inspection of the drone's exterior (1.3.1) → User removes casing (1.3.2) → User inspects mechanical fixtures (1.3.3) → AND → User inspects battery (1.3.4) / User inspects sensors and antennas (1.3.5) / User inspects wiring and connections (1.3.6) → Drone performs communication test (1.3.7) → Drone tests GNSS connection (1.3.8) → REF Package drone (1.4.0)

Package drone:
REF Package drone (1.4.0) → Fold drone (1.4.1) → Put drone in case (1.4.2) → REF Deploy drone (2.0)

Deploy drone:
REF Deploy drone (2.0) → Unpackage drone (2.1) → User performs final visual inspection (2.2) → Activate drone (2.3) → Drone gets location data if available (2.4) → REF Drone climbs (3.0)

Unpackage drone:
REF Unpackage drone (2.1.0) → Get drone out of case (2.1.1) → Unfold drone (2.1.2) → REF User performs final visual inspection (2.1.3)
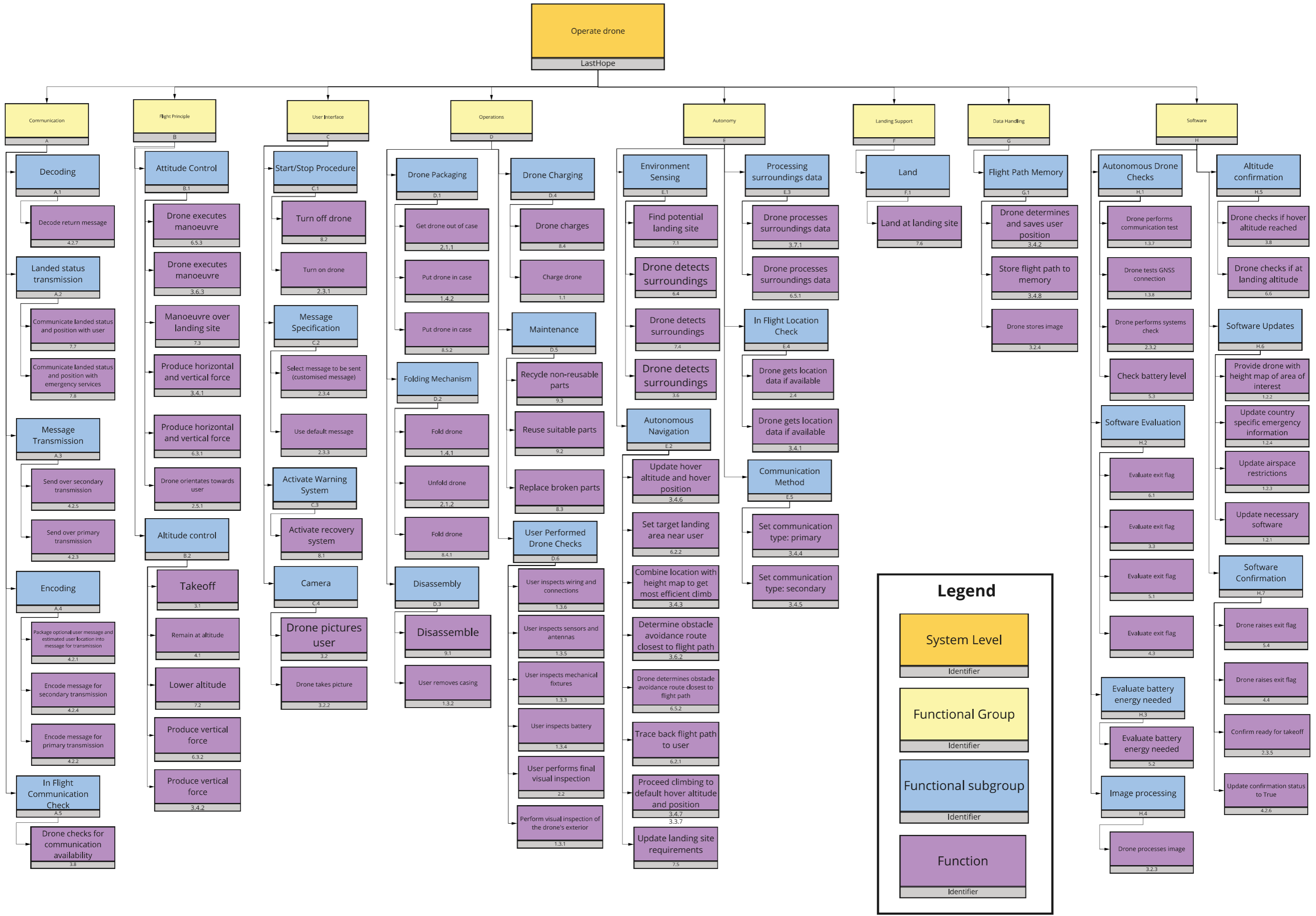
Activate drone:
REF Activate drone (2.3) → Turn on drone (2.3.1) → Drone performs systems check (2.3.2) → OR → Use default message (2.3.3) / Select message to be sent (customised message) (2.3.4) → Confirm ready for takeoff (2.3.5) → REF Drone gets location data if available (2.4.0)

Drone climbs:
REF Drone climbs (3.0) → Takeoff (3.1) → Drone pictures user (3.2) → Evaluate exit flag (3.3) → [Exit flag raised?] IF → G̅: AND → Drone determines flight path (3.4) / Drone ascends (3.5) / Drone detects surroundings (3.6) → Drone avoids obstacles (3.7) → AND → Drone checks for communication availability (3.8) / Drone checks if hover altitude reached (3.9) → IF [Communication available?] / IF [Hover altitude reached?] → REF Drone hovers (4.0)
- G: REF Drone lands (7.0)

Drone determines flight path:
REF Drone determines flight path (3.4.0) → Drone gets location data if available (3.4.1) → [Location data acquired?] IF → G: Drone determines and saves user position (3.4.2) → Combine location with height map to get most efficient climb (3.4.3) → [Cellular communication possible?] IF → G̅: Set communication type: primary (3.4.4) / G: Set communication type: secondary (3.4.5) → Update hover altitude and hover position (3.4.6)
- G̅: Proceed climbing to default hover altitude and position (3.4.7) → Store flight path to memory (3.4.8)

Drone ascends:
REF Drone ascends (3.5.0) → [Flight path purely vertical?] IF → G̅: Produce horizontal and vertical force (3.5.1) / G: Produce vertical force (3.5.2) → AND → REF Drone checks for communication availability (3.7.0) / REF Drone checks if hover altitude is reached (3.8.0)

Drone avoids obstacles:
REF Drone avoids obstacles (3.7.0) → Drone processes surrounding data (3.7.1) → Determine obstacle avoidance route closest to flight path (3.7.2) → [Path found?] IF → G: Drone executes manoeuvre (3.7.3) → AND → REF Drone checks for communication availability (3.8.0) / REF Drone checks if hover altitude is reached (3.9.0)
- G̅: [# Attempts > 10?] IF → G̅ / G: REF Drone lands (7.0)

Drone performs battery check:
REF Drone performs battery check (5.0) → Evaluate exit flag (5.1) → [Exit flag raised?] IF → G̅: Evaluate battery energy needed (5.2) → Check battery level (5.3) → [Battery level ≤ bingo energy?] IF → G: Drone raises exit flag (5.4) → REF Drone lands (7.0)

Drone takes pictures:
REF Drone takes pictures (3.2.0) → Drone orientates towards user (3.2.1) → Drone takes picture (3.2.3) → Drone processes image (3.2.4) → Drone stores image (3.2.5) → [# images = 10?] IF → G: REF Drone Climbs (3.0.0)

Functional Flow Block Diagram Legend (2 / 2)

Top level function — Identifier

Sub level function — Identifier

Sub sub level function — Identifier

IF — If statement block, outputs are go and no-go

G — Positive outcome of if statement (go)

G̅ — Negative outcome of if statement (no-go)

AND block, indicates both branches need to be completed

OR block, indicates only one branch needs to be completed

Top level flow:
1. Store drone
2. Deploy drone — AND
3. Drone climbs
4. Drone hovers
5. Drone performs battery check
6. Drone traces back to user
7. Drone lands
8. Recover drone — OR
9. End of life

4.0 REF Drone hovers — AND
4.1 Remain at altitude
4.2 Drone communicates
4.3 Evaluate exit flag
Exit flag raised? IF — G / G̅
4.4 Drone raises exit flag
6.0 REF Drone traces back to user
Confirmation status true? IF — G / G̅

4.2.0 REF Drone communicates
4.2.1 Package optional user message and estimated user location into message for transmission
Primary communication? IF — G / G̅
4.2.2 Encode message for primary transmission
4.2.3 Send over primary transmission
4.2.4 Encode message for secondary transmission
4.2.5 Send over secondary transmission
Confirmation received? IF — G / G̅ — AND
4.2.6 Update confirmation status to True
4.2.7 Decode return message
4.3.0 REF Evaluate exit flag

6.0 REF Drone traces back to user
6.1 Evaluate exit flag
Exit flag raised? IF — G̅ / G — AND
7.0 REF Drone lands
6.2 Drone determines flight path
6.3 Drone decreases altitude
6.4 Drone detects surroundings
6.5 Drone avoids obstacles
6.6 Drone checks if at landing altitude
Landing altitude reached? IF — G̅ / G
7.0 REF Drone lands

6.5.0 REF Drone avoids obstacles
6.5.1 Drone processes surrounding data
6.5.2 Drone determines obstacle avoidance route closest to flight path
Path found? IF — G / G̅
6.5.3 Drone executes manoeuvre
6.6.0 REF Drone checks if at landing altitude
Attempts > 10? IF — G̅ / G
7.0 REF Drone lands

6.3.0 REF Drone decreases altitude
Flight path purely vertical? IF — G̅ / G
6.3.1 Produce horizontal and vertical force
6.3.2 Produce vertical force
6.6.0 REF Drone checks if at landing altitude

6.2.0 REF Drone determines flight path
6.2.1 Trace back flight path to user
6.2.2 Set target landing area near user
6.6.0 REF Drone checks if at landing altitude

7.5 Update landing site requirements
7.0 REF Drone lands
7.1 Find potential landing site — AND
7.2 Lower altitude
7.3 Manoeuvre over landing site
7.4 Drone detects surroundings
Attempts > 10? IF — G̅ / G
Landing site suitable? IF — G̅ / G

7.6 Land at landing site
Drone stationary? IF — G̅ / G — OR
7.7 Communicate landed status and position with user
7.8 Communicate landed status and position with emergency services
8.0 REF Recover drone

8.0 REF Recover drone
8.1 Activate recovery system
8.2 Turn off drone
8.3 Replace broken parts
8.4 Drone charges
8.5 Repackage drone — OR
1.0 REF Store drone
9.0 REF End of Life

8.5.0 REF Repackage drone
8.5.1 Fold drone
8.5.2 Put drone in case — OR
1.0 REF Store drone
9.0 REF End of Life

9.0 REF End of life
9.1 Disassemble
9.2 Reuse suitable parts
9.3 Recycle non-reusable parts

Operate drone — LastHope

A. Communication

- **A.1 Decoding**
  - Decode return message — 4.2.7
- **A.2 Landed status transmission**
  - Communicate landed status and position with user — 7.7
  - Communicate landed status and position with emergency services — 7.8
- **A.3 Message Transmission**
  - Send over secondary transmission — 4.2.5
  - Send over primary transmission — 4.2.3
- **A.4 Encoding**
  - Package optional user message and estimated user location into message for transmission — 4.2.1
  - Encode message for secondary transmission — 4.2.4
  - Encode message for primary transmission — 4.2.2
- **A.5 In Flight Communication Check**
  - Drone checks for communication availability — 3.8

B. Flight Principle

- **B.1 Attitude Control**
  - Drone executes manoeuvre — 6.5.3
  - Drone executes manoeuvre — 3.6.3
  - Manoeuvre over landing site — 7.3
  - Produce horizontal and vertical force — 3.4.1
  - Produce horizontal and vertical force — 6.3.1
  - Drone orientates towards user — 2.5.1
- **B.2 Altitude control**
  - **Takeoff** — 3.1
  - Remain at altitude — 4.1
  - Lower altitude — 7.2
  - Produce vertical force — 6.3.2
  - Produce vertical force — 3.4.2

C. User Interface

- **C.1 Start/Stop Procedure**
  - Turn off drone — 8.2
  - Turn on drone — 2.3.1
- **C.2 Message Specification**
  - Select message to be sent (customised message) — 2.3.4
  - Use default message — 2.3.3
- **C.3 Activate Warning System**
  - Activate recovery system — 8.1
- **C.4 Camera**
  - Drone pictures user — 3.2
  - Drone takes picture — 3.2.2

D. Operations

- **D.1 Drone Packaging**
  - Get drone out of case — 2.1.1
  - Put drone in case — 1.4.2
  - Put drone in case — 8.5.2
- **D.2 Folding Mechanism**
  - Fold drone — 1.4.1
  - Unfold drone — 2.1.2
  - Fold drone — 8.4.1
- **D.3 Disassembly**
  - Disassemble — 9.1
  - User removes casing — 1.3.2
- **D.4 Drone Charging**
  - Drone charges — 8.4
  - Charge drone — 1.1
- **D.5 Maintenance**
  - Recycle non-reusable parts — 9.3
  - Reuse suitable parts — 9.2
  - Replace broken parts — 8.3
- **D.6 User Performed Drone Checks**
  - User inspects wiring and connections — 1.3.6
  - User inspects sensors and antennas — 1.3.5
  - User inspects mechanical fixtures — 1.3.3
  - User inspects battery — 1.3.4
  - User performs final visual inspection — 2.2
  - Perform visual inspection of the drone's exterior — 1.3.1

E. Autonomy

- **E.1 Environment Sensing**
  - Find potential landing site — 7.1
  - Drone detects surroundings — 6.4
  - Drone detects surroundings — 7.4
  - Drone detects surroundings — 3.6
- **E.2 Autonomous Navigation**
  - Update hover altitude and hover position — 3.4.6
  - Set target landing area near user — 6.2.2
  - Combine location with height map to get most efficient climb — 3.4.3
  - Determine obstacle avoidance route closest to flight path — 3.6.2
  - Drone determines obstacle avoidance route closest to flight path — 6.5.2
  - Trace back flight path to user — 6.2.1
  - Proceed climbing to default hover altitude and position — 3.4.7 / 3.3.7
  - Update landing site requirements — 7.5
- **E.3 Processing surroundings data**
  - Drone processes surroundings data — 3.7.1
  - Drone processes surroundings data — 6.5.1
- **E.4 In Flight Location Check**
  - Drone gets location data if available — 2.4
  - Drone gets location data if available — 3.4.1
- **E.5 Communication Method**
  - Set communication type: primary — 3.4.4
  - Set communication type: secondary — 3.4.5

F. Landing Support

- **F.1 Land**
  - Land at landing site — 7.6

G. Data Handling

- **G.1 Flight Path Memory**
  - Drone determines and saves user position — 3.4.2
  - Store flight path to memory — 3.4.8
  - Drone stores image — 3.2.4

H. Software

- **H.1 Autonomous Drone Checks**
  - Drone performs communication test — 1.3.7
  - Drone tests GNSS connection — 1.3.8
  - Drone performs systems check — 2.3.2
  - Check battery level — 5.3
- **H.2 Software Evaluation**
  - Evaluate exit flag — 6.1
  - Evaluate exit flag — 3.3
  - Evaluate exit flag — 5.1
  - Evaluate exit flag — 4.3
- **H.3 Evaluate battery energy needed**
  - Evaluate battery energy needed — 5.2
- **H.4 Image processing**
  - Drone processes image — 3.2.3
- **H.5 Altitude confirmation**
  - Drone checks if hover altitude reached — 3.8
  - Drone checks if at landing altitude — 6.6
- **H.6 Software Updates**
  - Provide drone with height map of area of interest — 1.2.2
  - Update country specific emergency information — 1.2.4
  - Update airspace restrictions — 1.2.3
  - Update necessary software — 1.2.1
- **H.7 Software Confirmation**
  - Drone raises exit flag — 5.4
  - Drone raises exit flag — 4.4
  - Confirm ready for takeoff — 2.3.5
  - Update confirmation status to True — 4.2.6

Legend

- **System Level** — Identifier
- **Functional Group** — Identifier
- **Functional subgroup** — Identifier
- **Function** — Identifier

7.   Operations

In this chapter, the design of the various aspects related to the operation of the drone will be explained and the results will be shown. This consists of the case which holds the drone, the primary user interface and the external system for warnings.

The storage of the drone and how it fits into the container is done in conjunction with the Structures Department and can be found in section 7.1. The charging system is developed alongside the Electronics Team similarly and is also mentioned in section 7.1. Sections from those departments will be referenced when needed to give added reasoning. The user interface and the process used to design it will be covered in section 7.2. The warning system is then covered in section 7.3 followed by a requirements compliance overview to end the chapter in section 7.4.

7.1. Drone Container

In this section, the final design for the container that will house the drone will be presented along with the steps taken to design it. First off, the requirements that influence the design will be reviewed followed by a functional analysis of the container. Then, a market analysis will be performed to discern what options are currently available on the market. Using the previous three subsections as guidance, initial concepts for the container are created and are traded off. The criteria and weights are explained following the trade-off. After the concept has been chosen, the material for the outer shell is traded off and then the final design is worked out in further detail. The final design can be seen below in figure 7.1 and its main characteristics in Table 7.1.

Going beyond the requirements and functions that will be outlined, it is worthwhile to define a design philosophy for which the container will be designed. As the drone is unlikely to be made fully out of sustainable materials, it is decided to try and compensate for this shortcoming by placing a large focus on sustainability in the container itself. This will be reflected in the materials chosen to be evaluated in the material trade-off such that they are either recyclable or come from a naturally-occurring source. The rest of the aspects that influence the design are described in the requirements and functional analysis subsections.
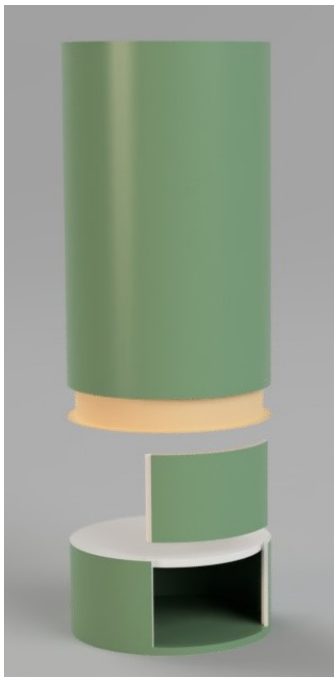
Figure 7.1: Exploded View of the Drone Container

Table 7.1: Drone Container Main Specifications

Components	Outer shell, inner liner, base, spare parts, charging system
Total Mass (excl. drone)	1.36 kg
Dimensions	diameter=12cm height=27cm
Total Cost (Material + Production)	€ 40.85
Outer Shell & Base Material	Polylactic Acid (PLA)
Inner Liner Material	Thermoplastic Polyurethane (TPU)
Cushioning Material	Coir Fibre

Container Requirements Review

It is necessary to design a case for the user to carry the drone while hiking or working in remote areas. The basic need for the case results from the following stakeholder requirements:

- **SYST-GENR-03:** The maximum dimensions of the drone in storage mode shall not exceed 200x100x100 mm (length, width, height)
- **STAK-STOR-01:** The drone shall have a protective casing for travel

At first glance, it is clear that the case must protect the drone and have the required storage space. It is also worthwhile mentioning that **SYST-GENR-03** refers to the drone when it is in storage mode and does not restrict the size of the case around it. Beyond that, there are requirements which do not influence the main need for the case, but do add other functions or constraints which it must abide by. These include:

- **STAK-COST-02:** The cost of the drone for the end-user shall not exceed EUR 700
- **STAK-DFPP-02:** The flight parameters of the drone shall be valid after 1-month storage after full charging.
- **STAK-ELEC-01:** The drone shall be able to be charged in field environment
- **SUBSYST-STOR-01:** The storage system shall protect the drone from any functional damage from a drop of <tbd> meter
- **SUBSYST-STOR-02:** The storage system shall protect the drone of any functional water damage after being submerged for <tbd> hours in saline water
- **SUBSYST-STOR-03:** The storage system shall have an IP rating of IP57
- **SUBSYST-OPER-02:** The system shall be operable by the user with their non dominant hand

As can be seen, the cost of the case will be factored in when summing up the total price. From **STAK-DFPP-02**, it is clear that the case must be equipped with a battery to keep the drone's battery up to charge for up to one month. The Electronics Department will size the battery needed for this and a space must be provided for it within this section. Beyond the requirements mentioned above, the sustainability requirements SYST-SUST-04 to 12 shall be followed to ensure that non-toxic materials are chosen and that the designed parts are recyclable and repairable.

Container Functional Analysis

Keeping the requirements mentioned in section 7.1 in mind, all functions of the container should be identified before starting the concept generation. The functions of the container can be divided into four categories being that it shall protect, store, charge, and serve as the launch platform for the drone. The latter has been added by the team at this stage from a user-friendliness point-of-view. A launch platform will greatly reduce the difficulty for the user to launch the drone in situations where there is a lack of a suitable launch location or where they only have one-hand to use due to an injury. Given that space is limited, it is even more important that the case is designed it in a way that parts have a dual functionality. If the launch platform can be built into one of the other parts of the container, that is optimal.

Other options would include the user just placing it down on the ground or launching it by hand. Although these options will still be possible even with the inclusion of the launch stand, they are not desired as they require extra work and knowledge to an extent for the user to deploy the drone successfully. It will be further discussed in the detailed design aspects, but it will be designed such that the drone is connected to the battery which keeps the drone's battery charged in the field through this launch setup. This also eliminates the step where the user must disconnect it from the charging system. In the case that the user only has their non-dominant hand available, the elimination of the steps to disconnect the drone and set it up for launch themselves improves the system's compliance with **SUBSYST-OPER-02**, stated in section 7.1. Overall, the value added through the improved ease-of-setup for the user justifies the inclusion of the launch stand function, even though there is no explicit requirement governing it.

1. Protection

- Protect from fall of a height of 2.5m
- Protect from water while submerged at 1m for 30 minutes
- Protect from dust which would damage the drone

2. Charge the drone

3. Storage

- Provide a storage space of 200 x 100 x 100 mm
- Store the battery
- Store the critical replacement parts
- Store the charging cord

4. Provide a launch platform for the drone

Container Market Analysis

After conducting some research, it can be reasoned that most available options consist of a hard container similar to a briefcase, a backpack, a soft case, or the container itself is built into the drone. Many options are larger than what would be needed to hold the LastHope drone, but evaluating these options is still relevant as information on the materials, mechanisms, and structure is helpful.

The first example is the briefcase-like-option shown in figure 7.2 created by Explorer Cases [1]. This case (355x860x765mm) is much larger than what would be needed for the LastHope drone. It has a hard shell exterior made of polypropylene and an inner foam to cushion the drone. It weighs 16.4kg and uses a latch mechanism to keep the case shut.

The second example, pictured in figure 7.3, is a backpack made by Go Professional Cases [2]. The backpack weights 3.2kg and is 530x440x250mm, which is a couple sizes larger than what would be needed for the drone being designed. The outer material is a soft shell made of nylon and the inner material is a foam to cushion the drone. It uses a zipper to close the bag.

The next example is a soft shell cylinder made by RC Geek [3] and shown in figure 7.4. Its dimensions are 155x98x123mm and it weighs 0.16kg. This example is maybe the closest to the storage requirement for the LastHope drone of 200x100x100mm as it was made for the DJI Mavic Mini Drone which is another small drone option weighing 0.249kg. The case is made of polyurethane leather and uses cloth as the inner cushion. The case is opened and secured with a zipper.

The last example, the PowerVision Egg Drone as shown in figure 7.5, is somewhat different than the others as the case is integrated into the drone itself [4]. This allows it to be stored in any backpack or other container. In its storage mode, the drone is 448x272x176mm in its storage mode and weighs 2.1kg, four times larger than LastHope's upper mass requirement (0.5kg). Given the tight mass requirements and the critical nature of the drone, it can be decided already that the drone's case will not be integrated into the design of the drone. Even if the case could be integrated into the design, the drone would have to lug that empty mass through its flight and its performance, would be worsened.

Figure 7.2: Box Case Example

Figure 7.3: Backpack Example

Figure 7.4: Soft Shell Bag Example

Figure 7.5: Built-in Case Example

From this market analysis it was seen what options currently exist on the market, what sizes they are, what materials they use, and how they work. Polypropylene, polyurethane leather, and nylon were used for the outer material for the reviewed options. Polypropylene is recyclable whereas polyurethane is not.[8] If the container is desired to be made in a sustainable manner, other options may have to be considered. It can be reasoned already that building the case into the drone itself shall not be considered given the driving mass requirements on the drone. Building a into the drone would drive up the mass unacceptable amount.

Container Concept Generation

From the functions identified in Table 7.1 and options already existing in the market in Table 7.1, concepts for the container can be generated. It has already been established that the drone will take on a long, slender shape optimised for its climb[2]. This was kept in mind when establishing the concepts such that a case is designed which fits the drone best and is the easiest for the user to store.

For each of the options, assumptions must be made about the other things the case must store besides the drone itself. These include the charger, the battery which charges the drone in the field, and any spare parts.

---

[1]Black Explorer Case https://www.bol.com/nl/nl/p/explorer-cases-7630-b-zwart-apparatuur-tas-met-trolley-plukschuim/9200000123183614/, [accessed 7.6.2021]

[2]Go Professional DJI Drone Backpackhttps://www.bhphotovideo.com/c/product/1306332-REG/go_professional_cases_gpc_dji_p4_bp_blk_ltd_dji_phantom_4_backpack.html, [accessed 7.6.2021]

[3]RC Geek DJI Mavic Mini Casehttps://www.amazon.com/RCGEEK-Compatible-Controller-Installed-Anti-Shock/dp/B081QBPX63, [accessed 7.6.2021]

[4]Power Vision Egg Dronehttps://www.powervision.me/en/product/poweregg, [accessed on 7.6.2021

Regarding the space needed for the charger, cord, and battery, it is assumed that a space of 80x80x40 mm is needed. This was generated from measuring similar charging units used on drones among the team.

In chapter 15, it was decided to include space for two spare propellers and two spare arms as these were deemed the most likely to fail . Using the preliminary design from the midterm report [2] and the sizes for the parts from , it was decided that the spare parts would need a 160x90x30mm space. The assumptions are later given in the unit of cm^3 for clarity with the concept analysis. Additional assumptions regarding the shape of the drone and the way it will fit into the container have been made. All assumptions mentioned prior are compiled below and any additional ones are explained.

- A volume of 256cm^3 (80x80x40mm) has been used for the charging system for the drone
- A volume of 432cm^3 (160x90x30mm) has been assumed for the spare parts that the case will store
- The spare parts will consist of two backup propellers and arms
- The wall thickness of the case will be 1 cm
- The drone will come preset in its launch stand if possible
- The connection at the launch stand will also connect the drone to its charger
- The charging system will be located at the bottom of the stand to prevent gusts from blowing it over
- The drone uses a shape that is close to 200mm tall chapter 9
- The folding mechanism has been chosen in such that the arms fold alongside the body of the drone
- The user already possesses a backpack to carry the drone in or has another place to store it.

Using these assumptions and the earlier stated requirements, multiple options were compiled in a design option tree as shown in the figures below. Non-concepts which didn't feature a built-in landing stand or were an inconvenient shape for the user to store were cast out, resulting in the following five concepts.

Figure 7.6: Concept 1: Soft shell bag with zipper
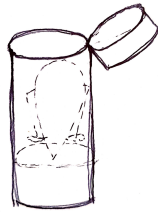
Figure 7.7: Concept 2: Hard shell cylinder with jar hinge cap
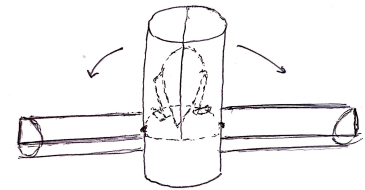
Figure 7.9: Concept 4: Hard shell cylinder with latched halves
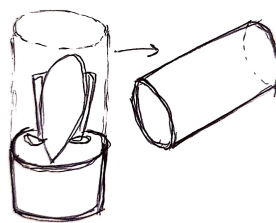
Figure 7.8: Concept 3: Hard shell cylinder with latched long cap
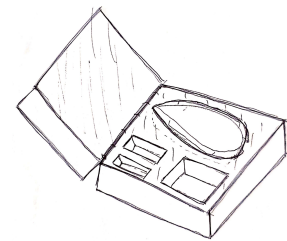
Figure 7.10: Concept 5: Hard shell normal case

Before moving onto the trade-off table, the result, being the third concept, can be identified and the methodology used for the trade-off between the five concepts will be explained. First, an explanation of the trade-off criteria and their weights are shown followed by the trade-off table itself in Table 7.10. For the trade-off table and weights table, a scoring method from zero to three is used where three is excellent, two is good, one is correctable and zero is unacceptable. A brief sensitivity analysis is performed afterwards to ensure that the method used is sound and that the best option was chosen.

Drone Container Trade-off Criteria
The trade-off criteria considered consist of seal-ability, protection, risk, size, ease-to-assemble, packing efficiency, and one-hand operability. The motivation for including each criteria, the scoring system used, and why each concept performed the way it did will be explained.

Seal-ability: First, seal-ability was included due to the requirement on the IP rating for sealing the container, **SUBSYST-STOR-03**. This is crucial when protecting the drone from dust or water damage. The main idea behind the scoring method is that concepts with a larger total edge length to seal will be harder to seal. Longer edges require additional clamps or latches to give sufficient pressure. Using the assumptions from figure 7.1, the length of the edges for each concept was found and the standard deviation was taken as described in section 4.1. This led to the three cylindrical concepts to perform the best as the length of the edges they must seal was above one standard deviation greater than the average. This lead to the scoring system as shown in Table 7.2.

Protection: Secondly, a criteria for protection was included mainly as protecting the drone is the main function of the container. This is also described by the requirements regarding the need for a protective case and the drop height, **STAK-STOR-01** and **SUBSYST-STOR-01**. For the analysis of each concept in regard to this criteria, a more qualitative method was used as it was infeasible to predict the toughness of the structure without having chosen a material yet. This led to the scoring method shown in Table 7.3. Concept one was given a score of one as it is a soft bag and would need extra support. Concepts two and three are hard shells and have only a single gap. As it is divided into two halves, concept four has constant interruptions to its structure meaning additional reinforcement is needed. Concept five received an excellent score as it is a hard shell and has edges which the that can absorb an impact.

Table 7.2: Scoring system for Seal-ability

Category	Length of Edges to Seal
Excellent	< 33cm
Good	33-58cm
Correctable	58-83cm
Unacceptable	> 83cm

Table 7.3: Scoring system for Protection

Category	Protection Effectiveness
Excellent	Extremely well protected
Good	Protected
Correctable	Needs extra support
Unacceptable	Not protected enough

Risk: The next criteria used was risk which was evaluated by the number of failure-prone components that each concept uses to open. It is desired to minimise the number of components required to open the drone. It is crucial that the container opens properly in an emergency situation as the user could be in danger. It is assumed that each type of hinge, latch, or zipper has the same probability of failure in this case. This is acknowledged to vary in reality, but is a reasonable assumption given the level of depth at this stage. The scoring method and its ranges are based on what was observed across the five concepts and is displayed in Table 7.4.

Size: Size was chosen as a criteria as the container must be small enough to be carried by most hikers or people when they are outdoors in remote areas. Hiking packs use liters to measure their volume[5], so the scoring method will be based on that and how much a like-sized item a hiker will have to carry takes up. Based on the drone's storage requirement **SYST-GENR-03**, it is known that at least 2L are needed to house the drone. An upper bound of 5L will be set for the scoring method as the drone shouldn't be taking up more than a sleeping mat, one of a hiker's larger items[6]. It is assumed that the cylinder options have a radius of 60mm and a height of 270mm whereas the box option is 120x200x220mm, which come out to volumes of 2.83L and 5.28L. The scores received follow the system shown in Table 7.5.

Table 7.4: Scoring system for Risk

Category	Number of Components Which Can Fail
Excellent	1
Good	2
Correctable	3
Unacceptable	>3

Table 7.5: Scoring system for Size

Category	Volume Taken Up By Case [L]
Excellent	<2.5L
Good	2.5L<V<3L
Correctable	3L<V<5L
Unacceptable	>5L

Ease-of-assembly: The ease-to-assemble criteria was included to help separate the differences between each of the concepts and their opening mechanisms. Opening the container should take the fewest number of steps possible. The steps which the user would have to take from opening the container to being ready to launch the drone were found. The main differences arose from whether the drone came preset in a stand and

---

[5]REI Hiking Packs`https://www.rei.com/learn/expert-advice/backpack.html`, [accessed 17.6.2021]
[6]Insulated Sleeping Mat `https://www.amazon.com/Exped-DownMat-camping-mat-black/dp/B00BT018CK/`, [accessed 17.6.2021]

how difficult it is to open the container. Concepts three and four performed best as they both required only three steps before being ready to launch the drone. The other three options were in the correctable category as they needed extra steps. The scoring system can be seen in Table 7.6.

Packing Efficiency: Packing efficiency was chosen to judge how well each container concept stores the drone, its spare parts, and its charging system using the assumed sizes from figure 7.1. The volume of those components minus the total volume and divided by the total volume to get a packing efficiency percentage. The scoring system goes from greater than 90 percent down to below 70 and can be seen in Table 7.7.

Table 7.6: Scoring system for Ease-of-Assembly

Category	# Steps to Assemble
Excellent	2
Good	3
Correctable	4-6
Unacceptable	>6

Table 7.7: Scoring system for Packing Efficiency

Category	% of Total Volume Used
Excellent	>90%
Good	80-90%
Correctable	70-80%
Unacceptable	<70%

One-hand operability: The final criteria was chosen to reflect how well the user could still use the container and set up the drone in a situation where they only have one-hand to use. The steps identified for the criteria on ease-of-assembly will be used as a basis and analysed for how much more difficult they would be with one-hand.

Table 7.8: Scoring system for One-Hand Operability

Category	One-Hand Operability
Excellent	Easy
Good	Medium Difficulty
Correctable	Hard
Unacceptable	Extremely Difficult

The scoring system is qualitative, similar to that of the protection score and can be seen in Table 7.8. Concepts one, two, and five received a score of one as they require the user to use their legs or something else for assistance when pulling out the drone. Concept four received a score of two as it takes longer using one-hand, but is still possible. Concept three was the only one that received a three as it's operation does not change greatly while only having one-hand.

Drone Container Trade-off Criteria Weights

The weights for each of the specified criteria followed the same method outlined in section 4.1. Protection, seal-ability and size are some of the more important criteria given that the main function of the container is to protect the drone, the requirement regarding water/air sealing and the need for it to be a reasonable size for a hiker to carry. Risk, ease-of-assembly, packing efficiency and one-hand operability all had weights that were single digits as they are aspects which separate concepts from each other but are not as driving as the previous three mentioned. The AHP table and the weights can be found in Table 7.9

Table 7.9: Container Concept Trade-off AHP

	Seal-ability	Protection	Risk	Size	Ease to Assemble	Packing Efficiency	One-hand Operability	Average (Consistency)
Seal-ability	1.0	0.3	5.0	0.3	3.0	3.0	3.0	**0.16 (7.41)**
Protection	3.0	1.0	5.0	1.0	5.0	5.0	5.0	**0.31 (7.30)**
Risk	0.2	0.2	1.0	0.2	0.3	0.3	0.3	**0.04 (6.59)**
Size	3.0	1.0	5.0	1.0	5.0	3.0	5.0	**0.29 (7.38)**
Ease to Assemble	0.3	0.2	3.0	0.2	1.0	1.0	3.0	**0.07 (8.57)**
Packing Efficiency	0.3	0.2	3.0	0.3	1.0	1.0	3.0	**0.08 (8.31)**
One-Hand Operability	0.3	0.2	3.0	0.2	0.3	0.3	1.0	**0.06 (7.14)**

Container Concept Trade-off

Below in Table 7.10, can be seen. It should be noted that the weights do add up to 1.01, which is attributed to rounding error after performing the AHP calculations. The result of the third concept can be seen in the last column in dark green.

Table 7.10: Drone Container Concept Trade-off

Criteria	Seal-ability	Protection	Risk	Size	Ease to Assemble	Packing Efficiency	One-hand Operability	Total
Weights	0.16	0.31	0.04	0.29	0.07	0.08	0.06	
Concept 1	2	1	3	2	1	3	1	**1.68**
Concept 2	2	3	2	2	1	3	1	**2.26**
Concept 3	2	3	2	2	2	3	3	**2.45**
Concept 4	1	2	0	2	2	3	2	**1.84**
Concept 5	1	3	1	1	1	0	1	**1.55**

From this trade-off, it can be seen that the cylinder with the latched cap clearly outperforms the competitors with its excellent performance in protection, packing efficiency, and one-hand operability. The second concept, the cylinder with the hinge cap, also came quite close, having a total of 2.26 compared to the third concept's 2.45. Concepts one and four, the soft shell bag and the cylinder with the separable halves, received the nearly the same score, but this will not be looked into further as the score is much lower compared to the top two concepts. Concept five, the normal hard shell case, performed the worse due to it's low packing efficiency and all-around correctable performance in most other categories.

Container Concept Discussion

Given the preliminary level of design for each concept and the assumptions made, a quick reflection on the outcome should be made to verify that the correct concept was chosen. Looking first at the assumptions, the premise of how much space would be required for the spare components and battery might mean that each concept was sized to be a bit larger than what they would be. This can be discarded however as they would each decrease or increase by roughly the same amount. Regarding size, additional time could have been given to sizing the normal hard shell case option. Although it still performs poorly in other criteria, it is unlikely that it would have taken up as much space as it did and would've maybe been in the good category with the other concepts. The assumption outlined in the Risk criteria description about hinges, latches, and zippers having the same chance of failure probably made the soft bag perform better than it did. Intuition would say that a zipper would get jammed much more frequently than a latch or hinge would stop working. The other shortcomings of the soft bag in protection and ease-of-assembly meant that this did not matter very much in the end.

Regarding the criteria themselves, the more qualitative criteria such as protection and one-hand operability could have been improved by asking various members on the team for how they would rate the different options to get the most accurate answer. It is likely that any of the concepts could have worked for seal-ability and protection, but it is difficult to fully establish without knowing what material is being used and what loads are expected. In the end, the level of analysis at this stage was sufficient given the resources available and further aspects to be considered are outlined in Table 7.1.

Container Material Selection

In this subsection, the materials for the components of the drone will be chosen. To further elaborate on the concept selected, it will consist of three main parts being the outer shell, inner liner, and base. The outer shell will be the primary protective piece of the container whereas the inner liner will provide the seal. Two separate parts are created here for sustainability. Any cracks that develop in the outer shell will not lead to a compromise of the seal as the inner liner sits just inside, avoiding the case where someone would throw away the whole case if just one crack were to develop. The base will contain the charging system and is the component which the drone will sit on as a stand. Inside the container, cushioning material will also be used to protect the drone. As the outer shell is the main protective component, a trade-off will be performed on its material. As discussed at the start of section 7.1, only sustainable materials will be evaluated for the container.

For the trade-off of the outer shell material, three materials were chosen being a Flax epoxy composite, Polylactic Acid (PLA), and Birch wood. All three are bio-based except for the epoxy in the flax composite. All

three materials were researched in Pharos[7] and found to have no high hazards with high confidence in their finished state. The container will be constructed from scratch for the flax composite and PLA options whereas the Birch wood is a pre-bought tube[8].

They will be compared on toughness, sustainability, cost, specific yield strength, and manufacturability. Sustainability was conducted using the Ecolizer[9] score. For all criteria expect manufacturability, a score system based on the standard deviation of the results of each option was used. It is assumed that the flax epoxy option would be constructed using manual layup with prepreg sheets, that the PLA option would be done using injection moulding, and the Birch tube is bought commercially. Injection moulding and prepreg layup are considered very resource-intensive for this early on and their score reflects it. Furthermore, CES Edupack [8] was used to obtain information on each material and the upper bound was assumed if a range was given for a certain material value. The trade-off results can be seen in Table 7.12.

The weights were derived using the AHP method similarly done throughout this report and can be seen in Table 7.11. Toughness received one of the highest weights given that the container's main function is to protect the drone and sustainability was also given one of the highest weights due to the chosen design philosophy outlined in the beginning of section 7.1.

Table 7.11: Outer Shell Material AHP

	Toughness	Sustainability	Cost	Specific Yield Strength	Manufactur-ability	Average
Toughness	1.00	4.00	3.00	1.00	4.00	**0.35**
Sustainability	0.25	1.00	4.00	3.00	3.00	**0.25**
Cost	0.33	0.25	1.00	4.00	1.00	**0.16**
Specific Yield Strength	1.00	0.33	0.25	1.00	4.00	**0.17**
Manufacturability	0.25	0.33	1.00	0.25	1.00	**0.07**

Table 7.12: Outer Shell Material Trade-off

	Toughness	Sustainability	Cost	Specific Yield Strength	Manufactur-ability	Total
Flax/Epoxy Composite	2	1	1	0	1	**1.18**
PLA	2	1	3	1	1	**1.66**
Birch	0	3	1	3	3	**1.63**

Container Detailed Design

At this stage, not much further design work will be done on the container for the drone, but a couple of aspects can be further worked out. It was deemed unnecessary to do a full trade-off for the materials used for the inner liner and cushioning due to lack of resources in this final phase.

For the inner liner, a material which is somewhat elastic and sustainable is desired. For this purpose, Thermoplastic Polyurethane (TPU) was selected. It has the flexibility desired such that it can slide inside the outer shell easily and has excellent water performance [8] so that it can help keep a water tight seal in case of a crack. Regarding sustainability, it is not a bio-based material, but is recyclable and is 3D printable. 3D printing is relevant here as a replacement part can be made by the user without having to discard the whole case and the emissions during the transportation of a replacement part are avoided.

For the cushioning inside the case, which is decided to be at the top and bottom of the container such that the drone sits in there tightly, coir fibre has been chosen. Coir fibre comes from the husk of a coconut and is frequently used in mattresses[10]. Although it is highly flammable given its high oxygen content [8], this is mitigated as the battery is surrounded by a protective fire-proof sheet inside the drone as described in chapter 9

Regarding the charging system, a battery has been selected in chapter 11. A battery charger is required to regulate the charge of the three cell battery inside the drone properly. Such a system would need to be adapted to accept the field battery that has been chosen by the Electronics Department. For now, an option

---

[7]Pharos Project`https://pharosproject.net/`, [accessed 15.6.2021]

[8]LignoTube `https://lignotube.de/`, [accessed 9.6.2021]

[9]Ecolizer Tool`https://www.ecolizer.be/`, [accessed 15.6.2021]

[10]Coir Mattress`https://www.slumbersearch.com/polyurethane-foam-vs-coir-comparison`, [accessed 14.6.2021]

that would require input from the user can be chosen[11], but it is recommended that an option that can do so autonomously be designed in the future. The interface between that and the charging port which the drone sits on must also be worked out, including how the drone would separate from this when launched. Beyond that, a port should be included which allows the user to plug in existing charging options which they may possess in the field. Nowadays, hikes often carry a small solar panel which can be used to charge their phones and other electronic devices. Future iterations of the drone's charging system should keep this mind and include a system which is adaptable to these systems.

Container Conclusion

In this section, the drone's container was designed in line with a sustainable design philosophy. This resulted in an outer shell and base made out of injection-moulded PLA and an inner liner made out of 3D printed TPU. After choosing a cushioning material and battery charging system, the total mass of the case including the drone came out to be 1.86kg. Even though the total cost is relatively low, being €40.85, the cost of production must be further evaluated, especially for the cushioning material and 3D printed inner liner. It is recommended to do a more in-depth analysis for different drop heights and ways the container could land to determine the loads that it must be able to endure. This would lead to a more efficient structure and most likely weight savings to further reduce the total weight of the container. A battery charging system could also be designed which does not require input from the user. It would also be worthwhile to do testing on a prototype to verify that a seal rating of IP57 could be reached referring to requirements **SUBSYST-STOR-02** and **SUBSYST-STOR-03**. A sectioned view of the drone inside of the container can be seen in figure 7.11.

Figure 7.11: Section View of the Drone Container

7.2. User Interface

The user interface encompasses the interaction between the users and the system itself. This section shows all the functions analysed and the options available. It includes:

- How the user interacts with the drone
- What the user needs to input to the drone

- How the drone is going to interact with the user
- The locations of the interfaces

Firstly for the design user interface, it is focused on the take-off procedure, therefore analysing from the moment when the primary user identifies that they are in an emergency situation, to the end of the mission. From the Baseline report [1], the requirement **STAK-OPER-01** "the user interface shall be intuitive to use to a range of users" is stated, hence emphasis should be put in practicality, convenience and universal. The interfaces should also be prominent and placed at instinctive locations so to require as little thought process as possible when deploying the drone, but not too overbearing so to avoid accidentally triggering the functions causing a false alarm.

In order to design the user interface, it is necessary to first identify all the tasks that are required from the user before deploying the drone. This is as shown in figure 7.12.

---

[11]LiPo Charger Example`https://www.amazon.com/ICQUANZX-Charger-Balance-Discharger-Battery/dp/B08CKCPXNN/ref=sr_1_11?dchild=1&keywords=3s+lion+battery+charger&qid=1624267517&sr=8-11`, [accessed 21.6.2021]
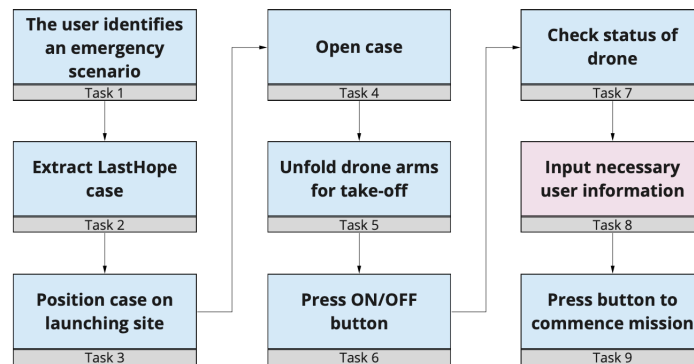
Figure 7.12: User procedure for drone deployment where the blue box means functions that must be performed and pink means optional

Moreover, the drone will have two user interfaces. The primary interface is where with the press of one button, the user switches the drone on, acquires the necessary user information and deploys automatically after running a successful system diagnostics, meaning Tasks 6 to 9 are combined into one. The primary user interface is situated on the drone protected by a security cover in order to minimise the chances of a false alarm. This serves as an override button in the case that the secondary user interface fails or when the user is in an extreme critical condition where they need immediate action. The secondary user interface contains more separate distinct functions where the user is able to interact and view the feedback provided by the drone.

Additional User Information

In figure 7.12, Task 4 and 5 are to be further elaborated in section 7.1 and section 9.2 respectively, as it depends heavily on the type of mechanisms used to open the case and to unfold the drone's arms. Task 8 depends on the source of information that shall be used to transmit the primary user's data. Data types can be in the form of:

- Video
- Photo
- Voice recording
- Text messages

It is not feasible to use all the different media hence an analysis to which one is the most optimum is performed. It should be noted that these are all extra data that could be sent to the emergency services in addition to the predefined calling for help message and user's location. This user information received will be stored and sent to the emergency services once cellular connection is established, as explained in section 12.4. It should be noted that large files such as videos, photos and voice recordings are not feasible to be sent by satellite as it will take a lot of time, in the scale of hours, and can be very costly, hence it will be performed by the secondary communications method.

The additional user information is used to assist the emergency services with what kind of situation the user find themselves in. Regardless of what the content of the additional information will be, the situation is still life threatening, hence it will not impact the services to an extent that forces them to change their course of actions. However, there is only one situation identified that the user might deploy the drone and not need full medical assistance. This is when the user is lost meaning that there should be an explicit way to indicate this to the services in the interface. Instead of sending a fully equipped medical search and rescue team on a helicopter, an experienced local hiker would be sent instead for instance. It should be noted in the user manual which functions to trigger depending on which situations.

Before deciding on which of the options aforementioned is the most effective given the situations, an analysis must be done regarding what information the emergency services need on top of what is sent by the drone automatically already. At this point in time it is determined that one would only use the drone under emergency life threatening situations, hence the services will come fully equipped and prepared for any conditions. The other identified scenario where the user might deploy the drone is when the person is lost. Further analysis of each individual emergency cases can be implemented for future development/improvements of the drone.

Emergency services generally divide the situations into four different categories[12], as can be seen in Table 7.13. However, due to the nature of this mission, the drone only deals with categories 1 and 2, which cover their respective conditions.

---

[12]Emergency categories, `https://www.yas.nhs.uk/our-services/emergency-ambulance-service-999/what-happens-when-you-call-999/`, [accessed 4.6.2021]

Table 7.13: Categories for severity of the emergency condition

Category	Conditions
1	Cardiac arrest, serious allergic reaction, life threatening injuries
2	Stroke, burns, epilepsy
3	Late stages of labour, non-severe burns, diabetes
4	Diarrhoea and vomiting, urine infections
NA	Lost

With severity of the incidents and the different conditions that a user would be in to deploy the drone identified, it is possible to determine which source of information is the most optimal for the mission. Since categories 1 and 2 fully cover all the different conditions that a user can potentially find themselves in, there is no need for extra information to be sent in that regard for this version of the drone. However, photos and videos can assist rescue teams to great lengths for when the user is lost. This could be done automatically as the drone flies off taking snapshots of the environment periodically for a determined number of times, or recording as it takes off and reaches a certain altitude. Voice recording is highly dependent on the external conditions as loud wind or rain would mask the voice of the user. Text messages would mean an implementation of a keyboard or touch screen which increases the overall mass and typing during rainy or minus zero degrees conditions adds another layer of risk. Therefore, the best medium for transmitting user's additional information is through photos and videos. Photos will be prioritised since it has a smaller size and takes shorter time compared to videos. Further analysis of this is shown in section 12.3.

Additionally, from the market analysis performed in the Baseline report [1], one of the most difficult parts of a search and rescue mission is locating the user, hence using a video recording or snapshots of the surroundings as the drone flies off would significantly assist the services. Last, but not least, it should be noted that all the parties involved with transmitting, handling and receiving the additional information of the primary user should acknowledge to a consensual agreement. Unwanted problems may arise from sharing and viewing unauthorised imagery hence it is to be included in a terms and conditions policy of the drone.

How does the user interact with the drone?

The primary user can interact with the drone through different methods. These are:

- Touch screen
- Buttons

- Voice command
- Phone application

The buttons are deemed the best method to interact with the drone. It should be noted that with the technology available today, voice commands are possible without having established internet connection beforehand[13]. However, it is not as reliable as physical buttons or touch screen as the user might be in conditions where voicing speech commands is not possible. This adds another layer of unwanted risk. Touch screens on the other hand allow for a larger variety of functions, however, due to the capacitive technology[14] it does not function as intended when under high levels of moisture or wet conditions. Moreover, touch screens are made out of heavy materials such as glass and plastic covered with conducting metal compounds like indium tin oxide and copper increasing the mass of the whole system. Phone application is also an alternative which enables a larger range of interface options. However, it relies on a charged phone operable at any conditions, which essentially means the user must also be dependent on their mobile devices. Hence, the best way for the primary user to interact with the system is through the use of buttons.

What are the user inputs?

For the user to interact with the system, a set of buttons with dedicated functions is present. Each function will have a separate button enabling the user to see all the options laid out explicitly. This is not the case for the primary user interface, where with the press of one button, the drone goes from switching on to deploying automatically. It should be noted that large number of buttons will overwhelm the user, hence the buttons are restricted to:

---

[13]Voice commands `https://www.techtimes.com/articles/89419/20150929/`, [accessed 1.6.2021]

[14]Touch screen `https://www.hp.com/us-en/shop/tech-takes/how-do-touch-screens-work`, [accessed 2.6.2021]

- **SOS override button**
  This primary interface button is situated on the drone ready to override all the interfaces. This button has two functions integrated, namely, switching the drone on and deploying the drone once all systems are nominal. The user shall not worry about all the other features of the system when using this interface as it will serve one purpose, establish connection with the emergency services. As mentioned before, it will have a plastic cover protecting the button from being accidentally pressed, hence the user will have to lift the cover and engage the button.

- **Start and shut off button**
  The ON/OFF button is the first apparent input from the user that the drone receives through the secondary user interface. It initialises the system and performs internal diagnostics for commence of mission.

- **SOS Take-off button**
  After the drone has ran the diagnostics and detected no faulty measures, the system is optimal and ready to commence mission. Once the user presses this button, the drone will wait for 10 seconds while the warning system is active for clearance and then proceed with take-off.

- **I am lost Take-off button**
  One of the identified scenarios where the primary user does not need fully equipped emergency services is when the user is lost. This is situated in the secondary user interface as the user would have more time and able to select this option. The main difference between this and a standard Save Our Souls (SOS) mission would be the message sent to the services. This button will also have a protective layer decreasing the chances of accidentally triggering this button instead of the SOS button. It is safer to accidentally trigger the SOS button when lost than accidentally triggering the I am lost button when in critical emergency condition.

- **Abort mission ***
  This is an optional function because it is unlikely that the user will have to abort a mission since one will have to be in a really critical condition to have launched the drone in the first place. However, it is subject to further discussion as it might be a way to retrieve the drone if the user manages to find help through an alternative way.

How is the drone going to interact with the user?

The users must be able to identify the status of the drone in order to react accordingly and adapt to the given situation. Many different ways in which the drone can interact to the users are analysed, however, the use of red, blue and green (RGB) lights is deemed the best method as it is light, effective and feasible. For battery status a separate battery icon was considered, however, it adds extra weight to the drone of which the user will only use once before commencing a mission. Realistically, once the user opens the case and turns the drone on, all they will need to know is whether the drone can perform its mission without running out of capacity, because in the case that the drone is critically low in battery, the user is not able to replace it. Therefore, the drone will self-evaluate the amount of charge it has, decide whether it is enough to perform a full mission, climb 2km and hover for 20 minutes, only able to perform a percentage of the full mission, or is critically low in charge and not be able to take-off. In any case, the drone's priority is to establish connection, hence it will still run the communication modules regardless of having sufficient energy to take-off or not.

Before determining how the drone will interact with the user, it is important to identify all the status that the drone would go through that needs informing to the user. With these identified, a way to express each can then be determined as well. This can be seen in Table 7.14.

Table 7.14: Drone to user interface

System	Condition	RGB indicator		
Diagnostics	Turning on and self diagnostic testing	Alternating	Alternating	Alternating
	Systems compliant/ready to commence mission		Flashing	
	IMU error	Flashing		
	Critical error	Continuous		
	Too many obstacles for safe flight		Alternating	Alternating
	Critical low battery	Alternating	Alternating	
	Compass calibration required	Alternating		Alternating
	Commence mission		Continuous	

Location of interface

It is important to have the interface at a location where the user can easily find and interact conveniently. While the primary user interface is going to be situated on the drone, the location for the secondary user interface is going to be on the drone's case. The options available to for the location of the secondary user interface are:

- On the drone itself
- On the case

- On a separate remote control
- On the user's phone

Having the interface on the case will allow for the drone to not carry all the user interfaces when performing the mission, hence less mass. The user will have to rely on the case in order to communicate with the drone. This means that a transceiver module is needed. With the presence of Wi-Fi and Bluetooth micro-controller present on the flight computer chosen in section 10.6, it no longer requires an additional external transceiver. This could be a method in saving some mass on the drone. However, it adds another level of risk if connection between the drone and the case is not successful. In that case the override button is to be used to mitigate this risk.

Having the interface on a separate remote control would decrease the mass on the drone, however increases the risk due to failure in connection between the drone and the remote control making it a reliability. After analysing all the possible options, the best location for the secondary user interface is deemed to be on the drone's case.

Criteria

From the trade-off performed in Table 7.16, the approach and the results are shown. The four different locations are compared to each other respective to:

- **Ease of access**: this is how easily the user can identify where the interface is located. On the drone is the most intuitive location whereas one might struggle finding where the remote controller is stored. Having the interface on the drone itself is the most natural place, whereas on a remote control can cause difficulties in locating it.
- **Added mass on the drone**: extra components and elements added on the drone for operability of the secondary user interface, such as the presence of cables, transceivers, circuitry and inputs. Adding all the UI system on the drone would be the least ideal, whereas this can be avoided by locating it somewhere else instead, hence on the drone scores the least amount of points.
- **Reliability**: the more steps the signals has to take before reaching the services the higher the chance of failure. Hence having the UI on the drone is deemed as the most reliable whereas having a separate remote controller is the deemed as the least.
- **User friendliness**: this describes the condition in which the user can perform its procedures, safely, effectively and efficiently. Having the UI on the drone is deemed to be the best as it is the least stressful interaction the user would have out of all the options.
- **Cost**: last but not least, it is important to keep in mind how feasible each of the options are and keeping the cost cap within the budget. Similarly to added mass on the drone, the additional elements for each of the options must be taken into account, hence the more components needed, the higher the cost and the less the score.

Criteria Weights

The weights of the criteria are as shown in Table 7.15. The added mass on the drone is the most important criteria followed by reliability. The options for location of the user interface are then scored relative to each other within the criteria described.

Table 7.15: Relative importance table and the final weights with a CR of less than 0.1

	Ease of access	Added mass on drone	Reliability	User friendliness	Cost	Final weights
Ease of access	1.0	0.2	0.3	1.0	0.5	0.08
Added mass on drone	5.0	1.0	1.3	5.0	2.5	0.38
Reliability	4.0	0.8	1.0	4.0	2.0	0.31
User friendliness	1.0	0.2	0.3	1.0	0.5	0.08
Cost	2.0	0.4	0.5	2.0	1.0	0.15

Trade-off

The preferred location for the secondary user interface is on the drone's case. Coming joint second are on the drone and on a mobile phone app. Having the secondary user interface on the remote control is deemed to be the least favourable. With the scoring system of 1 being the worst and 3 being the best, the trade-off is performed as shown in Table 7.16. This will be located on the top surface of the platform where the drone will sit when stored inside the case as it is the most apparent location for the user to access the user interface. The four buttons identified, namely SOS override, start and shut off, SOS take-off and I am Lost, are placed surrounding the drone and embedded into the under layer of the platform in order to not hinder the movements of the arm when unfolding.

Table 7.16: Trade-off results showing that having the user interface on the case would be the most ideal

User Interface locations:	Ease of access	Added mass on drone	Reliability	User friendli-ness	Cost	Final Score:
Drone	3	1	3	3	1	1.8
Case	2	3	2	2	2	2.1
Remote control	1	3	1	2	1	1.7
Mobile phone app	2	3	1	2	3	1.8

Discussion & Recommendations

The criteria determined earlier to evaluate the different options available for the secondary user interface location, are assessed qualitatively instead of quantitatively. For example, for ease of access, having the interface on the drone scores the highest due to resemblance to other new electronic items used today such as robot vacuum cleaners. It is out of intuition that one would expect the interface used to communicate with the device is on the device itself.

Moreover, for the criteria "added mass on the drone", it has been assumed that anything that is not on the drone would be beneficial to the total weight, however, at the cost of connectivity delay or failure. The individual components and elements that would be used for the four different options were not identified and analysed, due to the limited time and resources available, to see how they would contribute to the take-off mass. However, using the assumption that four buttons with all its necessary components and elements weighs more than one transceiver, it has been determined that having a remote user interface is the better option. A more in depth detailed analysis for each of the concept could be carried out for a more accurate assessment. Last but not least, the use of WiFi and Bluetooth are assumed to be the same, hence it is the number of devices or steps required for connectivity that indicates the higher chance of failure.

In the previous sections, the user interface with the primary user is described. However, it is also important for other users to know what to do in the case that they find the drone. This would be after the drone has performed its mission, whether the drone manages to establish connection or not, it will eventually descend and land somewhere as safely as possible to be retrieved. Once located the drone with the help of a warning system, further explained in section 7.3, the same primary user interface button, namely SOS override button, is used to shut off all systems including the warning system. The drone will then flash its RGB light sequentially three times and turn itself off. On top of that, there will also be a sticker on the drone indicating the founder what number to contact if the drone is found . This contact directs the founder straight to the rescue coordination centre in the case that the drone hasn't yet established connection with the services yet. The sticker will also contain the user's identification code. An example of how this would look like on the drone is shown in figure 7.13 and figure 7.14.

Post-DSE

In order to integrate this product into the market, an emergency service infrastructure relating to the use of the drone should include the handling of the drone by the rescue operations. The training modules should include the steps, procedures and tools needed regarding how to extract the SD card from the drone when retrieving it. They should also carry a mobile device that can read the SD card to access the user and flight information stored in it protected by the black box.

A mission status update indicator was considered, however, for this to be possible the drone shall be equipped with a telemetry transmitter able to send live data to the user interface constantly. This would provide the user with live feedback on the mission status, namely; mission success, mission abort and mission failure.

The transmitter in question operates with 100mA at 7.2V. It has a mass of 20g, a 62mm x 30mm x 15mm size and able to establish connection with the interface at ranges up to 10km[15]. This allows for more advanced interface to be possible between the user and the drone. This is a smart feature, but not a requirement, hence is subject to further elaboration and development for the next version of the drone at the post-DSE phase.

7.3. Visibility approach and Warning System

This section elaborates on the design process of the visibility approach and warning system. This system is designed to warn its surroundings on approach, and to increase visibility during and after flight. Firstly, the results are presented. These results are followed by the design strategy, which consists of a design option tree, a trade-off and lastly a discussion.

Results

The Visibility approach and Warning system consists of both active and passive techniques. The active techniques consist of 4 white LED's to increase visibility during night time. These LEDs are positioned on the start of a motor arm. They will be turned on if light levels dip below a certain level, measured by the Light Dependant Resister (LDR), as described in chapter 10. A buzzer is also included, which is turned on once the drone has landed and shut down its motors to help locate the drone. For passive measures, a yellow paint with a fluorescent compound is used and reflectors are placed on the arms. Yellow paint increases visibility during dusk conditions and reflective strips increases the visibility by reflecting light.

Design process

Following from the grouping of requirements, which are repeated down below, it becomes clear that some system on the exterior of the drone has to be developed.

- **STAK-GENR-08** The drone shall implement measures to maximise the visibility of its location for rescue operation
- **SYST-GENR-08-A** The drone shall be visible from a distance of 200 metres under normal weather conditions
- **STAK-LEGL-04** The drone shall not cause harm or endanger people while conducting the mission

This system, based on the requirements, has two main functions to perform. It has to maximise visibility, to aid in the rescue operation. Additionally, it should have the ability to warn its surroundings on approach. For this system, passive and active measures can be designed.

From the design options tree, some options have already been discarded. This will be explained and justified down below.

Passive; Whistle

It will be elaborated on whether a whistle can be used on the drone to warn the surrounding environment that it is going to land. This was deemed unfeasible as high speeds would need to be achieved in order to produce a loud enough whistle to be heard over the drone itself. For example, tests have shown that at a velocity of 12 m/s, a sound of 58dB can be produced, which is comparable to normal conversation[16]. These results came from a whistle with a diameter of 58mm, which would be quite large for the drone at hand. Due to this and the aforementioned reasons, the whistle concept can be discarded.

Active; light

For lights, which are the most helpful for locating the drone or warning the environment when it is dark, the options other than LED's were discarded as LED's are the best light source in terms of efficiency[14]. Due to the limited on board storage of energy, efficiency was deemed very important.

---

[15]Long range transmitter https://hobbyking.com/en_us/frsky-r9m-eu-version-lite-long-range-telemetry-transmitter-module.html?queryID=1d4dd6948b6816bd8a51ec65bc4796e9&objectID=79183&indexName=hbk_live_products_analytics, [accessed 8.6.2021]

[16]Geluidssterkte en decibel,https://www.schoonenberg.nl/blog/gehoorbescherming/geluidssterkte-en-decibel/, [accessed 22.6.2021]

Active; Buzzer

Buzzers would be a helpful addition to help with auditory warning from the drone. These will not be considered for warning during flight as the drone already makes 70-81 dB during flight which can also serve as a warning[17]. After the drone successfully performed its mission and has landed, retrieval of the drone might be an option depending on the state of the user. Even if the landing location is known via GPS, it can still be difficult to localise the drone. In this case, an audible ping for localisation can be use full. Due to the low power use, and low weight of the buzzer, it was decided to be included into the design[18].

Paint trade-off

From the design option tree, 3 different types of paint were identified being fluorescent, phosphorescent and radio luminescent paint. Criteria used, presented in order of importance, were safety, sustainability, light emitting properties and cost. Due to the often-toxic nature of the compounds in these paints, safety and sustainability were deemed very important. The light emitting properties were the next deemed important criteria as that could greatly help with locating the drone in the night and it helps separate phosphorescent and radio luminescent paint from fluorescent paint. It is expected that the prices of these compounds do not differ much between options, but for completeness cost was included. The AHP matrix for the weights is shown in Table 7.17 and the trade-off itself is in Table 7.18.

Table 7.17: Weights accredited to each criteria for paint trade-off

	Safety	Sustainabiliy	Light emmitance	Cost	Weights
Safety	1.0	1.0	2.0	4.0	**0.36**
Sustainability	1.0	1.0	2.0	4.0	**0.36**
Light emmitance	0.5	0.5	1.0	3.0	**0.20**
Cost	0.3	0.3	0.3	1.0	**0.08**

Table 7.18: Paint trade-off

Criteria	Safety	Sustainability	Light emmiten	Cost	Total
Fluorescent	2	3	0	3	2.04
Phosphoresence	1	1	2	3	1.36
Radio luminecent	0	0	3	1	0.68

The scores given in Table 7.18, were determined in a qualitative manner. The scores given to safety and sustainability were determined using the Project Pharos. Pharos collects and organises toxicity information on compounds. To demonstrate an example, when analysing fluorescent paint, it was assumed the paint to contain fluorescing as the main fluorescent compound. According to Pharos, fluorescien has two potential safety concerns being toxic ingestion and sensitive upon contact with skin. Using their confidence levels and hazard levels, fluorescent paint was given a two and a three for safety and sustainability.

For the light emitting criteria the scores were determined in the following way. Fluorescent options do not or barely emit light after being exposed to a light source, and were given a score of 0. Phosphorescent options do emit light after exposure to UV light. It can emit a faint glow for up to 8 hours after exposure, and was therefore given a score of 2. Radio luminescence on the other hand, emits light without being exposed. This is the main reason for the inclusion of radio luminescent substances in the trade-off, and a score of 3 was assigned.

The scores accredited to cost were determined in a qualitative way, as the pigment is not expected to drive costs up substantially. The price of fluorescent and phosphorescent pigments are relatively similar, at 104 and 117 euros per kilogram respectively[19,20]. A single tritium tubes of 3 mm by 22.5 mm cost roughly 25 euros[21]. Even though the difference between pigment and tritium tubes is hard to quantify, three points are given to the

---

[17]Drone Noise Levels and How to Keep Them Quiet,`https://3dinsider.com/drone-noise-levels/`, [accessed 22.6.2021]

[18]Buzzer,`https://www.allekabels.nl/buzzer-en-sirene/7374/1064517/buzzer.html`, [accessed 22.6.2021]

[19]Fluorescent Pigment Golden Orange,`https://www.kremer-pigmente.com/en/shop/pigments/56200-fluorescent-pigment-golden-orange.html`, [accessed 22.6.2021

[20]Phosphorescent Pigment Green,`https://www.kremer-pigmente.com/en/shop/pigments/56500-phosphorescent-pigment-green.html`, [accessed 22.6.2021]

[21]Tritium Flesjes 3X22.5 mm,`https://nl.grandado.com/products/tritium-flesjes-3x22-5-mm-trit-flesjes-tritium-buis-zelflichtgevend`, [accessed 22.6.2021]

fluorescent and phosphorescent options with one point being given to the radio luminescent option due to the small amount of pigment necessary for large quantities of resin[22].

Resulting from the trade-off, it can be decided that fluorescent pigment will be used. A pattern of fluorescent and phosphorescent resin was also considered, however, the faint glow of phosphorescent after exposure does not out weight the safety and sustainability concerns regarding zinc sulphide that come with the phosphorescent paint and is thus discarded

Colour

The most visible colour during daylight is green, followed by yellow[23]. In low light situations the most visible colour shifts towards yellow. Since forests are widespread in Europe, and dusk/night rescue operations also have to be considered, a bright, fluorescent, yellow colour is chosen as the colour of the drone as shown in figure 7.13. To aid in reflectively when light is shined upon, the drone will also be equipped with reflectors, to increase visibility. These will be placed on top of the arms/motor.

Warning System Conclusion & Recommendations

The final design consists of the following components and techniques. The drone is equipped with 4 white LED's to increase visibility during night time. To aid in the recovery of the drone, a buzzer has been selected to buzz once every minute after landing. The drone will be painted yellow with a bright fluorescent paint, and on the arms reflector strips are presented.

For future development a study on Automatic Dependent Surveillance–Broadcast (ADS-B) is recommended. This allows for the possible detection of nearby aircraft, which in turn can be used to avoid collisions. In the current budgets, an ADS-B module was too expensive to be implemented.

Figure 7.13: Drone with fluorescent yellow livery and reflective stickers on the arms

EMERGENCY RESCUE DRONE
IF FOUND CONTACT

XXX.XXX.XXX.XXX.XXX

DIRECTLY

USER IDENTIFICATION NUMBER

XX.XXXXXXX.XX
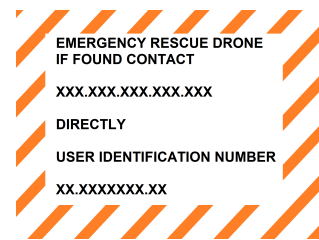
Figure 7.14: Reflective sticker on arms

7.4. Requirement Compliance

With the operations' subsystem established, it is to be checked with the requirements previously established. With the use of a compliance matrix as shown in Table 7.19 it can be seen which requirements are met and which are either omitted, failed to meet or need further evaluation in order to check for compliance. These will be further elaborated after the table in the feasibility analysis.

Table 7.19: Compliance Matrix for Operations

ID	Requirement	Met?	Comment	Validated by:
STAK-DFPP-02	The flight parameters of the drone shall be valid after 1-month storage after full charging.	✓		RoD
STAK-ELEC-01	The drone shall be able to be charged in field environment	✓		RoD
SUBSYST-STOR-03	The storage system shall have an IP rating of IP57		Verified at later stage	Test
SUBSYST-OPER-02	The system shall be operable by the user with their non dominant hand	✓		RoD
STAK-OPER-01	The user interface shall be intuitive to use to a range of users	✓		RoD
SYST-GENR-08-A	The drone shall be visible from 200 m under normal weather conditions	✓		Test
STAK-LEGL-04	The drone shall not cause harm or endanger people while conducting the mission	✓		RoD

SUBSYST-STOR-03 is all highly dependent on the final design of the drone's container. In a later stage when the structure and design is fully worked out, it could be determined if it has an IP rating of 57. Later on,

---

[22] The Perfect Pigment To Resin Ratio, https://www.artnglow.com/blogs/news/the-perfect-ratio, [accessed 27.6.2021]

[23] MEDICAL INSIGHTS: The most visible colors, https://www.postandcourier.com/aikenstandard/lifestyle/medical-insights-the-most-visible-colors/article_e031d15b-973a-5289-8f88-e014afab0a81.html, [accessed 22.6.2021]

SUBSYST-STOR-03 would be best demonstrated via a test with a prototype.

8. Drivetrain

The LastHope drone is a special drone as it spends most of its mission time hovering to communicate with the emergency services. Besides that a fast climb is beneficial as the time to climb reduces with climb velocity. Establishing communication with the emergency services more rapidly can make the difference between life and death of the user. Optimising propellers for these situation is not common. If a propeller geometry is optimised for the LastHope mission the propulsive efficiency is increased and battery mass can be saved. A lot of drone propellers available on the market are developed for recreational purposes. This is the main reason it was decided to develop a new drivetrain optimisation tool. Another reason to design the propeller from scratch is because propellers available on the market have a diameter that is part of a limited set of diameters for drone propellers. Developing the propeller from scratch results in more design freedom which can result in better performing propellers. The drivetrain consists of a propeller and a motor. Both the propeller and the motor have different efficiencies for different rotations per minute (rpm). Therefore it is important to carefully select a suitable motor to the designed propeller. This chapter first lists the most important system and subsystem requirements for the design of the drivetrain subsystem in section 8.1. Next, the drivetrain analysis tool that was developed is described in section 8.2. This analysis tool is used to optimise the drivetrain design using the HEEDS software. The optimisation process is described in section 8.3. The verification and validation of the drivetrain optimisation tool is described in section 8.4. After defining the geometry of the propeller a suitable material is selected. The material selection is explained in section 8.5. The material selection completes the drivetrain design. The current drivetrain design is showed in section 8.6. The influence of the assumptions is discussed in section 8.7. The implementation of sustainable development in the drivetrain design is summarised in section 8.8. The compliance of the drivetrain to its subsystem requirements is presented in section 8.9. Finally, the current drivetrain design is discussed and recommendations for the post-DSE phase are done in section 8.10.

8.1. Requirement Analysis

In order to assure that the system is fit-for-purpose first the requirements that apply to the drivetrain are analysed. From these the driving requirements are identified for this subsystem.

- **SYST-GENR-03**: The maximum dimensions of the drone in storage mode shall not exceed 200 x 100 x 100 mm(length, width, height)
- **SUBSYST-DFPP-03**: The propulsion subsystem shall allow for the generation of a lifting force of more than 10 N at the specified service ceiling of 4500 m
- **SUBSYST-DFPP-06**: The propulsion subsystem shall be able to maintain its position at the specified service ceiling for 20 minutes minimum
- **SUBSYST-DFPP-12**: The propulsion subsystem shall have a weight limit 110 grams
- **SUBSYST-DFPP-14**: The propulsion subsystem shall have a cost limit of 80 euros
- **SUBSYST-DFPP-15**: The propulsion subsystem shall have a temperature envelop of -33 to 40 °C
- **SYST-RISK-04**: The propellers shall be foldable
- **STAK-GENR-09:** The drone shall be able to operate in rain
- **SYST-SUST-02-B:** The drone shall not be manufactured out of toxic materials
- **SUBSYST-DFPP-07**: The propulsion subsystem shall allow for a maximum climb of 2000 m up until the specified service ceiling is reached

One important requirement to be numerically defined is **SUBSYST-DFPP-15**, which pertains to the temperature envelope the system should operate in. Using the starting numbers defined by **SYST-THER-01** and standard International Standard Atmosphere (ISA) properties it can be found that the temperature envelope the propulsion system should be able to operate in is -33 to 40 °C.

8.2. Drivetrain Analysis Tool

To come up with the current design for the drivetrain. First a short overview of the governing equations that were used to analyse the propeller performance are presented. Next, the assumptions made to develop the analysis tool are listed and briefly elaborated on. The drivetrain analysis tool consists of two separate analysis tools that were combined to form the drivetrain analysis tool. The propeller analysis tool is described first and the motor tool is described directly after. Lastly, the combination of the two analysis tools is described in this section.

Blade Element Theory

This section briefly describes the Blade Element Momentum Theory (BEMT). BEMT is used for analysing propeller and turbine geometries. BEMT combines two theories; the blade element theory and the momentum theory. The first theory divides the blade in small sections and independently calculates aerodynamic forces using available lift and drag data for the airfoil used. The second theory threats the rotor as a flat disk and evaluates the momentum lost by the work done by the rotor. As this chapter describes the design process of the drivetrain, only the equations for propellers are derived instead for both propellers and turbines. Power is applied to a propeller to generate thrust along the rotation axis. Induction factors are of great importance in BEMT. These inductions factors show the difference in flow velocity in axial and tangential direction compared to the actual incoming flow velocity and angular velocity of the rotor. For a propeller the actual axial velocity is increased due to downwash and the tangential velocity is reduced due to swirl[16]. These flow velocity components are sketched in figure 8.1.
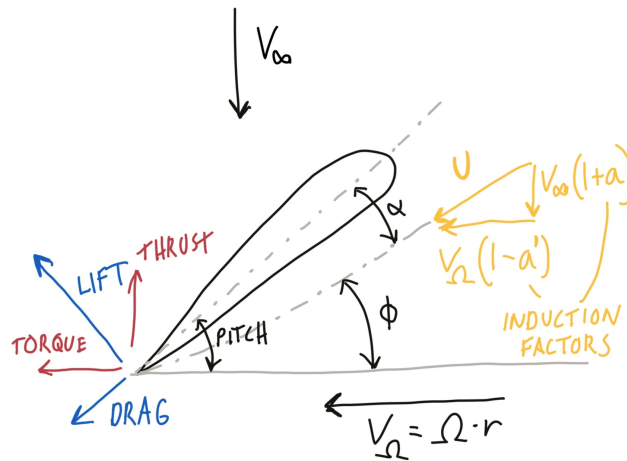
Figure 8.1: Schematic sketch of blade element [16]

From figure 8.1, Equation 8.1, Equation 8.2 and Equation 8.3 can be derived.

$$v = (1 + a)V_\infty \quad (8.1) \qquad v' = (1 - a')\,\Omega R \quad (8.2) \qquad U = \sqrt{v^2 + v'^2} \quad (8.3)$$

For a drone the axial inflow velocity can be seen as the climb velocity of the drone. The tangential inflow velocity is equal to the flow velocity resulting from the rotational motion of the propeller. $V_\Omega = \Omega * R$. The actual incoming flow velocity can be calculated by adding the axial flow velocity vector and the tangential flow velocity vector. From figure 8.1 also the following expression can be derived for the local inflow angle.

$$\tan \phi = \frac{(1 + a)\Omega R}{(1 - a')\,V_\infty} \tag{8.4}$$

From figure 8.1 it also becomes clear that the angle of attack of the section is equal to the pitch of the section minus the inflow angle.

$$\alpha = pitch - \phi \tag{8.5}$$

Combining the calculated angle of attack and airfoil data the drag and lift coefficients can be calculated. From the lift and drag coefficients, the thrust and torque coefficients can be calculated using Equation 8.6 and Equation 8.7.

$$C_T = C_l \cos \phi - C_d \sin \phi \qquad (8.6) \qquad \qquad C_Q = C_l \sin \phi + C_d \cos \phi \qquad (8.7)$$

The thrust and torque for every section can be calculated using Equation 8.8 and Equation 8.9.

$$\Delta T = \sigma \pi \rho U^2 C_T r \Delta r \qquad (8.8) \qquad \qquad \Delta Q = \sigma \pi \rho U^2 C_Q r^2 \Delta r \qquad (8.9)$$

Here the propeller solidity can be calculated by Equation 8.10.

$$\sigma = \frac{Bc}{2\pi R} \qquad (8.10)$$

From momentum theory Equation 8.11 and Equation 8.12 can be derived.

$$\Delta T = 4\pi \rho r V_\infty^2 (1+a)a\Delta r \qquad (8.11) \qquad \qquad \Delta Q = 4\pi \rho r^3 V_\infty \Omega (1+a)a'\Delta r \qquad (8.12)$$

Combing Equation 8.8, Equation 8.11, Equation 8.9 and Equation 8.12 results in the following expressions for the induction factors.

$$a = \frac{1}{\kappa - C} \qquad (8.13) \qquad \qquad a' = \frac{1}{\kappa' + C} \qquad (8.14)$$

$$\kappa = \frac{4\sin^2 \phi}{\sigma C_T} \qquad (8.15) \qquad \qquad \kappa' = \frac{4\sin \phi \cos \phi}{\sigma C_Q} \qquad (8.16)$$

It becomes clear that the previously stated equations form a system of equations without analytic expression for the solution. Therefore a numerical solver is necessary to solve the system of equations. This system of equations is solved using a bisectional solver. The equations presented in this chapter are implemented in a python code in the pyBEMT Github repository [16].

Assumptions

The drivetrain system is very complex, because of the advanced aerodynamics and the complexity of electric motors. Therefore, assumptions have to be made to be able to develop a propeller-motor combination analysis tool. This section states all assumptions made to be able to develop this drivetrain analysis tool. First the propeller tool assumptions are listed and then the motor tool assumptions are listed.

Assumptions propeller tool

- The air density to perform the analysis of the drivetrain in climb and loiter was assumed to be a constant value equal to the International Standard Atmosphere (ISA) air density at 4500 metres.
- The dynamic viscosity to perform the analysis of the drivetrain in climb and loiter was assumed to be a constant value equal to the ISA dynamic viscosity at 4500 metres.
- For the analysis of climb a constant climb velocity was assumed.
- The weight of the drone was assumed to be equal to 500 grams.
- A Cd value of 0.265 was assumed. This is the drag coefficient of the drone at a flow velocity of 20 m/s without the propellers mounted estimated by a preliminary Computational Fluid Dynamics (CFD) analysis of the drone.
- The characteristic surface of the drone was assumed to be 0.0235. This is an output of an initial CFD analysis at a flow velocity of 20 m/s without the propellers mounted.
- It is assumed that the climb is purely vertical.
- It is assumed that there is no wind or gust present.

The following assumptions result from the blade element momentum theory[1].

- Inviscid flow
- Incompressible fluid
- Irrotational flow
- Flow velocity is uniform in each cross section of stream-tube.
- Static pressure is uniform in each cross sec-
- tion of stream-tube.
- Blades are independent of one another.
- Thrust and torque are purely the result of lift and drag acting on airfoil.
- No wake expansion
- No tip losses

The last assumption is compensated for in the BEMT python tool retrieved from Github [16]. The assumption is listed for completeness.

Assumptions motor tool

- It is assumed that the battery voltage remains constant.

---

[1]Theoretical Model for Propellers, `http://edge.rit.edu/content/P14361/public/DDR_Documents/Helicopter%20Propeller/` `Theoretical%20Model%20for%20Propellers.pdf`, [accessed 22-06-2021]

- It is assumed that the voltage of each cell of the battery is 3.7 V.
- Friction in the motor bearing is assumed to be negligible
- Electrical losses in the ESC and wires are assumed to be negligible.

Propeller Tool

This section describes the propeller tool. An external Github repository is used to implement the BEMT into python. These python files were adapted to produce the desired outcomes. A block diagram is made to visualise the computing process of the "run" function of the imported python tool. The block diagram can be found in figure 8.2.
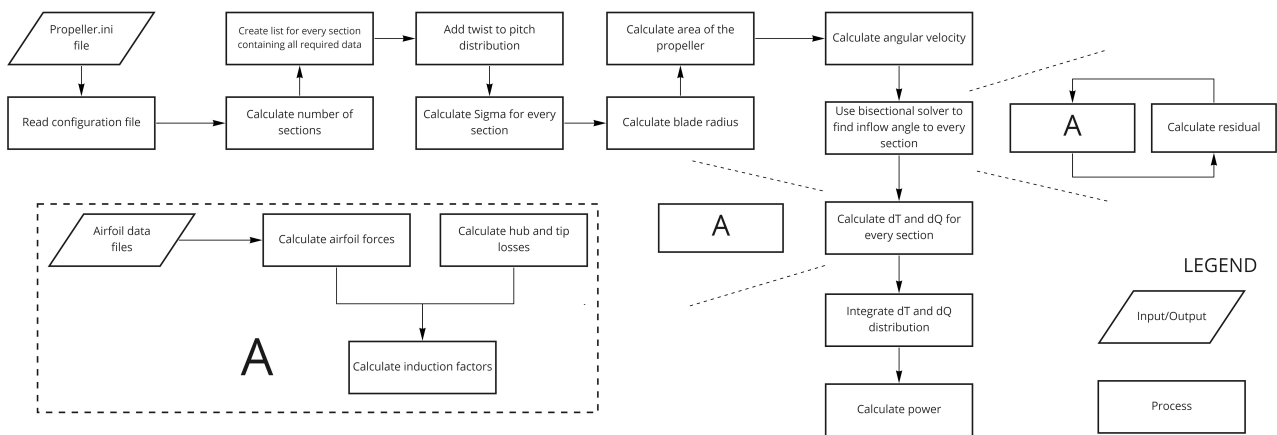
Figure 8.2: Block diagram visualising the propeller analysis tool

Below a step by step approach is described on how the 'run' function of the BEMT tool is working.

1. The first step of the program is to read the propeller.ini file. This file states the propeller geometry and other external parameters necessary to perform the analysis. The following parameters are stated in the propeller.ini file: V_∞, rpm, twist, diameter of the propeller, hub radius, number of blades, list of airfoils for every section, list of radius of middle point of the sections, list of chord length of the sections, list of pitch of the sections, air density and the dynamic viscosity of the air.

2. Based on the list given for the airfoil sections, the program calculates the amount of sections used for the analysis.

3. For every section of the propeller a list is generated that states all relevant specifications necessary to calculate the thrust and torque of that section.

4. The twist of the propeller is added to the pitch angles of the sections.

5. Sigma is calculated for every section using Equation 8.10 and added to the characteristic lists of the sections.

6. The blade radius is calculated using the propeller diameter.

7. The area of the propeller is calculated.

8. The angular velocity Ω is calculated.

9. Using the equation from section 8.2 the local inflow angle for every section is calculated. A bisectional solver is used. So therefore first a inflow angle is assumed. Combined with the airfoil data files the inflow angle is used to calculate the arifoil forces and the the hub and tip losses. To calculate the hub and tip losses the Prandtl tip loss factor is used. After calculating the airfoil forces and the hub and tip losses, the induction factors can be calculated. The assumed local inflow angle, the induction factors, the climb velocity, the angular velocity and the radius are used to calculate a residual. Based on the value of the residual a new local inflow angle is assumed. The whole process repeats itself and eventually this method will converge to a local inflow angle for every section.

10. After the bisectional solver has found a local inflow angle for every section the airfoil forces and hub and tip losses can be calculated again using the airfoil data files. The induction factors can be calculated again. These airfoil forces, losses and induction factors are used to calculate the thrust and torque generated by every section.

11. The thrusts and torques for the sections are added to get one thrust value and one torque.
12. The power is calculated by multiplying the torque with the angular velocity.

The 'run' function forms the basis of the propeller analysis tool. The propeller tool uses this 'run' function to evaluate the climb and hover performance of the propeller. The imported Github reposity also contains a function called 'run_sweep'. This function is performing the 'run' function multiple times and will change the inputted variable over a specified range defined by the user. For hover, the climb velocity is equal to zero. To analyse the hover phase the following procedure is used.

1. Set minimum rpm, maximum rpm and step size for the rpm interval.
2. Use the 'run_sweep' function to calculate the thrust, torque and power for every rpm in the interval. As stated before the climb velocity is equal to zero as the drone is hovering.
3. Calculate the weight of the drone and divide by four to calculate the required thrust for one motor-propeller combination to hover.
4. Remove all rpm values that do not generate enough thrust required from the dataframe.
5. Select the lowest rpm that still meets the required thrust level. The rpm and required power are inputs for the motor tool. This will be explained in more detail in Equation 8.2.

For the analysis of the climb a new function was developed based on the functions present in the BEMT python tool. This function can be described as a 'run_sweep_sweep' function. It gives the possibility to sweep over two different parameters. For climb these two parameters are the climb velocity and the rpm. The procedure to analyse the climb for the propeller is described below.

1. Define minimum rpm, maximum rpm and step size for the rpm interval.
2. Define minimum climb velocity, maximum climb velocity and step size for the climb velocity interval.
3. Use the 'run_sweep_sweep' function to calculate thrust, torque and power for every combination of rpm and climb velocity.
4. Calculate the drag and weight for the drone for every climb velocity using Equation 8.17 and divide by four to find the required thrust.
5. Remove all rpm-climb velocity combinations that do not generate enough thrust from the dataframe.
6. For every climb velocity, select the lowest rpm. The lowest rpm implies the lowest power necessary to generate the required thrust.
7. Use the remaining dataframe as an input for the motor tool. This will be explained in more detail in Equation 8.2.

$$D = C_d 0.5 \rho V_\infty^2 S \tag{8.17}$$

Motor Tool

This section describes the motor tool. A Python script was written which parses through a database of over 2000 motors[2] and using the rpm and power output of the propeller tool calculates the total energy needed to climb to altitude and loiter for 20 minutes. A block diagram is made to visualise the computing process of the propeller analysis tool.

---

[2]Home of the Drive Calculator, `http://www.drivecalc.de/`, [accessed 27.06.2021]
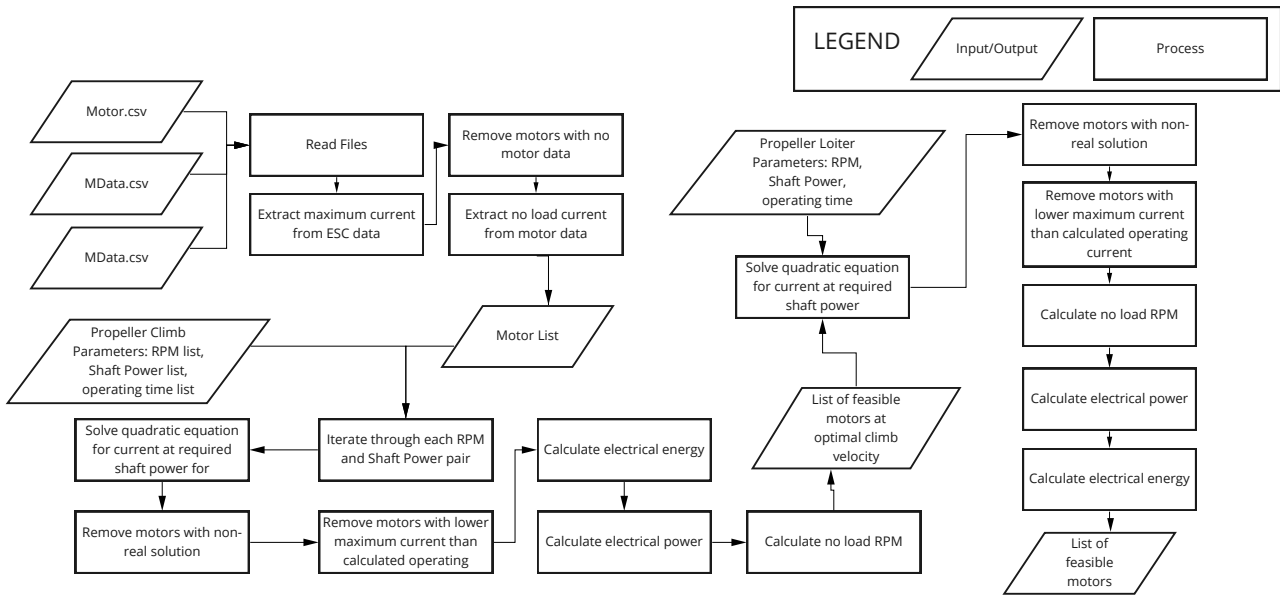
Figure 8.3: Block diagram visualising the motor tool

First the governing equations describing the performance of Brushless direct current (BLDC) motors will be presented[5]. The required motor parameters to perform these calculations are the internal resistance of the copper winding in the motor R_m and the no load current I_{noload} which is the current it takes for the motor to overcome friction with no load. The inputs are the shaft power P_{shaft} and the operating voltage V. Equation 8.18 computes the current required to operate a BLDC motor at a given shaft power.

$$I = \frac{V - \sqrt{V^2 - 4 \cdot R_m \cdot (V \cdot I_{noload} + P_{shaft})}}{2 \cdot R_m} \tag{8.18}$$

This equation solves the quadratic equation shown in Equation 8.19.

$$R_m \cdot I^2 - V \cdot I + (V \cdot I_{noload} + P_{shaft}) = 0 \tag{8.19}$$

The no load rpm calculated for a given input current is calculated using Equation 8.20.

$$\left(V - \frac{R_m \cdot I^2}{I} \right) \cdot KV \tag{8.20}$$

The electrical power and energy are calculated using Table 11.12 and Table 11.12 respectively.

$$P_{elec} = V * I \tag{8.21} \qquad\qquad E_{elec} = P_{elec} \cdot time \tag{8.22}$$

The motor tool contains three main functions, one to read the three files containing all pertinent information on the motors, another function which calculates for every motor the electrical energy consumed based on a series of rpm, shaft power and time inputs. Each rpm, shaft power and time input is associated to a flight velocity hence by calculating the electrical energy for each flight velocity and for each motor the function then outputs the performance for the most efficient flight velocity. The final function calculates for every motor the electrical energy consumed based on an rpm, shaft power and time input. Each function will be explained step by step in the same order as they were introduced.

1. First the Motor.csv, MData.csv and ESC.csv files are read. The first file contains the entire list of motors and general parameters such as maximum current, KV and internal resistance. The second file contains test data of each motor and finally the third file contains data regarding ESCs.
2. Next the motors with no information on winding resistance and weight are removed
3. Motors which have a mass larger than 25 grams are eliminated as they do not fit the budget.
4. If no information of max current is given the max current is extrapolated from the associated ESC.
5. Next the no load current is extrapolated for each motor from the MData.csv file. If the no load current is not present the motor is deleted.

6. the output is an array containing the motor's ID, name, weight, KV, winding resistance, maximum current, maximum test volateg and no load current

Next the function iterating through a list of propeller outputs is explained.

1. First two loops, one iterating through every motor and one iterating through every propeller output are initiated.
2. For every motor and every flight velocity the operating current is calculated using Equation 8.18
3. If the current is non-real the flight velocity and propeller outputs associated are discarded.
4. As a sanity check the rpm at operating current with no load is calculated using Equation 8.20. If the calculated rpm is lower than the operating rpm associated the flight velocity and propeller outputs associated are discarded.
5. The electrical power is calculated using Equation 8.21.
6. The electrical energy is calculated using Equation 8.22.
7. After iterating through all flight velocities the one with minimum electrical energy is selected.
8. The process repeats for every motor.
9. Once the iteration through both loops is finished an array containing all feasible motors their parameters and they calculated performance is outputted.

Finally the function calculating motor performance solely for one value of rpm, shaft power and time is explained.

1. For every motor the operating current is calculated using Equation 8.18
2. If the current is non-real the motor is discarded.
3. As a sanity check the rpm at operating current with no load is calculated using Equation 8.20. If the calculated rpm is lower than the operating rpm associated the motor is discarded.
4. The electrical power is calculated using Equation 8.21.
5. The electrical energy is calculated using Equation 8.22.
6. The process repeats for every motor.
7. Once performance is calculated for all motors an array containing all feasible motors their parameters and they calculated performance is outputted.

Drivetrain Tool

This section describes the integration of the propeller analysis tool and the motor tool. Several additional functions are added which results in one drivetrain analysis tool. A block diagram shows the sequential order of the functions executed to generate the output. This block diagram can be found figure 8.4.
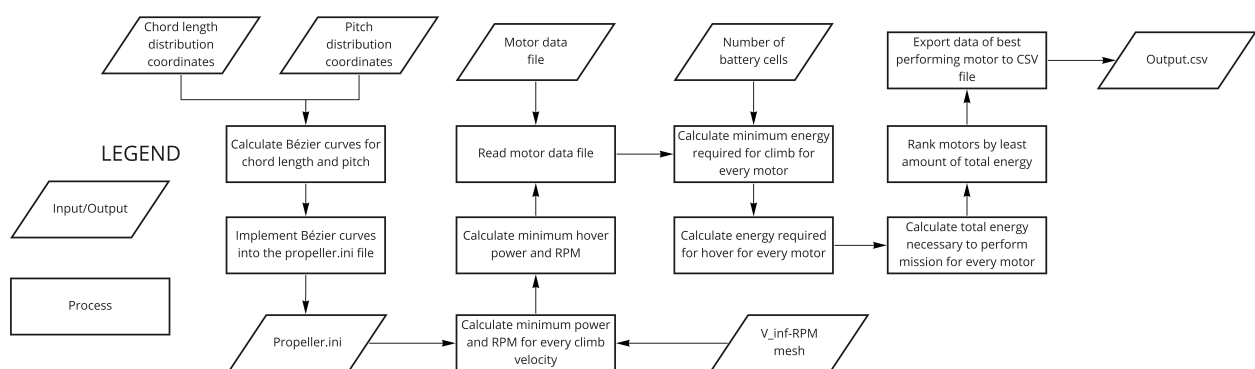
Figure 8.4: Block diagram visualising the drivetrain analysis tool

Below a step by step approach describes the drivetrain analysis tool.

1. First the propeller.ini file is updated. This is done by replacing the pitch and chord distributions by points on a Bézier curve formed by four data points. An example of a Bézier curve can be found in figure 8.5. Eventually these coordinates will be parameters for the HEEDS software to define a propeller design.

The Bézier curve generated for the given datapoints are sampled for the amount of sections present in the propeller. The sampled values represent the chord and pitch distibutions for the propeller. The implementation of the Bézier curves was to generate smooth chord and pitch distributions as it was found that optimising the propeller geometry using HEEDS without the Bézier curves resulted in propellers with large chord and pitch fluctuations.

2. When the propeller.ini file is changed the function explained in Equation 8.2 is used to calculate the minimum power and rpm for every velocity. For the function to work the V_{∞}-rpm mesh should be defined.

3. The function described in Equation 8.2 is used to find the minimum power and rpm necessary to hover.

4. After calculating the necessary power and rpm for climb and hover, the motor database is read as explained in Equation 8.2.

5. Given the number of battery cells, the minimum energy for climb for every motor can be calculated as explained in Equation 8.2.

6. The hovering energy for every motor can be calculated using the method described in Equation 8.2.

7. For every motor the minimum energy for climb is added to the energy necessary for hover for 20 minutes.

8. The motor database is sorted on minimum energy required to climb and hover.

9. The data on the motor that requires the least amount of energy for performing the mission is exported to a csv file. This output.csv file contains the motor data, the required energy for performing the mission, the most efficient climb velocity and the rotational speed of the propeller for climb and hover.
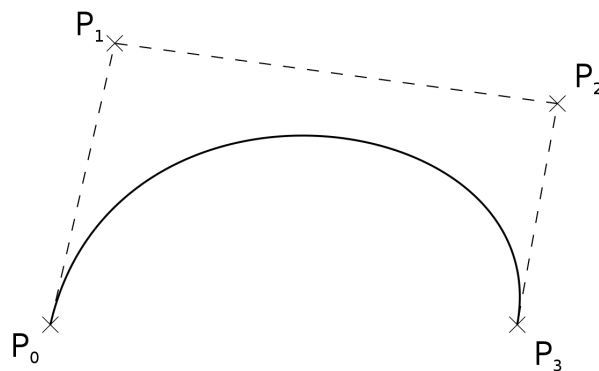
Figure 8.5: Example of a Bézier curve generated by specifying four data points [3]

8.3. Drivetrain Optimisation

After developing the drivetrain analysis tool, the motor-propeller combination has to be designed to minimise the required electric energy to perform the primary mission. This section discusses the optimisation process of the drivetrain subsystem using the HEEDS software from Siemens.

To summarise the drivetrain analysis tool: The drivetrain analysis tool takes a propeller geometry as input which is defined by the number of blades, the twist, the diameter, and radius of the hub. For every propeller section the airfoil, chord, pitch and radius are given. The chord and pitch distributions are determined by inputting four coordinates for both distributions that define unique Bézier curves. The output of the drivetrain analysis tool is the most energy efficient climb velocity for the drone, the most energy efficient motor and the total energy required for climbing 2000 metres and hovering for 20 minutes.

Before implementing the analysis tool, it must be known which parameters are fixed and which vary. The number of blades is set to two as more blades make it harder to comply with the storage volume requirement (**SYST-GENR-03**). Following suit, the maximum diameter of the propeller is equal to 16 cm and the hub radius has a minimum radius of 1.5 cm since a larger hub raidus will only reduce the thrust generated by the propeller. The number of sections used for the propeller was set to ten equidistant sections because of computational power restrictions. Combining the fixed hub radius, propeller diameter and amount of sections resulted in a fixed list of radii for the sections. To generate feasible Bézier curves, the x-coordinate for both the first and last data points of the four have to be fixed. For the first data point, the x-coordinate is set to 0 and is set to 1 for the last.

The remaining propeller parameters that are optimally adjusted by HEEDS are the six remaining coordinates to define the Bézier curve for the pitch and length distribution, and the specific airfoil for each section. This results in 22 parameters that can be altered by HEEDS. After defining the input variables, HEEDS requires a minimum, maximum and baseline value for all continuous values, such as the Bézier curve points whereas a set of inputs and baseline are needed for discrete values, such as the airfoil sections. All airfoil.dat files that were included in the Github repository were included except for the CLARK-Y airfoil as the numeric values in the file are not realistic. For the Bézier curve points, these boundaries are tabulated in Table 8.1 and are based on distributions from propellers found in literature [20].

The baseline for the optimisation was chosen such that it represents a propeller that is currently available on the market (APC 19 x 12 Thin Electric propeller). As the designed propeller has an unconventional diameter, it is not possible to compare the performance for exact geometries of the two. As HEEDS changes the airfoil distribution while iterating, it was decided to use a standard baseline for the airfoil distribution. The baseline for the airfoils was set to the NACA 4412 airfoil for all sections. It was not possible to set the baseline for the airfoils to the distribution of the APC 19 x 12 Thin Electric propeller as those airfoils were not present in the available data base. To make a better comparison with propellers that are available on the market, the airfoil database should be expanded in the future.

Table 8.1: Parameter ranges and baseline value to initiate the HEEDS software

Parameter	Minimum	Baseline	Maximum
Chord y1	0.01	0.025	0.04
Chord y2	0.03	0.045	0.06
Chord y3	0.01	0.035	0.05
Chord y4	0	0.01	0.02
Chord x2	0.05	0.1	0.39
Chord x3	0.4	0.5	0.6
Pitch y1	15	35	45
Pitch y2	20	55	65
Pitch y3	5	10	25
Pitch y4	0	15	30
Pitch x2	0.1	0.2	0.25
Pitch x3	0.3	0.4	0.8

After setting up all the files and initialising the study was run. After analysing over 150 designs the HEEDS software found a motor-propeller geometry that resulted in 21215 J for the total energy required for performing the climb and hover phases. This is the energy required for only one motor. This propeller geometry was selected as the final design for the DSE. The propeller geometry can be found in section 8.6

After finding the optimal propeller geometry with motor combination in HEEDS a manual check was performed with the three best iterations HEEDS found. The three designs yielded very similar propeller geometries with only one or two chord and pitch dimensions being slightly different. This provides confidence that the design has converged to at least a near local optimal design. From the three iterations it was noticed that the order of the motors arranged in ascending required capacity values was the same. Furthermore all the motors performed best in the first best iteration.

Up to this point the propeller-motor combinations were selected based only on the lowest energy in order to perform climb and loitering mission, however this does not take into account other important factors such as weight and cost. It was decided to perform a trade-off on the five motors with lowest required energy from the best iteration found in HEEDS. As the database of motors used contains motors since from 2006 onward some of the motors which are suitable are not present in the market anymore. The top 5 performing motors which are still available in the market are shown below:

1. T-Motor F20II 3750
2. RCX 1804-2400
3. Turnigy Multistar 1704-2300
4. HXT 2730 1300
5. Sunny Sky X2204 1800

From these 5 motors a trade-off was performed which found the T-Motor F20II KV3750 as the winner as seen in Table 8.2. This was mainly due to the motor having lowest weight, size and required capacity.

Table 8.2: Trade-off results showing T-Motor F20II KV3750 is winning

Motor	Weight	Cost	Size	Required Capacity	Sustainability	Final Score:
1 T-Motor F20II 3750	2	0	3	3	1	1.91
2 RCX 1804-2400	2	2	1	2	0	1.73
3 Turnigy Multistar 1704-2300	2	2	2	1	0	1.36
4 HXT 2730 1300	0	2	0	1	0	0.84
5 Sunny Sky X2204 1800	1	2	0	0	1	0.76

The T-Motor F20II 3750 is a high performance BLDC 3750 KV motor. It weighs 15.2 grams without cables, has a diameter of 18.8 mm and a height of 27.7 mm. Its peak current is 19.8 A and it is rated for 2-4 3.7V cell batteries[4]. Furthermore this motor has the CE marking and follows the ROHS directives [5].

The trade off criteria that will be taken into account are weight, cost, size, required capacity and sustainability. Weight, cost and required capacity are taken into account as they are the restricting budgets for motor selection. Required capacity is the amount of mili amp hours required to perform climb and loitering. We want to minimise this values as much as possible as a reduction in required capacity reduces the weight of the battery significantly. The size criteria refers to the diameter of the motor. This dimension should be minimised in order to reduce the drag in vertical climb and to make the arm smaller which facilitates folding of the mechanism. Finally sustainability will be taken into account as there are requirements such as **SYST-SUST-16** and **SYST-SUST-17** which require the manufacturer to have an ISO14001 and FLA certification.

The weight selection for each criteria is performed using analytical hierarchy process. The relative importance table is shown in Table 11.7.

Table 8.3: Relative importance table and the final weights with a CR of 0.0015

	Weight	Cost	Size	Required Capacity	Sustainability	Final Weight
Weight	1	1	5	0.5	2	0.22
Cost	1	1	5	0.5	2	0.22
Size	0.2	0.2	1	0.13	0.33	0.04
Required Capacity	2	2	8	1	4	0.41
Sustainability	0.5	0.5	3	0.25	1	0.11

From Table 8.3 and the final weight column it can be seen that the required capacity is the most important criteria. This is because we are sizing to minimise capacity due to its strong dependence on battery weight and size. Cost and weight are weighed the same and lower than the required capacity as they are both restricting budgets however in this trade off capacity is most important. Furthermore thanks to a preliminary check the weight of all motors fits within the technical budget. Regarding sustainability there are requirements which have to be met, however due to a preliminary market analysis on motors and manufacturers it was evaluated that finding components with certifications such as the ISO14001 and FLA is unlikely, hence Conformité Européene (CE) and Restriction of Hazardous Substances (ROHS) certificates are also taken into account. Finally size is weighed the least as this criteria does not directly affect the performance of the drivetrain subsystem but should still be taken into account for the frame design. It is important to note that although the speed controllers are sized with respect to the current drawn by the motors all of the ESCs taken into account in the ESC trade off are rated higher than the peak current of all motors.

The scoring system for the weight, cost size and required capacity criteria will be using standard deviation approach as explained in section 4.1. Sustainability will be scored using the scoring method shown in Table 8.4.

Table 8.4: Scoring system for Motor sustainability

Category	Score
ISO 14001 or FLA	2
CE or ROHS	1
none	0

Having an ISO 14001 or FLA certification would be recommended as these would satisfy the sustainability requirements however due to the market analysis CE marking and ROHS are also acceptable. However, no

---

[4]F20□ KV3750, `https://store-en.tmotor.com/goods.php?id=560`, [accessed 22.06.2021]

[5]T-Motor , `https://rctmotor.en.alibaba.com/?spm=a2700.details.cordpanyb.2.3a531552Rp5j5E`, [accessed 22.06.2021]
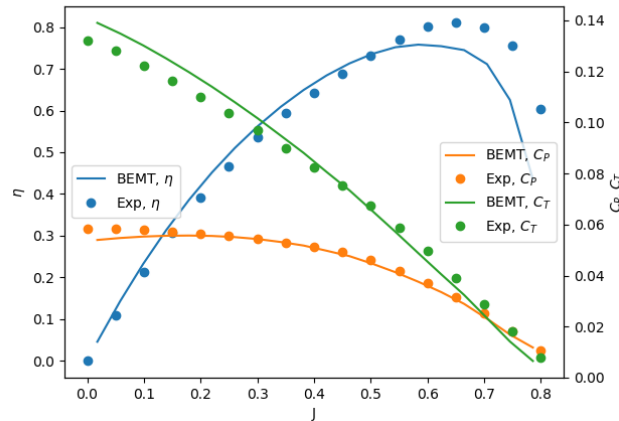
Figure 8.6: Simulated power and thrust coefficients along with the propeller efficiency compared to experimental results [16]

marking leads to no proof that the part was manufactured with a sustainable approach or design which leads to this category to yield zero points.

Table 8.2 shows the T-Motor F20II 3750 motor as the winner of the trade off. This motor has the lowest required capacity weight and diameter hence it scores high in all three categories. The cost however is higher than the other motors. Although it is only 3.73 euros more than the second highest scoring motor all other 4 motors have comparable prices between 10-12 euros which lead to a small standard deviation causing the T-Motor F20II 3750 motor to perform poorly in this criteria. Finally this motor is one of two motors which have the CE and ROHS markings.

Now that a motor is selected there is a remark on the usage of the motors. Requirement **SYST-THER-01** defines the temperature envelope. If the drone takes off at an ambient temperature of -20°C and ascends 2 km, the ambient temperature at altitude will be -33°C. While the motor is operating the waste heat will likely keep it within the operating limits. However, startup can be problematic as the viscosity of the grease in the bearings increases with decreasing temperature. This can cause a motor to operate less efficiently due to the increased friction or, in extreme cases, can cause the motor to seize. In order to mitigate this the grease in the bearing has to be carefully selected. The SKF 'Grease selection chart'[6] specifies a range of commercially available greases. Specific greases exist for low ambient temperature applications for small electric motors, namely the 'LGLT 2' type (DIN 51825 code K2G-50). These can also operate up to temperatures of 110 °C. The life of this grease 1000 operating hours at 20.000 rpm. Thus the low temperature envelope is not a killer requirement on the system, as long as some precautions are made.

8.4. Verification & Validation

This section describes the steps taken and the steps planned to verify and validate the drivetrain optimisation tool and the current drivetrain design. First, this section will discuss the verification and validation of the BEMT python tool. Then, the verification steps for the tools that were developed from scratch and the implementation into HEEDS are discussed. Lastly, suggestions how to validate the drivetrain optimisation tool are made.

The python tool that was retrieved from Github already contained validation data on the tool itself. The data will be summarised in this section. To validate the tool the thrust, torque and efficiency of an airplane propeller is compared against results from experiments [16]. The experimental data compared to the calculated values are presented in figure 8.6. From figure 8.6 it can be concluded that the used BEMT tool is validated as the predicted values by the tool closely resemble the experimental data.

As the basis of the drivetrain tool is validated the newly developed functions should be verified and validated. To verify the code several steps were taken. The first step of the verification of the code was to debug the code. After debugging the code several unit tests were performed ranging from tests that print the correct dataframe to tests that test if files are correctly changed by running the python code. After testing the individual functions in the code larger system tests were performed. The same approach was used for the drivetrain analysis tool into HEEDS. So, first debugging, then unit tests and finally system tests. Combining these two verification

---

[6]Lubricant selection, `https://www.skf.com/group/products/lubrication-management/lubricants/lubricant-selection`, [accessed 03-06-2021]

processes makes sure the drivetrain optimisation tool is working as expected.

Now that the drivetrain optimisation tool is verified it should still be validated. Given the limited resources, validation steps were out of reach for this project and will be part of the post-DSE plan described in section 8.10.

Regarding the motor tool, verification was performed using unit tests on the functions and comparing the results with the drive calc tool [7] which uses the same database of motors. The results produced by the motor tool and drive calc were similar when comparing the same motor side by side. Furthermore using the manufacturer data of the selected motor, although the motor was tested using different type and size of propeller, it was possible to see that the power and RPM calculated by the motor tool are achievable in real life.

In order to further validate the drivetrain tool a motor test could be performed in which the power, current drawn and rpm are measured. These could then be compared to the drivetrain tool outputs when calculating the performance for the same voltage and current settings.

The test setup shown in figure 8.7 was used in order to perform the validation test. The setup consists of the drivetrain subsystem including ESC, a wattmeter, and a stand for the motor with a load cell. With this setup The power current voltage consumption of the battery can be measured using the wattmeter, the thrust can be measured using the load cell and the RPM can be measured using a tachometer. The motor used was not the selected motor for the drivetrain but its performance parameters, namely the no load current and internal resistance were measured. The propeller used in the setup is the 3D printed propeller which was designed in section 8.3.

The motor was run at different throttle settings and the current voltage, power and RPM were measured. At each RPM measurement the measured voltage and the motor characteristics were inputted into the drivetrain tool to calculate the expected electrical power. The measured power and calculated power were then graphed in figure 8.8. Due to problems with the test setup it was not possible to measure accurate readings of the thrust, however this measurement is not strictly necessary as the thrust would be used to validate the propeller tool which was already validated.
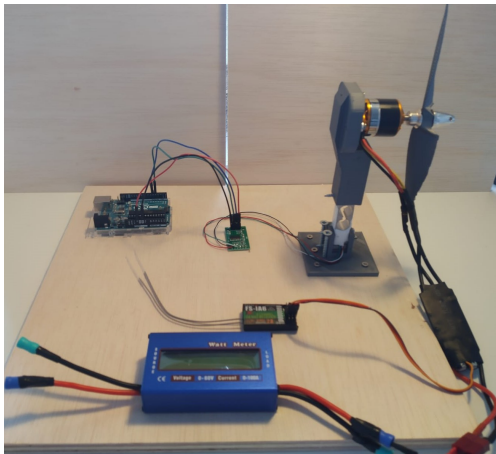
Figure 8.7: Drivetrain Validation Test Setup
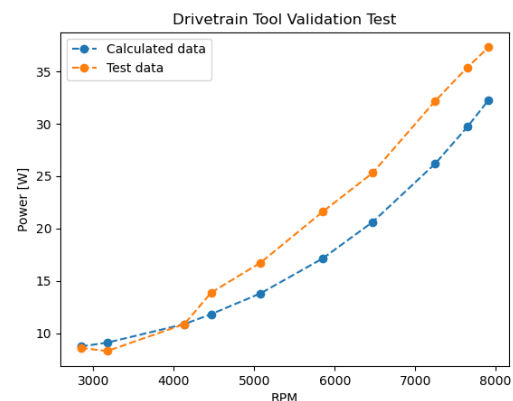
Figure 8.8: Power vs. RPM graph experimental and drivetrain tool

From figure 8.8 it is possible to see that the measured power is mostly higher than the calculated one. This is most likely due to losses in the wires and in the ESC. Furthermore excluding the 3 lowest RPM data points the percentage error between the measured and calculated powers is almost constant with an average of 17.1%. The discrepancies for the three lowest values of RPM are most likely due to the fact that during those measurements there was more noise in the measurements with the tachometer. This may have lead to a overestimation of the RPM leading to higher calculated values for the power. This experiment has shown that drivetrain tool is capable of estimating the motor and propeller performance to an acceptable amount in order to design the drivetrain subsystem. The results extrapolated were expected as it was shown in the assumptions of the tool that losses in wires and ESCs were neglected. However with this test setup it is not possible to validate the tool due to inaccuracies in measurements. Finally it is recommended to repeat this experiment with a more accurate test setup, perhaps also testing the effects of temperature by varying the ambient temperature. The entire drivetrain subsystem, electronics subsystem integration could also be validated using this setup if the same motor, battery, and ESC are tested.

---

[7] Home of the Drive Calculator, `http://www.drivecalc.de/`, [accessed 27.06.2021]

8.5. Propeller Material Selection

In order to select the material the propeller is made of a trade off was performed. An initial market analysis found that the 6 most common materials used for propellers are Polycarbonate (PC), Carbon Fibre Reinforced Polymers (CFRP), Beechwood, PC + 10% glass fibre, Nylon 6 (PA6) and PA6 + 15% glass fibre, hence these will be evaluated.

The trade off criteria taken into account are density, cost, Young's modulus, toughness, sustainability and coating. Density is taken into account as the volume of the propeller is already fixed hence this takes into account the weight of the propeller. Cost refers to the cost per unit volume and as with density since the volume is constant this resembles the material cost for the propellers. Furthermore the Young's modulus and toughness are taken into account. The first determines the elasticity of the material. We would like to minimise the deformation of the propeller in order to not alter the shape of the propeller which leads to different performance characteristics. Toughness on the other hand would be favourable to have a larger value as it evaluates the ability of energy absorption hence this is important in the case of the drone hitting a leaf or Branch of a tree. The need for coating is another criteria as some materials need a coat to remain water proof. Finally sustainability will be taken into account using the ecolizer tool.

The weight selection for each criteria is performed using analytical hierarchy process. The relative importance table is shown in Table 11.7.

Table 8.5: Relative importance table and the final weights with a CR of 0.0016

	Density	Cost	Young's Modulus	Toughness	Sustainability	Coating	Final Weight
Density	1	0.5	1	4	4	5	0.25
Cost	2	1	2	4	4	5	0.35
Young's Modulus	1	0.5	1	2	2	4	0.19
Toughness	0.25	0.25	0.5	1	1	2	0.08
Sustainability	0.25	0.25	0.5	1	1	2	0.08
Coating	0.2	0.2	0.25	0.5	0.5	1	0.05

From Table 8.5 and the final weight column it can be seen that the cost is the most important criteria. This is because most of the drivetrain budget is allocated to the motors hence cost is the most restricting budget. Density comes after as weight is also an important factor in the budgets. Young's modulus is also an important criteria as the propeller spin fast which causes the blades to deform. The deformation, as previously explained, can cause the performance and efficiency of the propeller to decrease which is undesirable. Young's modulus is weighed more than toughness as collisions should be avoided by the collision avoidance system and crashing into is not desirable. Sustainability is weighed the same as toughness as performance is considered mostly important for such a critical component such as the propeller. However sustainability is still taken into account. Finally the need for coating is weighed the least.

The scoring system for all the criteria except coating will be using standard deviation approach as explained in section 4.1. Coating will be scored with a 0 if coating is needed and 1 if coating is not needed.

Table 8.6 shows that beechwood material wins the trade off. This material has the lowest density and cost. The sustainability score is also the highest. Compared to the second best option which is PA6 it outperforms it in all categories except for toughness.

The result of the trade off is shown in Table 8.6. Beechwood was found to be the best material due to its low density and high sustainability score.

Table 8.6: Trade-off results showing Beechwood material is winning

Material	Density	Cost	Young's Modulus	Toughness	Sustainability	Coating	Final Score
1 Polycarbonate	1	2	1	1	1	1	1.35
2 CFRP	0	0	3	1	1	1	0.78
3 Beechwood	3	2	1	1	3	0	1.96
4 PC + 10% glass fibre	1	2	1	2	2	1	1.52
5 PA6	2	2	1	3	1	0	1.71
6 PA6 + 15% glass fibre	1	2	1	2	1	0	1.38

8.6. Final Design Drivetrain

This section provides an overview of the final drivetrain design. figure 8.9 shows a render of the propeller. The drivetrain consists of two foldable propellers made out of beechwood. The propeller is coated to make it water proof and less flammable. The outer diameter of the propeller is equal to 16 cm. This is an unconventional diameter for propellers that are available on the market. The current propeller maximises the diameter that is allowed by the volume constraint. As mentioned in the introduction, designing the propeller from scratch paid off due to the fact that it was possible to enlarge the diameter, which is in general more efficient[8]. The propeller only uses one airfoil, the NACA 63815 airfoil. The hub radius of the propeller is equal to 1.5 cm. To design the propeller, the propeller was divided into 10 sections. For every section the radius to the middle of the section, the pitch and the chord length are given. These values can be found in Table 8.7. The motor that was selected is the T-Motor F20II kv3750.

Figure 8.9: Render of the designed propeller attached to the drone arm

Table 8.7: Radius, chord length and pitch angle distribution of the sections

Section	1	2	3	4	5	6	7	8	9	10
Radius [m]	0.018	0.025	0.031	0.038	0.044	0.051	0.057	0.064	0.070	0.077
Chord Length [m]	0.025	0.027	0.027	0.026	0.024	0.021	0.017	0.013	0.0092	0.0055
Pitch Angle [deg]	38.7	33.7	29.1	24.8	21.1	18.0	15.6	14.2	13.7	14.3

8.7. Sensitivity Analysis

This section describes the influence of the assumptions made on the drivetrain design. Some assumptions will influence the design a lot and the effects of other assumptions are negligible.

- **The air density used is the ISA air density at 4500 m altitude**: The surface ceiling of the drone is equal to 4500 m. Therefore the air density taken into account for the design of the drivetrain is lower than the average air density the drone will operate in. The air density is therefore a conservative assumption. A larger air density would increase the thrust and torque generated by the propeller as can be seen in Equation 8.9 and Equation 8.8. This conservative assumption was made to make sure the propeller can generate enough thrust to hover at every altitude below its surface ceiling.

- **Constant climb velocity**: The assumption of constant climb was used to simplify the calculations for the time to climb. In reality the drone first has to accelerate to the most efficient climb velocity and at the top of the climb the drone has to decelerate to be able to hover at altitude. Therefore this assumption underestimates the time to climb and therefore the energy required to climb to 2000 m altitude. As the time to climb is approximately 100 seconds, the acceleration and deceleration phases of the climb will not significantly impact the time to climb. If climb thrust is used to accelerate the drone to its nominal climb velocity, the time to climb would increase by approximately six seconds. Assuming that the time to climb would also increase by six seconds due to deceleration, the extra time to climb would be 12 seconds. This is 12% extra than the time used for the calculations. In reality, the thrust can be maximised

---

[8]Propeller efficiency rule of thumb, `http://www.nar-associates.com/technical-flying/propeller/cruise_propeller_efficiency_screen.pdf`, [accessed on 29.06.2021

to accelerate faster to the nominal climb velocity. This would reduce the error due to the constant climb velocity assumption.

- **The weight of the drone was assumed to be 500 grams, a C_d value of 0.265 was assumed, the characteristic surface of the drone was assumed to be 0.0235 and the climb is assumed to be vertical**: These four assumptions will be taken into account in the post-DSE phase. The assumptions on the values will be updated according to the latest technical budgets and CFD analysis. The vertical climb assumption is taken into account by adding a horizontal leg into the propeller analysis. A more detailed explaination is given in section 8.10.

- **Incompressible fluid**: To derive the blade element momentum theory incompressible flow is assumed. The validity of this assumption can be checked by calculating the Mach number at the tip of the propeller at maximum rpm. The maximum rpm is achieved during climb. From the output.csv file it was found that the current drivetrain design requires a maximum rpm of 11493. The highest Mach number can be found using the speed of sound at maximum altitude. For the drone the maximum altitude is 4500 m. At 4500 metres altitude the speed of sound is 323 m/s. The tip velocity can be calculated by Equation 8.23.

$$V_{tip} = \frac{rpm_{max} \cdot \pi \cdot D}{60} \tag{8.23}$$

Plugging in the maximum rpm and the diameter of the propeller results in a maximum tip velocity of 96.3 m/s. This results into a maximum Mach number of 0.298. As a rule of thumb compressibility effects are only present at Mach number larger than 0.3[9]. Therefore the assumption that the flow is incompressible is valid.

- **Inviscid flow**: To derive the BEMT, inviscid flow is assumed. The Reynolds number of inviscid flow is infinite[10]. For the propeller a minimum Reynolds number was found to be approximately 25,000. This Reynolds number was found for the rpm used for hover at the minimum radius of the propeller. A maximum Reynolds number of approximately 50,000 was found. This Reynolds number was found using the rpm setting for climb and the tip position of the propeller. As Re»0, for both the minimum Reynolds number found and the maximum Reynolds number found, the assumption of inviscid flow does not significantly influence the calculations.

- **Other assumption coming from BEMT.**: These assumptions are all regarding the airflow properties. The python tool has been validated by the author of the tool. This was already covered in section 8.4. From this validation data it is concluded that these assumptions have a small impact on the results.

8.8. Sustainability Assessment

Sustainability in the drivetrain subsystem was taken into account for the motor trade off and the material trade off. The approach for taking into account sustainability was different between the two trade offs. With regards to the motor selection sustainability was taken into account by including and searching for the ISO 14001, FLA, CE and ROHS certifications. The first two certifications come from requirements **SYST-SUST-16** and **SYST-SUST-17**. However finding electrical components which posses this certification is quite challenging hence the CE and ROHS marking were also included. These last two represent that the component conform with the European health, safety and environmental protection standards. The ROHS marking is a part of the CE marking which is specifically related to the use of hazardous substances in the component [11].

Sustainability in the propeller material trade off was taken into account using the Ecolizer tool which is also explained in chapter 19. Specifically for beechwood the Ecolizer tool did not contain a production estimate which included CNC machining hence an estimate was performed by estimating the volume of the chipped material using a safety factor of 1.5 and adding the environmental impact of that amount of material and its disposal. For future references this methodology could be expanded and should be verified to remain consistent with the other materials.

8.9. Requirement Compliance & Feasibility Analysis

In order to evaluate if the drivetrain design meets the requirements set at the start of this chapter a compliance matrix is made and presented in Table 8.8. Despite discarding some requirements, there are still some

---

[9]Mach Number, `http://www.engineeringarchives.com/les_fm_machnumber.html`, [accessed on 26-06-2021]

[10]Inviscid flow, `https://en.wikipedia.org/wiki/Inviscid_flow`, [accessed on 29.06.2021]

[11]RoHS Compliance FAQ, `https://www.rohsguide.com/rohs-faq.htm`, [accessed 22.06.2021]

requirements left that have undefined values and can therefore not be evaluated. Furthermore, there are also a number of requirements where there are not currently enough resources available to evaluate the requirement. An example of this is **STAK-GENR-09**. While it is possible to plan to waterproof the electrical components, it is not yet feasible to evaluate the size of added drag of flying through rain.

Table 8.8: Compliance matrix of the drivetrain

ID	Requirement	Comp-laint	Comment	Valida-ted by:
SUBSYST-DFPP-03	The propulsion subsystem shall allow for the generation of a lifting force of more than 10 N at the specified service ceiling of 4500 m	✓		Sim
SUBSYST-DFPP-07	The propulsion subsystem shall allow for a maximum climb of 2000 m up until the specified service ceiling is reached	✓		Sim
SUBSYST-DFPP-12	The propulsion subsystem shall have a weight limit 110 grams	✓		RoD
SUBSYST-DFPP-14	The propulsion subsystem shall have a cost limit of 80 euros		The current drive-train design has a cost of 84 euros.	Ana
SUBSYST-DFPP-15	The propulsion subsystem shall have a temperature envelop of -33 to 40 °C	✓		Test

SYST-RISK-01 is as yet unevaluated, due to problems with the complex geometry of the propeller. In the available time critical errors in the way the geometry is translated from one software package to the other could not be solved.

The current design is not compliant with **SYST-SUST-03-B**. This is because there were no non-flammable materials available that are suitable for making propellers out of that fit within the cost budget and sustainability constraints of this project. In order to remedy this breach of compliance in future reports fire resistant coatings, additives and impregnation's must be evaluated. These must be carefully weighed off against the sustainability and toxicity concerns these processes bring along with them.

8.10. Discussion & Recommendations

This section first lists steps that can be taken to improve the drivetrain analysis tool. Then future plans are given to improve the complete drivetrain design.

Steps that can be taken to improve the drivetrain optimisation tool are listed below. This was not yet implemented to generate the current drivetrain design, because of limited time and computational power.

- Include descent phase for drivetrain optimisation: in the current drivetrain tool only the climb and hover phase are included for optimising the propeller-motor combination. Adding the descent phase would result in a propeller-motor combination optimised for climb, hover and descent. It would also result in a more accurate prediction of the energy consumption of the drivetrain for performing the mission.
- Include horizontal flying in drivetrain optimisation: it is very likely that the drone should translate horizontally before climbing to altitude when used. Including a horizontal flying phase to the drivetrain optimisation tool would result in a better prediction of the total energy consumed by the drivetrain for performing the mission. The propeller-motor combination would also be optimised for climb, hover, descent and a horizontal leg.
- Expand the airfoil data set: at this point only five airfoils are present in the airfoil data set. This decreases the design freedom for the propeller geometry and it is not possible to compare the current design with propellers that are currently available on the market. Expanding the airfoil data set would require to find lift and drag coefficient estimates for angles from -180 ° up to 180 °. These lift and drag coefficients can be estimated by using Xfoil[12]. Coefficients estimated by Xfoil at high angles of attack are not accurate

---

[12]Subsonic Airfoil Development System

enough. Methods to increase the accuracy of these values are described later in this section.

- Updating the motor database: during the motor trade-off process it was found that some motors in the database are not available on the market anymore. It was also concluded that no 2021 motors are present. In general new motors outperform their predecessors in performance or efficiency. Therefore updating the motor database will probably result in more feasible designs and more efficient propeller-motor combinations.
- Refining the rpm - climb speed mesh: a finer rpm - climb speed mesh would result in smaller rpm and climb speed steps. The current propeller tool is always overestimating the rpm necessary for hovering. Reducing the rpm steps results in a smaller shaft power required for the propeller as the thrust required for hovering can be met more accurate.
- Rerunning the drivetrain optimisation using better mass and drag estimates: Running the optimisation again with better mass and drag estimates will result in a propeller-motor combination that would fit the drone. For the current design a mass of 500 grams is used and the drag is estimated using preliminary CFD analysis data. The expected mass of the drone is not exactly 500 grams and the estimated will also be different from the predicted values.

Below actions that would increase the accuracy of the calculations or confirm the validity of the drivetrain are listed. Again, these actions were not implemented in the current drivetrain analysis tool, because of time and computational power constraints.

- Increase the amount of sections for the propeller: Increasing the amount of sections will increase the accuracy of the calculation. This will not increase the performance of the propeller, but it will give a more reliable prediction of the performance.
- Increase accuracy of the airfoil data by using the methods described in literature [20]: In this paper several methods are described to increase the airfoil data for low speed drone propellers using BEMT. These methods include the extension of aerodynamic data to post-stall angles using idealised stall [29], including rotational effects [27, 10].
- Validation of the motor database: the data in the motor database is generated by experiments performed by the author of the database. Validation on this motor database is necessary to guarantee accurate motor performance predictions. As the database consists of over 2000 motors this can be an expensive procedure. Therefore it is recommended to first filter out the motors that are certainly too heavy to be used on the drone.
- Drivetrain testing to validate the drivetrain analysis tool: tests are necessary to validate the drivetrain analysis tool. This can be done by a siple test setup with a propeller-motor combination, a load cell and a rpm sensor. The energy consumption can be measured together with the thrust generated at a certain rpm. Testing the tool for different climb velocities would require a wind tunnel experiment.
- The airfoil data used for the propeller analysis tool should be validated. This can be done using CFD analysis on the airfoils or by a windtunnel experiment. This would require a lot of computational power or expensive test equipment. This should be taken into account for the post DSE planning.

For the future it is necessary to update the material selection. As explained in section 8.5, the manufacturing costs were not included in the trade-off. As injection moulding for plastics is very cheap for bulk production compared to CNC machining this could influence the outcome of the trade-off. At this point not enough information is available to make an estimate of the manufacturing costs of the beechwood propellers. More information can be obtained by approaching companies. Given the limited resources this is something left for the post DSE phase.

As the current design is formed by the NACA 63-815 airfoil, which is not a symmetric airfoil, the airflow over the propeller will also generate a moment. The moments generated by the blades due to the asymmetry of the airfoil have to be investigated in more detail. This is because the moments generated at high rpm might induce high stresses that can damage the propeller.

9. Frame Detailed Design

This chapter will present the design of the main components of the drone and their respective structural, aerodynamic and material characteristics.

9.1. Requirements Analysis

In order to assure compliance, first an analysis of the requirements is performed. The design driving requirements are presented below:

- **STAK-GENR-03**: The drone shall not have exposed electronics
- **STAK-GENR-07**: The drone or its element(s) shall stay on the water surface for at least 72 hours
- **STAK-GENR-07-A**: The drone or some indication mark shall have positive buoyancy
- **SYST-GENR-03**: The maximum dimensions of the drone in storage mode shall not exceed 200 x 100 x 100 mm (length, width, height)
- **SYST-GENR-13** The drone shall fit through an opening with minimum dimensions of 40x40 cm
- **SYST-RISK-01**: The critical components shall be designed to have safe life or fail safe philosophy implementation
- **STAK-SUST-01**: The drone shall be able to be repaired in a modular fashion
- **SYST-SUST-11**: Each structural component of the drone shall be evaluated to determine if it can be replaced with a 3D printed part
- **SYST-SUST-03-A**: The drone shall contain any sparks and fire within the system in case of short-circuit
- **SYST-THER-01**: The drone shall be able to operate in a temperature range from -20 to +40
- **SYST-RISK-10**: The drone shall be IP rated to at least IP 55

The electronics of the drone will have to be completely enclosed in order to comply with these requirements. This structure can serve multiple functions. It can provide the required positive buoyancy as well as protect the drone from the elements. Since such a structure is needed, it is expected that this shape can be tailored in order to give the drone aerodynamic advantages while gaining relatively little weight.

The maximum folded dimensions of the drone is critical to the structure. From this, as well as the chosen geometry and layout, constraints on the maximum length of propeller are found. The requirement on modular repairability constrains the design philosophy in this project. It excludes adhesives as a joining technique because this can often not be reversed without damage to the parts.

9.2. Folding Mechanisms Trade-Off

Before in depth structural analysis can be performed, the main configuration of the quadcopter has to be chosen. A requirement has been set on the maximum volume of the quadcopter and that the propellers should be foldable.

- **SYST-GENR-03:** The maximum dimensions of the drone in storage mode shall not exceed 200 x 100 x100 mm (length, width, height)
- **SYST-RISK-04**: The propellers shall be foldable

To make sure the quadcopter will fit in the designated protective case, the arms need to be foldable. Therefore, a design option tree has been made including the most used folding mechanisms in the market, shown in figure 9.1, where the egg/cylinder fold is deemed the best. Each folding mechanism category will be explained below.

The long fold will has two opposite folding arms on each side sharing a single rotating hinge. The Parrot Anafi[1] is a good example of a drone using this folding mechanism.

The box fold is one of the most popular folding mechanisms in the drone market. This is because the drone company DJI, the market leader covering 76% of the drone market[2], uses this folding technique for their small form factor drones. The DJI Mavic Mini[3] is shown in the design option tree. The two front arms rotate 135 degrees forward whereas the two arms at the back of the drone rotate a full 180 degrees to extend upwards.

The egg/cylinder fold category features drones with arms that fold down alongside the cylindrical or egg shaped body. The egg shaped drone is from a company named PowerEgg[4]. This drone features inward folding arms and a folding landing gear system so that when all folded up this drone will be a perfectly shaped egg.

---

[1]Parrot Anafi: `https://www.parrot.com/en/shop/buy-anafi`,[accessed 1.6.2021]
[2]DJI Market Share: `https://www.thedronegirl.com/2021/03/15/djis-market-share-2020/`, [accessed 17.6.2021]
[3]DJI Mavic Mini: `https://www.dji.com/nl/mavic-mini`, [accessed 1.6.2021]
[4]PowerEgg: `https://www.powervision.me/en/product/poweregg`, [accessed 1.6.2021]
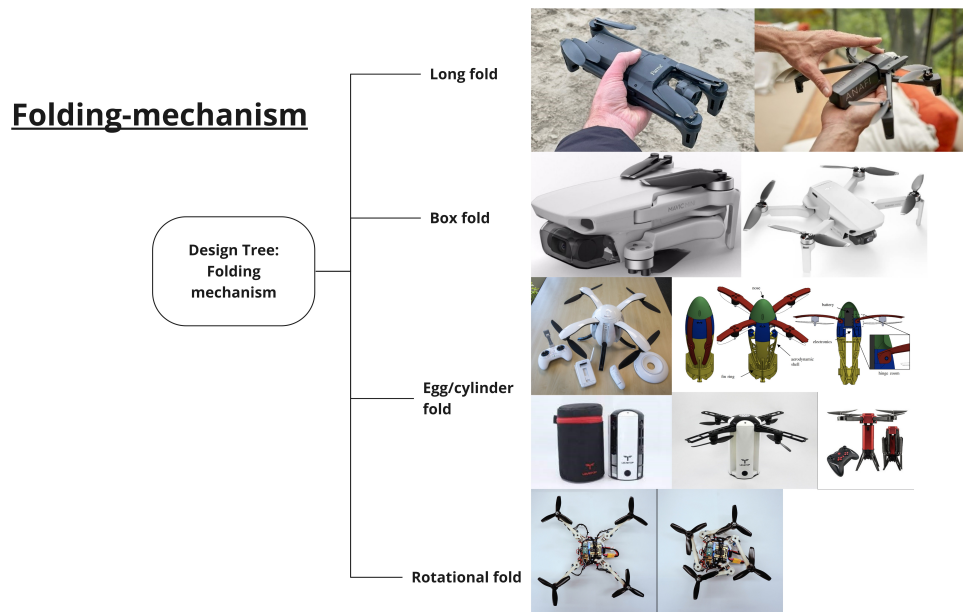
Figure 9.1: Design option tree for the folding mechanisms of the quadcopter

The arms can be folded up easily and a small button has to be pushed below the arms to release them again. The rugby shaped drone to the right of this is a ballistically launched research drone[5]. This drone is launched from a tube and has spring loaded arms that unfold themselves right after a wire that goes around the arms breaks. The cylindrically shaped drone is from a company named Levetop[6] and is a lot more compact than the previous two drones. The arms of this drone fold into the body protecting the motors and propeller during transport.

The rotational fold drone is an experimental concept coming from a research paper where morphing drone qualities were used to manoeuvre through tight spaces[7].

Criteria

Four criteria have been defined for the folding mechanism trade-off:

- Functionality
- Protection
- Aerodynamics
- Technical Risk

Functionality checks if the folding mechanism is functionally efficient, so that it can be used easily with one hand for example. Protection is taking into account if the way of folding protects the drone well in the stored configuration. Aerodynamics is concerned with how the unfolded configuration influences climb performance. Finally, technical risk checks if the way folding mechanisms have been implemented in the market and are proven to work well. Sustainability is not covered in this trade-off since it is too general to implement sustainability in this phase of the design.

Criteria weights

The criteria weights have been calculated using the Relevant Importance Table (RIT) that can be seen in Table 9.1. Between these four criteria only functionality is deemed to be slightly more important than aerodynamics giving the fairly similar criteria weight distribution.

Table 9.1: Relative importance table and the final weights with a CR of 0.02

	Functionality	Protection	Aerodynamics	Technical Risk	Weights
Functionality	1.0	1.0	2.0	1.0	0.30
Protection	1.0	1.0	1.0	1.0	0.25
Aerodynamics	0.5	1.0	1.0	1.0	0.21
Technical Risk	1.0	1.0	1.0	1.0	0.25

---

[5]Ballistic drone `https://arxiv.org/pdf/1911.05639.pdf`, [accessed 1.6.2021]

[6]Cylinder drone: `https://www.levetop.com/`, [accessed 1.6.2021]

[7]Rotational drone: `http://rpg.ifi.uzh.ch/docs/RAL18_Falanga.pdf`, [accessed 1.6.2021]

Trade-Off Results

The result of this are shown in Table 9.2 where it can be seen that the egg/cylinder concept is chosen.

Table 9.2: Trade-off results showing that the egg/cylinder type folding mechanism is winning

Criteria	Functionality	Protection	Aerodynamics	Technical Risk	Total
Weights	0.3	0.25	0.21	0.25	
1 Long fold	2	1	1	2	1.5
2 Box fold	2	1	1	3	1.8
3 Egg/Cylinder fold	3	3	3	2	2.8
4 Rotational fold	1	1	1	0	0.8

9.3. Hinge Mechanisms Trade-Off

Hinge mechanisms are used to fold the arms up and down. These mechanisms are the heart of the folding mechanism and there are multiple right ways to go about it, therefore a trade off is performed.

The concepts used in this trade off can be found in figure 9.2 and will be explained below.
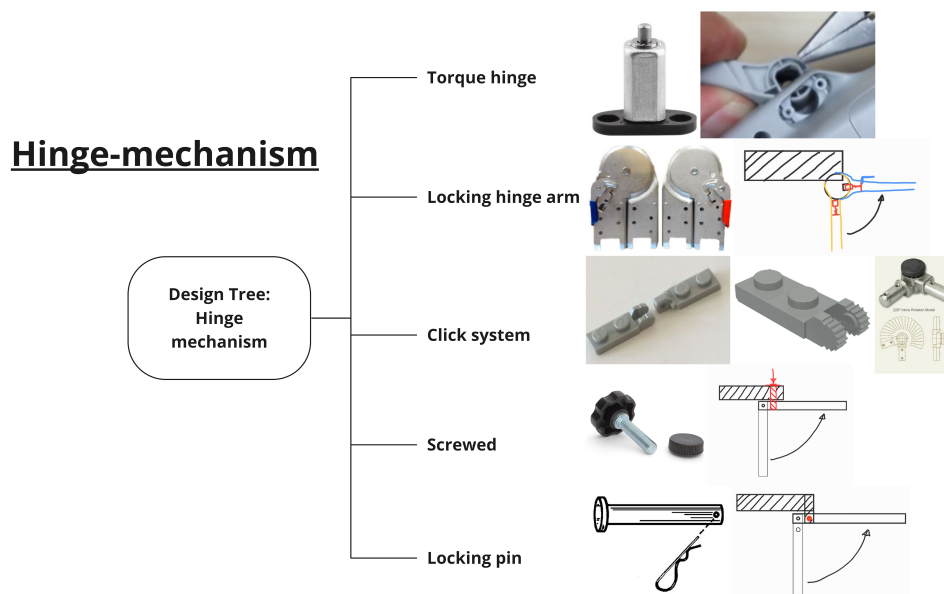
Figure 9.2: Design option tree for the hinge mechanisms of the quadcopter

The torque hinge[8] features a spring that supplies a torque which varies with how far the hinge is rotated. This results in a hinge that when folded against the drone body will click in place, and when folded out it will deliver torque in the opposite direction keeping the arm in the upright position. The locking hinge arm[9] features no torsional spring, the way it keeps the arm upright after unfolding is a little block with spring that will slide into a groove when the arm is unfolded. To release the arm and fold it in a small lever needs to be pulled to unlock the arm. The click system[10] simply clicks into place at different angles until the drone arm is unfolded. The screw system[11] is a simple yet effective system where the arm will be unfolded and properly secured by screwing it secure at the bulkhead. The final concept is the locking pin[12] where instead of screwing the arm into place the arm will be kept into place by inserting a locking pin. The relative importance table for this trade off can be found in Table 9.3.

9.3.1. Criteria Weights

The criteria weights have been calculated using the RIT that can be seen in Table 9.3.

---

[8] Torque Hinge `https://drone-parts-center.com/en/produit/dji-mavic-air-2-charniere-bras-avant/`, [accessed 20.6.2021]

[9] Locking hinge `http://www.ladderhinge.com/e_productshow/?25-folding-ladder-hinges-25.html`, [accessed 20.6.2021]

[10] Click system `https://nl.pinterest.com/pin/721983384003906629/`, [accessed 20.6.2021]

[11] Thumb screw `https://www.onderwaterhuis.nl/thumb-screws-voor-dl-ports-set-van-3-9249-7l`, [accessed 20.6.2021]

[12] Locking pin `https://www.vanguardmanufacturing.com/products/LOCKING-PIN%7B47%7DHAIR-PIN.html`, [accessed 20.6.2021]

Table 9.3: Relative importance table and the final weights with a CR of 0.04

	Cost	Ease of Use	Structural Performance	Technical Risk	Mass	Weight:
Cost	1.0	0.2	0.3	0.3	0.3	0.05
Ease of Use	6.0	1.0	2.0	4.0	2.0	0.41
Struct. Performance	4.0	0.5	1.0	2.0	2.0	0.24
Technical Risk	4.0	0.3	0.3	1.0	2.0	0.16
Mass	3.0	0.5	0.5	0.5	1.0	0.14

Trade-Off Results

The result of this are shown in Table 9.4 where it can be seen that the torque hinge concept is chosen.

Table 9.4: Hinge Mechanisms Concept Trade-Off

Criteria	Cost	Ease of Use	Structural Performance	Technical Risk (Safety)	Technical Risk (Failure)	Weight	Total
Weights	0.05	0.41	0.24	0.08	0.08	0.14	
1: Torque hinge	1	3	2	3	3	3	2.65
2: Locking hinge arm	1	2.5	2	3	3	2	2.31
3: Click system	1	2	1	2	1	3	1.76
4: Screwed	3	1	3	1	3	1	1.82
5: Locking pin	3	1	3	1	3	1	1.82

9.4. Part Design

The frame will be designed in CATIA V5. The design will be made fully parametrically. This is because at the start of the design the dimensions of many of the components are not yet known. Rather than having to remake each component for each subsequent iteration, a design table containing all the parameters can be updated. Because of the expected time savings during the iterative phase of the project the time investment to make a parametric design is deemed worth it.

Part Placement

The basic layout of the drone determined previously will be used to guide the design. Fundamentally the design consists of a cross shaped platform with most of the electronics mounted above this and the battery mounted below this. Because of the fact that the battery is the most volatile component this separation is desirable.

The drivetrain is mounted at the end of the arms in order to make as much space available as is feasible for the propellers, as this is expected to be aerodynamically advantageous.

The electronics are mounted above the bulkhead in order to give the communication and navigation modules a clear view of the sky. Part of the electronics will live in a black box . The blackbox will be placed on top of the bulkhead and will seal against it, housing the companion computer. The rest of the electronic components will be placed on scaffolding above it.

Lastly the electric components will be enclosed in a dust- and waterproof shell.

Bulkhead

The most critical structural component is the bulkhead at the heart of the drone. This transfers the loads from all the drive train to the heaviest single component, the battery. Because of its location and central importance, however, it is not easy to replace this in case of a breakage. Therefore, this part is designed with a safe-life philosophy. This will likely come at the cost of additional weight.
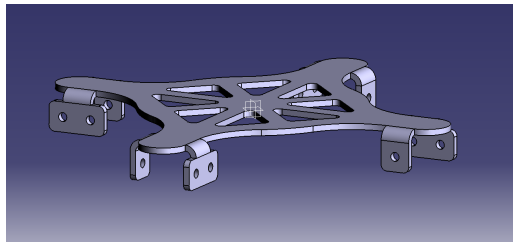
Figure 9.3: Possible geometry for the bulkhead

Arms

The next most critical structural components of the drone are the arms. These components are expected to be some of the first to break in the event of a crash or collision. Because these components are easily serviceable, spares will be provided for the user to exchange with the broken component.

Drone arms are traditionally flat plates or hollow tubes. This manner of construction incurs a lot of drag and requires very high performing materials such as carbon fibre reinforced composites. Sustainability is an important criterion, but sustainable materials perform significantly worse than the current industry leading materials. This can be counteracted, in part, by compensating for weak materials using better design. However, a much larger volume is needed to accommodate this.

Larger arms might, in theory, come at a significant cost in terms of aerodynamic drag. However, the shape of an object can matter much more than its size when drag is concerned. In figure figure 9.4 two shapes can be seen that have incur the same amount of drag. This shows that design choices regarding the aerodynamic shape of the drone can have great influence drag wise and thus overall have great impact on the performance of the drone as a whole.

Because of this the choice is made to shape the arms like symmetric aerofoils. The NACA four digit series is chosen due to the ease of parametrisation of this profile. Furthermore, the main loading of the arms will be a bending load due to the forces produced by the drivetrain and the inertia of the internal components. Due to the large moment of inertia of an aerofoil shape it is well suited for this dominant load case.

In order to ensure that it is accessible and replaceable it is decided that the electronic speed controller shall be placed on or in the arm.
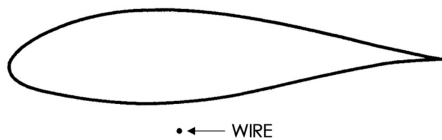
Figure 9.4: A wire and an airfoil with the same drag
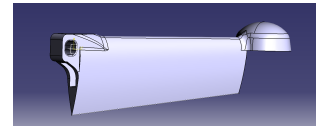
Figure 9.5: Possible geometry of the drone arms

Shell

The electronics are to be enclosed in a dust and waterproof shell. It is expected that shape can be tailored in order to make the drone more aerodynamic at relatively little extra cost or weight. The bottom half of the shell can also be shaped such that it features built-in landing gear to aid in landings. It can both act as feet to stabilise it during a normal landing, but also as a crumple zone to absorb energy in the case of a hard landing.
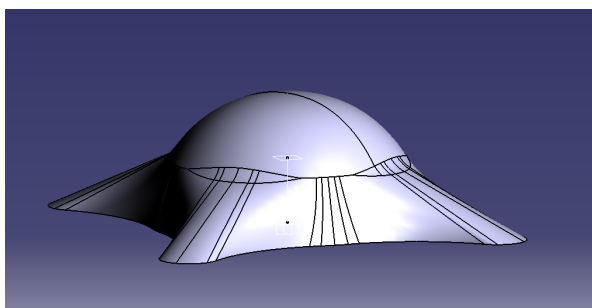
(a) Possible top half of the shell
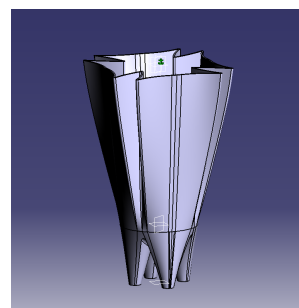
(b) Possible bottom half of the shell
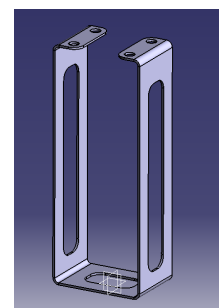
(c) Possible battery cage

Figure 9.6: Example geometries of the shell parts and battery cage

Battery Cage

In order to suspend the battery under the bulkhead a bracket must be designed to support it. Since the battery is likely to be the single heaviest component the bracket must be adequately strong to transfer the accelerations the drone experiences to the battery. These can be both rotational and linear accelerations.

9.5. Material Choice

Material choice is inextricably tied to the production methods available. Therefore this chapter will take a 'manufacturing first' approach to material selection. This means that first the geometries and constraints will be analysed in order to identify suitable production methods. From that applicable materials will be chosen for each part. If there is no clearly identifiable criteria to select a winning material a trade-off will be performed.

For this analysis a production size will be assumed of 500 drones. This is because this is an ambitious goal for the introduction of a new product, but one at which the powers of economies of scale can start to be leveraged. For more information see section 17.5. For detailed cost calculations related to the production see chapter 18.

Sustainability is a key criteria when evaluating materials for use in a product. The current standard in the performance drone market is to produce drone frames out of flat sheets of Carbon Fibre Reinforced Polymer (CFRP) material. The shapes are cut out using a cnc-controlled abrasive water jet or using a cnc-controlled milling machine. This is relatively cheap and because of how well this material performs the structurally inefficient shape does not impact the overall performance overmuch. However, CFRP is not at all recyclable. Non-recyclable materials will not be considered as candidates for the main components of the frame.

Bulkhead

For the bulkhead multiple options are available. It can be produced by plastic injection moulding, Selective Laser Sintering (SLS) 3D printing or Sheetmetal Lasercutting. In terms of cost and weight aluminium sheet metal is the most attractive option. However, parts of the bulkhead are exposed to the elements and it is a very high hazard with high confidence in terms of ecotoxicity. On the other hand plastic, either 3D printed or injection moulded, is much safer for the environment. Thus a trade-off is performed.

Trade-off Result

The material that performs best in the trade-off is the SLS printed Nylon PA12. Although it is more expensive than aluminium, it is more affordable than injection moulding at the expected production scale. In terms of weight it is slightly performs less well but it makes up for this in its low toxicity and other hazards to humans. While it is not 'non-flammable' like the Aluminium, it is slow burning, which is acceptable for this part.

Criteria

For the selection of the bulkhead material four criteria were analysed: Cost, Weight, Environmental Hazard and Risk. The structural performance of the materials was considered indirectly through the weight of the parts. Example geometries were designed for the plastic and sheet metal options and they were analysed using FEM and reworked accordingly. Therefore at each weight, each material performs sufficiently.

Weight This is a critical criterion and limited by one of the driving requirements of the project.

Cost This is a critical criterion and limited by one of the driving requirements of the project. Cost estimations are based on a production volume of 500 drones. More information about this can be found in chapter 18

Environmental Hazard When comparing the candidates many sustainability-related aspects were similar. For example, when adjusting for the weight of each material the carbon footprint of each material was too similar to be used to discern meaningfully between them. However, one dimension stands out: environmental hazard. This is the complicating factor that makes the trade-off necessary.

Risk One other aspect that is taken into account is the performance of the material in the presence of a fire. Since the bulkhead is directly connected to the battery cage and in near proximity of both the battery and power distribution board how it performs of in case of a fire is an especially relevant performance dimension. However, as is explained in section 11.2, the battery is contained in its own fireproof bag, mitigating the importance of this criterion.

Criteria Weights

The criteria weights have been calculated using the RIT that can be seen in Table 9.5.

Table 9.5: Relative importance table and the final weights with a CR of 0.04

	Cost	Weight	Enviromental Hazard	Risk	Weights
Cost	1.0	0.3	0.2	1.0	0.10
Weight	3.0	1.0	0.3	3.0	0.27
Sustainability	5.0	3.0	1.0	3.0	0.51
Risk	1.0	0.3	0.3	1.0	0.12

Trade off table

The trade off results can be seen in Table 9.6.

Table 9.6: Bulkhead Material Concept Trade-Off

Criteria	Cost	Weight	Environmental Hazard	Risk	Total
Weights	0.1	0.27	0.51	0.12	
SLS Nylon	2	2	3	2	2.51
Injection moulding ABS	0	1	2	1	1.41
Injection moulding PLA	0	0	3	2	1.78
Lasercut Aluminium	3	3	0	3	1.46

Discussion

Due to resource constrains a few factors were not evaluated. The first is that the eco-toxicity of the aluminium which might be mitigated by using a coating. However, it is unknown to which degree this would work in practice and what level of additional cost and weight that would add. Furthermore, many different formulations of the analysed plastics exist. There are versions of the Nylon plastics that are more fire retardant, but it is unknown how much cost that would add and how both the material strength and the product's recyclability are affected.

Lastly, the numbers are contingent on the estimated production size. For smaller production runs, the price-advantage of the aluminium is even larger. For larger production runs, the price of an injection-moulded part can drop dramatically. One possible approach is to accept the high startup costs of the injection moulding process as an investment to be amortised over future production runs as well. The marginal cost of a part at any scale is almost negligible compared to the cost of the tooling. One downside of this is that it locks the design into place for all those future runs, which makes future design iterations very costly. It is recommended that these factors are evaluated again in later stages of the design.

Arms

The arms constitute the most complex part of the drone. They have complex internal and external features. Some of these featured can be simplified to adapt the part to injection moulding, but some of them are also imposed by requirements. Of the criteria by which candidate materials vary, cost is by far the most dominant. The cost is heavily dependent on the production size. Up to a size of 500 drones (which would constitute 3000 arms) additive manufacturing is by far cheaper. Beyond that point injection moulding becomes increasingly dominant. At those numbers the complexity of the mould has at most a small influence. More information about this can be found in chapter 18.

Therefore, at this stage of development, the Selective Laser Sintering (SLS) additive manufacturing process is chosen as the production method. Of the materials available from the assessed suppliers only Nylon PA12 recyclable. Therefore that material is chosen.

Shell

The complex thin-walled geometry of the shell restricts the possible production methods severely. From those left only vacuum forming is deemed economical. One of the main advantage of vacuum forming is that the cost of the tooling scales relatively flexibly with the size of the production. Of the types of plastics that can be vacuum formed two plastics are found to be suitable, ABS and PETG. Of these PETG has clear advantages. It has a ecological footprint half that of ABS (135 mPt versus 251 mPt) and where ABS is classified as a moderate respiratory hazard, PETG only has low confidence persistence & carcinogenicity.

One unexpected side-benefit found during simulation is that PETG can be made fully transparent, which might offer advantages in terms of routine inspections and for housing LED light indicators in a protected fashion.

One function preliminary assigned to the shell was containing the intense heat generated in the even of a battery fire. Due to the addition of a fireproof battery bag this constraint is no longer limiting the material choice, as discussed in section 11.2.

Battery Cage

The battery cage is a simple bracket that holds the battery to the bulkhead. Both plastics and sheet aluminium were examined, but due to the simplicity of the component if it were to be made out of sheet metal it is by far more economical unless very large production volumes are achieved. Of the available materials at the suppliers that were found AlMg3 EN AW 5754 is the most suitable.

One downside of this material is that it has a high eco-toxicity, but this is mitigated by the fact that this part is fully enclosed by a waterproof shell.

9.6. Aerodynamic Analysis

To be able to evaluate gust and climb performance, aerodynamic analysis needs to be performed.

Simple C_D estimation

A preliminary way to estimate the cd of the drone during climb is to simplify the shape of the drone and then use the respective C_D of the simplified shapes. The drone is assumed in this case to have the body of an ellipsoid and circular arms. The estimated C_D of those can be seen in figure 9.7.
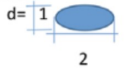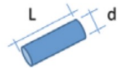
Body (Flow From left to right)	L/d	Re= V d/v	C_D
Bodies of revolution			
1) Sphere: D		10^5 $>3 \times 10^5$	0.50 0.20
2) Ellipsoid : d= 1 2		$>2 \times 10^5$	0.07
3) Circular cylinder axis vertical to follow: L d	1 5 20 ∞ 5 ∞	10^5 $>5 \times 10^5$	0.63 0.74 0.90 1.20 0.35 0.33

Figure 9.7: Drag coefficient estimation using basic shapes [3]

To be able to use these C_D values first the Reynolds Number needs to be calculated and checked to be in the vicinity of 10^5.

$$Re = \frac{\rho v l}{\mu} = \frac{vl}{v} \tag{9.1}$$

Where ρ, v, l, μ and v are the density of the air, velocity of the fluid, the characteristic length, the dynamic viscosity of the fluid and the kinematic viscosity of the fluid. Using $\rho = 1.225, v = 10, l = 0.3, v = 1.42181-^{-5}$ the Reynolds number is found to be 211164 which fits in the order of magnitude 10^5 used in figure 9.7.

The C_D of the ellipsoid that will represent the pod of the body is 0.07 and the C_D of the arms with a length over diameter of 15 is then rounded up to 0.90. In Table 9.7 the total frontal area of both shapes is calculated, then the C_D is calculated using the weighted areas of both shapes.

Table 9.7: Dimensions used for the C_D estimation

Diameter ellipsoid	Length arms	Area ellipsoid	Area arms	Total C_D
75mm	80mm	4418mm2	1707mm2	0.30

CFD Analysis in Ansys Fluent

CFD analysis has been performed to get the drag coefficient while climbing for the drivetrain calculations. Also CFD analysis was needed for GNCS where it was used to evaluate gusts and flows from all different directions

of the drone, which can be found in chapter 10. For two simple flows, one from directly on top and one directly from the side, the resulting C_D values can be seen in Table 9.8.

Table 9.8: C_D results

Flow direction (20m/s):	From top (0 degrees)	From the side (90 degrees)
Projected area:	0.0235m2	0.0328m2
Drone drag coefficient:	0.25	0.71

The resulting pressure of the side gust flow case can be seen in figure 9.8 and streamlines in figure 9.9.
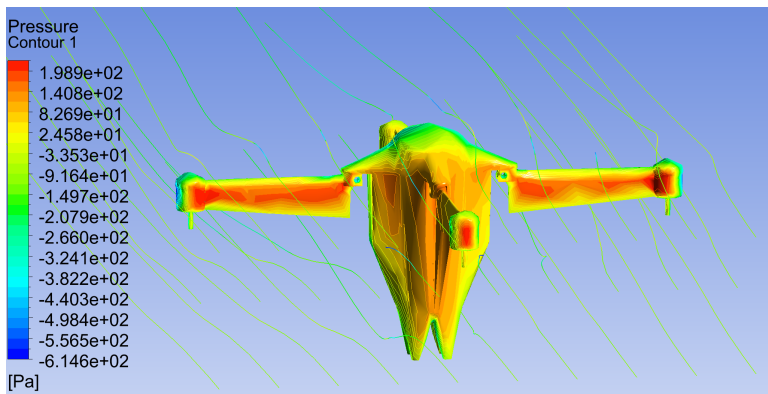
Figure 9.8: Pressure around the drone body when a 20 m/s gust is coming from the side
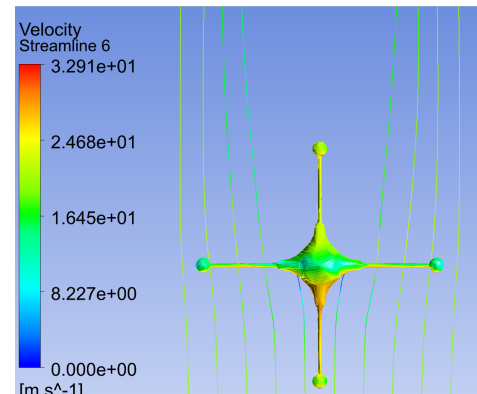
Figure 9.9: Streamlines around the middle of the drone body

Method

The first step of doing an CFD analysis in Ansys Fluent is to create an enclosure. This enclosure can be visualised as a box of air with the drone cut out of it in the middle. To have correct CFD results the outer boundary should be far away enough from the drone in the middle of the enclosure, otherwise the flow could become pinched between the drone and the wall. The upwind clearance is the clearance in front of the drone, downwind behind the drone. Since the flow is unobstructed upwind of the drone, the distance here is taken to be 0.6m between the drone wall and enclosure. Downwind the distance is taken to be one meter since the downwind flow is disturbed by the drone and vortices or pressure waves could be present that should be included in the enclosure for complete results. The side of the enclosure have a wall distance of 0.6m.

The next step is creating the mesh of the enclosure with the drone in there. The mesh generation can be done automatically by Ansys but it is preferred to do it manually so that detailing can be added wherever needed. For this analysis however the standard adaptive sizing was used since otherwise the mesh element count, now 188000, would go over 500000 requiring additional licenses. Since the basic shape and airflow of the drone this was deemed unnecessary. The resulting mesh of the enclosure can be seen in figure 9.10 and the resulting drone body inside the mesh in figure 9.11. During this step the faces of the mesh are given names that can be recognised by the Ansys Fluent program. So for example the top face of the square enclosure mesh is called "velocity inlet" to indicate that that face will be a velocity inlet in the CFD. The same is done with the walls, pressure outlet and drone body.
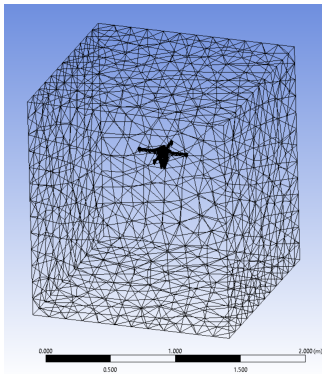
Figure 9.10: Creating the mesh in Ansys
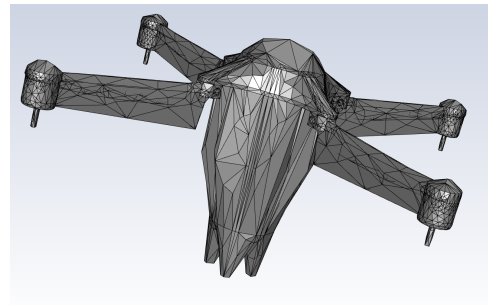
Figure 9.11: Close up of the mesh in Ansys Fluent

Now that the mesh is loaded into Ansys Fluent the flow properties and solver can be selected. First the flow velocity is set to 20m/s at the velocity inlet. This is the speed that will be checked for at different angles of this CFD analysis. Next to that the walls of the flow will be selected. A special setting that is used for the walls is setting the shear of them to 0 so that the flow next to the walls can flow uninterrupted just like in real life. Then a pressure outlet is selected with a gauge pressure of 0. The body of the drone is selected as a wall as well, and coupled to a monitor where the forces around the body wall are being calculated. These calculations are converted to display the C_D of the drone per iteration of the CFD to see if the simulation is converting or diverting. In this C_D calculation the projected area of the drone is used, which is 0.0329 m^2 from the side and 0.0235 m^2 from the top.

Furthermore, the energy equation is turned on in this CFD simulation. This adds negligible simulation time but adds extra realism to the simulation and is therefore not neglected. The air is changed from having a constant density, perfect gas, to be compressible and therefore an ideal gas where the density of the air changes according to the energy equation.

The first iteration will be ran with the Euler Inviscid solver, meaning the flow will be inviscid and now viscous forces will be present in the results. This generally gives a lower drag value but has to be done to properly initialise the CFD simulation.

Then after that the viscous forces are used with using the k-epsilon 2 equation viscous model. The k-epsilon model used is the Realizable one which can handle compressibility better than the standard model. Standard wall functions are used with standard model constants. The C_D monitor from both the inviscid and viscous simulation can be seen in figure 9.12
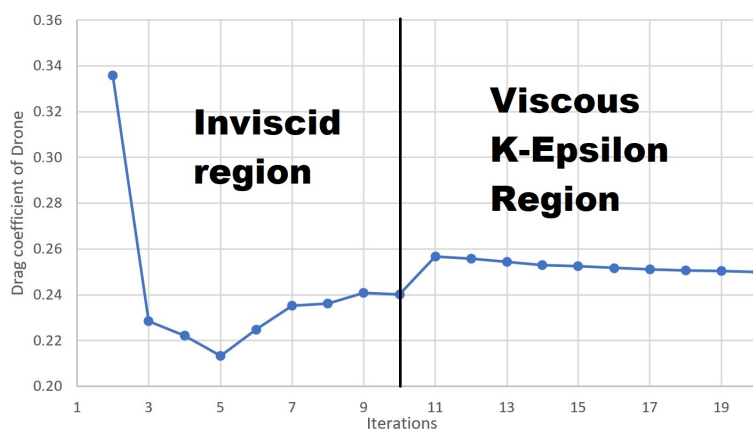
Figure 9.12: Drag coefficient from inviscid to viscous, looking closely the C_D can be seen to increase slightly when adding viscous forces which is expected and in the end the C_D ends up at 0.25

Validation

To validate the results four extra runs have been performed, varying the solver and the flow speed. These runs can be seen in Table 9.9. These results are as expected, since the results do not vary between speeds and that the C_D is indeed higher for K-Epsilon (viscous) vs the inviscid solver.

Table 9.9: Validation runs performed for the CFD C_D calculation

	Flow speed	Simulation	C_D pressure	C_D viscous	Total C_D
Run 1	10	Inviscid	0.243	0	0.243
Run 2	10	K-Epsilon	0.239	0.011	0.250
Run 3	20	Inviscid	0.246	0	0.246
Run 4	20	K-Epsilon	0.241	0.009	0.250

Another way to validate the CFD results is to look at the wall y+ values. Wall functions are used in CFD to estimate the flow speed behaviour close to the wall. The Y+ U+ curve that a wall function estimates can be seen in figure 9.13[13]. When a coarse mesh is chosen, the speed difference per mesh cell become really coarse making the CFD results less reliable. That is why looking at the Y+ values is something that is done to make sure all the parts of the mesh used have acceptable y+ values. For most flows using the standard wall functions having a y+ below 300 is deemed acceptable for the logaritmic log-law part of the velocity curve[14]. The average of the mesh used in this CFD simulation is 67 and can be seen in figure 9.14. The minimum and average value of the y+ are within the acceptable bounds but the maximum Y+ value is a little out of bounds. Since this covers only a small part of the mesh this can be neglected, but for more detailed CFD analysis the mesh would need to be refined to get these Y+ values to acceptable levels.
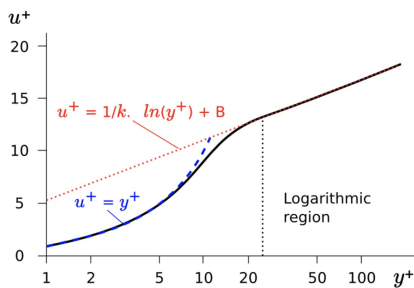
Figure 9.13: Wall Yplus approximation. Standard wall functions use a combination of the linear and logarithmic part to estimate the U+ behaviour
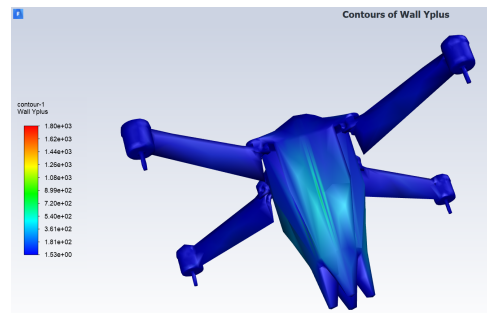
Figure 9.14: Wall Yplus values, minimum is 1.53, average is 67 and parts in the groove are 1790. There the mesh would need to be refined

9.7. Frame analysis

In this section the five main load carrying parts of the frame will be put into FEM analysis to see where reinforcements are needed or weight can be saved. The results of this structural analysis can be found in Table 9.10. Here it can be seen that for the pod bottom, bulkhead and the battery cage a second iteration was done either to save weight or to add weight to improve performance as was done for the bulkhead.

Table 9.10: Summary of performed structural analysis and design changes

	Load	Force	Factor	Max FEM	Material	Max MPa	Margin	Weight
Pod Top 1	Aero	300Pa	1.5	0.39MPa	PETG	63MPa	16000%	13.9g
Pod Top 2	**Aero**	**300Pa**	**1.5**	**1.34MPa**	**PETG**	**63MPa**	**4600%**	**4.3g**
Pod Bottom	**Fall**	**408.75N**	**2.5**	**16MPa**	**PETG**	**63MPa**	**294%**	**51.0g**
Arms	**Thrust**	**18.4**	**2.5**	**21MPa**	**PA12**	**48MPa**	**129%**	**45.6g**
Bulkhead 1	Thrust	14.715N x4	2.0	128MPa	PA12	48MPa	OVER	21.8
Bulkhead 2	**Thrust**	**14.715N x4**	**2.0**	**45MPa**	**PA12**	**48MPa**	**6.7%**	**32.3g**
Batt. Cage 1	Gust	4N & 19.27N	2.0	9.9 & 19MPa	Alu	209MPa	1000%	17.2g
Batt. Cage 2	**Gust**	**19.27N**	**2.0**	**32.8MPa**	**Alu**	**209MPa**	**537%**	**10.7g**

---

[13]Wall function picture `https://www.cfd-online.com/Wiki/Law_of_the_wall`, [accessed 22.6.2021]

[14]Log Law y plus `https://www.afs.enea.it/project/neptunius/docs/fluent/html/th/node99.htm`, [accessed 22.6.2021]

Factor of Safety

In order to ensure the reliability of the aircraft factors of safety are used in order to determine if a design is sufficiently strong. The factor of safety is defined as the load at which a component will fail divided by the expected load a component will endure. Common safety factors for aircraft industry lie between 1.5 and 2.5[15]. For components where all the expected loads can easily be quantified a safety factor of 1.5 shall be used. If the component is required to be design with a 'safe life' philosophy the safety factor will be increased to 2.0. For components where estimating the loads is infeasible, for example dynamic shock loads under an oblique angle on the drone arm, the component will be designed with a safety factor of 2.5 on the static load case.

This will likely make some components stronger and heavier than they in reality need to be. This is a deliberate conservative approach that is needed due to the limited time and resources available. In the post-DSE phases these factors should be evaluated again and perhaps more part- and situation-specific factors can be determined. In the end there is no substitute for real-world testing in realistic use-conditions.

Load cases

In the paragraphs below the chosen load case for each part of the frame will be explained. A picture from Ansys Static Structural will be shown where the load can be seen and in some cases the fixed faces used to solve the problem using the Finite Element Method (FEM).

Pod Top

The Pod Top is not a load carrying part in the assembly but merely there to protect the electronics from the outside and giving the drone an aerodynamic shape. The load case for this part is therefore the aerodynamic drag coming from climbing straight up at high velocity. For consistency with the aerodynamic analysis done a flow speed of 20 m/S has been chosen. From aerodynamic analysis in Ansys Fluent that can be seen in figure 9.15 a load of 200Pa is the result. In figure 9.16 the load case is translated to forces Ansys Static Structural can work with.

Because all the expected loads can be easily quantified a safety factor of 1.5 is used for the pod top resulting in a pressure load of 300Pa.
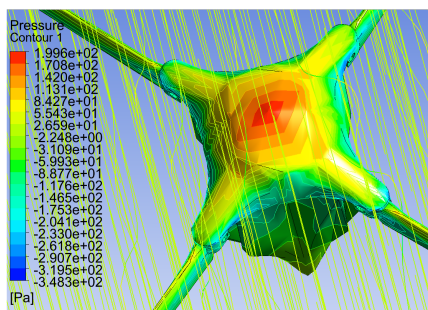
Figure 9.15: Aerodynamic analysis in Fluent showing pressure when flying at 20 m/s
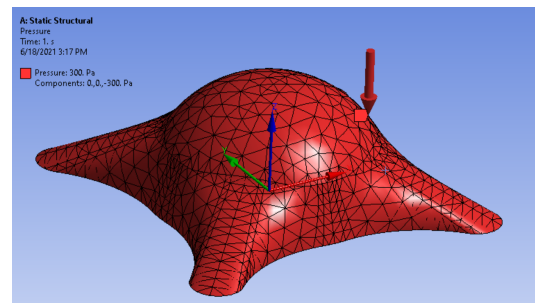
Figure 9.16: Load case of the Pod Top

Pod Bottom

The limiting load case chosen for the Pod Bottom is the load it will undergo when falling from a height of 1 meter. If there is a crash landing from that height, the pod bottom should not crumble more than the distance between it and the battery. The crumple zone in this drone is 3cm. Then using Equation 9.2 the average impact force is calculated to be 163.5N.

A safety factor of 2.5 is used for this load case since estimating the real load is infeasible since the dynamic shock loads are hard to predict. Therefore the final load used is 408.75N.

$$\text{Average impact force} = \frac{m \cdot g \cdot d}{c} = \frac{0.5 \cdot 9.81 \cdot 1}{0.03} = 163.5N \tag{9.2}$$

Where m is the mass of the drone equal to 0.5 kg, g is the gravitational constant equal to 9.81 m/s^2, d is the distance from which the drone is dropped which is 1m and c is the crumple zone distance equal to 0.03 m.

---

[15]Factors of safety, `https://www.engineeringtoolbox.com/factors-safety-fos-d_1624.html`, [Accessed 17-06-2021]
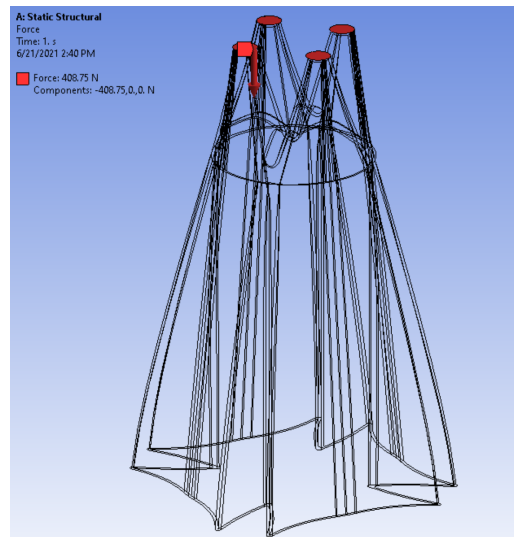
Figure 9.17: Load case of the Pod Bottom

Arms and Hinge

The load case that is used by the arms is based on the maximum thrust the drivetrain can provide. A TWR value of 6 has been used by the drivetrain resulting in a thrust of 7.36N per motor per arm. A safety factor of 2.5 is used for the arm because a safe life design philosophy is used here in combination with hard to predict shock and aerodynamic loads. Applying a safety factor of 2.5 to this load and the final load that will be tested in Ansys is 18.4 N as can be seen in figure 9.18.

Bulkhead

The bulkhead has the same load case as the Arms, being the thrust of the drivetrain. The bulkhead however needs to handle the thrust of four of those drivetrain combinations, so four times 14.715N. In Ansys Static Structural a remote force has been used to assign the force to the bulkhead. A safety factor of 2 is used for the arm because a safe life design philosophy is used here. Using a remote force automatically implements the moments and other forces that come with the load at that remote position, which is the motor location one arm length away from the bulkhead. This can be seen in figure 9.19.
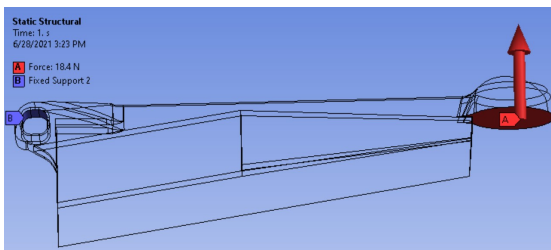
Figure 9.18: Load case of the Arm
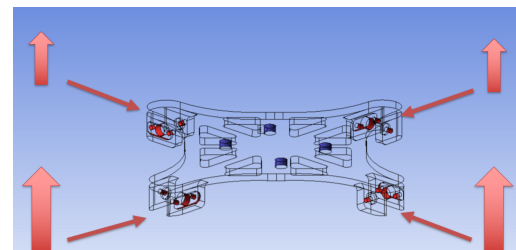
Figure 9.19: Load case of the Bulkhead with the remote forces

Battery Cage

For the battery case two different load cases were checked. The first load case is the load resulting from a gust of 20 m/s hitting the side of the drone. From the aerodynamic analysis in Ansys Fluent it was found to create a drag force of 6.11 N. Using F = ma with a weight of 500 g an acceleration of 1.25 m/s^2 can be expected. The battery weighs 163.7 g and with this acceleration will produce a force of 2.00 N. Since a safety factor of 2 is chosen for this part the final side load will be 4.00 N. This side way force has then been put into Ansys affecting both sides of the battery cage and can be seen in figure 9.20.

The second load case comes from the acceleration caused by the drivetrain. A TWR of 6 and instant thrust are assumed. This gives an acceleration of 6 m/s^2, resulting in a force of 9.635N from the battery. Applying a safety factor of 2 again results in a load of 19.27 N pointing downwards as can be seen in figure 9.21.
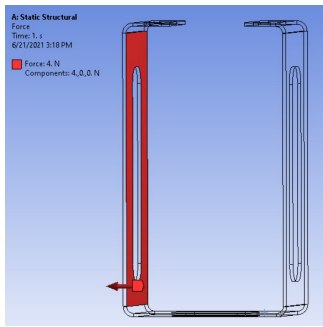
Figure 9.20: Load case of the Battery Cage with a side force from a gust
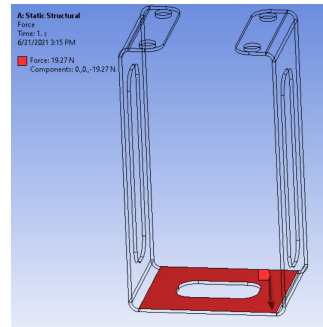
Figure 9.21: Load case of the Battery Cage with a straight force from instant thrust

Finite element analysis

Pod Top

The FEM results of the pod top can be seen in figure 9.22 with the scaled displacement. The maximum force found is 0.39MPa which is lower than the maximum tensile strength of 63MPa that is from PETG.
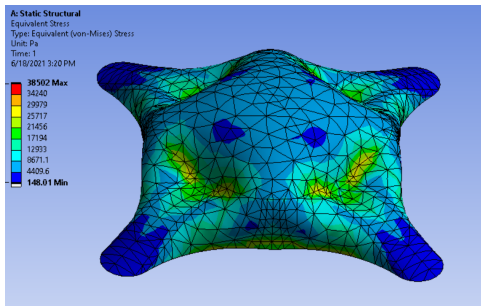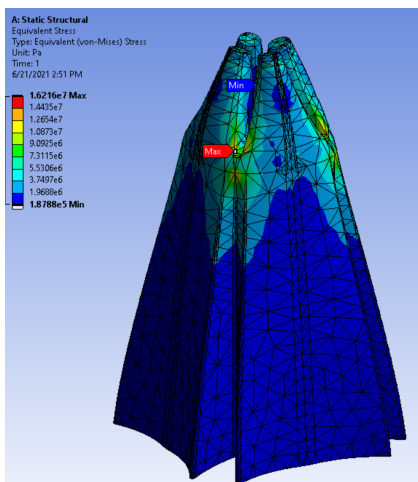

Figure 9.22: FEM of Pod Top with scaled displacements
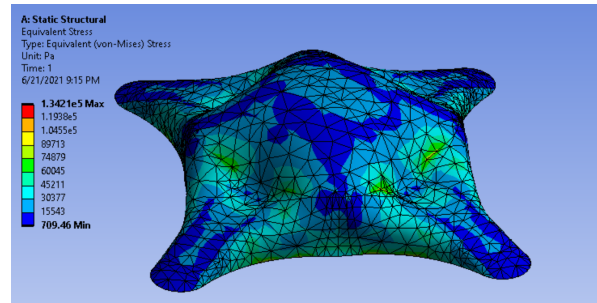
Figure 9.23: FEM of Pod Top with a wall thickness of 0.3mm instead of 1mm

Because the maximum stress compared to the maximum allowable stress is so small, weight can be saved by making the pod top thinner. The wall thickness is decreased from 1mm to 0.3mm and the new FEM results from this change can be seen in figure 9.23. The weight of the pod top decreased from 13.9 grams to 4.3 grams.

Pod Bottom

The FEM results of the pod bottom can be seen in figure 9.24 with the scaled displacement of the feet and in figure 9.25 with the true displacements. The maximum force found is 16MPa which is lower than the maximum tensile strength of 63MPa that is from PETG.

Figure 9.24: FEM of Pod Bottom with scaled displacements
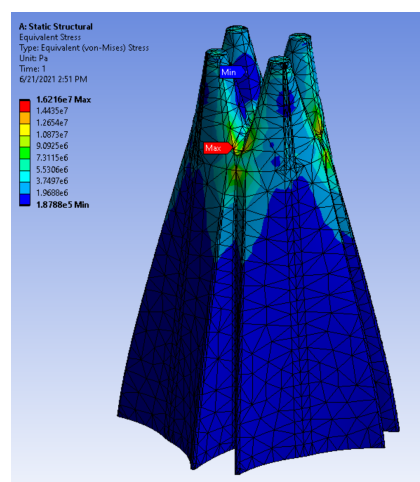
Figure 9.25: FEM of Pod Bottom with true displacements

Arms and Hinge

The FEM results of the arm can be seen in figure 9.26. The maximum force found is 21MPa which is lower than the maximum tensile strength of 48MPa that is from 3D printed PA12[16].
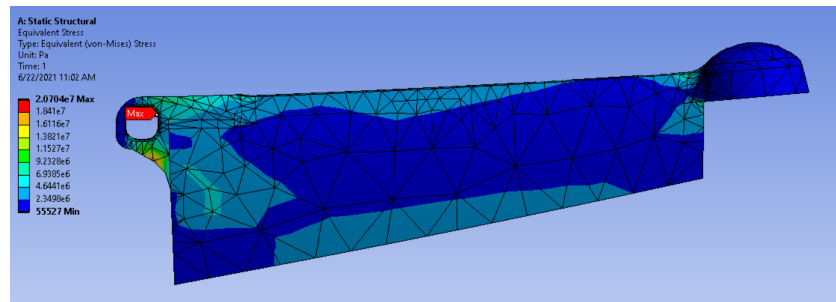
Figure 9.26: FEM of Arm with scaled displacements

Bulkhead

For the first iteration of the bulkhead the overall loads can be seen in figure 9.27. The maximum force here is 128MPa at the location that can be seen in figure 9.28. The maximum tensile strength of 3D printed PA12 is 48MPa so this bulkhead will fail under the given load case.
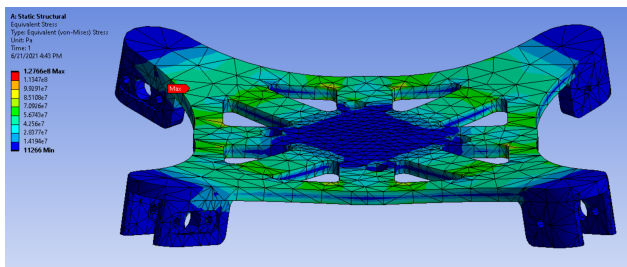
Figure 9.27: FEM of New Bulkhead with scaled displacements
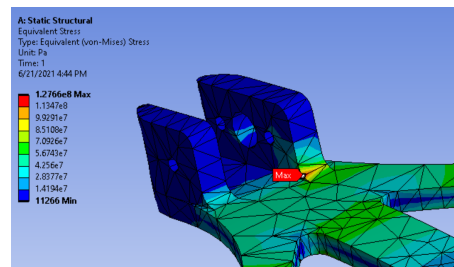
Figure 9.28: FEM of Bulkhead showing the maximum stress

Therefore the bulkhead got a new iteration to accompany for the high loads. The first big change that was made is increasing the thickness of the bulkhead from 3mm to 4mm. Then for the place where the maximum load has been observed to be a new chamfered edge has been added to facilitate better force transportation. Then new FEM analysis has been that can be seen in figure 9.29. In figure 9.30 the new chamfered edge can be seen as well as the place of the new maximum stress of 45MPa which is below the maximum tensile strength of 3D printed PA12.

Figure 9.30: FEM of Bulkhead showing the new maximum stress of 45MPa and the place where the old maximum was, which is now 38MPa instead of 128MPa

Figure 9.29: FEM of New Bulkhead with scaled displacements

To see how the bulkhead changed between the two iterations, look at figure 9.31 to see the old bulkhead and look at figure 9.32 to see the result of the new bulkhead. Changes made are increasing the thickness, creating a stronger chamfered edge coming from the hinge attachment of the bulkhead and finally decreasing the lightning hole size. The final weight increased from 21.8 grams to 32.3 grams.

---

[16]Tensile strength PA12 `https://www.hubs.com/3d-printing/plastic/nylon/hp-pa-12/`, [accessed 22.6.2021]
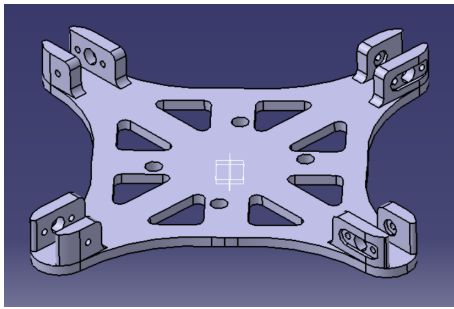
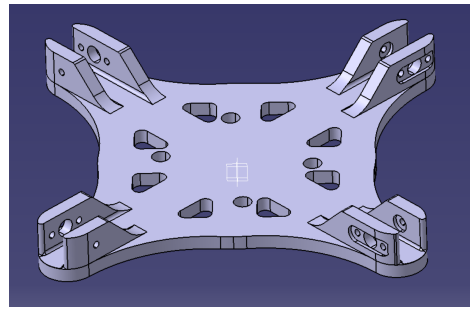**Figure 9.31:** Bulkhead before improvements

Figure 9.32: Bulkhead after improvements

Battery Cage

The battery cage is made of sheetmetal aluminium which has a maximum tensile strenght of 209MPa. The first load case that has been tested in Ansys is the side load case and can be seen in figure 9.33 with the scaled displacement and in figure 9.34 with true displacements. The maximum load found from this side load case is 9.9MPa.
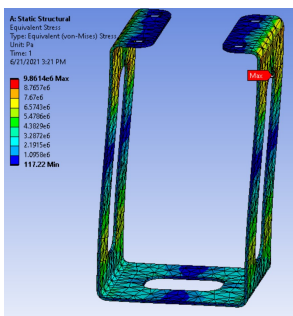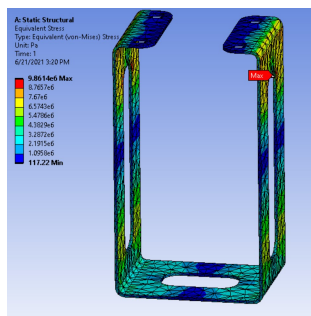

Figure 9.33: FEM of the old battery cage with scaled displacements

Figure 9.34: FEM of the old battery cage with true displacements
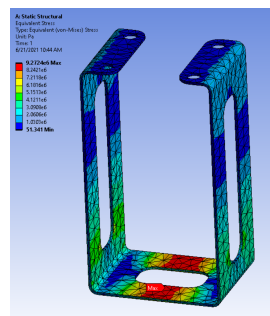
Figure 9.35: FEM of the old battery cage under a vertical load due to thrust
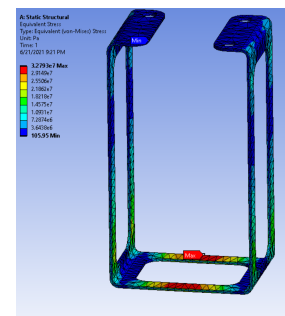
Figure 9.36: FEM of the new battery cage under a vertical load due to thrust

In figure 9.35 the FEM analysis can be seen from the vertical load of 19.27N. The maximum resulting stress is 19MPa which is higher than the side load case. Because of the high maximum tensile strength of the aluminium of 209MPa and the low resulting stressed of the FEM analysis, weight can be saved on this part. Increasing the hole sizes gives the new FEM analysis that can be seen in figure 9.36. Here the new maximum stress only increased to 33MPa while saving almost 7 grams of the final part.

To see how the battery cage changed between the two iterations, look again at figure 9.35 to see the old battery cage and look at figure 9.36 to see the result of the new battery cage. Changes made are increasing the hole size on the sides and bottom of the cage. The weight decreased from 17.2 grams to 10.7 grams.

9.8. Requirement Compliance

In this section the compliance of the frame with the set subsystem requirements is checked.

Buoyancy: The buoyancy of the drone has been checked based on the volumes of the parts in Catia. Adding up the volumes from the arms (0.044L), drivetrain (0.056L), the pod top (0.124L) and pod bottom (0.486L) gives a total volume of 0.71L resulting in a buoyancy of 710 grams. This is more than the weight of the drone and therefore it will be able to float, floating time of the water has to be validated by testing in the post DSE phase.

Table 9.11: Compliance matrix for the frame subsystem

ID	Requirement	Compliance	Comment
SUBSYST-STRC-01	The structure weight shall not exceed 55 grams	x	Struc. exceeds weight by 100 g
SUBSYST-STRC-04	The structure shall be able to operate in a temperature range from -20 to +40 °C	tbd	
SUBSYST-STRC-10	The structure cost shall not exceed 30 euros	x	Struc. exceeds cost by 45 euros
STAK-GENR-03	The drone shall not have exposed electronics	✓	
SYST-GENR-03	The maximum dimensions of the drone in storage mode shall not exceed 200 x 100 x 100 mm (length, width, height)	✓	
SYST-GENR-13	The drone shall fit through an opening with minimum dimensions of 40x40 cm	✓	
SYST-RISK-01	The critical components shall be designed to have safe life or fail safe philosophy implementation	✓	
STAK-SUST-01	The drone shall be able to be repaired in a modular fashion	✓	
SYST-SUST-11	Each structural component of the drone shall be evaluated to determine if it can be replaced with a 3D printed part	✓	
SYST-SUST-03-A	The drone shall contain any sparks and fire within the system in case of short-circuit	✓	
SYST-RISK-10	The drone shall be IP rated to at least IP 55	tbd	Requires real-world testing
SUBSYST-STRC-05	The structure shall be able to withstand a force of <tbd> N	tbd	*

* Iill-defined, but important. See section 9.7 and section 9.9

9.9. Conclusion

In the end a strong and sustainable frame has been designed in order to protect and provide structure to the other drone components. Due to the choice of only considering recyclable materials the drone is heavier that it otherwise would be. Furthermore the heavy emphasis on reduction of the drones environmental impact in terms of eco-toxicity contributes to the weight in the specific case of the bulkhead. Further research needs to be performed if the risk of eco-toxicity can be mitigated using coating or other means. For now the risk avoided by avoiding these hazardous materials altogether.

In future phases the strength requirements placed on the frame need to be re-evaluated. In the currently allotted time-span it was not possible to define every possible load case for each component and as such conservative safety factors were used. It is important that values are defined for each load case that are meaningful in the real world. Especially aero-elastic effects stemming from the interaction between the propeller and the airstream could pose an unexpected failure mode.

It is also likely that the weight of this subsystem could be significantly reduced using further design iterations. For example, preliminary investigations show that at least 35% of the weight of the arms could be removed without reducing the failure load, but actualising these results was not possible given the time budget. The advantages of the choice for additive manufacturing for many parts could be further leveraged since it allows for heavily optimised organic structures.

10. Guidance, Navigation, Control and Stability

This chapter will elaborate on the design decisions made regarding guidance, navigation, control and stability. In section 10.1 the results of the chapter are combined and summarised. References to relevant sections are made, and the general navigation strategy is laid out.

10.1. General Navigation Strategy

This section aims to introduce and present the results of this chapter. It will elaborate and summarise the full navigation strategy. To aid in this overview, several diagrams are made, which can be found down below.

For example, an accident in a forest will be considered. The autonomous decisions will be mentioned and referenced where necessary. On start up, the drone will use its Light Dependent Resistor (LDR) to measure the surrounding light levels and decides to activate the warning LEDs if necessary. Before take-off, the drone checks if a GNSS connection can be established. If established, the drone will execute the height map algorithm. A path of least resistance with respect to elevation is estimated, which yields a starting heading. Moreover, the user location will be stored in memory. In case a GNSS signal cannot be established, a heading will arbitrarily selected until GNSS signal is established. The path of the drone travelled will be estimated by using Inertial Measurement Unit (IMU) data and a drag model. This is elaborated upon in section 10.9.

Using the algorithms as described in section 10.8, combined with the field of view provided by the senors in section 10.3, the drone will traverse the forest. The computation of these algorithm is performed by the companion computer, of which a detailed description can be found in section 10.7.

To minimise backtracking, this traversal will be done in the selected heading. If the drone does not find suitable paths out of obstacles, it will rotate in hover to obtain a new field of view. During traversal, stability and control is of most importance. A more detailed description of the stability and control characteristics and be found in section 10.4 and in section 10.5 respectively. The control of the motors to ensure stability and control is taken care of by the flight controller, which is elaborated upon in section 10.6.

While traversing the forest, the space above the drone will continuously be sampled for obstructions. If the sky is clear of obstacles the drone will probe up and breach the canopy if possible. The drone will slowly ascend until a certain height is estimated, from whereon it will start ascending faster and faster, until connection with the emergency services can be established, or the maximum height is reached. If secondary communication coverage is close by and GNSS available and it is expected to be more economical to fly towards this position, the drone may opt to pursue this way point instead of climbing up, with safety margin in altitude with regards to the local terrain. There are cases where the canopy cannot be breached, or the drone seems to get stuck in the forest. The longer the drone samples around in the forest, the higher the risk tolerance will get. This means, that the margin necessary to pass through a found hole will shrink the longer time proceeds. This is only the case in the default SOS mission type. In the "I am lost" mission type the drone will not take unnecessary risk and eventually try to return close to the user, or not takeoff at all, until re-positions the drone to a new start site.

After a certain amount of time of probing around, the drone will estimate the density of the obstruction, and attempt to proceed/ breach the canopy in that way. This should however really be considered a last hope attempt, since damage to the drone is almost inevitable. Assuming hover altitude is reached the drone starts broadcasting the message. If confirmation is received, the drone descents back to earth, backtracking the way it flew up. If confirmation is not received, the drone will continue climbing up till the maximum altitude is reached. It will hover there as long as possible, which is approximately 25 minutes when fully charged and in good weather conditions, where after the drone will return back to earth.
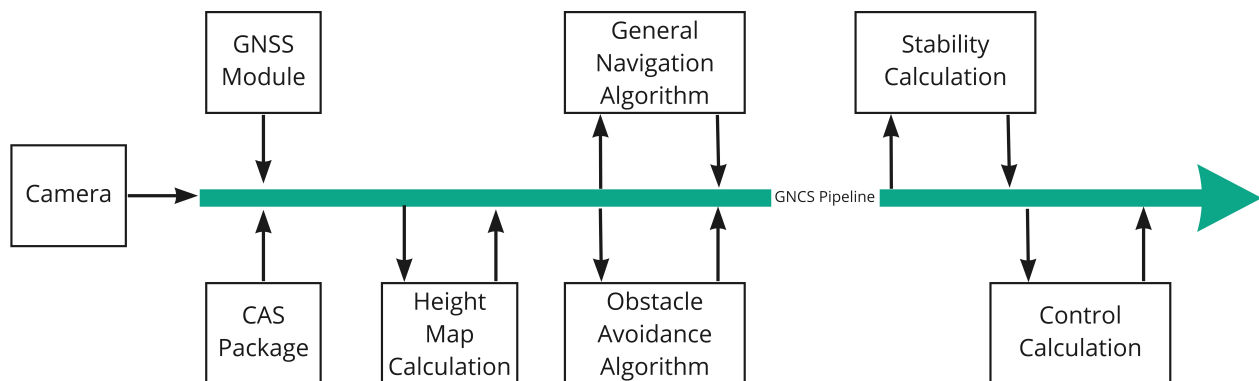

Figure 10.1: GNCS pipeline

A safe distance above the first obstacles on the way down, the drone will evaluate its battery level. It will either attempt to land right there on the spot, or if battery allows, attempts to trace back the path to the user as far as possible, before landing. This required landing with no message confirmation has a few advantages.

The energy spend for landing is comparatively small compared to the amount of energy spend during hover as described in chapter 8. Not a lot of extra hover time could be achieved staying at altitude. While on contrast after landing, the visibility of the drone might aid in the rescue operations. When landed, the motors of the drone will shut down, and the buzzer locator will be activated. This descriptive process can be found in detail in diagram form in the software diagram presented down below, and the functional flow diagram in chapter 5. The GNCS pipeline in figure 10.1 presents the above described description in a graphical way.

10.2. GNCS Requirements

Initially a number of requirements were conceived in [1] that were to be utilised in designing the GNCS subsystem. However in the detailed design phase, a critical reflection on the requirements resulted in a number of requirements being dropped, as some were outdated and still largely tied to the possibility of a fixed wing concept. The following requirements were kept as they were deemed relevant for the concept at hand.

- **SUBSYST-GNCS-02-REV-1**: The guidance and navigation subsystem shall be able to locate the drone with an accuracy of 30 m if GNSS data is available
- **SUBSYST-GNCS-09**: The control subsystem shall ensure the drone is flying within its flight envelope
- **SUBSYST-GNCS-13**: The guidance and navigation subsystem shall have a power at most 3 W
- **SUBSYST-GNCS-14**: The guidance and navigation subsystem shall use at most 12 V
- **SUBSYST-GNCS-15**: The guidance and navigation subsystem cost shall not exceed 175 euros
- **SUBSYST-GNCS-16**: The guidance and navigation subsystem weight shall not exceed 35 grams.

10.3. Navigation Sensor Selection

The starting point of the GNCS subsystem is the determination of the onboard sensors. This is an important first step, since this dictates other aspects of the GNCS.

The flow of sensor selection starts with a qualitative look at the types of sensor available and selects a few to analyse in more detail. A catalogue of sensors of the identified is created, from which several sensor packages are created. These packages are then formally traded off via the AHP method.

Literature Study

In the Baseline report [1], several types of sensors were identified, namely: Cameras, Lidar, Radar, Ultrasonic and GNSS. Now the concept has been chosen, and the operating environment better defined, these sensors types will be re-evaluated, aside from GNSS, which is now handled by the communications subsystem.

- **Cameras:** Using a camera, the received images can be used to identify objects. This, however, is computationally heavy as some form of neural network would be needed to recognise objects. Furthermore, a camera is significantly hindered during nighttime operations, and is discarded as a CAS sensor. It should however be noted that a camera is being considered for the purposes of the operation subsystem, so this can perhaps have a secondary use for the CAS.
- **Lidar:** Lidar, or light detection and ranging, uses reflected light to calculate the position of objects. Lidar sensors can be categorised into major groups: rotating and non-rotating. Although a rotating sensor gives a better view of the surrounding environment, it is unlikely to be suitable for this project given the cost and mass budgets. Furthermore, lidar is perceptible to weather conditions[1].
- **Radar:** Radar uses reflected radio waves to detect objects. Radar can also detect the velocity of an obstacle. However, in the initial search, the smallest radar module was found to be outside of the budgets. Furthermore, as dynamic obstacles are no longer considered, one of the advantages of radar is neglected[2].
- **Ultrasonic:** The last sensor type to be examined is the ultrasonic sensor. Though ultrasonic works on a similar principle as radar, it instead uses sound waves. As these propagates through a medium, ultrasonic is sensitive to changes in the medium, e.g. temperature fluctuations[3].

---

[1] Rain on Lidar Sensors – What is the effect on Performance?, `https://blog.lidarnews.com/rain-lidar-sensor-effect-performance/`, [accessed 22.06.2021]

[2] What is a radar sensor?, `https://www.fierceelectronics.com/sensors/what-a-radar-sensor`, [accessed 22.06.2021]

[3] Advantages of Ultrasonic sensor | Disadvantages of Ultrasonic sensor, `https://www.rfwireless-world.com/Terminology/Advantages-and-disadvantages-of-Ultrasonic-Sensor.html`, [accessed 22.06.2021]

Examining these sensors, the camera and radar sensors are excluded for the CAS package. Specific Ultrasonic and lidar sensors will now be evaluated to generate the CAS sensor package.

CAS Sensor Package Generation

Though this section examines all of the onboard sensors, a majority are contained within other components (e.g. the IMU within the flight controller). However, the CAS still need to be chosen. In the literature study, Lidar and Ultrasonic sensor types were chosen, from which specific sensors can now be analysed. The starting point of this was to compile a catalogue of possible sensors. From this catalogue, the sensors were ranked based on the ratios of range / cost and range / weight, since range, cost and weight are considered to be the most important factors. These ratios are then normalised and multiplied together to find the best sensors, as shown in Table 10.2. The mass and cost are equally important. The higher the result, the better the sensor. The top sensors are then used in the concept generation.

Table 10.1: Sensors from which CAS packages generated

Name	Minimum Range [cm]	Maximum Range [cm]	Sensing Angle [deg]	Cost [€]	Mass [g]
Ultrasonic Distance Sensor (HC-SR04)[4]	2	400	30	2.33	9
Benewake Lidar TFmini 0.3-12m[5]	30	1200	1.15	45.26	5
TFmini-S Lidar Module[6]	10	1200	2.3	39.95	6.1
SRF01 Ultrasonic Sensor[7]	18	600	-	30.74	2.7
SRF02 Ultrasonic Sensor[8]	16	600	38	19.56	4.6
Maxbotix Ultrasonic Rangefinder - LV-EZ4[9]	0	645	45	22.11	4.23
US-100 Ultrasonic Distance Sensor[10]	2	450	15	6.21	9

Table 10.2: Index Values

Name	Range / Cost [cm / €]	Normalised [-]	Range / Weight [cm / g]	Normalised [-]	Result
Ultrasonic Distance Sensor (HC-SR04)	171.67	1.000	44.44	0.185	0.185
Benewake TFmini 0.3-12m	26.51	0.154	240.00	1.000	0.154
TFmini-S Lidar Module	30.04	0.175	196.72	0.820	0.143
SRF01 Ultrasonic Sensor	19.52	0.114	222.22	0.926	0.105
SRF02 Ultrasonic Sensor	30.67	0.179	130.43	0.543	0.097
Maxbotix Ultrasonic Rangefinder - LV-EZ4	29.17	0.170	152.48	0.635	0.108
US-100 Ultrasonic Distance Sensor	72.46	0.422	50.00	0.208	0.088

From these sensors, four CAS sensor packages are then created:

1. 4 x Ultrasonic Distance Sensor (HC-SR04), 1 x Benewake TFmini 0.3-12m

2. 1 x TFmini-S Lidar Module , 1 x US-100 Ultrasonic Distance Sensor, 2 x Ultrasonic Distance Sensor (HC-SR04)

3. 2 x US-100 Ultrasonic Distance Sensor, 2 x Ultrasonic Distance Sensor (HC-SR04)

4. 3 x Ultrasonic Distance Sensor (HC-SR04), 2 x SRF02 Ultrasonic Sensor

---

[4]Ultrasonic Distance Sensor, `https://thepihut.com/products/ultrasonic-distance-sensor-hcsr04`, [accessed 14.06.2021]

[5]Benewake TFmini 0.3-12m 100Hz LiDAR Module, `https://24loop.com/shop/benewake-tfmini-0-3-12m-100hz-lidar-module-laser-radar-ser` [accessed 14.06.2021]

[6]TFMINI-S LIDAR MODULE, `https://www.antratek.nl/tfmini-lidar-module`, [accessed 14.06.2021]

[7]SRF01 ultrasonic sensor, `https://thepihut.com/products/srf01-ultrasonic-sensor`, [accessed 14.06.2021]

[8]SRF02 Ultrasonic Sensor, `https://wiki.dfrobot.com/SRF02_Ultrasonic_sensor__SKU_SEN0005_`, [accessed 14.06.2021]

[9]Maxbotix Ultrasonic Rangefinder - HRLV-EZ4, `https://thepihut.com/products/maxbotix-ultrasonic-rangefinder-hrlv-ez4`, [accessed 14.06.2021]

[10]US-100 Ultrasonic Distance Sensor, `https://thepihut.com/products/us-100-ultrasonic-distance-sensor-3v-or-5v-logic`, [accessed 14.06.2021]

The sensors are arranged for the best coverage, whilst also aiming for diverse packages to be fed into the trade-off. These four CAS options can now be traded-off to find the most suitable option.

CAS Package Trade-off

Concept 4, utilising 3 x HC-SR04 and 2 x SRF-02 sensors, won the trade-off. This concept has a good field of view. The CAS sensor trade-off criteria, and their pairwise comparisons, are presented in Table 10.3.

Table 10.3: CAS sensor trade-off criteria relative importance table

	Mass	Cost	Maximum Range	Sphere Coverage	Condition Limitations	Power	Redundancy
Mass	1.00	1.00	1.00	1.00	3.00	2.00	4.00
Cost	1.00	1.00	1.00	1.00	2.00	2.00	4.00
Maximum Range	1.00	1.00	1.00	1.00	2.00	2.00	3.00
Sphere Coverage	1.00	1.00	1.00	1.00	1.00	2.00	2.00
Condition Limitations	0.33	0.50	0.50	1.00	1.00	1.00	2.00
Power	0.50	0.50	0.50	0.50	1.00	1.00	1.00
Redundancy	0.25	0.25	0.33	0.50	0.50	1.00	1.00

A few of the criteria are explained in more detail:

- **Sphere Coverage:** A measure of the coverage the sensors give at a moment in time. A higher sphere coverage is preferable. Lidar, for example, has a good maximum range, but poor field of view. This criteria is scored based on the top coverage and side coverage, since these are distinct directions the drone needs to sense.
- **Condition Limitations:** How much are the sensors affected by the ambient conditions, e.g. weather. Criteria scored on percentage of sensors that are resilient to weather conditions.
- **Redundancy:** How prone is the package to total failure. If a sensor fails, the drone should still be able to sense in one direction. Criteria scored on the number of additional sensors per sensing direction.

The other criteria (mass, cost, maximum range and power) and quantitative and are scored using the method explained in section 4.1. The concept scores are presented in Table 10.4

Table 10.4: CAS packages trade-off scores

	Mass	Cost	Maximum Range	Sphere Coverage	Condition Limitations	Power	Redundancy	Weighted Result
Weight	0.206	0.193	0.184	0.162	0.104	0.088	0.063	
Concept 1	1	0	2	2	1	0	1	1.066
Concept 2	1	3	2	1	0	2	2	1.617
Concept 3	3	2	0	1	2	2	2	1.675
Concept 4	1	2	1	3	2	1	2	1.684

Final CAS Sensor Package Analysis

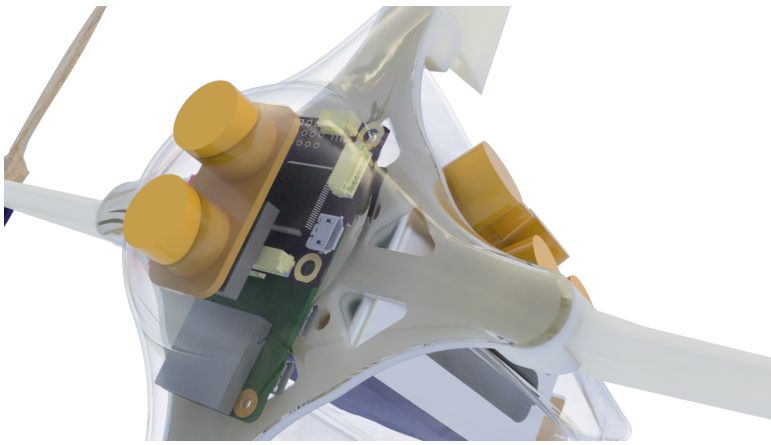The selected concept is now analysed in further detail. The sensor package field of view is seen in figure 10.3.
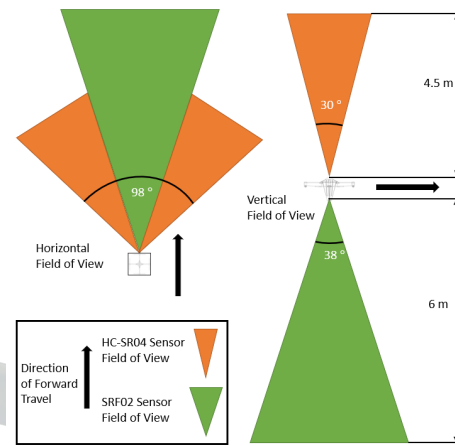
Figure 10.2: CAS sensors layout

Figure 10.3: CAS sensors field of view

In the horizontal view, the front-facing SRF02 sensor can confirm that the drone has a clear path at a distance of 1.5m and can indicate obstacles at a distance of up to 6m. The front facing HC-SR04 sensors are used for a peripheral view in case the drone finds its path blocked. The vertical sensors act in a similar way. The primary use of the vertical sensors is to help the drone find an opening to climb and descend through, though this can also aid in the obstacle avoidance. It should be noted that the sensors need a clear view, so they stick through the case, as can be seen in figure 10.2.

Other Sensors

So far, this section has focused on the CAS sensors, but a few other sensors also need to considered in this section, namely a smoke sensor and a light sensor. The light sensor is used to differentiate between day and night, whereas the smoke sensor is used primarily to avoid forest fires.

The light sensor is facilitated through the inclusion of an Light Dependant Resistor (LDR), which changes its resistance based on the amount of light received. A quick market search found cost-effective LDRs[11] for less than €1. The LDR can be wired from the companion computer.

The smoke sensor however requires some more analysis. First, it is important to consider what is meant by a smoke sensor. As the sensor should be able to detect and avoid forest fires, the sensor needs to be able to detect smoke, carbon dioxide, methane or carbon monoxide[28]. The MQ range of sensors was considered, specifically the MQ-2[12], MQ-7[13] and MQ-135[14]. Each sensor is designed to detect different types of aerosols. However, the addition would violate the cost budget by 20 %. Therefore, a smoke sensor is excluded. Furthermore, it can only indicate the presence of smoke (And thus a forest fire). No indication is given of the direction and the drone still has to guess a direction to fly in, so the usefulness is low.

Discussion & Conclusion

This section has examined the CAS and other sensors needed in the operation of the drone. The chosen sensor package provides a simple sensing option which is sufficient in aiding the drone to find open sky.

In the CAS sensor package generation, several sensor packages were generated from a catalogue of sensors. Here some deficiencies can be identified. Though some time was spent analysing current market solutions, it is noted that some more suitable sensors could have been missed. Furthermore, the generation of concepts only considers four possible packages that met the budgets. These two points mean that more appropriate sensor packages could exist, but the chosen package is sufficient given the resource constraints.

It also noted that the ultrasonic sensors can only return an obstacle range, as opposed to an exact location as with other sensors (e.g. lidar). This has implications later for the obstacle avoidance algorithm, as discussed in section 10.8. Though packages using lidar were considered, ultrasonic-only packages performed better as the total sphere coverage is higher (consider the prime ultrasonic sensor (HC-SR04) versus the prime lidar

---

[11]Silonex, LDR, `https://uk.rs-online.com/web/p/ldr-light-dependent-resistors/4661996/`, [accessed 20.06.2021]

[12]MQ-2 Gas Sensor Module, `https://www.tinytronics.nl/shop/en/sensors/temperature-air-humidity/mq-2-gas-sensor-module`, [accessed 20.06.2021]

[13]MQ-7 Gas Sensor, `https://www.tinytronics.nl/shop/en/sensors/temperature-air-humidity/mq-7-gas-sensor-module`, [accessed 20.06.2021]

[14]MQ-135 Gas Sensor, `https://www.tinytronics.nl/shop/en/sensors/mq-135-gas-sensor-module`, [accessed 20.06.2021]

sensor (Benewake TF mini)). The ultrasonic sensor has a field of view of 30 degrees, whereas the lidar has a field of view of 2.3 degrees - a considerable difference. A constraint also stemmed from the mass and cost budgets - competing sensors would typically score well on one parameter, but rarely both. This is another reason why lidar is not included. If the cost and mass budget of the sensor package were increased in later iterations, an option including lidar could be included, giving a better obstacle map. It was also mentioned that lidar sensors are typically rotated. A rotating lidar returns a larger field of view, but at the added mass and volume. This also adds a point of failure, as the rotating mechanism needs to continually rotate. The lightest commercial package found weighed 200g, which is outside the budget. In terms of weather conditions, lidar was found to be more susceptible to weather conditions, such as rain, whereas ultrasonic sensors are sensitive to short term changes in the medium (for example, heat from a forest fire).

Another downside of the chosen sensors is the impact on repairability. This is because the requirement of the ultrasonic sensors needing a clear view of the environment has to be balanced against keeping the drone sealed from water. To achieve this, sealant of some form is needed, thus another step to swapping out faulty sensors, though this should be evaluated

Recommendation: If the mass or cost budgets was larger, the ideal sensor package would rely on a combination of sensors, combining the advantages of lidar and ultrasonic. Furthermore, some rotating sensor would be included, as this would provide a larger field of view with more detail, though this needs to be weighed against the increased computational cost.

10.4. Drone Stability

Attitude stabilisation

A quadcopter is inherently unstable[2], as by itself there are no restoring forces that would lead to a a restoring motion towards the assumed stable state[23]. Therefore, an active control strategy needs to be implemented to keep the drone from crashing. Setting up a dedicated controller is not required, as the chosen flight computer is able to run the chosen Autopilot system, Ardupilot, with all included features. Attitude control is implemented via a standard Proportional Integral Derivative (PID) control loop.

For a more in depth overview of the inner workings of a traditional PID controller, and the Ardupilot implementation, the reader is recommended to refer to literature[23].

Evaluation of Wind Response

In order to analyse the performance of the drone with respect to wind influence, the following strategy was chosen: For a small selected number of angles, the fluid simulation module of Ansys was used to estimate the frame drag generation of a constant wind of 20 m/s. Rotor drag is neglected for simplicity. In general, the method relies on the following simplifications:

1. The frame is assumed to be completely rigid
2. The presence of rotors is ignored
3. Thrust and rotor torques are modelled as static forces
4. Moments around the symmetry axis are assumed to be negligible for symmetric angle
5. Constant frame drag is assumed to be the only influence of wind
6. The individual thrust contributions are assumed to stay aligned with the longitudinal axis of the quad copter

After literature [23], the thrust and torque of the propulsion units can be modelled as follows:

$$\sum_{i=1}^{i=4}(\frac{C_M}{C_T})_i(-1)^{i+1} = -\frac{M_z}{D}$$
(10.3)

$$T = C_T\rho(\frac{N}{60})^2D^4 \quad (10.1) \qquad Q = C_M\rho(\frac{N}{60})^2D^5 \quad (10.2)$$

In Equation 10.1 and 10.2, N represents the rpm, D the rotor diameter, and C_M, C_T the torque and thrust coefficient respectively. Requiring the sum of moments around the z-axis to be zero, Equation 10.3 can be derived. Furthermore the assumption of C_M/C_T=constant is made for the linear system presented in Equation 10.4. Note that a positive torque corresponds to a clockwise orientation around an axis. The system can
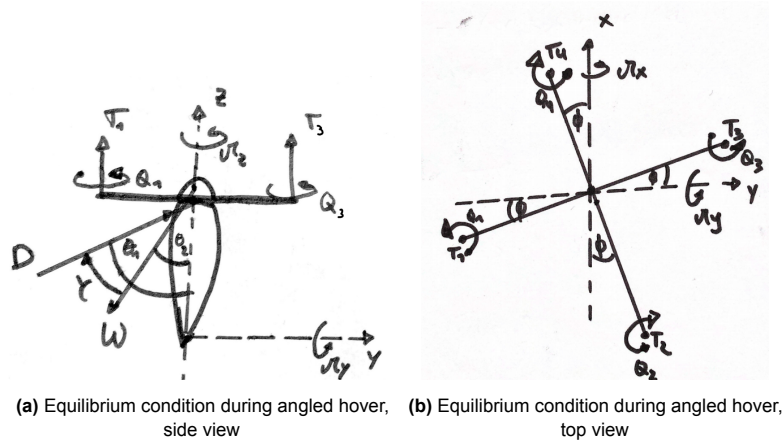
(a) Equilibrium condition during angled hover, side view

(b) Equilibrium condition during angled hover, top view

Figure 10.4: Equilibrium conditions from different view

be expressed in matrix form, d represents the horizontal distance from rotor center to center line, d_{cg-rp} the vertical distance between center of gravity and rotor plane :

$$
\begin{bmatrix}
1 & -1 & 1 & -1 \\
1 & 1 & 1 & 1 \\
-sin(\Phi)d & -cos(\Phi)d & sin(\Phi)d & cos(\Phi)d \\
cos(\Phi)d & -sin(\Phi)d & -cos(\Phi)d & sin(\Phi)
\end{bmatrix}
\begin{pmatrix} T_1 \\ T_2 \\ T_3 \\ T_4 \end{pmatrix}
=
\begin{pmatrix}
-\frac{M_z}{D} \\
cos(\theta_2)W - cos(\theta_1)D \\
-M_y + d_{cg-rp}W sin(\theta_2) \\
-M_x
\end{pmatrix}
\tag{10.4}
$$

Additionally, it is clear that all thrusters are essentially providing control in one direction only. As a result, all forces perpendicular to the thrust directions need to equate to zero without the direct input of thrust. This can be achieved by selecting a suitable angle θ_2, such that the perpendicular components of weight and drag with respect to the thrust line cancel out. This condition can be represented as:

$$
D sin(\theta_1) - W sin(\theta_2) = 0
\tag{10.5}
$$

Technically, this condition would already be enough to establish a flight path angle first and subsequently the resultant thrust levels required for the individual thrusters. The angles θ_1 and θ_2 however are coupled by the rotation of the drone. Therefore the interpretation of the output of this tool is as follows: For a given discrepancy between the flight path angle θ_2 and relative wind angle θ_1, what thrust levels are necessary to fulfil a steady state condition. The motivation here lies in the fact that as the drone rotates, θ_1 and θ_2 may change, but their difference will not. Therefore, $\gamma = \theta_1 - \theta_2$ is constant. An additional consideration is the drag force. In total, only five measurements were conducted in Ansys due to effort that has to be spent on acquiring the data. By assuming the drone to be symmetrical, the evaluation space was restricted to $(\theta_1, \phi) \in [0, 180] x [0 x 45]$. The actual evaluated angles were $\theta_1 \in \{0, 45, 90, 135, 180\}$ and $\phi \in \{0, 45\}$ as a result of limited resources. For a given value of ϕ, the gathered drag force values were interpolated with a fourth order polynomial to yield estimates for angles that were not part of the sample set. For an initial relative discrepancy angle of γ, the corresponding tuple (θ_1, θ_2) is found such that Equation 10.5 is fulfilled. Then for these two angles, the corresponding linear system presented in Equation 10.4 is solved, yielding the thrust values. Furthermore, M_y was only evaluated for $\phi = 0°$, as it was relatively small, with a maximum value around 3.5 mNm. For all angle combinations, M_x and M_z were assumed to be negligible due to symmetry of the composition for $\phi = 0, 45$ degrees. The estimated sampled drag values and corresponding interpolation can be found in figure 10.5.

Results and Discussion

Evaluation has been performed on the latest version of the system, with a mass of 586 g. The results are presented in figure 10.6a-10.6b.
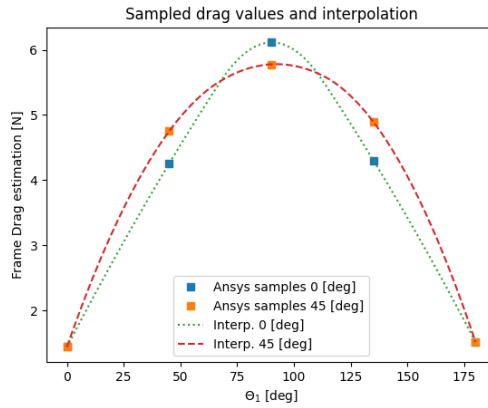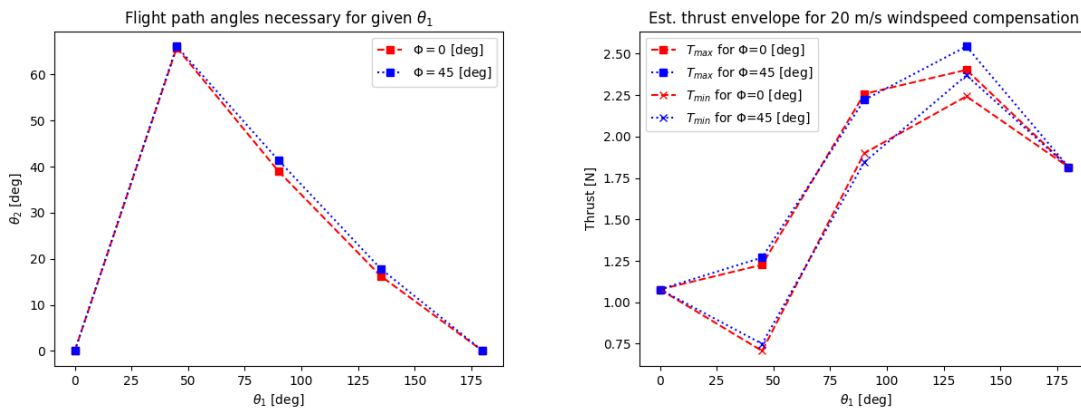
Figure 10.5: Sampled drag values and associated interpolation for frame drag estimation

(a) Flight path angle θ_2 evaluated at $\Phi =$0,45 degrees. Note that θ_1 represents the initially set θ_1, not the final resultant.

(b) Estimated thrust envelope for wind speed compensation of 20 m/s for $\Phi =$0, 45 degrees

It is seen that the overall maximum requirement stemmed from side wind of 45 degrees, with a maximum value of a single thruster of about 2.5 N. The minimum overall value was found at 0 degrees, with a thrust per motor slightly above 0.7 N. Furthermore, The maximum angle required to fulfil a steady state condition is slightly larger than 67 degrees at max. As the maximum thrust value of the implemented thrust system is about 4.24 N per propulsion unit, the selected thrust configuration is expected to be able to comply with the wind requirements in a steady state. With the initial upper mass bound of 500g, the maximum thrust required corresponded to 2.25 N and the minimum 0.5 N with maximum θ_2 around 70 degrees.

Limitations and Sources of Error

The motivation of the method at hand is that in case the propulsion system is under-designed with respect to the required thrust in steady state, compliance in the transient, dynamic state is unlikely. In reality, a steady state is not reached instantly. However after some time, assuming the disturbance stays constant, the transient state is expected to fade and the steady state is expected be approached. This represents an idealised scenario. In reality, the wind is most likely not constant, and the control system cannot reach arbitrarily fine control inputs. Furthermore, the above evaluation is not ideal for gust performance; Though the gust value of 20 m/s was consciously chosen, the nature of a gust is that it appears suddenly and abruptly. The interest here would thus lie more with the transient state. This is especially important in the context of close-ground flight with local obstacles, as a certain ability of disturbance rejection may be important to avoid close obstacles and follow a predefined path. Additionally, within the scope of the approach, there are a number of potential sources of error:

- Interpolation was conducted for only five data points per Φ value with a polynomial of degree 4
- Only symmetrical cases were evaluated with $\Phi \in \{0, 45\}$
- Apparent flow angle is not taken into account for the maximum available thrust for the flight envelope

The first point is rooted in the fact that it is uncertain if a higher polynomial degree may be required to accurately represent the behaviour of drag under angular change. Additionally, since only five data points were available for evaluation, an additional discretisation error is introduced. The second point stems from the fact that moments around the x- and z-Axis were assumed to be negligible as the flow essentially sees a symmetrical obstacle. If different angles were to be evaluated, such that the apparent obstacle to the flow is not symmetrical, an additional moments around the x- and z-axis are expected to be present. One of the conditions incorporated into the linear system is that no moment around the z-axis should be present in the rotor frame. Lastly the maximum available thrust may be slightly lower than the incorporated value here, as the apparent flow fed into the rotors is streaming in under an angle.

Verification and Validation

From literature[33], a similar approach can be found, in which the wind rejection capabilities of a hybrid Unmanned Aerial Vehicle (UAV) in quadcopter mode is evaluated. The evaluation is more complex and extensive, however at the heart lies a steady state evaluation. The method aims to quantify the wind resistance capabilities in the opposite direction as outlined above: From the maximum thrust and torque that can be provided, the maximum wind speed is found in a steady state such that force equilibrium is fulfilled. Both crosswind and headwind situations were evaluated in three dimensions[33].

For verification of the associated code, the following unit tests and system tests were carried out and passed successfully by the implementation:

- For a values of $\theta_1 = 0, 180$ degrees, the thrust values of all propulsion units should be the same and amount to the weight of the drone $\pm$ the drag force respectively
- For an angle $\theta_1 \neq 0$, the associated thrust values should again be the same and amount to the weight of the drone if a drag of 0 N is applied
- Dedicated inspection has been performed to ensure consistency in all angular units

10.5. Drone Controllability

Available Control Authority Index

Controllability is an important aspect of the system at hand. Generally speaking, the quadcopter dynamic model can be represented in the following, general state space form[23]:

$$\dot{\mathbf{x}} = \mathbf{A}\mathbf{x} + \mathbf{B}\mathbf{u} \tag{10.6}$$

In Equation 10.6, $\mathbf{x}$ represents the space vector, $\dot{\mathbf{x}}$ the derivatives with respect to time and $\mathbf{u}$ the input vector. Furthermore, $\mathbf{A}$ and $\mathbf{B}$ represent the matrices relating the systems inputs, together with the current state to the derivative with respect to time. Generally speaking, controllability for a system of the form presented in Equation 10.6 can be defined in the following way [23]:

The system described in 10.6 is controllable if for any $\mathbf{x}(t_0)$ there exists a bounded, admissible control $\mathbf{u}_{[t_0,t_1]}$ defined on the finite time interval $[t_0, t_1]$ which steers $\mathbf{x}(t_0)$ to zero. Else, the system is uncontrollable. It can be shown, that this is equivalent to steering any state $\mathbf{x}(t_0)$ towards a different state $\mathbf{x}(t_1)$.

A procedure was found that aims to answer the question, "is a given multicopter system is controllable or not?" and if so, how it compares to other configurations in terms of controllability.[11]. The mathematical details of the underlying procedure will not be repeated here, however they may be found in literature [23] and [11]. For this procedure, the following assumptions are taken:

- The dynamical model is based around the hover condition
- Gravity is the only disturbance and acts as a constant force perpendicular to the symmetry plane
- Aerodynamic damping and stiffness effects are negligible
- The multirotor is symmetric about its centre of mass

The procedure furthermore takes the following parameters as inputs:

- Principal moments of inertia J_{xx}, J_{yy}, J_{zz}
- Total mass of the multicopter M
- Thruster amount m
- Positioning of the thrusters with respect to the centre of mass. In polar coordinates: ϕ_i and d_i for thruster $i \in \{1, 2.., m\}$ as seen in figure 10.7
- Maximum thrust available per thruster K_i
- Health status of each thruster $\eta_i \in [0, 1]$
- Spinning direction of rotors $w_i \in \{1, -1\}$
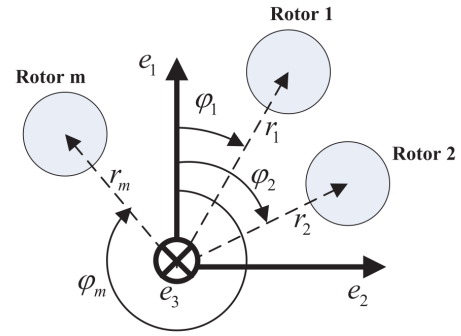- Torque, thrust coefficient of thrusters c_M, c_T

Figure 10.7: Parametric representation of quadcopter configuration [11]

The output of the procedure is the Available Control Authority Index (ACAI), a measure of how controllable the system is, if at all. Two scenarios are possible:

- $ACAI > 0 \longrightarrow$ controllable
- $ACAI < 0 \longrightarrow$ uncontrollable

A higher positive $ACAI$ relates to a higher degree of controllability between two systems. The authors of the underlying paper[11] also provide a *Matlab* implementation of the approach, which can be found online.[15]

Results and Discussion

The input parameters have been changed to the drones parameter of the last iteration. The most recent estimates were put in, resulting in the following input parameters:

Table 10.5: Drone parameters used to evaluate controllability

J_x	$0.003\ kgm^2$
J_y	$0.003\ kgm^2$
J_z	$0.005\ kgm^2$
m	0.586 kg
T_{max}	4.24 N
c_M/c_T	0.07 -
d_{arm}	0.1743 m

Table 10.6: Results for current configuration: ACAI in non-degraded state, maximum applied torques and minimum rotor health factor η such that ACAI is still > 0. All torques have been applied separately.

$ACAI_{healthy}$	0.3129 −
L_{max}	$0.5\ Nm$
M_{max}	$0.5\ Nm$
N_{max}	$0.40125\ Nm$
η_{min}	0.3386 −

All results for the present configuration can be found in Table 10.6. Since $ACAI > 0$ it can be seen that the system is controllable in hover. The output of this method can be interpreted as how much control authority (in the form of thrust/control torque) is present after compensating for the disturbance[11]. It is also of interest how much thrust degradation the system is able to withstand. As the quadcopter configuration with the applied force is symmetric, an arbitrary thruster can be degraded. The η_1 parameter has been reduced, until the system was not controllable any longer, denoted by η_{min}. The symmetry is lost if a moment is included in the disturbance: Introducing a pitch, roll or yaw moment will lead to a difference in importance between thrusters: E.g. if yaw is introduced, a degradation to one of the thrusters generating an opposing moment to the yaw is more detrimental than one generating an aligned moment, as less moment can be generated to counter the applied yaw. This has been verified with the system at hand, introducing a yaw of 0.25 N, and a degradation of $\eta = 0.5$ to all rotors individually. The overall conclusion is that in hover, without any applied moments, the thrust level of the rotors such that the weight is offset is the governing factor for the current configuration.

The maximum disturbance torques of the healthy system were evaluated as well. Although the paper specifically goes through the system in case of the weight being the applied disturbance, after [23], the important aspect is that the disturbance is constant, and specifically suggests the DoC (Degree of Controllability) in the form of the ACAI can be used to establish wind resistance [23].

In Table 10.6 $L_{max}, M_{max}, N_{max}$ present maximum values for applied roll pitch and yaw torques. $L_{max} = M_{max}$ is an expected result, as the quadcopter is symmetrical around the vertical axis.

---

[15]BUAA reliable flight control group, `http://rfly.buaa.edu.cn/resources.html`, accessed: June 14th 2021

Verification and Validation

The underlying tool provided for a hexacopter has been assumed to be verified by the authors. The tool generally speaking is implemented in parametric form.The computation of the $ACAI$ is given as a seperate *matlab* function, where the inputs are directly stemming from the main script. Therefore the transition from hexacopter to quadcopter has been verified by inspection and comparison to the underlying mathematical procedures. Simple unit tests were carried out on the inputs of the $ACAI$ function regarding the shape of the input arrays and matrices. The underlying dynamical model in hover condition has been assumed to be validated. Furthermore, the code presented was evaluated for the parameters presented in [11] for the hexacopter, verifying that the output is the same for the configuration in a healthy and one degraded mode. Ideally additional validation procedures should be implemented. These would include

- Direct, additional validation of the underlying dynamical model including assumptions of negligibility of aerodynamic stiffness effects
- Experimental validation showcasing loss of controllability

However due to the scope of this project, these should be conducted at a future stage.

10.6. Flight Controller Trade-Off

For the first iteration, the MRO Pro flight computer was chosen. To arrive at this conclusion, a trade-off between different flight computers had to be performed. To start the trade-off process, trade-off criteria were chosen. Criterion identified were mass, cost, volume, clock speed, RAM and Inertial Measurement Unit (IMU) redundancy.

Due to the hard requirements set by the customer, **cost** and **mass** were deemed the the main design criteria. Cost is expected to be the most important in the trade-off process, followed by mass. This can be justified by the following reasoning. The average cost of the flight controllers selected to be traded off is €187, with a SD of €79. This accounts for a considerable amount in the total cost budget. Therefore cost is deemed as the most important trade-off criteria. For mass, the same situation can be observed, just to a lower extend.

Following in order of importance, the **IMU redundancy** criteria is introduced. Some flight controllers come equipped with a single IMU, while others come equipped with triple IMU's. Without the IMU, the flight controller has no sense of attitude, and makes flight impossible. Points were awarded for the amount of redundant IMU's available on the flight controller.

Next in order of importance, are the **RAM** and **clock speed** criteria. These are placed quite low in the line of importance. Since it was decided that a companion computer would be necessary to run the navigation algorithms (see trade-off companion computer in section 10.7), the emphasis on RAM and clock speed was lowered for the flight controller, and raised for the companion computer.

Last in line of importance, is the **volume** criteria. Since there exists a space constraint, it was decided to include volume into the trade-off. Since the volumes of (most of) the flight controllers is relatively small compared to the shell dimensions, it is not ranked high on the line of importance.

Filling in the AHP, as described in section 4.1 the following weights were devised, as shown below in Table 10.7. As can be observed, some form of **power draw** criteria is not considered in this trade-off. Although unexpected, for most flight controllers considered, power draw was not mentioned in the specifications sheet and was therefore excluded from the trade-off. For one of the flight computers, the power draw was mentioned. Since this is one of the more powerful models considered, this power draw was assumed across all unknown models as an upper estimate, for budgeting purposes.

As can be seen a **sustainability** criteria is not taken into account in the trade-off. This is due to the fact that all flight computers considered were ROHS certified.

In Table 10.8, the scores are presented for the remaining products[16,17,18,19,20,21]. These scores are accredited using the SD metric as explained in section 4.1 and scaled by the weights as found in Table 10.7. This resulted in the following finding. The mRo PixRacer Pro flight controller will be chosen in the first iteration of the design. It performs relatively good on all criteria set. If cost did not play a role, the mRo Control Zero H7 would be chosen. But due to the price tag of €287, this flight controller is not an option in the budget of this project.

[16]mRo PixRacer R15, `https://store.mrobotics.io/mRo-PixRacer-R15-Official-p/m10023a.htm`, [accessed 19-06-2021]

[17]Holybro Pixhawk 4, `https://docs.px4.io/v1.9.0/en/flight_controller/pixhawk4.html`, [accessed 19-06-2021]

[18]pix32 v5, `http://www.holybro.com/product/pix32-v5/`, [accessed 19-06-2021]

[19]Cube Orange, `https://docs.px4.io/master/en/flight_controller/cubepilot_cube_orange.html`, [accessed 19-06-2021]

[20]mRo Control Zero H7, `https://store.mrobotics.io/mRo-Control-Zero-H7-p/mro-ctrl-zero-h7.htm`, [accessed 19-06-2021]

[21]mRo PixRacer Pro, `https://store.mrobotics.io/mRo-PixRacer-Pro-p/m10064c.htm`, [accessed 19-06-2021]

Table 10.7: Weights determined by AHP for the flight controller trade-off

	Mass	Cost	Volume	Clock speed	RAM	IMU Redundancy	Weights
Mass	1.0	0.67	8.0	4.0	4.0	1.33	**0.29**
Cost	1.5	1.0	8.0	4.0	4.0	1.33	**0.34**
Volume	0.13	0.13	1.0	0.3	0.3	0.5	**0.03**
Clock Speed	0.25	0.25	3.0	1.0	1.0	0.57	**0.09**
RAM	0.25	0.25	3.0	1.0	1.0	0.57	**0.09**
IMU Redundancy	0.75	0.75	2.0	1.75	1.75	1.0	**0.16**

Table 10.8: Trade-off of the flight controller

Criteria	Mass	Cost	Volume	Clock Speed	RAM	IMU Redundancy	Total
Weights	0.29	0.34	0.03	0.09	0.09	0.16	
mRo PixRacer R15	2	2	1	1	0	0	1.38
Holybro Pixhawk 4	2	2	1	1	1	1	1.63
Pix 32 v5	1	2	2	1	1	1	1.37
Cube Orange	0	0	0	2	2	2	0.67
mRo Control Zero H7	2	0	3	3	2	2	1.44
mRo PixRacer Pro	2	2	2	2	2	2	2.00

Sensitivity analysis

As already described above, neglecting cost would shift the trade-off towards the mRo Control Zero H7. This module is perfect for the application at hand, being a very light weight, small, power full flight controller. This does not come cheap however. The best option according to the trade-off, mRo PixRacer Pro does perform good on all criteria considered, at a cost of €180. This price is considerably more than the three cheapest options. These are the mRo PixRacer R15, Pixhawk 4 and and the Pix 32 v5. These options come at a cost of €115, €116 and €118 respectively. However, both these options suffer in the Volume, clock speed, RAM and IMU redundancy department compared to the mRo PixRacer Pro. Since cost is deemed the most important criteria in this trade-off, and a measure of Mean and SD is used, the following sensitivity analysis is conducted.

To judge the influence of cost in a quantitative manner, to two most expensive options were removed, that being the Cube Orange and the mRo Control Zero H7. These flight controller cost €284 and €287 respectively. By including these options in the trade-off, the mean and the SD of the cost criteria increases and this in turn reduces the differentiation between the cheaper flight controllers. However, since these were deemed valid options at the time, they were included in the trade-off. By removal of these flight controllers in the sensitivity analysis, the cost scores will be accredited in a different manner and thus may differentiate more between the remaining flight controllers.

The advantage of the mRo PixRacer Pro shrunk considerably. This can be explained due to the extreme emphasis on cost in the trade-off. The Pixhawk 4 now becomes the most an attractive option. A low price, combined with a low mass makes it score great in the trade-off. However, it scores less great on the IMU redundancy score, since it only comes equipped with a single redundant IMU. It has to be noted, that the mRo PixRacer Pro will still be selected as the flight controller option in the first iteration. If budgets do not allow, the Pixhawk 4 turns out to be a great alternative. This sensitivity analysis shows the great influence of the cost on the trade-off.

10.7. Companion computer trade-off

In order to open the door to more computationally expensive strategies regarding autonomous behaviour, and more advanced methods regarding general mission planning, a companion computer should be implemented [22]. The companion computer in this case is specifically intended to provide local path planning solutions and to keep the possibility of more advanced autonomous decision making open.

Although the companion computer should ideally be more powerful than the flight controller, there is an upper limit set in place, as usually computational power seems to strongly correlate with power draw and weight of the unit. Therefore a trade-off has to be set in place based on a range of companion computers that are commonly

---

[22] Ardupilot Companion Computer, `https://ardupilot.org/dev/docs/companion-computers.html`, accessed: June 15th 2021

used. The companion computer will communicate with the flight controller via the *MAVlink* interface [23]. Similarly to the flight controller, a number of different criteria were taken into account, presented in Table 10.9

Table 10.9: AHP weighting for trade-off criteria regarding companion computer selection

	Mass	Cost	Power	Volume	Clock speed	RAM	Weights
Mass	1.0	1.0	4.0	8.0	1.0	1.0	**0.24**
Cost	1.0	1.0	2.0	2.0	1.0	1.0	**0.18**
Power	0.25	0.5	1.0	2.0	0.2	0.2	**0.06**
Volume	0.13	0.5	0.5	1.0	0.2	0.2	**0.05**
Clock speed	1.0	1.0	6.0	6.0	1.0	1.0	**0.24**
RAM	1.0	1.0	6.0	6.0	1.0	1.0	**0.24**

As can be seen by comparing the above table to Table 10.7, the criteria selection is similar but not exactly the same. Mass, clock speed and RAM were deemed the most important criteria. In contrast to the flight controller, **mass** is deemed more important than **cost** in this trade-off. The mass across products varies more than cost varies across products, and would thus have a bigger influence on the budgets.

On the same importance as mass are **clock speed** and **RAM**. As explained in introduction of this section, most of the computation will be done by the companion computer. Both criteria are used to estimate the computational power of the underlying computing unit. It should be mentioned that these criteria were given an equal AHP scores, as it was beyond the scope the project to conduct an analysis of the relative hierarchy between the two. Additionally, **power** can be taken into account as data on power draw of the underlying computing units are more readily available.

As with the flight controller, **sustainability** was not taken into account in the trade-off. It was checked however, that the components to be traded-off were ROHS compliant.

The strategy for determining the boundaries of scoring performance of candidates[24,25,26,27] in criteria was chosen the same as for the flight computer using the SD metric (section 4.1). The result of the trade-off process can be found in Table 10.10. The Raspberry Pi turns out to be the most attractive option for the companion computer.

Table 10.10: Results of trade-off for the companion computer

	Mass	Cost	Power	Volume	Clock speed	RAM	Result
Weights	0.24	0.18	0.06	0.05	0.24	0.24	
Arduino Nano	2	2	3	2	0	1	1.34
Odroid XU4	1	1	0	0	3	2	1.61
Odroid C4	0	1	1	1	1	3	1.24
Raspberry Pi Zero	2	2	2	2	2	1	1.76

Sensitivity analysis

The same case as for the flight controller applies here. The inclusion of certain components influences the mean and the standard deviation, and thus the scores accredited. In contrast to the flight controller however, where 2 of the products turned out to be too expensive to consider in the budgets, the companion computers traded-off are all viable options within the budgets. Therefore the following strategy was executed. The most influential product(s) were removed from the computation of the mean and SD, but still scored along the newly found range. In this trade-off, the Arduino Nano scores extremely well on the Mass, Cost, and Power criteria, and was therefore removed from the calculation in the first sensitivity analysis. The Odroid XU4 scores great on the clock speed and RAM criteria and was therefore removed from the calculation in the second sensitivity analysis. In both analysis, the Raspberry Pi zero was still the clear choice of component. This sensitivity analysis showed the inclusion of the Arduino Nano as a relative light weight competitor and the XU4 as a heavy weight competitor did not influence the trade-off in a negative way.

---

[23]MAVlink,`https://ardupilot.org/dev/docs/mavlink-commands.html`,accessed: June 15th 2021

[24]Arduino Nano, `https://www.hobbyelectronica.nl/product/arduino-nano-compatible-ch340/`, [accessed 22-06-2021]

[25]ODROID-XU4, `https://www.hardkernel.com/shop/odroid-xu4-special-price/`, [accessed 22-06-2021]

[26]ODROID-C4, `https://www.hardkernel.com/shop/odroid-c4/`, [accessed 22-06-2021]

[27]Raspberry Pi Zero W, `https://www.kiwi-electronics.nl/raspberry-pi-zero-w`, [accessed 22-06-2021]

10.8. Navigation Algorithms

Ardupilot - built in solutions

For the software, the Ardupilot system was chosen, as it allows for heavy customisation and has a range of features available related to obstacle avoidance and other aspects of autonomous navigation. Therefore it was deemed a generally good representation for off-the shelf options available. [28] These built in solutions regarding obstacle avoidance and path planning will be briefly introduced and their characteristics brought forward. Please note that for this subsection, all information and images are taken from the Ardupilot website [29]

Object avoidance in ALT_HOLD (AH) and Loiter mode

AH mode requires no GNSS. This is a benefit, as GNSS is not necessarily guaranteed in the close ground environment at hand. In this mode, the quadcopter tries to hold a steady altitude based on barometer measurements. The included obstacle avoidance is incorporated as follows [30]:

1. Obstacles are detected
2. Obstacle distance vectors are converted into a roll/lean angle by a predefined mapping
3. Maximum and minimum roll/pitch angles are combined and the copter takes on a lean angle that tends to move it away from the obstacle. Pilot input is combined with the final pitch/roll angle.

This is the simplest form of built in object avoidance. It does not take into account velocity and exact deceleration is therefore impossible.

Loiter mode does require GNSS for velocity estimation. The flow is as follows[31]

1. Distances are measured from onboard sensors

2. Mini fence is constructed around measured distance points as illustrated in figure 10.8

3. Desired velocities coming from the pilot are adjusted to stop before a certain distance to the obstacle.
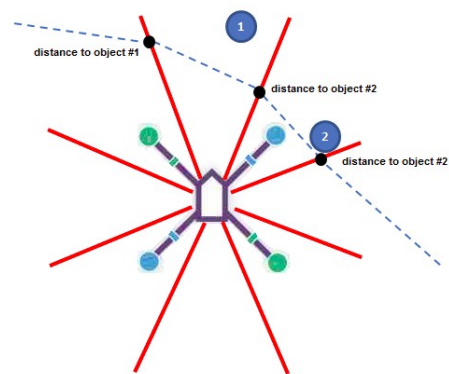

Figure 10.8: Mini fence construction around drone in loiter mode [32]

Although loiter mode requires a pilot, the obstacle avoidance mode implemented in the loiter mode seemingly only requires an estimated velocity. The custom firmware should enable this mode to be used in an autonomous fashion, with the desired speed stemming from the autonomous path planning.

Bendy ruler local path-planning and obstacle avoidance

This mode is the most advanced. It is run in the AUTO mode. The quadcopter, following a predefined path utilises its distance sensors to probe around an obstacle. If the probed area is sufficiently open, the quadcopter will pursue a local updated path around the obstacle while trying to follow the overall GNSS waypoint.[33].

Although a number of solutions are present in the Ardupilot system, the more advanced approaches largely rely on GNSS. Therefore there is a need for either

- Adapting the current implementations such that GNSS is not required
- Providing a proposal that does not rely on GNSS

---

[28] Ardupilot, `https://ardupilot.org/`, accessed: 22.06.2021

[29] Ardupilot documentation, `https://ardupilot.org/ardupilot/index.html`, accessed: June 22nd 2021

[30] AH avoidance, `https://ardupilot.org/dev/docs/code-overview-object-avoidance.html`, accessed: June 21st 2021

[31] Loiter avoidance, `https://ardupilot.org/dev/docs/code-overview-object-avoidance.html`, accessed: June 21st 2021

[32] Loiter avoidance `https://ardupilot.org/dev/docs/code-overview-object-avoidance.html`, accessed: June 21st 2021

[33] Bendy Ruler, `https://ardupilot.org/copter/docs/common-oa-bendyruler.html`, accessed: June 22nd 2021

The first approach is most likely possible, as the avoidance in loiter mode only needs an estimate of the current speed in order to be able to compute the necessary deceleration. For the bendy ruler approach it could be argued that localised path planning, within the visbility of the drone could be used to present a fictitious GNSS way point for the drone to follow. For the chosen approach to estimate velocity and position values, please refer to section 10.9. It might be a possibility to neglect the drift in current position, if local path planning is done step-wise only within the current field of view. To showcase that such an approach might be an option for exploring the unkonwn terrain based only on sensor data and to propose a local path planning solution for the problem at hand, three additional approaches have been set in place that will be presented in the subsequent section.

Proposed Substitutions to the Bendy Ruler Approach

Algorithm #1: Simple Algorithm

The first algorithm is simple algorithm. If the path in front of the drone is blocked (as in an obstacle), the flight computer tries to send the drone to the left. If that direction is blocked, then the drone flights to the right. Already, one disadvantage of the algorithm is clear. If the drone senses an obstacle in the front, left and right directions, it has no path forward. This can be countered by stopping and allowing the drone to rotate on its z axis and trying to repeat the process. This algorithm has two major advantages; firstly, it's computationally cheap, which means the reaction time is faster and the drone can then fly faster (as the top speed is limited to the sensing and reaction times). This is preferable for an emergency drone. Secondly, the algorithm is suited to the chosen sensor package, as it does not require the exact location of obstacles, but rather an indication of whether a direction is available. However, this algorithm will not be suited for obstacle-rich environments, such as the dense forest outlined in section 5.1

Algorithm #2: RRT Based Algorithm

The second algorithm uses Pygame as a virtual environment, simulating a random forest. Its main incentive was to design a more robust algorithm compared to algorithm 1, attempting to fix some of the disadvantages described. To aid in the design, an algorithm called Rapidly exploring Random Tree, or RRT for short, was studied in a literature study.

The problem with this algorithm is that it assumes the full space considered is known and can be sampled. In the drone application however, this is not the case. Obstacle information is only available within the range of the sensors. Outside this "field of view", the territory is unknown and sampling would be useless. Moreover, drawing random samples during drone flight is not very efficient. Without storing the previously visited locations, this enables backtracking to occur that wastes precious energy. Therefore the following modifications were made to an existing implementation of an RRT algorithm[34].

The sample space is taken care off by 2 normal distributions. Firstly, a heading in degrees is selected. The first normal distribution is centred around the heading, and a bias is provided. The second normal distribution accounts for the range sample. A sample following a normal distribution is drawn from within the maximum range of the sensors. Bias can of course be adjusted. To aid in this explanation the following figure 10.9 is provided. By adjusting the bias the shape of the sampling cloud can be adjusted.
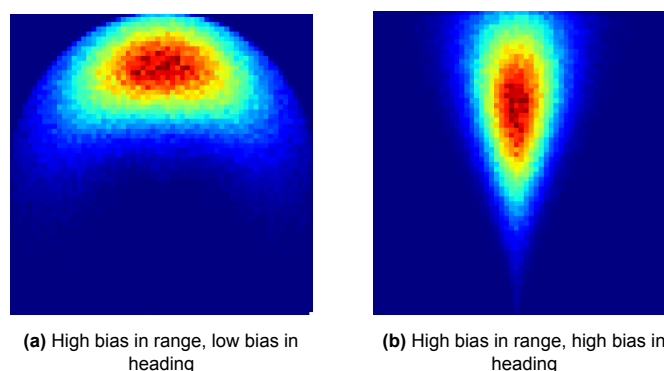

(a) High bias in range, low bias in heading

(b) High bias in range, high bias in heading

Figure 10.9: Bias influence samples

---

[34] Algobotics, The RRT path planning algorithm simulated with python, https://www.youtube.com/watch?v=TzfNzqjJ2VQ, [accessed on 22-06-2021]

Based on the bias, a sample/node is drawn from within the range of the sensors. The space itself and around the sample is checked for obstacles, and line from the current position towards the obstacle is checked for obstructions. If a valid sample is drawn, the node is added to the tree and the drone moves to the next node location. If the node is invalid, a new sample is drawn. The more samples are drawn, the lower the bias towards heading becomes. After a few thousand samples, it will look like random sampling. This makes this algorithm more robust than the previous mentioned algorithm. In case the drone is obstructed from movement in the forward direction, eventually it will find a node in the backwards direction and start to sample again. This has one obvious flaw. If the size of the "trap" is much larger than the field of view range, the drone will remain stuck. After backtracking, it will sample forward again and a loop will arise. In forests however, simulated via a Pygame environment filled with random obstacles of roughly the same size of the drone, this algorithm performs very well.

Algorithm #3: A* Based Algorithm
The last approach is an implementation based on the A* algorithm. A* is one of the most popular pathfinding algorithms used in the field of robotics together with RRT. For a detailed outline the reader is referred to [32].

Generally, cost is defined as the sum of a heuristic cost function and a direct cost function. [32]. In the implementation presented in this section, given a specific node A, the heuristic cost function is the euclidean distance between that node and the destination node D. The direct cost between two given adjacent nodes is taken as the euclidean distance between them. This equates to 1 for horizontal and vertical nodes and $\sqrt{2}$ for diagonal neighbours. The direct cost of the specific node A is the path cost up until that node was in evaluation. Note that this cost is continuously updated if a lower cost path is found.

For a given run, the current implementation requires the storage of at least 6 arrays of the same size: The field of view map, where occupied space is given a value of 1. The heuristic and direct cost, the total cost, the node visited/not visited array and the previously visited node array. The array size is tied to the desired resolution of the surrounding field of view. A first run with a memory profiler showed a total usage of around 160 megabytes for a map size of $100 \; x \; 100$ elements. It should be noted that this is relatively inefficient and has not been optimised. The necessity of including A* in to the path finding algorithm can be argued, as the optimisation aspect is essentially reduced to finding a straight line to a desired point, since the obstacles have to be assumed to take up the complete sector of the sensor field, from the distance onwards where it is spotted. Currently three sensors as presented in Table 10.1 provide local field of view information. The algorithm at hand has been adapted to the local field of view, meaning the drone is simulated to have a field of view of 98 degrees, with the symmetry line lying in direction of the current heading. Again, the exploration is essentially driven by a bias. If an obstacle does not permit a waypoint in the bias direction, a position within the field of view is chosen that is closest to the bias heading. This position represents the destination node for the A* algorithm. The distance to the point selected within the field of view is always smaller than the field of view itself, such that finer paths can be generated that react to the obstacles more continuously. The implicit assumptions here are:

- The drone is assumed to be capable of perfect hover
- The drone flies at a low horizontal speed

The first point is related to the overall strategy:

1. Hover, hold position
2. Evaluate surroundings
3. Select next point in local field of view

4. Transverse to point

5. Repeat

The second point is related to the feasibility of the paths generated. If the drone moves too fast, it is expected that the paths cannot be followed by an appropriate trajectory. Therefore the drone should fly slow enough, such that stops can be carried out almost immediately. This is an ideal case, as there could be wind gusts that make hover more unlikely or almost impossible, introducing drift. In the current implementation, one map entry corresponds to 0.25 x 0.25 m^2. The visibility radius is 16 units (4 m) and the mapsize is 800 x 800 entries corresponding to $40000 \; m^2$. This in turn with 5000 obstacles corresponds to an average obstacle density of $125000 \; km^2$. figure 10.10a shows a closeup of the path taken with a bias of 315 degrees. It should be noted that no collision occurs, however no feature was implemented to adhere to a minimum safety distance to obstacles, therefore close encounters are present. Lastly, figure 10.10b illustrates the sensor view at a given position. An obstacle is detected to the lower left, and the complete sensor area is deemed an obstacle from the distance of the actual obstacle itself onwards.
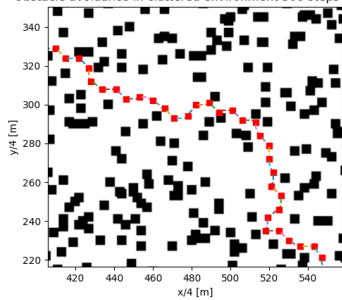
(a) Close-up of covered path
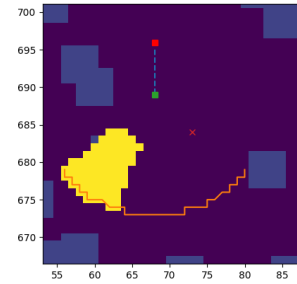
(b) Showcasing of local field of view of the drone. Lower, green dot: Current position. Blue squares: Unknown obstacles. Yellow sector: ultrasonic sensor triggered by an obstacle. The red dot: previous position,not known to the drone

Conclusion and Recommendations

From these implementations the following conclusions were drawn:

- In case of continuous saturation of the sensors, the drone should adjust its heading bias to avoid becoming trapped in symmetrical obstacles
- A safety radius should be implemented to decrease the drones chances of hitting obstacles by random disturbances such as gusts. This radius should more than half of the maximum drone span.
- With a safety region around obstacle, A* might become useful after all, as the optimum paths will no longer be straight lines anymore. However it can be debated whether the drone is able to follow a non-straight line with position estimations other than GNSS

These conclusions were incorporated as follows: Local path planning will be conducted with a variation or combination of the above exploration algorithms. Furthermore, the built in obstacle avoidance mode of the Ardupilot loiter mode as outlined in the previous section will be active during manoeuvring. The minimum distance, such that action is taken by this mode should be set lower than the proposed minimum distance to an obstacle by the local path planner. This should give an active layer of security during transversal. At distinct steps, the path planner carries out its task and during transition it is not active, while the loiter mode obstacle avoidance is active at all times, most notably during transition to the new proposed waypoint.

An additional set of assumptions come into play here:

- A local waypoint can be set with within the field of view that can be translated into a desired acceleration, speed and heading, without the use of continuous map building.
- The loiter mode obstacle avoidance of Ardupilot can be adapted, utilizing horizontal velocity estimates based on one of the methods proposed in section 10.9

Recommendations: Numerical comparison and analysis should be conducted for all three proposed algorithms. The exploration aspect should be taken into account: How likely is the drone to find a vertical opening using one of the given algorithms? Vertical movement should be incorporated for path planning and exploration: Currently path planning is conducted in 2D with these algorithms. Plane changes in the form of altitude changes could provide an additional layer of planning and exploration. Lastly Alternatives to the bias-exploration should be explored.

10.9. Special Considerations: GNSS-denied Environment

One major obstacle the system needs to overcome is the state estimation of the UAV in case GNSS is unavailable. Estimating the current position and velocity based on the on board IMU may simply not be enough. Drift and rounding errors will lead to a divergence in accuracy over a short period of time. [15] Typically, velocities and positioning stemming from GNSS can be taken into account by fusing the measurements with expected values for the states by means of an Extended Kahlman Filter (EKF) for example,in order to compensate for these introduced errors. For a more detailed outline of the EKFs strucuture, please refer to [23]. An overview of the implementation of the EKF within Ardupilot can be found in the documentation.[35] While automatic stabilisation is a feature of Ardupilot that works without the availability of GNSS, wind cannot be compensated in

---

[35]EKF-Ardupilot,`https://ardupilot.org/dev/docs/extended-kalman-filter.html#extended-kalman-filter`

this mode. [36]. Furthermore, for a constant wind, it is expected to be impossible for the drone to hold a steady hovering position among the surrounding obstacles without a velocity estimate. Additionally,the built in obstacle avoidance methods of Ardupilot require an estimate of the current velocity in order to perform abrupt stops, usually provided by GPS [37]. Therefore, a strategy has to be set in place to minimise the chance of collision in the cluttered, GNSS denied environment. After literature, two possible solutions were found:

1. Using the on-board camera capturing ground footage coupled with the companion computer and the bottom mounted ultrasonic sensor to conduct an optical flow method in order to estimate current position and more importantly in-plane velocity based on current implementations [12, 4].

2. Estimating the in plane velocity based on a more refined dynamical model of the quadcopter, including a drag term, based on [19]

The first approach is expected to enable:

- Integration into EKF, dynamic obstacle avoidance with wind influence
- Rough estimation of current position
- Active resistance and countermeasures against wind

The second approach is expected to enable:

- Dynamic obstacle avoidance without wind drift
- Very rough first estimation of current position without wind drift

Drag model approach

In this approach, a typical representation of the dynamical model of a quadcopter is extended by including a term representing drag force. The overall scheme is implemented with the use of a Extended Kalman filter. The method relies on IMU data alone and is therefore not dependent on any form of GNSS. [19]. Testing was conducted in a controlled indoor environment, therefore it can not be expected to yield any form of benefits with regards to wind opposition.

Raspberry Pi optical flow

Literature [12] provides an implementation of optical flow for the raspberry pi 3 and the Picam V2.0. Velocity and position are estimated without the use of external inputs such as GNSS. Outdoor flight is performed and compared to values obtained with GPS data. The only additional sensor required is an ultrasonic sensor or equivalent range finder sensor. The computational load is relatively low due to the dedicated hardware acceleration of the Pi for motion sensing. [12]. [4] gives an implementation of optical flow for object tracking on on the chosen companion computer, the raspberry pi zero. All Raspberry Pi models up until the Raspberry Pi 3 support hardware acceleration in this context. [38]. The camera chosen in figure 12.4b is designed for the Pizero system and the user manual suggests the output to be the H.264 format that is required for the hardware acceleration block to utilise it. [39]. Drawbacks of this approach are the same as most optical flow methods: Inconsistent lighting and environmental conditions such as rain or bad visibility may render the method problematic.[18]. Furthermore, the camera sensor at hand is the previous version of the one implemented in [12]. The expectation is that the older lens might lead to a drawback in performance.

Mitigation approach

Both approaches suffer from different problems. The drag model estimate is expected to provide questionable performance during wind associated drifts. It could be argued however that the presence of cluttered obstacles may inhibit strong wind generation. The optical flow is expected to perform better in context of wind, but is susceptible to lighting, weather conditions and nighttime.[18]. Furthermore, it bounds the maximum and minimum velocity depending on altitude above ground. [12]. Additionally, it is expected but it can not be guaranteed that the hardware at hand will provide the capabilities as expected. Overall the drag method is preferred at this stage as less uncertainties are involved.

It should be noted that the EKF is evaluated on the flight computer, not the companion computer. Ardupilot gives the opportunity to customize firmware to the required needs and therefore there should be no issue in

---

[36]Stabilisation mode Ardupilot, `https://ardupilot.org/copter/docs/stabilize-mode.html`, accessed: June 20th 2021

[37]Copter object avoidance, `https://ardupilot.org/dev/docs/code-overview-object-avoidance.html`, accessed: 20.06.2021

[38]Pi model comparison, `https://www.raspberrypi.org/documentation/faqs/#hardware-compare`

[39]PiCam zero, `https://www.waveshare.com/wiki/RPi_Zero_V1.3_Camera`, accessed: June 20th 2021

adapting the sensor fusion methods such as the EKF already present in the system. The upper limit in customisation is computational performance and the flash size available on the respective flight computer chosen.

Vertical Linear Velocity Estimation

An approach for the estimation of the vertical linear velocity can be found in [25]. In this approach, IMU data is fused with barometer output to generate an estimate of the vertical velocity. Furthermore an EKF is applied on the inertial measurements to estimate the current body frame attitude. At the time of writing, the authors were in the midst of implementing the approach to a microcontroller, significantly less powerful than the flight controller. Therefore it can be argued that it is not unrealistic to run the given approach on the hardware present in the drone, and hence this approach will be selected in order to estimate the vertical velocity.

10.10. Height Map Implementation

General Outline

Local obstacles such as trees or natural barriers blocking the line of site to various satellite signals may render the drone unable to establish connection to both the GNSS system as well as the primary communication system of the Iridium constellations.

In [2], an initial estimate for the maximum climb increment that the drone would have to perform in Europe was estimated to be 2 km, with the terrain chosen to be local terrain around mount Elbrus. A number of sizing decisions have been performed around this climb interval value. In order to verify that this is indeed an appropriate estimate, the following strategy was devised: From literature, [22] it can be found that Iridium satellites can be seen by the user with a minimum elevation angle of 8.2 degrees. Effectively that means that if the user is at the outskirts of the coverage area of a satellite, the elevation angle will correspond to the minimum elevation angle, as shown in [6]. Usually, the minimum elevation angle is set larger than zero in the sizing of the satellite constellation to avoid line of sight blockage of terrain and additional atmospheric attenuation. [6]. The worst case situation with regards to line of sight is at this minimum elevation angle, as the line of sight is more susceptible to interception by local obstructions.

A simple tool was developed that for a given position on a digital elevation map (DEM) performs a check for a line of sight requirement of 8.2 degrees that might be violated by any surrounding natural barriers of the terrain. The DEMs were taken from the ALOS Global Digital Surface Model [40] from the Japanese Aerospace Exploration Agency. Subsequently a climb requirement is given, such that all surrounding obstacles become neutralised with regards to open sky visibility for the primary communication means. A number of simplifications were made:

- Satellite orbit and constellation parameters are neglected, except for the minimum elevation angle
- Local obstructions such as trees or crevices are neglected

Furthermore, obstacles are classified in the following way:

1. The view from the position is discretized into 128 directions between (0,360) degrees.
2. The line of sight under an angle of 8.2 degrees is cast in all directions
3. The obstacle requiring the highest climb is found per direction
4. Out of all directions, the most dominant one is selected once more
5. The climb interval required for this obstacle is considered as the estimation for the minimum climb value such that local terrain does pose a threat to the Iridium connection.

The above simplifications are expected to yield an overestimation of the required climb height: Generally speaking, the modelled situation is harsher than the reality at hand. The Irridium NEXT constellation consists of 66 satellites, spaced out in 6 equally sized orbital planes, with 11 equally spaced units per plane.[41]. Either one or two satellites should be visible at any given time [22] assuming open sky. Furthermore, orbital parameters are not taken into account and the most dominant obstacle in any direction is seen as the obstacle to overcome, regardless of orientation towards the satellites orbits. Lastly, satellite movement is not taken into account. While an obstacle might be a problem for a short duration of time, it may be possible to establish a connection to a satellite after line of sight has passed the obstacle. figure 10.11b illustrates an example of an evaluation in

---

[40]ALOS Global Digital Surface Model, `https://www.eorc.jaxa.jp/ALOS/en/aw3d30/`, accessed: June 19th 2021

[41]Irridium NEXT,`https://earth.esa.int/web/eoportal/satellite-missions/i/iridium-next`, accessed: 19.06.2021

the area surrounding mount Elbrus, shown in figure 10.11a. The red points represent the dominant obstacle in each direction. If no red dots are present in one direction, then no obstacle is found high enough to influence the line of sight.

In an effort to find the maximum climb value that would be expected for a given DEM area, the DEM can be sampled and the above method applied for each sampled position. It was decided to analyse two different areas within europe: The area containing Mount Elbrus and the area containing Mont Blanc. Both maps are of size 3600x3600 units and the DEM has a resolution of around 30 m and an associated uncertainty of 5 m for the elevation measurements[42]. The evaluation parameters were *sampling_interval=100*, *step_count* = 150, meaning samples are taken every 100th entry over the map, corresponding to a distance of ≈ 3000 m and rays are cast out to a distance of 150 entries ≈ 4500 m to allow for overlap between samples. In total 1296 equidistant samples were evaluated for both the Mount Elbrus and Mont Blanc region.
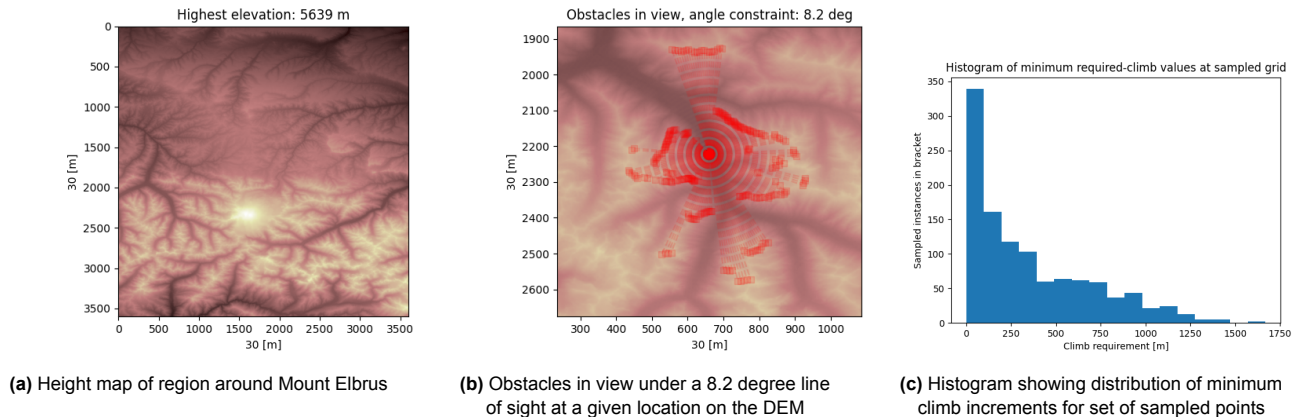

(a) Height map of region around Mount Elbrus

(b) Obstacles in view under a 8.2 degree line of sight at a given location on the DEM

(c) Histogram showing distribution of minimum climb increments for set of sampled points

Table 10.11: Average and maximum values of minimum climb increments for selected terrains

Area	Average min. Climb [m]	Max. min. Climb [m]
Elbrus	356.74	1669.58
Mont Blanc	505.25	2126.07

As can be seen, the values for Mont Blanc actually exceed the intital 2 km estimate. However after further analysis the distribution showed that 99.98 % of all climb increments are below 1800 m. Therefore this was deemed acceptable.

Verification and Validation

A number of test were carried out to ensure the implementation is working as intended. The DEM was verified by the following:

- Map images were crossreferenced by visual features on google maps to ensure the data tiles contain Mont Blanc and Mount Elbrus respectively
- The largest elevation on the data map should correspond to the Mont Blanc and Mount Elbrus for each tile. This was successful within ± 5 m , as this is the resolution of the DEM

Additionally, the following system test was carried out and passed successfully: A custom map was generated. The map was filled with elevation values of 0, except for 7 different points in equally spaced directions: {0,60,120,180,240,240,300} degrees. These points had an associated elevation value of {0,10,15,30,35,20,20}, located a distance of 30 entries from the mid-point. The angle constraint was set to 25 degrees. By trigonometry, the first two entries did not violate the line of sight with this angle. The following associations for the points were returned as expected: {No obstacle, Obstacle not problematic, obstacle in direction , obstacle in direction, Overall dominant obstacle, obstacle negligible in direction, obstacle in direction}. The minimum climb altitude was 21 units as expected since this is the climb necessary to have a 25 degree line of sight in any direction.

---

[42]FAQ JAXA, `https://www.eorc.jaxa.jp/ALOS/en/faq/faq_aw3d30_e.html`, accessed June 19th 2021

On board Implementation

In theory, if a GNSS signal is available, an estimation could be made on how high the drone would need to fly to be able to receive a primary communication signal. This estimation with some safety margin could provide the targeted loiter altitude. However it is very difficult to evaluate the level of open sky with the constraints at hand. This is a problem, because loitering at an altitude governed by natural barriers might underestimate the required altitude,if a different source of strong attenuation is present in the sky. The iridium communication line between satellite and local receiver module is situated between 1616 MHz to 1626.5 MHz [22]. After literature [17] attenuation by rain and clouds is about $0.1\,dB$ and negligible for a frequency band slightly lower than than the one at hand. However after an extensive literature survey, the influence of events such as smoke plumes and strong thunderstorms could not be established. Therefore, even though loitering around the estimated minimum altitude may have benefits in terms of efficiency there could be other sources apart from terrain that would require a higher climb. This strategy was therefore discarded for the first iteration in order to increase the robustness of the climb strategy and is left as a recommendation to be further investigated.

Therefore, for the first iteration the implementation is limited to the following:

The first implementation is the cross reference of the current position with regards to a coverage map for the secondary communication module. Online, coverage maps for 2G and 3G are available [43]. An assumption is made that these datasets can be obtained for offline-use in the future. Combining saved coverage data with DEMs on board may yield a shorter path for the drone to establish communication via its secondary communication strategy. The drone will only evaluate an actual flight path to the position where coverage is available, if the point falls within a circular area governed by a maximum radius around the current position. The extent of this maximum radius is not only coupled to the flight capabilities of the drone itself, but the capabilities of the companion computer to efficiently generate a suitable path, tied to the size of data to be analysed. Therefore, this radius should be relatively tight. If a location with coverage is found within this radius, a path will be generated by the use of e.g. A* or RRT, under consideration of a minimum altitude above local ground and additional constraints such as potential areas of GNSS loss. It should be noted that the exact implementation of the complete approach has not been conducted at this stage of the design.

Additionally, literature [31] has shown that the combination of GPS, GLONAS and GALILEO provides a very robust coverage against natural barriers by example of the alpine region. The argument could be made that due to the constellation differences between the Iridium network and these GNSS networks, there might a possibility where a GNSS signal is received, but a Iridium signal is not received. Therefore the extended case should be considered, where a GNSS signal is received but due to local obstructions, the drone is not able to immediately climb and has to transverse a horizontal path in search of an opening.

In such a case, instead of arbitrarily selecting an initial heading, the above algorithm can be carried for the current position of the drone. The angle constraint can be changed to a constraint suitable for a flight path angle. Therefore, a heading can be chosen by the drone, based on e.g. the largest uninterrupted line of sight in any direction on the DEM as this gives information about the overall terrain shape of the surrounding area. For a sparse forrest this would not yield a lot of benefits as the DEM resolution is around 30 m per pixel. However in more cluttered environments, where a larger horizontal distance would need to be covered, it would be beneficial for the drone to select a less demanding flight path. It is clear, that the DEMs do not provide any information about local obstacles, but for larger distances the influence of the overall terrain shape may become significant. Therefore, in case the situation arises where GNSS is available, the drone cannot immediately climb and no communication link is present, the drone will select a heading based on the above implementation and commence exploration.

It should be noted that both the DEM and the coverage map will be transferred onto the drone before the user commences their hike/exploration/trip in a larger region by a provided software interface. The storage required by the DEMs is around 26 megabytes for a map size of $3600\,x\,3600$ entries, corresponding to 11664 km^2, an area much larger than required. The coverage maps are assumed to be of a similar size/resolution. These data sets will be stored on the companion computer's micro-SD card, offering more than enough space. Transfer can be facilitated by the built in wifi/bluetooth module of the companion computer, without a need of opening the drone.

---

[43]Coverage Map,https://www.gsma.com/coverage/, accessed: June 20th 2021

10.11. Requirement Compliance

Table 10.12: Comliance matrix for the GNCS subsystem

ID	Requirement	Compliance	Comment	Valid. by
SUBSYST-GNCS-02	The guidance and navigation subsystem shall be able to locate the drone with an accuracy of 30 m	✓		RoD, Comp
SUBSYST-GNCS-09	The control subsystem shall ensure the drone is flying within its flight envelope	✓		RoD, Test
SUBSYST-GNCS-13	The guidance and navigation subsystem shall have a power at most 3 W	✓		RoD, Test
SUBSYST-GNCS-14	The guidance and navigation subsystem shall use at most 12 V	✓		RoD, Test
SUBSYST-GNCS-15	The guidance and navigation subsystem cost shall not exceed 175 euros		190 euros	RoD
SUBSYST-GNCS-16	The guidance and navigation subsystem weight shall not exceed 35 grams		54.4 grams	RoD, Test

As can be seen, a number of requirements is not fulfilled. These are mainly of budgetary concern: Stemming from a previous design phase, both the cost and mass budget did not take into account the possibility or necessity of a companion computer. The cost requirement is deemed feasible to be fulfilled: As outlined in section 10.6, the second option for the flight controller would still yield good performance aspects, while being around 60 euros cheaper. In terms of mass, it was found that the initial budget available is simply outdated and not appropriate. The mass restriction is deemed infeasible for the current application and needs to be revised in collaboration with other subsystems.

10.12. Software Diagram

On the following page, in figure 10.12, the software diagram is presented. A description on the general navigation strategy is given in section 10.1 and should be read together with the software diagram. As can be seen the software diagram also includes a "black box". Here the (estimated) user location and estimated travelled path is stored. In case of retrieval of the drone the external party could read out the data and locate the user. In the post-DSE phase the design of the black box will be expanded upon. The accuracy of the location estimations will be analysed and if sufficient a dedicated UI has to be designed.
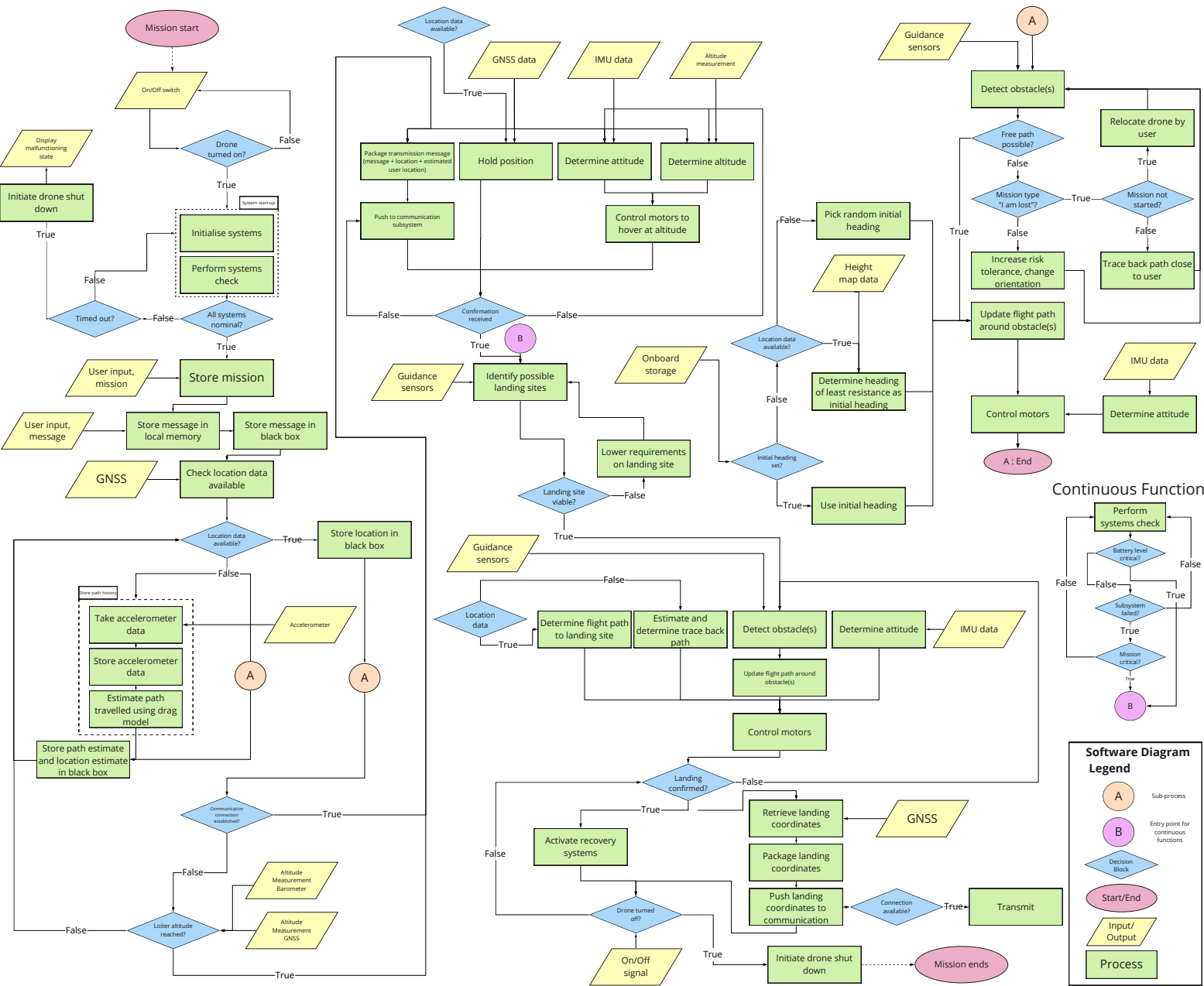
Figure 10.12: Software diagram

10.13. Conclusion and Recommendations

In the end, a GNCS subsystem was designed to fulfil the stability and control requirements of the design as well as enable the autonomous behaviour required to successfully follow the mission at hand. Cost and mass were found to be most restricting in incorporating appropriate sensing and obstacle avoidance strategies. Solutions such as lidar/ultrasonic sensor combinations should be investigated for the sensor selection. The obstacle avoidance and exploration strategies should be extended and further analysed to include altitude changing actions. For control and stability aspects additional steps should be taken to incorporate the analysis of dynamic responses. For the second iteration, a switch in flight computers is recommended to comply with the cost requirement.

11. Electronics

This section analyses the electronics subsystem, which comprises the design of the battery, section 11.2, the Battery Management System (BMS), section 11.5, Electronic Speed Controller (ESC), section 11.3 and finally the Power Distribution Board (PDB) in section 11.4. As stated in the chapter 3, all of these components shall

be chosen as off the shelf components. The resulting power distribution diagram can be found in chapter 13.

11.1. Requirement Analysis

First, the requirements that apply to the electronics are analysed in order to assure that the system is fit-for-purpose. The requirements related to the electronics subsystem can be found below.

- **STAK-GENR-03**: The drone shall not have exposed electronics
- **SYST-RISK-01**: The critical components shall be designed to have safe life or fail safe philosophy implementation
- **SYST-THER-01**: The drone shall be able to operate in a temperature range from 20 to +40◦C
- **STAK-SUST-01**: The drone shall be able to be repaired in a modular fashion
- **SYST-SUST-02-A**: The drone shall be electrically powered
- **SYST-SUST-02-B**: The drone shall not be manufactured out of toxic materials
- **SYST-SUST-13**: The drone shall be able to be disassembled to a subsystem level by the user with standard household tools within 10 minutes
- **SYST-SUST-03-A**: The drone shall contain any sparks and fire within the system in case of short-circuit
- **SUBSYST-ELEC-01**: The power storage subsystem shall have an energy capacity of 106 kJ
- **SUBSYST-ELEC-02**: The electronics subsystem weight shall not exceed 200 grams
- **SUBSYST-ELEC-03**: The electronics subsystem shall be able to be recharged
- **SUBSYST-ELEC-06**: The power storage unit shall deliver a voltage of 11.1 V
- **SUBSYST-ELEC-07**: The power storage unit shall deliver a power of 162.8 W
- **SUBSYST-ELEC-09**: The electronics subsystem shall not exceed 30 euros

11.2. Battery

The battery is the primary power source of the drone and constitutes the largest component by mass. Though the battery will power the entire system, the driving requirements are derived from the drivetrain. The parameters of concern for the battery are:

- **Total capacity required, mAh**: The battery must be able to store enough energy for the duration of the mission. This parameter is driven by the loitering phase
- **Max current required, A**: In a strict sense, power is the limiting factor, but as the voltage remains constant, the current is the parameter of concern. This is driven by the climbing phase.
- **Mass, g**: As the battery makes up a large portion of the drone, the mass needs to be carefully considered.

The requirements stemming from the drivetrain, and budgets taken into account for the other subsystems are stated in. This includes a margin of 10 %, 5% of which accounts for losses in the electrical system and the other 5% a general margin. The breakdown of the battery specifications is presented in Table 11.1.

Table 11.1: System electrical requirements

	Drivetrain	Other Subsystems	Total	Margin	Total
Required Capacity [mAh]	2274	450	2724	300	2996
Power [W]	153	10	163	16.3	179
Voltage [V]	11.1	5	11.1	-	11.1

Literature Study

Batteries can be constructed using different chemistry types, with these types giving different performance specifications. The considered battery types, and a short explanation of their characteristics, is given below.

- **Lipo**: Lipo, or Lithium polymer, is the chemistry type most frequently found in drones. This is because they are slim and are packaged in flexible cases.[1]

---

[1]BU-206: Li-po, `batteryuniversity.com/article/bu-206-lithium-polymer-substance-or-hype`, [accessed 20.06.2021]

- **Li-ion**: This chemistry type has a high energy density, making it preferable for use in a drone[2]. However, some safety concerns exist around Li-ion with Thermal Runaway (TR)d at high voltages. Furthermore, capacity and reliability depreciate over time. This isn't a large problem for this system, as the emergency nature of the drone means the battery *can* be used only once.
- **LiHV**: A variant on the Lipo cells, LiHV, or High Voltage Lipo. However, this comes at an increased cost and a lower reliability[3].
- **NIMH**: Nickel-metal-hydride (NiMH) chemistry batteries have a good cycle life with a high depth of discharge[4]. However, there are two major disadvantages when considering this application. Firstly, this chemistry type has a high self-discharge rate, which means frequent charging will be required. Secondly, voltage is not as high as other chemistry types (1.2 V vs 3.7V for lipo cells). Therefore, more cells would be required.

Battery Selection

With the battery specifications listed in Table 11.1 and the chemistry types identified, a battery can be selected. It is decided not to run a trade-off, as the design space is already sufficiently restricted. The batteries that meet the requirement shall be scored on their mass, since this appeared to be the most critical budget. The following batteries considered are listed in Table 11.2.

Table 11.2: Batteries considered

Battery Name	Chemistry	Capacity [mAh]	Nominal Voltage [V]	Available Current [A]	Mass [g]	Cost [€]
SONY | MURATA VTC6 18650[5]	Li-ion	3000	11.1	15	142.5	14.82
Turnigy Graphene Professional LiPo Pack w/XT60[6]	Lipo	3000	11.1	45	214.5	23.08
Turnigy High Capacity LiHV Pack w/XT60[7]	LiHV	3000	11.1	36	258	12.97

The mass of the Li-ion option is considerably lower than the rest. This would leave 50g, or 10% of the drone's budgeted mass free to be allocated elsewhere or lower the overall mass of the drone. Thus the chosen option is the **SONY | MURATA VTC6 18650** in a 3 Series 1 Parallel (3S1P) configuration.

Concept Analysis

Now a battery has been chosen, it is important to consider the performance characteristics, for example temperature performance. The studied characteristics were guided from literature[7].

Discharge Characteristic

As the battery is discharged, the output of the battery will change. In Table 11.1, the maximum required current is just below 17 A. As the maximum available current is 30 A, this is easily met. However, over the typical mission duration of 25 minutes, this would require a capacity of over 7000 mAh; over double the specified battery capacity. Therefore, the use of the current must be managed at any one time, though a further breakdown of the required currents is given the in section 11.4.

Charge Characteristic

One of the requirements calls for the drone to have the ability to be charged in the field. Two types of charging can be identified, trickle charging, where the battery is continually charged and topping charging, where the battery is charged discontinuously, e.g. once an hour. To quantify the charging requirements, the energy loss whilst in storage needs to be evaluated, or the self-discharge. The self-discharge for Lithium-ion batteries is

---

[2]What is a lithium-ion battery and how does it work?, https://www.cei.washington.edu/education/science-of-solar/battery-technology/, [accessed 21.06.2021]

[3]LiHV Battery vs. Lipo-Introduction, https://www.large.net/news/8nu43n7.html, [accessed 22.06.2021]

[4]Nickel Metal Hydride Batteries, https://www.mpoweruk.com/nimh.htm, [accessed 22.06.2021]

[5]SONY | MURATA VTC6 18650 3000MAH 15A https://www.18650batterystore.com/products/sony-vtc6, [accessed 20.06.2021]

[6]Turnigy Graphene Professional 3000mAh 3S 15C LiPo Pack w/XT60,https://hobbyking.com/en_us/turnigy-graphene-3000mah-3s-15c-w-xt60.html?, [accessed 20.06.2021]

[7]Turnigy High Capacity 3000mAh 3S 12C LiHV Pack w/XT60, https://hobbyking.com/en_us/turnigy-high-capacity-battery-3000mah-3s-12c-drone-lihv-pack-xt60.html, [accessed 20.06.2021]

estimated to be 5 % over 24 hours, then 1 - 2 % each month, with a 3 % margin[8]. With the rated capacity of 3000 mAh, a month at full charge would see a capacity degradation of around 300 mAh. Furthermore, temperature negatively affects the self-discharge. If the cell is at 60 °, the capacity can degrade by a third over a month. It is acceptable for the capacity to degrade, as some margin is built into the battery specifications. The acceptable limit is therefore placed at 2750. The 24 hour degradation of 5% listed reduces the capacity by 150 mAh, which is acceptable. Therefore, a topping-off charging strategy shall be chosen. The recommended charging current varies with the ambient temperature, but a current of 2 A and a voltage of 3.7 V is reasonable[9]. Assuming the battery degrades by 150 mAh every 24 hours, and the battery needs to be at (near) full charge for a month, a charging battery of 4650 mAh is required. Taking a 5 % margin into account, the required capacity of the charging battery is 4882 mAh.

Temperature Characteristic
The temperature affects the capacity of the battery. As the ambient temperature gets colder, the capacity decreases. For example, when the ambient temperature lowers to -10 °, the capacity drops to around 60 % of the rated capacity (1860 mAh). Though a conservative margin was taken into account with the battery specifications, this still poses a problem. Furthermore, as the battery is likely to heat up during use, this can't be exactly quantified. If early prototypes prove this to be a problem, a thermal control system could be implemented into the system. The battery also has a top temperature limit, at 80 °. This, however, is less of a problem. Though the battery will heat up during use, the most intensive phase of flight is during climb, which occurs during the early part of the mission.

Depth of Discharge
As the battery is cycled through charge and discharge cycles, the capacity of the battery is negatively affected. Furthermore, depth of discharge of the cycle also affects the capacity. As this is an emergency drone, the performance of one cycle is much more important the the overall lifetime. Therefore, the depth of discharge can be 100%.

Fireproof Bag
Lithium-based batteries need to keep the voltages across cells balanced during discharge, something which is expanded on in section 11.5. If the voltages differ too greatly, then Thermal Runaway (TR) can occur.[30] For this reason, the inclusion of a fireproof bag is examined. If TR occurs during flight, the mission success is critically threatened by the battery performance, so the inclusion of the a fireproof bag is not useful. Instead, the intended purpose of the fireproof bag is to keep the user safe during transport, for example during charging. Taking a reference fireproof bag and scaling it to the required battery size would lead to a bag mass of 9g.[9] Due to time constraints, full budgeting and integration will be left to subsequent phases.

11.3. Electronic Speed Controller
An ESC is an electronic circuit which controls the speed of a motor. An ESC is required in order to run the quadcopter's brushless direct current motors. ESCs connect the flight computer to the motors just like a gear box in a car. Just as a gear box controls the speed of the wheels, the ESCs use the flight computer output to rotate the motors at the required speed for the given throttle setting. There are two different types of ESCs that can be chosen being 4-in-1 ESCs, which are printed circuit boards with four speed controllers, and Individual ESCs. Before specific speed controllers are selected, a trade-off needs to be performed between these two.

The result of the trade-off can be seen Table 11.4 where individual ESCs won. This was mainly due to the fact that 4-in-1 ESCs would constrain the design for repairability, as they would be placed inside the shell of the drone. The individual ESCs on the other hand could be placed in the arm which would facilitate repairability.

ESC Concept Trade-off Criteria
The trade-off criteria used are weight, cost, repairability and reliability/risk. Sustainability is not included as both components are similar and the materials they are made of will generally also be similar. Furthermore, the weight criteria will indirectly take into account sustainability, as the heavier the component, the more material it

---

[8]What does Elevated Self-discharge Do?, `https://batteryuniversity.com/article/bu-802b-what-does-elevated-self-discharge-do`, [accessed 19.06.2021]

[9]Anself Fireproof Explosionproof Lipo Battery Guard Safe Bag, `https://www.amazon.in/Anself-Fireproof-Explosionproof-Portable-Resistant/dp/B07S18DKQT/`, [accessed 26.06.2021]

requires. Sustainability will be taken into account during the trade-off between different off-the-self components. The different criteria and how they are evaluated is now explained.

To evaluate weight and cost criteria, a database of over 200 recent ESCs (2018 onward) was found [10]. The database included both 4-in-1 and Individual ESCs, their prices, weights and more parameters. The average cost and weight of one 4-in-1 ESC was found to be 54.6 euros and 12.8 grams respectively. The average cost and weight of four Individual ESCs was found to be 55.0 euros and 24.3 grams respectively. As it can be seem the prices of both costs are comparable and the weight varies significantly, approximately twice the weight for Individual ESCs.

The repairability criteria comes from the stakeholder requirement **STAK-SUST-01**. This criteria states that the drone shall be able to to be repaired in a modular fashion and as previously mentioned, using a 4-in-1 ESC might restrict the design in this capacity. The weight and cost of each concept are taken into account given their restrictions in the budget on this subsystem. Finally the reliability/risk criteria entails the failure rates and technical risks associated with both concepts. For example, if an individual ESC were to be damaged, only one of the ESCs would have to be replaced whereas a 4-in-1 ESC would have to be fully replaced.

ESC Concept Criteria Weights

The weight selection for each criteria is performed using the AHP method explained in section 4.1. The relative importance table is shown in Table 11.3.

Table 11.3: Relative importance table and the final weights with a CR of 0.0015

	Weight	Cost	Repairability	Reliability/Risk	Final Weight
Weight	1.0	2.0	0.333	1.0	0.19
Cost	0.5	1.0	0.2	0.5	0.10
Repairability	3.0	5.0	1.0	3.0	0.53
Reliability/Risk	1.0	2.0	0.333	1.0	0.19

As can be seen, Repairability is the most important criteria given **STAK-SUST-01**. Cost and weight are less important as the repairability affects the cost of the components and what structure is needed to facilitate it. Weight and reliability/risk were given the same weight as the mass budget is quite restricting and the ESCs failure likelihood is similarly critical. Cost, on the other hand, is weighed less important than weight as its budget is less restricting. All four criteria have the same scoring system, being a five for excellent, a four for good, a three for satisfactory, a two for poor, and a one for unacceptable. As this trade-off is mostly qualitative and based on market analysis, the scoring system used is also qualitative.

Table 11.4 shows individual ESCs as the winner of the trade off. The 4-in-1 performs very well for the weight criteria but poorly in repairability and acceptable in reliability/risk. Individual ESCs perform satisfactorily in weight and cost and good in repairability and reliability/risk. As previously explained, having a 4-in-1 ESC means that the entire drone shell and electronics stack would have to be removed to replace it. This makes the fulfilment of **STAK-SUST-01** complicated which resulted in the poor score compared to the Individual ESCs better score being placed in the arm. Regarding reliability/risk the 4-in-1 ESC was only satisfactory as it is placed in the electronics stack and heats up significantly over time which could lead to failure or a decrease in performance. However, it is important to mention that smaller individual ESCs can potentially heat up quicker than 4-in-1 ESCs. This can be mitigated by choosing an ESC which is rated quite higher than the peak current of the chosen motors. Individual ESCs a higher current rating do not necessarily incur a larger weight and cost.

Table 11.4: Trade-off results showing that the Individual ESC is winning

ESC concept	Weight	Cost	Repairability	Reliability/Risk	Final Score:
1 Individual	3	3	4	4	3.72
2 4-in-1	5	3	2	3	2.84

ESC Off-the-shelf Selection

Given the selection of the Individual ESC concept and motor in chapter 8, the specific COTS ESC can be selected. The database of ESCs used in the concept trade-off was used with a couple newer speed controllers.

---

[10]FPV Drone ESC Buyer's Guide, `https://oscarliang.com/choose-esc-racing-drones/`, [accessed 22.06.2021]

The result of the trade-off can be seen Table 11.8 where the XILO 40A ESC won. This was mainly due to the low cost and size of the ESC compared to all other competitors.

The XILO 40A ESC is a low cost ESC at 6.7 euros. It weighs 6 grams excluding wires and the dimensions are 40x14x4 mm. It is rated for 40 amps but can tolerate a burst current of up to 50 amps. It runs the DSHOT 600 protocol and comes with a capacitor which protects the battery from voltage spikes [11].

The trade-off criteria that will be taken into account are weight, cost, size, ΔI/W, protocol and sustainability. The size criteria refers to the thickness of the ESC. As the ESC needs to fit into the drone's arm, a thickness smaller than 5mm is required in order to maintain a slender and aerodynamic shape. The ΔI/W criteria is a computed parameter which is equal to the difference between the current rating of the ESC divided by the weight of the ESC. This parameter was chosen as the larger the ΔI, the less the ESC overheats and the higher its reliability. However, the ΔI was divided by the weight as the difference in current ratings should not be the result of an increase in mass. The protocol of an ESC is comparable to the Operating System (OS) of a computer or phone. The protocol determines how fast the ESC and and flight computer are able to communicate together. This criteria was selected as, although the difference in protocols leads to small changes in timing in the order of microseconds, these differences can still affect the performance of the drone greatly [12]. Finally, sustainability will be taken into account as there are requirements such as **SYST-SUST-16** and **SYST-SUST-17** which require the manufacturer to have an ISO14001 and FLA certification. The weight selection for each criteria is again performed using the AHP method.

The relative importance is shown in Table 11.7. Weight was found to the most important criteria, followed by cost, size and sustainability. ΔI/W and protocol as ΔI/W is used to separate higher rated ESCs and protocol as the differences between the options are relatively small. The scoring system for weight, cost size and ΔI/W criteria will be using standard deviation approach as explained in chapter 3. For protocol and sustainability, the scoring methods shown in Table 11.5 and Table 11.6 will be used respectively.

Table 11.5: Scoring system for ESC protocol

Category	Score
latency<15 μs	3
15<latency<50	2
50<latency<100	1
latency>100	0

Table 11.6: Scoring system for ESC sustainability

Category	Score
ISO 14001 or FLA	2
CE or ROHS	1
none	0

Table 11.7: Relative importance table and the final weights with a CR of 0.0015

	Weight	Cost	Size	ΔI/W	Protocol	Sustainability	Final Weight
Weight	1	2	2	4	9	3	0.33
Cost	0.5	1	1	5	7	4	0.24
Size	0.5	1	1	5	7	4	0.24
ΔI/W	0.25	0.2	0.2	1	2	0.5	0.06
Protocol	0.11	0.14	0.14	0.5	1	0.25	0.03
Sustainability	0.33	0.25	0.25	2	4	1	0.09

Table 11.8 shows the XILO 40A ESC as the winner of the trade off. As seen this ESC performs best in cost and size which are the second most weighed criteria. The ESC performs well in both protocol and ΔI/W but less well in weight. The ESC is still quite light weighing only 6 grams. The second best ESC is the Lumenier Razor Pro F3 45 which outperforms the XILO 40A in all of the opposite criteria, namely weight, ΔI/W, and protocol. Unfortunately for all the ESCs no certification for sustainability was found. A market analysis specifically for ESCs which would meet the ISO 14001 and FLA requirements was performed however it yielded no results. Perhaps for future development the production of the ESCs can be performed by a separate manufacturer who has the capabilities of producing ESCs and possesses the ISO 14001 and FLA certifications, or at least the CE and ROHS markings.

---

[11]XILO 40A BLHeli_S 2-4s ESC, `https://www.getfpv.com/xilo-40a-blheli-s-2-4s-esc.html`, [accessed 22.06.2021]

[12]How to choose ESC, `dronenodes.com/drone-esc-electronic-speed-controller/`, [accessed 22.06.2021]

Table 11.8: ESC Component Trade-off Matrix

ESC	Weight	Cost	Size	∆I/W	Protocol	Sustainability	Final Score
1 Flyduino KISS ESC 24A	2	0	2	1	3	0	1.30
2 Lumenier Razor Pro F3 45A	3	1	1	3	3	0	1.75
3 XILO 40A	1	3	3	2	2	0	1.96
4 Lumenier 35A	1	2	1	1	3	0	1.21
5 Spedix IS45 45A	1	1	1	2	2	0	0.99
6 Lumenier 30A	2	2	1	1	3	0	1.55
7 SPEDIX ES30 HV 30A	0	1	1	1	3	0	0.63
8 Spedix GS30 30A	1	2	1	1	3	0	1.21

11.4. Power Distribution Board

The PDB is a printed circuit board that is used to distribute the power of the battery to different components of the quadcopter. There are two main requirements to be considered in the selection of the appropriate PDB, namely the voltage capabilities and current capabilities. It is important to find out what voltages the components connected to PDB require, as voltage inputs that are too high may result in failure of electrical components of the quadcopter. Luckily, the PDBs considered during the trade-off are integrated with a voltage regulator. It should be noted that the amount of power that can be supplied by the integrated voltage regulators is limited. [13] If the maximum rated current of the voltage regulator is exceeded, it is likely to overheat and gets damaged[14]. For this reason an overview needs to be made of the maximum current draw of all components connected to the PDB to make sure that the PDB does not need to provide more power than it is capable of.

The other important factors which should be considered during the selection of a PDB are the size, cost, weight and the sustainability. The size is important since the PDB should fit in the designed case of the drone. The wires connecting to the ESC are often the heaviest and thickest wires of the quadcopter, after the wires connecting to the battery, and for that reason it is of great importance to consider where the wires of the ESC will connect to the PDB. The cost and weight are of importance since the chosen PDB should fit in the budget given to it. Finally, one should aim for a PDB which is as sustainable as possible.

Three types of PDBs are considered, namely a separate PDB, a PDB integrated in the flight computer and a PDB integrated in a 4-in-1 ESC[15]. A PDB integrated in a 4-in-1 ESC has the advantage of being compact, lightweight, relatively cheap and it reduces the complexity of the wiring. However, due to the trade-off performed in section 11.3, it is decided not to use a 4-in-1 ESC, mainly due to the lack of repairability in a modular fashion (**STAK-SUST-01**). This trade-off was explained in section 11.3.

A PDB which is integrated in the flight computer is ideal for frames with tight spaces as it reduces the height of the stack, it simplifies the wiring and reduces the weight. The drawback of a PDB being integrated in the flight computer is that it is prone to electrical noise interference. Due to a trade-off performed in section 10.6, a flight computer is chosen which does not include a PDB.

This means the only separate PDBs are considered in the selection process. The advantages of using a separate PDB are that the voltage regulators of a separate PDB are more efficient than the PDBs integrated in a flight computer, it reduces stress on the flight computer and it is better filtered from electrical noise. It is also logical that using a separate PDB increases the amount of wiring needed. The PDBs usually consists of two Battery Eliminator Circuits (BECs), which is basically a step down voltage regulator. The BECs will take in the battery voltage and reduce it down to a voltage that can safely power other components of the quadcopter. A PDB have four different locations at which each separate ESC can be connected.

PDB Selection

An overview has been made of PDBs which can be connected to the chosen battery. The PDBs chosen to be considered in the PDB selection can all be connected to a 3S Li-Ion battery and all can work properly with the voltage input range of 10.8 V up to 11.1 V from the battery. Being able to deliver the requisite output voltages, the maximum output current to the other components connected to the PDB of the quadcopter and the maximum output current to the ESCs have been included as a pass/fail criteria to decide whether a PDB

---

[13]PDB, www.dronetrest.com/t/power-distribution-boards-how-to-choose-the-right-one/1259, [accessed 07-06-2021]

[14]PDB, https://www.getfpv.com/learn/new-to-fpv/all-about-multirotor-fpv-drone-power-distribution-board/, [accessed 07-06-2021]

[15]PDB types, https://dronenodes.com/pdb-power-distribution-board/, [accessed 07-06-2021]

will be included in the trade-off. The requisite output voltages are 5 V and 12 V. An overview has been made of the total maximum current draw of the components connected to the 5 V output of the PDB. This overview can be seen in Table 11.9.

Table 11.9: Current draw of components connected to the 5V output of the PDB

Component	Maximum Current Draw
Iridium module	100 mA
Cellular module	2000 mA
GNSS	30 mA
4x LED	80 mA
Buzzer	30 mA
Flight computer	250 mA
Companion computer	120 mA
3x ultrasonic sensor 1	60 mA
2x ultrasonic sensor 2	8 mA
Light dependant resistor	5 mA
Total	2683 mA

As seen, the PDB should be able to deliver (in an extreme case) a total maximum current of at least 2683 mA to the components connected to the 5 V output voltage. This is the case when the drone is actively using its secondary communication means and the iridium module is at rest mode as it was decided that the primary and secondary communication means will not be used at the same time. As can be seen in the electrical block diagram in section 13.1 no components will be connected to the 12V output of the PDB. The maximum output current to each ESC the PDB should be able to provide is 7 A. Many PDBs were found which passed the criteria of being able to provide the requisite output voltages and to provide the maximum output current to each ESC. However, only one PDB was found which met the criteria related total maximum current draw of the 5 V output of the PDB, namely the Matek Mini Power Hub [16]. An overview of the parameters of the Matek Mini Power Hub can be found in Table 11.10 and a visual representation of how the PDB looks can be seen in figure 11.1[17]. As no information is provided on the sustainability certifications by the distributor, the sustainability of the PDB could not be estimated.

Table 11.10: Overview of Matek Mini Power Hub PDB

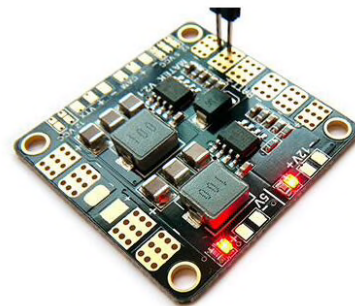| Name	Matek Mini Power Hub
Output voltages	5V and 12V
Maximum output current to each ESC	20A
Maximum output current of BEC's	3A (5V) and 2A (12V)
Weight	6g
Dimensions	36 x 36 mm
Cost	€ 7,52

Figure 11.1: PDB Mini Power Hub PDB

11.5. Battery Management System

The BMS is the electronic system that manages the quadcopter's rechargeable battery. It can can be characterised as the brain of the battery. The BMS performs two main tasks: controlling and monitoring the battery.

The controlling task of the BMS includes cell balancing, safe and optimal utilisation of the battery and thermal management[26]. To minimise the chances of overcharging or discharging, and to ensure that the state of charge remains the same or within a very narrow band while charging or discharging, the BMS performs cell balancing. The battery is kept within safety margins by controlling the charging and discharging schemes of

---

[16]PDB Matek Mini Power Hub, `https://nl.aliexpress.com/item/1005001555971144.html?spm=a2g0o.productlist.0.0. 5f7c1a72k17625&algo_pvid=d0a21b8b-0df2-4c9a-9baa-849b0020018d&algo_expid=d0a21b8b-0df2-4c9a-9baa-849b0020018d-2& btsid=2100bb4916226311886434211efd7d&ws_ab_test=searchweb0_0,searchweb201602_,searchweb201603_,` [accessed 07-06-2021]

[17]PDB Matek Mini Power Hub, `https://nl.aliexpress.com/item/1005001555971144.html`, [accessed 07-06-2021]

the battery. The BMS collects data regarding the ageing of the battery such that the lifetime of the battery can be optimised. Finally, an advanced BMS can decide to heat or cool the battery system by collecting information of the temperature distribution over the battery.

The monitoring task of the BMS includes measurement and estimation of important parameters and health monitoring[26]. The voltage and current of the battery cells, as well as the temperature distribution in- and outside the battery, are typical parameters being measured by the BMS. The important parameters which cannot be measured are being estimated by the BMS. These estimated parameters include the State of Charge (SoC), State of Health (SoH) and State of Life (SoL). Actuator faults, sensor faults, network faults, battery faults and electronic circuit faults are all examples of sources of different types of faults within the BMS and battery. The responsibility of the BMS is detecting and isolating the faults and generating alarm signals.

The choice of the BMS is dependent on the the battery that will be used in the quadcopter. The Battery Management Systems considered in the trade-off are all compatible with 3S Li-Ion batteries. Due to factors such as different ageing processes, temperature distribution in the pack and imbalance in the battery characteristics from production, cell imbalancing is introduced. The cells do not possess the same amount of charge due to these existing mismatches and for that reason charging or discharging the pack at the same rate might lead to overcharging and overdischarging some of the cells. Cell balancing is crucial for Li-Ion batteries as overcharging or overdischarging can cause serious cell damage, such as a decrease of the battery capacity. There are two important parameters for the BMS to monitor: The BMS should ensure the correct overdischarge voltage and overcharge voltage is being applied. The manufacturer of the cells chosen to use in the battery specify that an overcharge voltage detection of 4.25 V and a overdischarge voltage detection of 2.5 V is required to keep the battery in a good state[18]. Thus, this is included as a pass/fail criteria for choosing the BMS resulting in the options listed in Table 11.11 being considered in the trade-off.

On top of that, the manufacturer of the cells specifies that the maximum constant discharge rating of the cells is 20 A. However, as insufficient information was provided on the capabilities of detecting the overcurrent of off-the-shelf battery management systems, this was not included as a pass/fail criteria. All BMSs considered are able to protect against short circuits. It should be noted that the weight of the options is not included in the as they were not available for all options. Also, it was not possible to find any information on the RoHS certification of the companies selling the battery management systems and ISO-14001 as well as FLA certification of the BMS products and for that reason the sustainability of the different options could not be evaluated.

Table 11.11: Overview of BMSs considered during trade-off

Name	Tinytronics BMS 3S[19]	HX-3S-FL25A-A[20]	HX-35-01[21]
Dimensions	56 mm x 45 mmx 2.6 mm	56 mm x 45mm x 1.2mm	50 mm x 16 mm x 1mm
Cost	€ 4,50	€ 6,53	€ 10,70
Over charge detection voltage	4.25 V	4.25 V	4.25 V
Over discharge detection voltage	2.5 V	2.3-3 V	2.3-3.0 V
Name	ANMBEST[22]	Songhe 3S[23]	
Dimensions	41 mm x 62 mm x 3.4 mm	56 mm x 45 mm x 4.0 mm	
Cost	€ 8,24	€ 6,50	
Overcharge detection voltage	4.25 V	4.25 V	
Over discharge detection voltage	2.5 V	2.3-3.0 V	

---

[18]Li-Ion cell, https://www.18650batterystore.com/products/sony-vtc6, [accessed 07-06-2021]

[15]Tinytronics BMS, https://www.tinytronics.nl/shop/nl/batterij-en-accu/overige/li-ion-li-po-protectiecircuit-(bms)-3s, [accessed 10-06-2021]

[15]HX-3S-FL25A-A, https://www.hlhv.nl/Webwinkel-Product-253449009/3S-11.1V-25A-18650-Li-ion-Lithium-batterij-BMS-Protection-PC.html, [accessed 10-06-2021]

[15]HX-35-01, http://www.amppower.nl/12V-3S-10A-BMS, [accessed 10-06-2021]

[15]ANMBEST, https://www.amazon.com/ANMBEST-Charger-Protection-Lithium-Battery/dp/B08GFRXHNL/, [accessed 10-06-2021]

[15]Songhe 3S, https://www.amazon.com/Lithium-Battery-Protection-Balanced-Discharge/dp/B082VLCDYM, [accessed 10-06-2021]

[15]ZkeeShop 3S 25A, https://www.amazon.nl/ZkeeShop-3S-25A-Batterij-Protection/dp/B073MJ6J8R/, [accessed 10-06-2021]

As no real distinction could be made on the performance of the BMS options considered, the BMS will be chosen based on how well it is able to fit within the given budgets. As all options considered have approximately the same dimensions, the final choice is made based on the price of the options making the Tinytronics BMS 3S the winner. This BMS is made for 3S Li-Ion batteries and is capable of detecting the correct overcharge and overdischarge voltages as specified the battery manufacturer. It costs € 4,50 and and has dimensions of 56 mm x 45 mm x 2.6 mm making it perfectly fit in the given budgets. As no information was given by the distributor on the weight of the BMS, a BMS of similar size was found with the weight indicated as comparison resulting in an assumed weight of 10 grams.

11.6. Requirement Compliance

With the electronic's subsystem established, it is to be checked with the requirements previously established. With the use of a compliance matrix as shown below it can be seen which requirements are met and which are either omitted, failed to meet or need further evaluation in order to check for compliance. These will be further elaborated after the table in the feasibility analysis.

Table 11.12

ID	Requirement	Compliance	Comment
STAK-GENR-03	The drone shall not have exposed electronics	✓	
SYST-RISK-01	The critical components shall be designed to have safe life or fail safe philosophy implementation		No components have been designed
SYST-THER-01	The drone shall be able to operate in a temperature range from 20 to +40◦C	✓	
STAK-SUST-01	The drone shall be able to be repaired in a modular fashion	✓	
SYST-SUST-02-A	The drone shall be electrically powered	✓	
SYST-SUST-02-B	The drone shall not be manufactured out of toxic materials		Battery made out of toxic materials
SYST-SUST-13	The drone shall be able to be disassembled to a subsystem level by the user with standard household tools within 10 minutes		Omitted
SYST-SUST-03-A	The drone shall contain any sparks and fire within the system in case of short-circuit	✓	
SUBSYST-ELEC-01	The power storage subsystem shall have an energy capacity of 106 kJ	✓	
SUBSYST-ELEC-02	The electronics subsystem weight shall not exceed 200 grams		212,50 grams
SUBSYST-ELEC-03	The electronics subsystem shall be able to be recharged	✓	
SUBSYST-ELEC-06	The power storage unit shall deliver a voltage of 11.1 V	✓	
SUBSYST-ELEC-07	The power storage unit shall deliver a power of 162.8 W	✓	
SUBSYST-ELEC-09	The electronics subsystem shall not exceed 30 euros		55,06 euros

11.7. Discussion & Conclusion

The battery focused on different chemistry types that met the system electrical requirements and scored on their weight. From a point of thoroughness, a more rigorous analysis of the chemistry types could have been carried out, but instead the literature study was inline with resources available. Furthermore, an analysis of how the market selection might change in line with technological improvements.

For the selection of the PDB, an overview has been made of PDBs which can be connected to the chosen battery. However, since only one PDB was found which passed the criteria of being able to withstand the maximum output current to the components of the drone which are connected to the 5V output of the PDB, no trade-off was performed during the selection of the PDB. By getting in contact with shops which are very experienced with the electronics of drones, the team could be able to get an overview of more PDBs which are suitable for the LastHope drone, which can eventually result in a PDB which fits better within the given budgets as a trade-off could be performed. On top of that, it could clarify the sustainability of the PDBs as currently no information was found on the sustainability certification by the distributor.

A BMS was chosen that could correctly manages the quadcopter's rechargeable battery. The manufacturer of the cells of the battery specifies that the maximum constant discharge rating of the cells is 20 A. However, since no sufficient information was provided by the distributors on the capabilities of detecting the overcurrent by off-the-shelf battery management systems, the team should get in contact with the distributors to make sure the BMS chosen is capable of doing this. On top of that, like for the PDB chosen, there was no available on the sustainability certifications of the distributors, so the team should check that as well.

It should be noted that during the final design phase of the DSE, the wiring of the LastHope drone has not

been investigated. By getting a clear overview of what the wiring scheme will look like, the team can try to make it as effective as possible which will eventually result in a decrease in cost and weight. Extra attention should be made for the wiring connecting to the ESCs and the battery of the drone, as they are generally the thickest and heaviest wires. In order to decrease the risk of power loss in case of a collision, the team should design the connectors such that they fit correctly and the connectors should be rated to the conditions it is expected to operate in.

12. Communications

This chapter addresses the communications subsystem for the LastHope drone. The primary communications method has already been determined in the Midterm report [2], namely Iridium 9603. This is to be revisited once the costs for each of the subsystems has been determined allowing for a clearer overview and reiteration of budget allocation to be possible. Nevertheless, for the second communications method, in the case that there is failure in the first communications system, a back up method is to take over and make sure that contact with the emergency services can still be established. On top of this, the secondary communication system allows the drone to send photos and videos of the emergency situation using cellular connection.

The second means of communication shall be different to the first, as this decreases the chances that the same failure would happen twice. Therefore, instead of relying on satellite, the second means of communication will depend on non-satellite communication methods, such as cellular or radio. This also allows for the drone to increase the amount of mission options, offering a broader range of alternatives to reach connectivity. Moreover, data transfer rates would be a lot faster and cheaper when using systems such as cellular communications in comparison to satellite. As an example, a standard photo on an iPhone 6 of a 2448 x 3264 pixels size would generally take over three hours to transmit through satellite and cost over € 200[1] hence the Iridium module will only be used for coordinates and distress messages, as it can only only send 340 bytes per message[2].

First, the requirements related to the communication subsystem are shown in section 12.1, followed by an explanation of the primary communication system in section 12.2. section 12.3 explains the trade-off performed regarding the secondary communication system. Finally, section 12.5 shows which GNSS module is chosen in the design.

12.1. Requirement Analysis

The requirements related to the communication are analysed in order to guarantee that the system is fit-for-purpose. The requirements related to the communication subsystem can be found below.

- **STAK-COST-03**: The subscription costs of the additional service shall not exceed EUR 15 per month
- **SYST-THER-01**: The drone shall be able to operate in a temperature range from -20 to +40 $^\circ$C
- **SYST-THER-02**: The drone should be able to operate in a temperature range from -30 to +50 $^\circ$C
- **STAK-COMM-01**: The drone shall have at least 2 different means of communication with emergency services
- **STAK-COMM-02**: The drone shall be able to communicate with emergency services at areas with cellular reception
- **STAK-COMM-03**: The drone shall communicate user location to the emergency services
- **STAK-COMM-04**: The drone shall communicate user data to the emergency services
- **STAK-COMM-05**: The drone shall send landing coordinates for easy recovery of the drone
- **STAK-COMM-06**: The drone should transmit its live location to the user
- **SYST-COMM-01**: The drone shall have at least one mean of communication, between drone and emergency services, that is "two-way"
- **SUBSYST-COMM-10**: The communication subsystem shall have a weight limit 30 grams
- **SUBSYST-COMM-12** The communication subsystem shall have a cost limit of 200 euros

---

[1]Satellite transmission costs, `http://www.globalmarinenet.com/how-to-send-photos-over-your-satellite-phone/`, [accessed 09.6.2021]

[2]RockBLOCK 9603, `https://cdn.sparkfun.com/assets/2/5/3/2/e/RockBLOCK-9603-Product-Information-Sheet.pdf`, [accessed 15.6.2021]

12.2. Primary Communication

The primary communication method consists of an Iridium 9603 modem chosen from the Baseline report [1]. The other options analysed failed to offer rapid pinging location, no global coverage or were not within the budget with respect to size, weight or costs.

This two way communication product offers global coverage constellation as it consists of 66 low orbiting satellites. However, it only supports Short Burst Data (SBD) capability, hence it can not operate with short message service (SMS), circuit switched data nor voice messages. This transceiver relies on wireless data application integrated with other hardware and software subsystems of the drone. The modem itself serves as a black box, meaning that other functions such as microprocessor, digital and analog inputs and outputs, antenna, cable distribution system and power supply must be provided for full functionality. It should be noted that the 9603 does not comply with Subscriber Identity Module (SIM) as it solely depends on the standards for Radio Emissions Compliance, Electromagnetic Compatibility, and AC Safety in the United States, European Union and Canada[3].

The transceiver itself weighs 11.4g, has a size of 31.5 x 29.6 x 8.1 mm and costs € 187. Moreover, there is a fee to using this product however, it depends on the distributor. The cheapest one seems to be provided by the Satphonestore[4] for $15.99 or €13.26 per month. Other hardware components must be selected in order for the Iridium 9603 to be integrated in the drone. This is addressed in section 12.4.

12.3. Secondary Communication

The secondary communication's module is used not only as a redundancy measure with establishing connection with the emergency services, but also to allow the drone to have a broader range in options to increase the reliability of mission success. This means that before the commence of the mission, the drone evaluates which option is most feasible in the scenario that it is in. With all the information provided beforehand, as explained in section 10.10, it can choose secondary or primary communication method.

Secondary communication's method

Many different options were considered for the secondary communication's method. Satellite was omitted to avoid committing the same failure twice, therefore narrowing the most feasible options to be cellular radio and cellular non-radio, which will be further elaborated in the next subsections.

Cellular communications

Cellular communication is the most common means of transferring information from person-to-person, making mobile phones a convenient and necessary day-to-day tool. Unlike the primary means of communication, the secondary method does not depend on Earth orbiting satellites, but on ground cells and cell towers instead.

Cells are areas which provide mobile network from the presence of a base station, also known as a cell tower[5]. These cell towers receive electromagnetic waves from its users and transmits the data to its respective cell towers in the form of radio waves through optical fibre cables. These cables are laid under the ground or the ocean for international and national connectivity. This enables users to call other users and connect to the internet anywhere around the world where cellular signal is available.

The frequency used by the electromagnetic waves generally ranges from 800MHz to 2100MHz. Europe uses dual bands, namely 900MHz and 1800MHz[6], meaning that the communications module must be able to transmit and receive waves with these frequencies. The lower band of the spectrum is used for covering larger areas as less energy is lost in travelling through the medium compared to high frequencies. On the other hand, the higher band of the spectrum provides high data speeds and connectivity[7]. The terminology used to describe data connectivity are 1G, 2G, 3G and 4G. The G means Generation where:

- **1G** Analogue mobile network only used for voice calls, very limited with the amount of users.
- **2G** Digital technology provides the ability to share calls, text messages and limited amount of data using General Packet Radio Service (GPRS)[8].

---

[3]Iridium 9603 `https://www.cls-telemetry.com/wp-content/uploads/2018/12/Iridium-9603-9603N_Developers-Guide.pdf`, [accessed 16.6.2021]

[4]Iridium SBD Rates `https://www.satphonestore.com/airtime/iridium-sbd.html`, [accessed 17.6.2021]

[5]Spectrum, `https://www.vodafone.com.au/red-wire/demystifying-mobile-networks`, [accessed 07.6.2021]

[6]Dual bands, `https://www.worldtimezone.com/gsm.html`, [accessed 10.6.2021]

[7]Spectrum, `https://www.vodafone.com.au/red-wire/demystifying-mobile-networks`, [accessed 07.6.2021]

[8]Mobile generations, `https://hutch.lk/difference-2g-3g/`, [accessed 07.6.2021]

- **3G** The same as its previous generation, however, 3G supports additional features such as video calls and mobile TV. A disadvantage is that it has a lower coverage than 2G due to higher frequencies used in 3G and larger amount of 3G users.
- **4G** The same as its predecessor, but allowing higher speeds of data transfer. The main downside is that 4G's coverage is a third of 3G's[9].

1G is not considered as it uses analogue technology, meaning data quality is poor, signal bandwidth is low and it's sensitive to external influences. 4G's coverage is too low for the purpose of the mission. Another characteristic is the upload speed. This will determine how long it would take for the drone to transmit the necessary information to the emergency services. The average upload speed for 2G and 3G are 0.1 Mbps[10] and 0.4 Mbps[11] respectively. These will be the assumed speeds for future calculations. It should be noted that the speeds are very much dependent on the strength of the signal. It is also evident that 3G covers only a third of what 2G covers, but, due to the higher transfer rates, further evaluation is needed to determine whether the advantage would outweigh the risk related to using 3G.[12]

With these speeds the time taken for transferring of data for both 2G and 3G can be determined as shown in Table 12.1.

Table 12.1: Transfer time between 2G and 3G for different activity comparisons

Activity	Data size	2G	3G
Upload a high resolution photo (figure 12.1a)	5.8MB	7.7 minutes	1.9 minutes
Upload a low resolution photo (figure 12.1b)	66kB	5.3 seconds	1.3 seconds

There are two major criteria when it comes to deciding what quality of image to upload to the emergency services. The first criteria is the speed at which the files are uploaded and the second criteria is how much help will the photos provide. The low resolution is the best choice out of the two.

As can be seen in figure 12.1, two sides of the spectrum for image resolution are compared. With the figure 12.1a, one is able to identify each individual on the ground despite from an altitude of more than 50 meters. However, it takes approximately two minutes to upload one image with 3G and eight minutes with 2G. By the time one high resolution photo is uploaded, the drone could have uploaded 88 low resolution photos. Having many low resolution photos where one is still able to distinguish distinct objects, such as trees, fields, houses and lakes, would provide the services a lot more information and reference points for finding the person in need of rescue than one high resolution photo.

(a) A high resolution picture of 5.8 MB captured by a drone takes 7.7 minutes to transfer by 2G and 1.9 minutes by 3G

(b) A low resolution picture of 66 kB captured by a drone takes 5.3 seconds to transfer by 2G and 1.3 seconds by 3G

Figure 12.1: The comparison between a high and low resolution photo taken by different drones

---

[9]Mobile generations, `https://hutch.lk/difference-2g-3g/`, [accessed 07.6.2021]

[10]2G, `https://www.giffgaff.com/blog/is-2g-data-still-usable/`, [accessed 07.6.2021]

[11]3G, `https://www.4g.co.uk/how-fast-is-4g/`, [accessed 07.6.2021]

[12]Mobile generations, `https://hutch.lk/difference-2g-3g/`, [accessed 07.6.2021]

On the other hand, videos provide a wider scope of useful references, however, at the cost of longer upload times. There are many different configurations that can be chosen, as can be seen in Table 12.2. The most crucial specifications are:

- Frames per second: this rate determines the frequency at which a frame, or snapshot, appears on the screen. It is dependent on the motion of the camera as well, as the faster it moves, the blurrier the videos will appear, hence a higher frame rate should be used.
- Bitrate: this refers to the amount of video data transferred in a certain period of time. The higher the bitrate, the better the high resolution and high frame rate videos will look. The recommended bitrates are respective to the quality and frame rate of the video[13].
- Data size: this is the result from the parameters chosen, the higher the quality, frame rate and bitrate, the higher the size of the data, hence longer upload time[14].

Table 12.2: Time for transfer of data for different telecommunication methods for different video types with a time duration of 10 seconds

Quality	Frames per second	Recommended bitrate [Mbps]	Data size [MB]	2G [min]	3G [min]
1080p	60	12	15	20	5
	30	8	10	13.3	3.3
720p	60	7.5	9.4	12.5	3.1
	30	5	6.3	8.4	2.1
480p	60	4	5	6.7	1.7
	30	2.5	3.1	4.1	1.0

As an equal comparison, the videos will have a time duration of 10 seconds. This can be scaled down to 5 seconds or up to 20 seconds according to the mission type, the data size is linearly dependent on the video duration. Nevertheless, a 10 second video is able to capture sufficient data when the drone deploys for the emergency services to use. Recording this stage of the mission can provide the services with accurate reference points and narrowing down the victims' location when approaching the area. However, the video configurations shown in Table 12.2 are a few out of many that are possible, but this serves as a starting point for the analysis. Future iteration can take into account the different parameters such as frame rates and bitrates in order to adapt the video quality according to the mission type more appropriately.

The 480p, 30fps at 2.5Mbps is the video configuration most suitable for the mission as it would transmit the video the fastest and still comply with its functionalities. It should be noted that the drone is in motion when recording the video, hence the frame rate can be changed respectively. For example, when the motion becomes too high, the videos will start looking unnatural and have a "soap opera effect". This is a process when the system tries to display a video at a higher refresh rate than the original source by motion interpolation. This should be avoided as it can increase the blurriness of the video.

480p still provides a sufficiently clear picture of the surroundings. Examples are shown in figure 12.2[15] where figure 12.2a is used as a reference. It can be seen in figure 12.2b, that the person indicated in the red circle in figure 12.2a is still distinguishable at an altitude of approximately 50 meters. For example, a drone travelling at 10 meters per second covers 100 meters with 10 seconds of footage. This would provide the emergency services with solid data to pin point the user's location. In the case that the drone can not fly up due to obstacles, it will travel horizontally by tilting at an angle to which videos and photos can also be taken covering larger parts of the area, compared to if the drone were to take photos and videos up-right at the same altitude.

Sending larger files is also possible with the use of compressors. This compression process consists of reducing the total number of bits used to represent a video or photo. For this to be possible, a specific algorithm or formula is used to determine the best way to reduce the size of the data. Large areas with repetitive colour are the main target when removing areas. This is then reconstructed in the video when the file is opened, with the use of interpolation processes. The algorithms used are referred to as codecs. Some type of codecs

---

[13]Bitrate, `https://oscarliang.com/upload-dji-fpv-footage-youtube/`, [accessed 07.6.2021]

[14]Data size, `https://toolstud.io/video/filesize.php`, [accessed 14.6.2021]

[15]Video quality comparison, `https://oscarliang.com/upload-dji-fpv-footage-youtube/`, [accessed 07.6.2021]

(a) 2.7k   **(b)** 480p

Figure 12.2: Comparison of the same drone shot with different video quality where the spot in the middle of the red circle in 12.2a is a person for reference purposes at an altitude of 50 meters approximately

can reduce raw content data by 1000 times such as H.264/AVC or H.265/HEV[16]. There are two main types of compression, namely, lossless and lossy[17].

- **Lossless compression** resembles to that of a ZIP file. The data of the file is compressed into a smaller size, but no quality is lost when the file is opened and viewed at full size.
- **Lossy compression** discards some data by an amount chosen manually by the user allowing for space to be saved for easier uploading. However, everytime that the file is opened, modified and then resaved, some more detail is lost in the process

It should be noted that the receiver must also have the same codec in order to decode the sent file and be able to view the data sent. These procedures already exist in devices such as single-lens reflex (SLR) cameras[18]. The advantage in sending a compressed file for higher quality is in question with regards to the increase in transmission time due to the extra steps in encoding and decoding procedures the drone and the emergency services must carry out.

Radio communications

The International Distress Frequency is a radio frequency that is designated for emergency communications by international agreement. There are several frequencies in the Very High Frequency (VHF) band which are especially designated to search and rescue operations, namely 121.5 MHz, 123.1 MHz, 138.78 MHz, 172.5 MHz, 282.8 MHz and 406 MHz[19]. However, the drone cannot use these frequencies as a means of communication. 121.5 MHz is the International Aeronautical Emergency frequency. However, since one should first send a signal with a Personal Locator Beacon (PLB) via the 406 MHz satellite based frequency so to estimate the position of the victim who is in need for help before being able to use the 121.5 MHz for more precise locating, this can not be used as secondary communication means. The Aeronautical Auxiliary Frequency (123.1 MHz) is auxiliary to the 121.5 MHz frequency and is used for coordinated Seach and Rescue (SAR) operations by mobile and land stations engaged in the coordinated SAR operations[20]. The 138.78 MHz emergency frequency can not be used since it is designated to be used by the United States military for on-the-scene search and rescue. The 172.5 MHz is used by the United States Navy aircraft assigned to a search and rescue mission. The North Atlantic Treaty Organization (NATO) occupies the 282.8 MHz frequency for SAR actions[21]. The 406 MHz is a satellite based search and rescue frequency as it uses the Cospas-Sasat satellites it can not be used as secondary communication means as it was decided to use a communication means which is not based on satellites as secondary communication means[22].

---

[16]Codec, `https://www.haivision.com/resources/streaming-video-definitions/compression/`, [accessed 16.6.2021]

[17]Compression types, `https://www.lifewire.com/the-effect-of-compression-on-photographs-493726`, [accessed 16.6.2021]

[18]Codec, `https://www.camerastuffreview.com/en/canon-4000d-review/`, [accessed 16.6.2021]

[19]International Distress Frequencies, `https://www.skybrary.aero/index.php/Distress/Emergency_Frequencies`, [accessed 07.6.2021]

[20]Aeronautical Auxiliary Frequency, `https://www.icao.int/safety/FSMP/Documents/Doc9718/Doc9718_Vol_I_2nd_ed_(2018) corr1.pdf`, [accessed 15.6.2021]

[21]International Distress Frequencies, `https://en.wikipedia.org/wiki/International_distress_frequency`, [accessed 15.6.2021]

[22]406 Frequency `https://www.sarsat.noaa.gov/emerbcns.html`, [accessed 15.6.2021]

It should be noted that on top of the International Distress Frequencies other radio frequencies seemed feasible for communication. However, since these frequencies are based on the use of satellites they are not included in the trade-off for the secondary communication means.

Secondary communication's module

The selected secondary communication means is the SIM800L GSM / GRPS Module. As explained in the Cellular communications section previously mentioned, all modules using 4G have been disregarded in the trade-off since their coverage in Europe is too small. On top of that, it was shown in Radio communications section, that radio based communication methods will be disregarded in the trade-off as well because the feasible frequencies are already in use. The possible candidates considered in the trade-off are all cellular based and use 2G or 3G network. An overview of the modules considered can be found in Table 12.3 where all options are able to have two way communication and transmit User Defined (UD) messages. As they score the same on these parameters, they are not included in the trade-off as a criteria.

Table 12.3: Overview of communication modules considered during trade-off of secondary communication means

Name	Adafruit Fona 3G[23]	Adafruit Fona uFL version[24]	Adafruit Fona 808[25]
Data transfer rate	380 kpbs	100 kpbs	100 kpbs
Size of module	50 mm x 46 mm x 7 mm	45 mm x 34 mm x 8 mm	44 mm x 43 mm x 8 mm
Cost of module	€ 65,81	€ 32,86	€ 41,09
Mass of module	50 g	9 g	12.3 g
Name	SIM900A GPRS A6 Module[26]	SIM800L GSM/GRPS Module[27]	SIM900A MiniV4.0 Module[28]
Data transfer rate	42.8 kpbs	100 kpbs	100 kpbs
Size of module	22.8mm x16.8mm x16.8mm	25mm x23mm (height NA)	49mm x47mm (height NA)
Cost of module	€ 19,73	€ 5,34	€ 6,59
Mass of module	28 g	8 g	38 g

The options shown in Table 12.3 are a few of the many Global System for Mobile (GSM) communications modules available in the market. The choices are constrained however, by the cost and size budgeted the department as shown in Table 11.12. The modules analysed should also provide the necessary data and specifications for a trade-off to be possible within the parameters.

Criteria

Five criteria have been defined for the secondary communication means trade-off. The scoring system uses four types of categories where the different options evaluated are compared against each other under the same criteria. The highest points achievable is three whereas the lowest is zero. The criteria used are as follows:

- **Data transfer rate** This criteria checks if the module is able to send messages and photos within a certain time frame. From the bandwidths with which the module can operate in, the type of telecommunication technology is determined. In Europe specifically, the bandwidths used for 2G is 900 MHz and 1800 MHz, whereas 3G uses 2100 MHz. Depending on what technology for telecommunication the modules can use, unless explicitly specified, the average upload rate can then be determined.

- **Size of module** Each of the modules analysed should be able to fit in the drone compartment. However, the smaller it is the better it will be scored as it would increase the configurability of the internal layout of the drone.

- **Cost of module** From the requirement **STAK-COST-01** stating "the cost of the drone for the end-user shall not exceed EUR 700", the cost of each component should be taken into account. Communications

[23] Adafruit Fona 3G, `https://www.adafruit.com/product/2691`, [accessed 10.6.2021]

[24] Adafruit Fona uFL version, `https://www.adafruit.com/product/1946`, [accessed 10.6.2021]

[25] Adafruit Fona 808, `https://www.adafruit.com/product/2542`, [accessed 10.6.2021]

[26] SIM 900A GPRS A6 Module, `https://alexnld.com/product/sim900a-smart-electronics-gprs-a6-module-wireless-extension-module-gsm-` [accessed 10.6.2021]

[27] SIM800L GSM / GRPS Module, `https://nettigo.eu/products/sim800l-gsm-grps-module`, [accessed 10.6.2021]

[28] SIM 900A Mini V4.0 Module, `https://nl.aliexpress.com/item/4000410644525.html`, [accessed 10.6.2021]

is prioritised when allocating budgets to the different departments since it is one of the most critical sub-systems in the drone. However, a balance of budget distribution is still important for the system to achieve its maximum potential.

- **Mass of module** The mass of the module is important as the communications module will be mounted inside the drone, meaning a lighter module translates to less power needed.
- **Coverage** The amount of coverage each module is determined by the type of telecommunication generation used. As explained in the Cellular communications' section 3G's coverage is a third of what 2G can cover due to the different frequency used.

Criteria Weights

The criteria weights have been calculated using the AHP as shown in in Table 12.4. The calculated weights are logical, as the criteria determining the overall performance of the secondary communication means, namely the data transfer rate and coverage, have the highest weights and are more important than the criteria related to the budgets.

Table 12.4: Relative importance table and the final weights with a CR of 0.0029

	Data transfer rate	Size of module	Cost of module	Mass of module	Coverage	Final weights
Data transfer rate	1.0	3.3	2.5	2.5	0.5	0.29
Size of module	0.3	1.0	0.5	0.5	0.3	0.09
Cost of module	0.4	2.0	1.0	0.5	0.5	0.13
Mass of module	0.4	2.0	1.0	1.0	0.5	0.15
Coverage	2.0	3.0	2.0	2.0	1.0	0.34

Trade-off

The winner of the trade-off is the SIM 800L GSM/GRPS Module as can be seen in Table 12.5. The cost of this module is € 5.34 and weighs 8 grams. The data transfer rate of the module is 100 kpbs which means that it takes 5.3 second to upload a low resolution photo of 66 kB and 7.7 minutes to upload a high resolution photo of 5.8 MB. It should be noted that the upload speed is very much dependent on the strength of the signal and for that reason dependent on the area the drone is flying in. On top of that, the module is able to upload a 10 seconds video of 480p with 30 frames per second in 4.1 min. Videos of longer duration or higher quality are discarded as it will take too long to upload them. For that reason, a camera is chosen in section 12.6 which is able to record videos with a 480p quality. Based on these results, the following upload strategy is chosen. As soon as the module is connected to the cellular network, it will first upload a few low quality photos to the emergency extraction services to give a preliminary overview of the emergency situation. Afterwards, it will upload a short, low quality video, which will take a few minutes to be uploaded, to further clarify and give a more detailed overview to the emergency situation.

Table 12.5: Secondary communication means Trade-off

Criteria	Data transfer rate	Size of module	Cost of module	Mass of module	Coverage	Total
Weights	0.29	0.09	0.13	0.15	0.34	
Adafruit Fona 3G	3	1	1	1	2	**1.92**
Adafruit Fona uFL version	2	2	2	3	3	**2.49**
Adafruit Fona 808	2	2	2	3	3	**2.49**
SIM 900A GPRS A6 Module	1	3	2	2	3	**2.13**
SIM 800L GSM/GRPS Module	2	3	3	2	3	**2.56**
SIM 900A Mini V4.0 Module	3	1	3	2	2	**2.34**

In order to use the cellular communication methods, a Subscriber Identitity Module (SIM) card is needed. This means that the user should have some sort of subscription to a telecommunications provider or mobile operator. There are many contracts that are available, however, due to the nature of the mission, a pre-paid card is all that the primary user needs. Roaming is possible in different countries within the European Union without extra fees[29], meaning that one would be able to purchase a card in their own country and use it abroad. The drone will be provided by the distributor with the SIM card included with a balance of € 5. The standard cost for a pre-paid card is € 3 per GB covering SMS, calls and data services. It was estimated that the drone will use in an extreme case 88 MB, from 10 high resolution photos and a 20 second long video with all the specifications maxed out according to Table 12.2, during an emergency flight. Therefore, the user or drone provider should check the balance before using the drone to make sure that a sufficient allowance is left (at least 250 MB), otherwise they should top it up before taking it out.

However, some EU countries, namely, Switzerland, Monaco, Andorra and San Marino, are not part of the free roaming agreement. In this case due to the main target audience that this product is focused on, explained in section 17.5, the local hiking organisations or adventure group clubs must make sure that the drone that they provide to their users does not have this problem by using a local SIM card instead. For the more fanatic users who carry their own drone when travelling to these countries, they must be made aware of the extra costs, or the possibility in switching out the SIM card for a local one. A list with the non-roaming countries is to be made very clear in the user manual when purchasing or renting this drone.

Discussion

The criteria used for the trade-off matrix consisted of assumptions based off from literature study. From the type of telecommunication technology used, a data transfer rate and coverage area is assumed. This is then used to compare with one another. Nevertheless, even if the values are not accurate, they are still representative for relative comparisons. Modules which do not explicitly show the data rates are assumed to have an average transfer speed as the generic 2G or 3G SIM card. For modules which can run both 3G and 2G, 3G is assumed as the weight for coverage and data transfer rate are close to each other, it does not make any substantial difference because both these criteria are inversely proportional to each other. However, a better understanding of the actual data transfer rate or coverage is to put the modules to the test. A simple test such as timing how long it takes to transfer a fixed size photo from each of the modules using 2G or 3G (if possible) would allow for a more accurate trade-off. Moreover, for the coverage, using the same module, both 2G and 3G can be tested with a signal strength reader providing a value in dBm (decibel milliwatts)[30] where:

- Close to deadzone = -110 dBm
- Poor signal strength = -85 dBm to -100 dBm
- Good signal strength = -65 dBm to -84 dBm
- Excellent signal strength = -64 dBm to -50 dBm

---

[29]Roaming, `https://europa.eu/youreurope/citizens/consumers/internet-telecoms/mobile-roaming-costs/index_en.htm`, [accessed 12.6.2021]

[30]Signal Strength, `https://www.weboost.com/blog/how-to-test-signal-strength-on-your-phone`, [accessed 18.6.2021]

The scoring system is determined relative to each other, hence, the best performing one from the all the options is scored the highest, whereas the worst is scored the least. Anything in between would be scored proportionally respective of the two ends of the spectrum. Unfortunately, this does not represent the actual performance of the module irrespective of the rest, meaning that it might be the case that all of the parameters for the different modules fall in the excellent window already, or the unfeasible category. With the budgets provided from the requirements and further testing aforementioned, a more representative trade-off can be carried out, however, it is safe to say that out of the six modules analysed, SIM800L GSM/GPRS is the best performing one.

It should be noted that major networks such as Vodafone and KPN have announced that they will stop supporting 2G networks in 2025 [31]. On top of that, they have announced that they will stop supporting 3G networks across Europe beyond 2020[32]. As the LastHope drone is using a module that supports 2G as the secondary communication system, it should move to another option from 2025 onwards. The team should consider the use of a module as secondary communication system that supports the 4G networks by 2025 as it is very likely that its coverage in Europe have really increased by that time. It should be noted that the communication options considered as primary communication system relying on satellite connection are not suitable to to replace the secondary communication system as they are too expensive for now. A module supporting the Starlink connection of Elon Musk could also be an interesting option as it is aiming to have full each coverage within the next years. However, as for now the Starlink module is very expensive (499 $ for the Starlink kit and 99 $ per month for the service), it is likely to be not suitable as this would mean that the cost budgets will be exceeded[33].

12.4. Communication Modules

Now that all the communication means have been determined, the next stage is figuring how it will be integrated with the rest of the subsystems. It is crucial to take into account the specifications and parameters for each of the communication means. This allows for the right power draw to be allocated, the right components to be selected and small, but crucial components to not be overlooked. Determining the interaction of the modules with the rest of the subsystems allows for a better understanding of what is happening and quicker identification of where a potential problem might arise from.
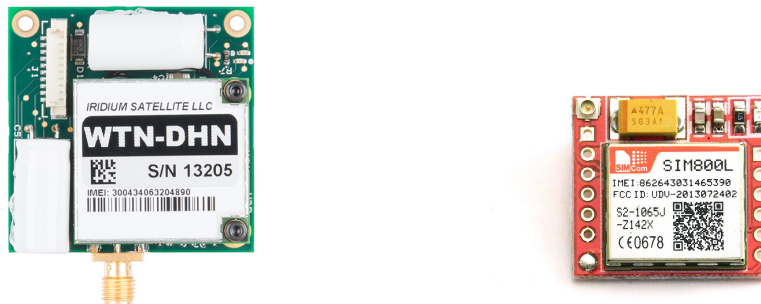
(a) Primary communication method RockBLOCK 9603   (b) Secondary communication method SIM800L GSM/GRPS

Figure 12.3: A visual representation of what the mean communication modules look like

The primary communication, as can be seen in figure 12.3a, is an Iridium 9603 modem which is put in a module called RockBLOCK 9603. This module allows for an easy integration to the system in subject. The features and specifications are shown in Table 12.6[34]. This mode of communication will be transmitting the user's coordinates acquired from the GNSS module and the distress signal.

---

[31]RTL Nieuws, https://www.rtlnieuws.nl/tech/artikel/5234122/t-mobile-2g-uit-3g-kpn-vodafone-gprs-oude-nokia

[32]Nu.nl, https://www.nu.nl/tech-achtergrond/6028318/dit-merk-jij-van-het-uitschakelen-van-het-3g-netwerk.html

[33]StarLink, https://www.inverse.com/innovation/spacex-starlink-global-coverage-when-available

[34]RockBLOCK 9603, https://cdn.sparkfun.com/assets/2/5/3/2/e/RockBLOCK-9603-Product-Information-Sheet.pdf, [accessed 15.6.2021]

Table 12.6: Primary communication RockBLOCK 9603 specifications

Feature	Parameters and specifications
Size	45.0mm x 45.0mm x 15.0mm
Weight	36 grams
Storage and operating temperature	-40 to 85 deg Celsius
Operating environment	<75% relative humidity
Operating power	5VDC, 100mA min/450mA max
Telecommunications	Integrated antenna and power conditioning
External antenna	Optional connector available subminiature version A (SMA)
Satellite communication	Plug-and-play
Message sizes	Upload 340 bytes per message
Cost	€ 206.13

The secondary communication is decided to be a cellular module, namely the SIM800L GSM/GRPS as shown in figure 12.3b. This also comes with all the specifications pre-determined and ready to be integrated into the system with the correct inputs and outputs as shown in Table 12.7[35]. The placement of the secondary communication system will be in the pod bottom as this will result in better connectivity with the cell towers on the ground while flying.

Table 12.7: Secondary communication SIM800L GSM/GRPS Module specifications

Feature	Parameters and specifications
Size	25 x 23 mm (height NA)
Weight	8 grams
Storage and operating temperature	-40 to 85 deg Celsius
Supply voltage	3.8V - 4.2V (4V recommended)
Power consumption	sleep mode <2.0mA idle mode <7.0mA GSM transmission (avg): 350 mA GSM transmission (peek): 2000mA
Interface	UART (max. 2.8V) and AT commands
Frequency bands	850 / 950 / 1800 /1900 MHz
Telecommunications	First wire antenna solded to NET pin on PCB Second PCB antenna with IPX connector
Cost	€ 5.34

Table 12.8 indicates the type of messages that the primary and secondary communication modules will be sending to the satellite and cellular towers respectively once connection is established. The end destination of the transfer of information are the emergency services for both the communication modules, however, using different methods.

Table 12.8: Message type which both communication modules will be sending when connection is established

Message type	Primary communication	Secondary communication	Comment
User's coordinates	✓	✓	Acquired from GNSS module
Distress signal	✓	✓	Acquired from user input
Photo of surroundings		✓	Acquired from camera module during take-off and if sufficient time and power allows for it
Video of surroundings		✓	Acquired from camera module during take-off and if sufficient time and power allows for it

---

[35]SIM800L GSM/GRPS, `https://nettigo.eu/products/sim800l-gsm-grps-module`, [accessed 15.6.2021]

It should be noted that it was chosen not to design an antenna or any subcomponents as the options provided by the respective companies are designed in-house to operate with the rest of the module, hence increasing its performance is relatively difficult considering the scope of this project. However, for the future of the project, an analysis can be made on the specifications of the antenna. Comparison can be done with respect to other better performing antennas to integrate driving features to the communication modules. Moreover, both these modules will be placed inside the frame protecting it from the externals.

12.5. GNSS Module

The Global Navigation Satellite System (GNSS) refers to a constellation of satellites providing signals from space that transmit timing and positioning to GNSS receivers which use the data to determine its location[36]. It is of great importance that the quadcopter is able to define its location as this is used in the path finding to communicate to the emergency extraction services as quickly as possible and to be able to sent the exact location of the one who is in need for help. For that reason a trade-off have been performed including six different GNSS modules. It should be noted that more than six GNSS modules were found, however since they did not fit in the budgets, they were excluded from the trade-off. Moreover, the GNSS module will also be used to determine the drone's location once landed and send it to the services in order to recovery.

The E108-GN01 module is the winner of the GNSS module trade-off. The two most important criteria included in the trade-off are the Time To First Fix (TTFF) and the number of GNSS constellations the module can use. The TTFF is a measure of the time required for a GNSS module to acquire navigation data and satellite signals to calculate the position. As the drone will be used in emergency cases, it is of utmost important that the drone is able to calculate the position of the emergency case as quickly as possible. The TTFF can be divided into two more specific scenarios, namely the TTFF with a cold start and the TTFF with a hot start. In case of a cold start the GNSS module is missing or has inaccurate estimations of its velocity, position, the time or the visibility of any of the GNSS satellites and needs to perform a full search of the sky for all satellites. In case of a hot start the GNSS module has valid data stored leading to an accurate initial estimate of its position which will eventually lead to a quick connection to the GNSS satellites. The four GNSS constellations that cover global coverage are the Global Positioning System (GPS), Galileo, Glonass and the BeiDou Navigation Satellite System (BDS). An overview of the four GNSS constellations can be found in Table 12.9.

Table 12.9: Overview of GNSS constellations

Name	GPS[37]	Galileo[38]	Glonass[39]	BeiDou[40]
Owner	United States	European Union	Russian Federation	China
Satellites in orbit	31	24	24	35
Frequencies	1.57542 GHz, 1.2276 GHz	1.164-1.215 GHz, 1.260-1.300 GHz, 1.559-1.592 GHz	1.602 GHz, 1.246 GHz	1.561098 GHz, 1.589742 GHz, 1.20714 GHz, 1.26852
Orbital altitude	20,182 km	23,222 km	19,130 km	21,150 km
Coverage	Global	Global	Global	Global

Multi-GNSS modules increase the quality of the location information and significantly reduces the TTFF as the more satellites the GNSS module can connect with, the faster the exact location can be determined. On top of that multi-GNSS modules increase the reliability of the connection as for example the case of poor Galileo coverage in a region, one can automatically switch to rely on GPS. GNSS modules can be included in the flight computer or in the communication module. However, as a GNNS module is not included in the flight computer and communication modules chosen in section 10.6 and section 12.3 respectively, it is chosen to only included separate GNSS modules in the trade-off. An overview of the GNSS modules considered during the GNSS trade-off can be found below.

---

[36]GNSS, https://www.euspa.europa.eu/european-space/eu-space-programme/what-gnss, [accessed 14.6.2021]

[37]GPS, https://www.geotab.com/blog/what-is-gps/, [accessed 10.6.2021]

[38]Galileo, http://www.esa.int/Applications/Navigation/Galileo/Galileo_a_constellation_of_navigation_satellites, [accessed 10.6.2021]

[39]Glonass, https://gssc.esa.int/navipedia/index.php/GLONASS_Space_Segment, [accessed 10.6.2021]

[40]Beidou, https://gssc.esa.int/navipedia/index.php/GLONASS_Space_Segment, [accessed 10.6.2021]

Table 12.10: Overview of GNSS modules considered

Name	SKLAB SKG09F[41]	Matek M8Q-5883[42]	Bynav BY682[43]
Time to first fix	15 s (cold), 1 s (hot)	26 s (cold), 1 s (hot)	45 s (cold), 30 s (hot)
Cost	€ 7,38	€ 38,50	€ 0,82
Weight	6 g	7 g	28 g
Size	10.1 x 9.7 x 2.2 mm	20 x 20 x 5 mm	71 x 46 x 11 mm
Number of constellations	GPS, BDS	GPS, Glonass, Galileo	GPS, Glonass, Galileo, BDS
Name	E108-GN01[44]	PA101D[45]	Delincomm MT3331[46]
Time to first fix	27.5 s (cold), 1 s (hot)	35 s (cold), 1 s (hot)	15 s (cold), 1 s (hot)
Cost	€ 5,38	€ 8,27	€ 8,29
Weight	5 g	2.75 g	7.6 g
Size	16 x 12 x 2.4 mm	10 x 10 x 6.8 mm	18.1 x 18.1 x 6.4 mm
Number of constellations	GPS, Glonass, Galileo, BDS	GPS, Glonass, Galileo	GPS, BDS

Criteria

Five criteria have been defined for the GNSS module trade-off:

- Time to first fix
- Cost
- Weight
- Size
- Number of constellations

The time to first fix criteria checks the average time it takes to determine the position solution in case of a cold start and in case of a hot start. The cost, weight and size criteria make sure that the chosen GNSS module perfectly fits within the given budgets. The number of constellations criteria is included as this gives an indication of the reliability and accuracy of a GNSS module. It should be noted that only the GNSS constellations that provide global coverage are counted in the number of constellations criteria. The accuracy determining the exact location of each GNSS module has been considered as a criteria as well. However, since the modules included in the trade-off all have approximately the same accuracy (within 2.5 m of the exact location), this criteria was not useful for the trade-off. It was chosen to not include a criteria related to sustainability in the trade-off as the sustainability tools introduced in chapter 19 can not be used to estimate the sustainability of the GNSS modules.

Criteria weights

The weights of the criteria have been calculated using the RIT as can be seen in Table 12.11. It makes sense that the TTFF and the number of constellations criteria end up having the biggest final weights as they determine the overall performance of the GNSS module and having the correct location of the person in need for help as quickly as possible is extremely important.

Trade-off

As can be seen in figure 12.4a, the E108-GN01 module, which can operate in temperatures between -35 and 80 degrees Celsius, is the winner of the GNSS trade-off. It costs € 5,38 and weighs 5 grams. The module uses four types of constellations with global coverage, namely GPS, Glonass, Galileo and Beidou. The hot start of the module is on average 1 s and the cold start on average 27 s. For the number of constellations criteria, only the four GNNSS constellations that have global coverage are considered. The highest score of 3 was given to modules that are able to use all four GNSS constellations as it was found in [13] that each GNSS satellite

---

[41]SKLAB SKG09, https://www.alibaba.com/product-detail/SKLAB-SKG09F-high-performance-GNSS-solution_10000001197479.html, [accessed 10.6.2021]

[42]Matek M8Q-5883, http://www.ftec-shop.nl/shop/FMPro?-db=Ftec%20Producten.fp3&-lay=CGI&-format=HWdetail.htm, [accessed 10.6.2021]

[43]Bynav BY682, www.alibaba.com/product-detail/Bynav-BY682-low-price-GPS-RTK_62583998536.html, [accessed 10.6.2021]

[44]PA101D, https://www.mirifica.it/cd-top/mediatek-mt3333/cdtop-technology-pa1010dv2-cd-pa1010d2_100011_1321/, [accessed 10.6.2021]

[45]Delincomm MT3331, https://dutch.alibaba.com/product-detail/delincomm-mediatek-mt3331-165dbm-sensitivity-gps-bds-module-nmea-html, [accessed 10.6.2021]

[46]E108-GN01, alibaba.com/product-detail/E108-GN01-GPS-GLONASS-Tracker-GSM_62571773406.html, [accessed 10.6.2021]

Table 12.11: Relative importance table and the final weights with a CR of 0.0030

	Time to first fix	Cost	Weight	Size	Number of constellations	Final weights
Time to first fix	1.0	5.0	6.0	2.5	1.0	0.36
Cost	0.2	1.0	1.0	4.0	0.3	0.12
Weight	0.2	1.0	1.0	0.2	0.2	0.06
Size	0.4	0.3	0.3	1.0	0.2	0.07
Number of constellations	1.0	4.0	5.0	6.0	1.0	0.38

system used added to the GPS system increased the total number of satellites observed and thus increase the accuracy of the position estimated and increase the reliability.

All modules considered were at least able to use two different GNSS constellations as it is required to have a back-up constellation available if one is for some reason not properly working in an area. The scores for the cost, weight and size criteria were given based on how well the modules fit in the given budgets. An unacceptable score of 0 was given to a criteria if the module did not fit in the given budgets, leading to the Matek M8Q-5883 not being able to become the winner of the trade-off.

Table 12.12: GNSS Trade-off

Criteria	Time to first fix	Cost	Weight	Size	Number of constellations	Total
Weights	0.36	0.12	0.06	0.07	0.38	
SKLAB SKG09F	3	2	2	3	1	**2.05**
Matek M8Q-5883	2	1	2	0	2	**1.74**
Bynav BY682	1	3	1	2	3	**2.08**
E108-GN01	2	2	2	3	3	**2.45**
PA1010D	2	2	3	3	2	**2.13**
Delincomm MT3331	3	2	2	2	1	**1.98**

(a) E108-GN01 GNSS Module

(b) Camera module Zero Spy Camera

Figure 12.4: Images of selected electrical components

12.6. Camera Module

However, a camera is used to provide additional user information for the services to locate the person in subject faster and bring medical assistance as soon as possible. Therefore, the camera module shall not compromise with other performances of the drone, however should still be compatible with the performances of the drone explained in section 10.4. The module chosen for the system is the Zero Spy Camera for Raspberry Pi Zero[47] as it is compatible with the chosen flight controller explained in section 10.6.

The camera weighs a total of 1.1 grams, has a size of 8.6 x 8.6 x 5.2 mm and lens diameter of 6.9 mm with a 52 mm long cable. With a resolution of 5 megapixel it is able to record video at 480p, 30fps, 2.5Mbps and

---

[47]Camera, `https://www.adafruit.com/product/3508`, [accessed 18.6.2021]

take approximately ten low resolution snapshots of the surrounding to send to the emergency services. This shall be attached to the current flight controller and provide the necessary footage to the cellular module where it will be sent to the emergency services. This module can be seen in figure 12.4b.

12.7. Weather conditions

Weather conditions have great influence on the performance of the radio waves sent by the modules. **Rain with large droplets** can scatter and weaken cell signals, however, it is more likely that the drone fails to fly in heavy rainfall before failure in cellular transmission. On the other hand, some moisture in the air can be a beneficial by facilitating signal transmission, but in excessive amounts, it can become an interference[48].

Fog and clouds also affects the performance of the transmission, however, it is strongly dependent on the frequency the drone is operating in. Any bandwidth above 2000GHz are significantly affected, meaning 2G will not be affected as it does not fall in the that range[49].During cold conditions, **snows and hails** can indirectly affect the performance of the communications module such as power outage, however, it does not have any substantial direct affects on the mobile signals themselves. Snow and hail are composed of solid ice so compared to liquid water, it is unlikely to refract signal propagation causing any problems[50].

In circumstances where **lightning** bolts are present, electrical interference might cause antenna damage or power outages. However, this is quite of an extreme scenario not likely to happen[51]. **Physical obstructions** are most often the case. Having trees, buildings or even mountains in between the user and the cell tower can interfere with the signal. The presence of abundant amount of metal used in buildings, vehicles, towers can also influence the radio waves[52].

12.8. Communication Flow Diagram

The drone operates autonomously, hence having a clear overview of how information flows through the system is crucial. The flow diagram shown in figure 12.5 indicates a mixture of hardware and software blocks due to the fact that from the communication's point of view, the commands and data change from block to block. It should be noted that communication between the sensors and the flight controller is absent here as it will be shown in more detail in section 13.2.
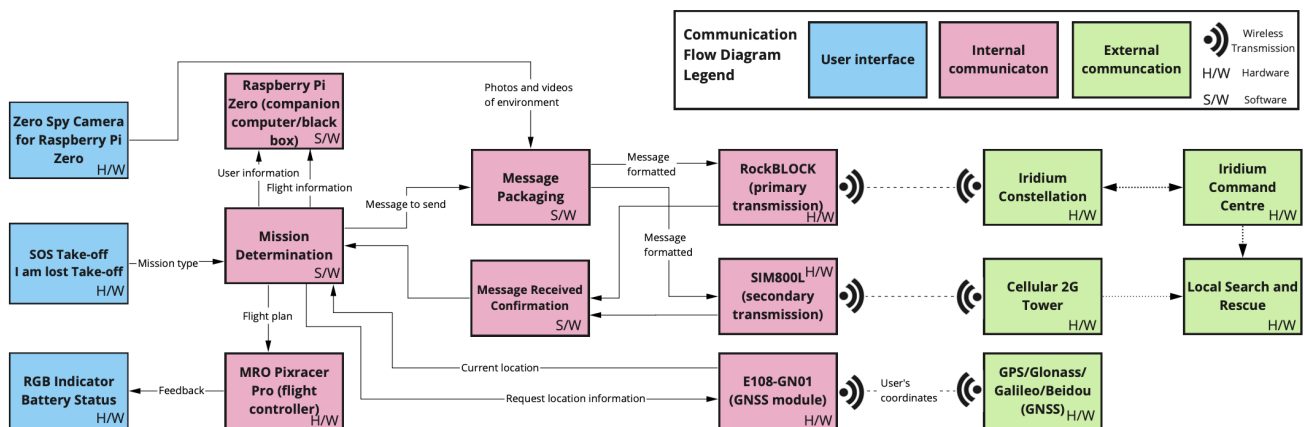

Figure 12.5: Communication flow diagram

12.9. Sustainability

The sustainability of such models dealt with in the chapter is complicated to estimate using the tools introduced in Table 11.12. Moreover, due to the lack of information online and unavailable ISO-14001, FLA and RoHS

---

[48]Rain, `https://www.outsideonline.com/2186591/how-weather-affects-your-phones-signal`, [accessed 17.6.2021]

[49]Fog and cloud, `https://www.outsideonline.com/2186591/how-weather-affects-your-phones-signal`, [accessed 17.6.2021]

[50]Snow and hail, `https://cellboosteronline.com/mobile-signal-weather-conditions/`, [accessed 17.6.2021]

[51]Lightning, `www.outsideonline.com/2186591/how-weather-affects-your-phones-signal`, [accessed 17.6.2021]

[52]Physical obstruction, `www.outsideonline.com/2186591/how-weather-affects-your-phones-signal`, [accessed 17.6.2021]

certifications of the cellular modules, it was chosen to not include a criteria related to sustainability in the trade-off. Therefore, the module will be assumed to be more sustainable the smaller it is as all the modules use the same material for their individual components, such as circuitry, indicator LEDs and antenna connectors. On the other hand, for the primary means of communication, the Iridium 9603 is Restriction of Certain Hazardous Substances (RoHS) certified, meaning that the proportion of difficult to dispose materials or hazardous substances is monitored. This leads to more environmentally friendly manufacturing processes as well such as unleaded soldering[53].

The company that produces the GNSS module is ISO-14001 certified meaning that the company is actively measuring its environmental impact and constantly trying to improve it. On top of this, the product itself has an RoHS certification. Moreover, the camera module chosen for the system is RoHS2 2011/65/EU and 2015/863/EU certified.

12.10. Requirement Compliance

With the communication's subsystem determined, it should be checked whether it complies with all the requirements previously established. With the use of a compliance matrix as shown in Table 12.13 it can be seen which requirements are met and which are either omitted, failed to meet or need further evaluation in order to check for compliance. These will be further elaborated after the table in the feasibility analysis.

Table 12.13

ID	Requirement	Compliance	Comment
STAK-COST-03	The subscription costs of the additional service shall not exceed EUR 15 per month	✓	€13.26
SYST-THER-01	The drone shall be able to operate in a temperature range from -20 to +40 °C	✓	-35 to +80 °C
SYST-THER-02	The drone should be able to operate in a temperature range from -30 to +50 °C	✓	-35 to +80 °C
STAK-COMM-01	The drone shall be able to communicate with emergency services at areas with cellular reception	✓	Verified at later stage
STAK-COMM-03	The drone shall communicate user location to the emergency services	✓	Verified at later stage
STAK-COMM-04	The drone shall communicate user data to the emergency services	✓	Verified at later stage
STAK-COMM-05	The drone shall send landing coordinates for easy recovery of the drone	✓	Verified at later stage
STAK-COMM-06	The drone should transmit its live location to the user		Not met.
SYST-COMM-01	The drone shall have at least one mean of communication, between drone and emergency services, that is "two-way"	✓	
SUBSYST-COMM-10	The communication subsystem shall have a weight limit 30 grams		49 grams
SUBSYST-COMM-12	The communication subsystem shall have a cost limit of 200 euros		221,85 euros

Before starting with the feasibility analysis, all the requirement regarding communicating with the emergency services are considered to be met given the assumption that the modules work as intended, however will be verified during the test analysis phase at a later stage after DSE. It should be noted that all these components are to be tested before introducing it to the market. It can be seen in Table 12.13 that all the communication modules meet the respective requirements except for one in particular, namely, transmitting its live location, **STAK-COMM-06**. It should be noted that this was an optional requirement. To make the drone being able to sent its live location, the drone should be equipped with a transmitter able to reach the user interface on the case for live updates on the status of the drone. Since the mission of the drone is to establish connection with the emergency services, this feature is considered a bonus hence it was killed and not used to drive the design. However, as mentioned in chapter 7, a transceiver can be implemented for the next version of the drone in order to meet this requirement. Last, but not least, the requirement **STAK-COMM-06** is an optional

---

[53]9603 RoHS, `ott.com/blog/2017/07/what-does-the-rohs-certification-mean-for-ott-products/`, [accessed 16.6.2021]

requirement established internally hence it will not pose a substantial compromise to to the performance of the drone. It will also be further elaborated in the post-DSE phase in chapter 7.

12.11. Discussion & Recommendations

There are a lot of further investigations possible for the development of the drone. Regarding the sustainability aspect, some of the components and modules used are not legitimately certified in terms standards in environmental management. However, this can be overcame with SIM800L V2.0 5V Wireless GSM GPRS MODULE[54] for the secondary communication. This newer version of the SIM800L GSM/GRPS Module does contain a RoHS certification, weighs less, has many more functions, but is four times more expensive than the current one used.

Another subject to discussion and further elaboration is the knowledge on the data connectivity coverage and strengths. Due to lack of information found online, this was a huge assumption coming into the design of the communications system for the drone. With a better understanding of the locations high and low cellular connectivity, the drone will be able to make smarter decisions for path planning.

Further research and usage of new technology can be implemented in the type of video recorded for additional user data transferred to the emergency services. An experiment can be proposed to determine at what altitude and speed would the drone stop being able to distinguish an average sized human being when taking off. This would help having a deeper understanding to what configuration of video should be used to best assist the emergency rescue team. Research can also be done on the modules used in mobile phones, due to their size and mass, it would be beneficial to the drone.

13. Technical Analysis of Design

Here the electrical block diagram, power distribution diagram, data handling diagram, exploded view, systems characteristics and performance analysis will be presented.

---

[54]SIM800L V2.0, `https://irishelectronics.ie/SIM800L-V20-5V-Wireless-GSM-GPRS-MODULE`, [accessed 15.6.2021]
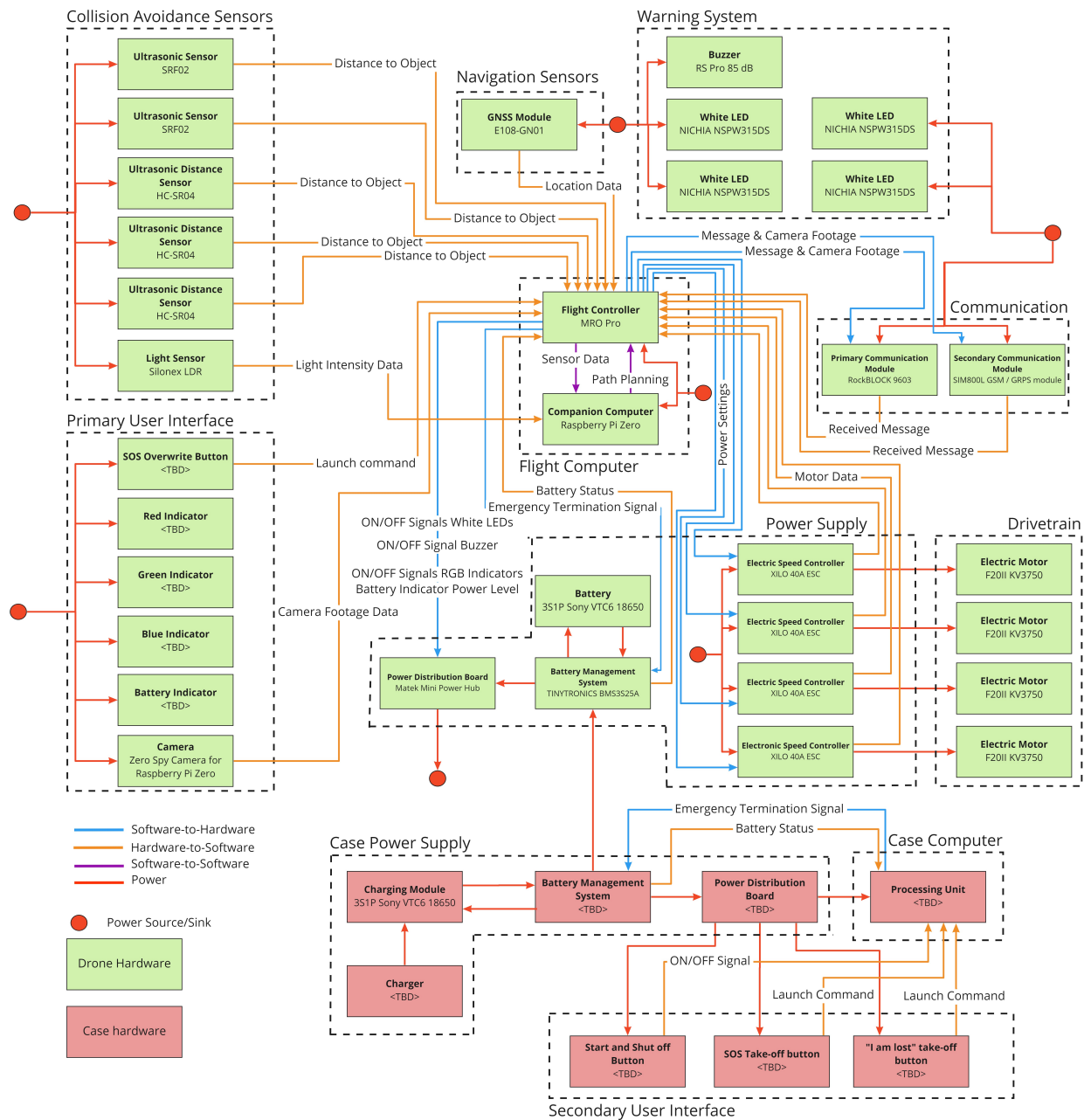
13.1. Electrical Block Diagram

Figure 13.1: Electrical block diagram

In this section the electrical block diagram is shown. The electrical block diagram shows all electrical components and their relations to each other. It can be seen that the PDB is the centre of the power supply. The flight computer is the centre of the drone regarding data exchange between components. From the electrical block diagram diagram it also becomes clear that the case and the drone are connected by means of their battery management systems. The BMS of the case delivers energy to the BMS of the drone which will recharge the battery of the drone. The diagram is seen in figure 13.1. The electrical block diagram is supplemented by the power distribution diagram, which shows the exact voltage and current requirements over each connection. This diagram also serves as the hardware diagram which houses the software diagram illustrated in figure 10.12.

Now the electrical subsystem has been designed in more detail, this information can be compiled into the updated electrical block diagram. This is shown in figure 13.2.
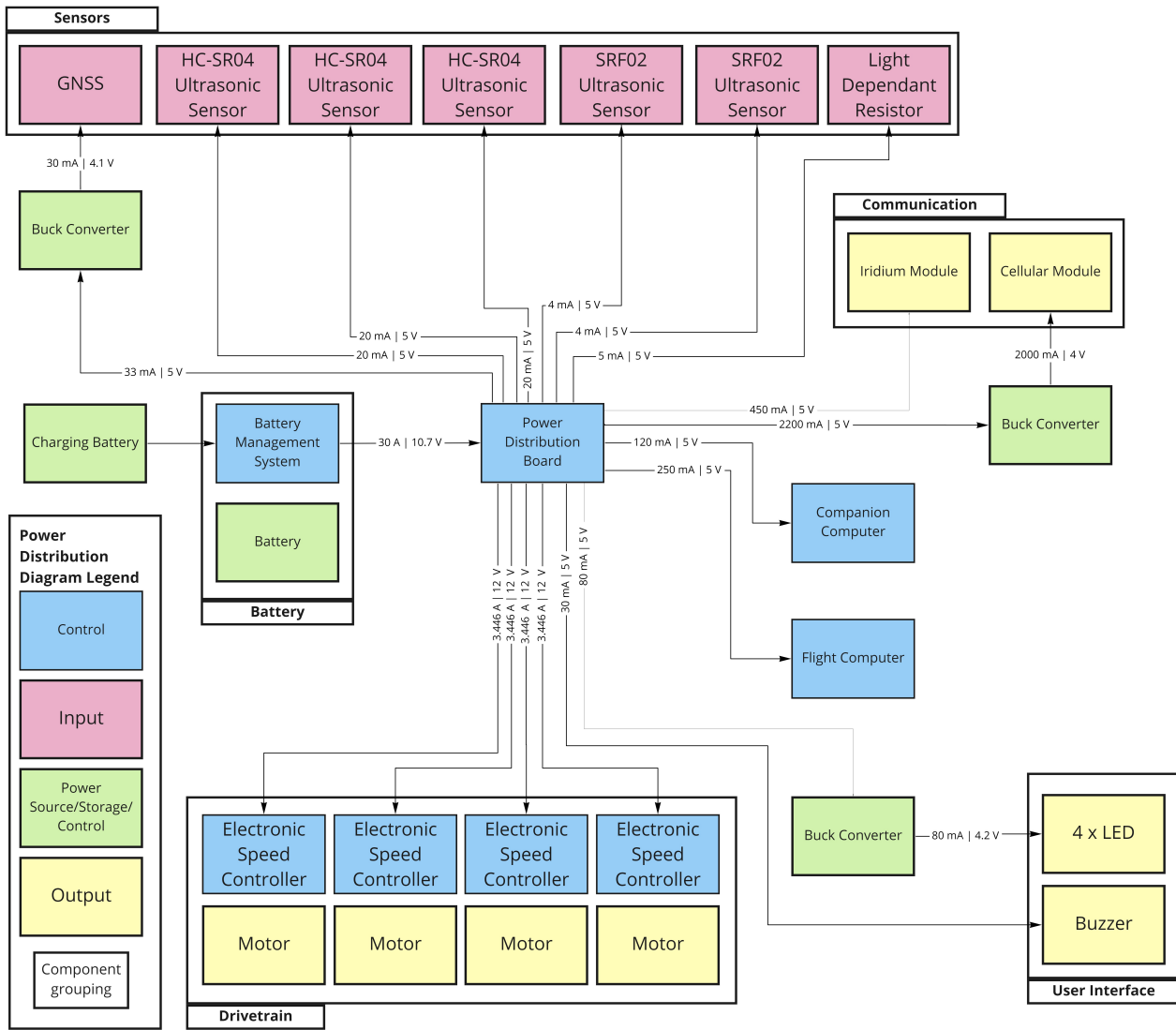
Figure 13.2: Power Distribution Diagram

13.2. Data Handling Diagram

The data handling diagram is now presented in figure 13.3. This shows the interaction between the various information systems and data flowing between them.

13.3. Exploded view

In order to illuminate the placement and geometry an exploded view has been made in figure 13.4, the descriptions corresponding to the numbers inside the balloons can be found in Table 13.1.

Figure 13.3: Data handling diagram

Isometric view
Scale: 1:2

Figure 13.4: Exploded view of the drone with annotations

Table 13.1: Components from exploded view with their respective numbering

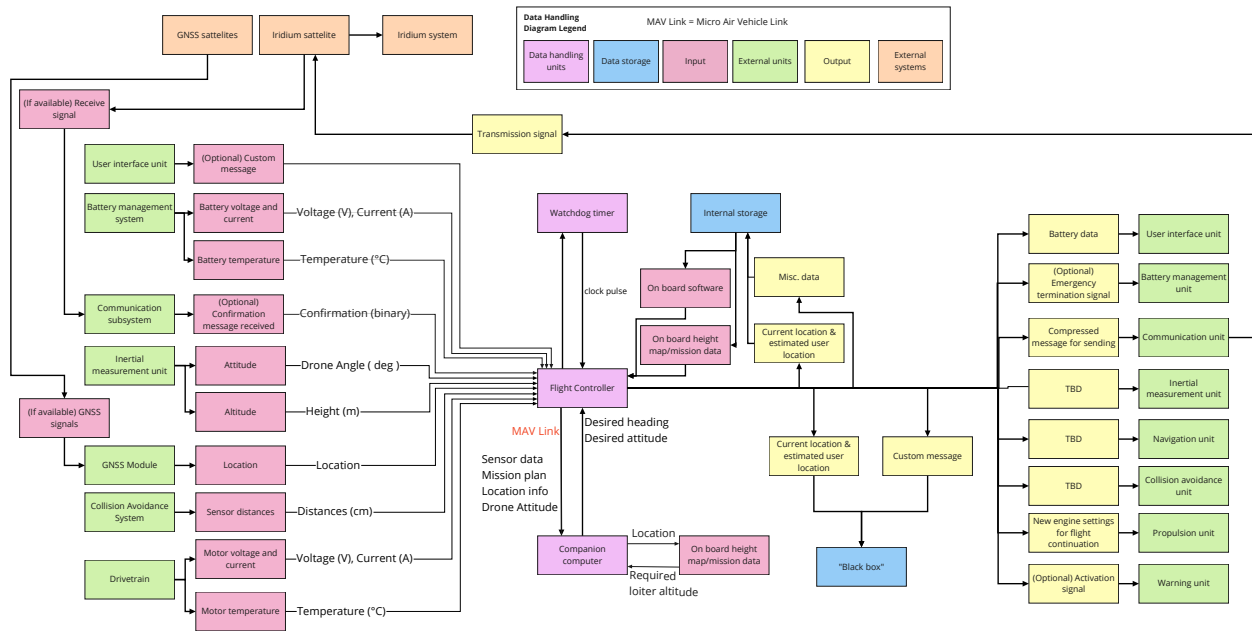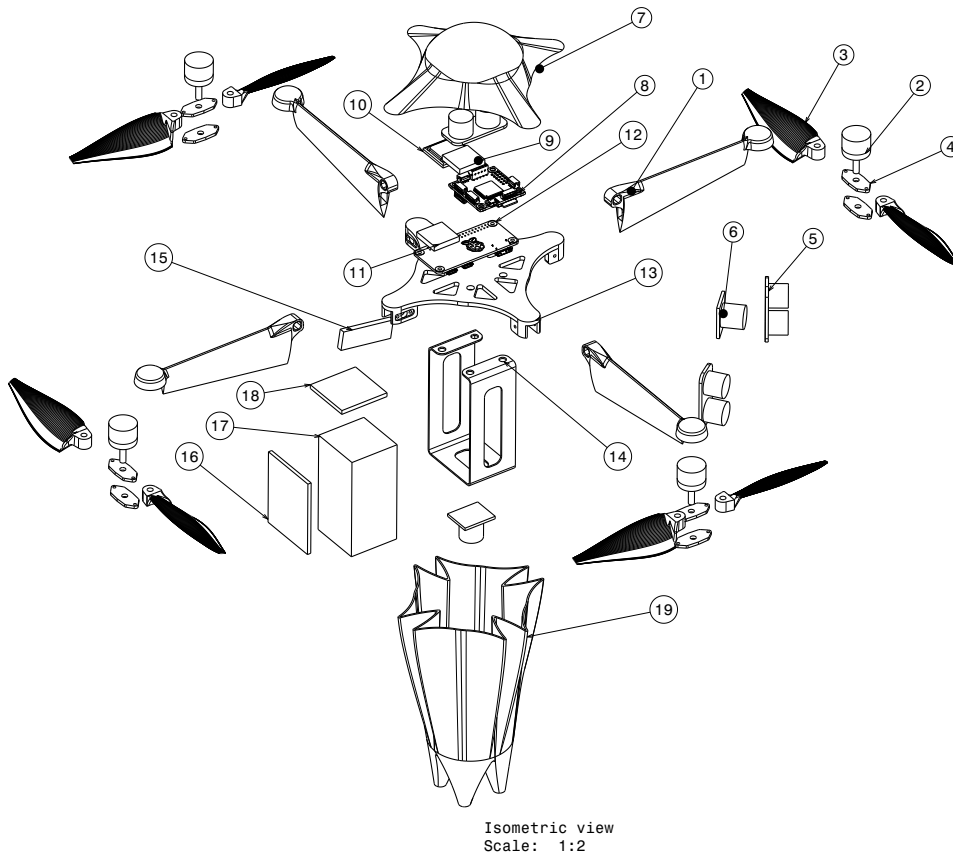|			
1	Arm	11	Satellite communications module
2	Motor	12	Companion computer
3	Prop half	13	Bulkhead
4	Prop hub	14	Battery cage
5	Ultrasonic sensor	15	Electronic speed controller (ESC)
6	Ultrasonic sensor	16	battery management system (BMS)
7	Pod top	17	LiPo battery
8	Flight computer	18	Power distribution board (PDB)
9	GNSS module	19	Pod bottom
10	Secondary communications module		

13.4. Aircraft system characteristics

This section serves as an overview of all the subsystems. Within the chapters, these subsystems are explained in more detail. The first subsystem mentioned in this report is the Operations subsystem which focuses on the case design, user interface and warning and visibility system of the drone. These detailed descriptions of these designs can be found in section 7.1, section 7.2 and section 7.3 respectively. The next subsystem covered in this report is the drive train which covers the design of propeller and motor selection. This is presented in section 8.2. Following the drive train subsystem is the frame subsystem which connects all other subsystems physically by the frame. Apart from design, this chapter also includes the structural analysis and an aerodynamic analysis. This can be found in section 9.7.

Next subsystem in line is the Guidance Navigation, Control and stability subsystem. This subsystem starts of by selecting the on board sensors (section 10.3), which the drone uses to autonomously perceive its surroundings. This is followed by a stability and control analysis in section 10.4 and section 10.5. Ensuring the control commands are executed properly is done by the flight controller, which is selected in section 10.6. To run the autonomous algorithms a companion computer is chosen in section 10.7. After these components have been selected, several navigation algorithms and techniques are analysed from section 10.8 till section 10.10.

The GNCS subsystem is followed by the electronics subsystem. This subsystem selects a battery in section 11.2 as the power source of the drone. The power for the motors is drawn from the battery, and provided via an Electronic Speed Controller, selected in section 11.3. To prevent battery failure a battery distribution board and battery management system needs to be selected, as described in section 11.4 and section 11.5 respectively. Furthermore, in this chapter the electrical block diagram is provided. Lastly, the communications subsystem is presented The secondary communication system is selected, together with a Global Navigation Satellite System (GNSS) module. At last a camera module is selected. This can be found in section 12.3 from section 12.6. This chapter also includes the communication flow diagram.

13.5. Performance Analysis

This section will summarise the performance characteristics of the Last Hope drone. Within the chapters of each subsystem the performance of each subsystem is described however the complete performance of the drone will be presented here.

The performance of the drone is evaluated based on evaluating the flight speed, flight time and energy consumption for each of the possible flight phases this drone may be operating in. By evaluating the energy consumption of all electronic components the sizing of the battery may also be verified.

Three different specific missions were defined in order to asses the performance of the Last Hope drone. The first mission (M1) occurs during the night, hence requires the LEDs to be turned on, and consists of climbing 2000 m to maximum service ceiling of 4500m, loitering for 20 minutes in order to request emergency services through the primary communication module and finally descending. The second mission (M2) occurs during the day, hence the camera, in a worse case scenario, may be used by the GNCS subsystem for obstacle avoidance, and consists of the same steps as mission 1; climbing 2000 m to maximum service ceiling of 4500m, loitering for 20 minutes in order to request emergency services through the primary communication module and finally descending. The third and final mission (M3) which will be considered occurs during the day and consists of the drone recording the user's surrounding area during a slow climb, flying 5 km in range in order to upload the recorded images and request emergency services through the secondary communication module, and finally

descending. Table 13.2 shows a more detailed breakdown of the flight phases for each of the mission. It is important to note that at this stage the use of a camera for guidance and navigation is not expected however as the performance is evaluated for worse case scenario the camera will be considered active while the CAS sensors are active.

Table 13.2: Flight profile breakdown for each mission

	Mission 1	Mission 2	Mission 3
Flight phases	Drone Startup	Drone Startup	Drone Startup
	Horizontal flight (100m) with CAS	Horizontal flight (100m) with CAS	Vertical climb (100m) with CAS
	Vertical climb (100m) with CAS	Vertical climb (100m) with CAS	Horizontal flight (5km) without CAS
	Vertical climb (2km) without CAS	Vertical climb (2km) without CAS	Landing (100m) with CAS
	Loiter (20min)	Loiter (20min)	
	Descent (2km) with CAS off	Descent (2km) with CAS off	
	Landing (100m) with CAS on	Landing (100m) with CAS on	

The performance for each of the flight phases was analysed using the drivetrain tool from section 8.2, adapting it to run only for the chosen motor and for horizontal flight. Furthermore all electronic components such as the flight computer (FC), companion computer (CC), GNSS module (GNSS), CAS sensors (CAS), primary communication module (COM1), secondary communication module (COM2), camera (CAM), LEDs and LDR were included in the energy consumption calculations[1]. Table 13.3 shows the performance calculations for each of the flight phase.

Table 13.3: Performance evaluation for each flight phase

Flight Phase	Working Electronics	Flight speed	Phase time	Total Energy Consumption
Horizontal flight (100 m) with CAS on	FC, CC, GNSS, CAS, Propulsion M1: COM1, LEDs M2: COM1, CAM	2.5 m/s	40 s	M1: 73.0 mAh M2: 73.5 mAh M3: NA
Vertical climb (100 m) with CAS on	FC, CC, GNSS, CAS, Propulsion M1: COM1, LEDs M2: COM1, CAM M3: CAM	2.5 m/s	40 s	M1: 73.3 mAh M2: 73.8 mAh M3: 72.6 mAh
Landing (100 m) with CAS on	FC, CC, GNSS, CAS, Propulsion M1: LEDs M2: CAM M3: CAM	2.5 m/s	40 s	M1: 60.9 mAh M2: 61.3 mAh M3: 61.3 mAh
Horizontal flight (5 km) with CAS off	FC, CC, GNSS, Propulsion M3: COM2	18.2 m/s	275 s	M1: NA M2: NA M3: 796.2 mAh
Vertical climb (2 km) with CAS off	FC, CC, GNSS, Propulsion M1: COM1, LEDs M2: COM1	18.4 m/s	108 s	M1: 445.1 mAh M2: 442.7 mAh M3: NA
Descent (2 km) with CAS off	FC, CC, GNSS, Propulsion M1: LEDs	21.1 m/s	95 s	M1: 89.2 mAh M2: 87.1 mAh M3: NA
Loiter (20 min)	FC, CC, GNSS, Propulsion M1: COM1, LEDs M2: COM1	NA	1200 s	M1: 1967.5 mAh M2: 1940.8 mAh M3: NA
Drone Startup	FC, CC, GNSS, CAS, LDR M1: COM1, LEDs M2: COM1, CAM M3: CAM	NA	20 s	M1: 3.7 mAh M2: 3.9 mAh M3: 3.3 mAh

---
[1]The abbreviations included are not for acronyms but are as identifiers used in the upcoming tables.

The total energy consumption for mission one, two and three were found to be 2713, 2683 and 933 mAh respectively. As all three these values are below the total battery capacity of 3000 mAh, it is possible to conclude that the drone Last Hope is capable of fulfilling its entire mission profile. Furthermore it is shown that operating the drone during night consumes more battery than during the day. Finally it is shown that for all three mission types enough battery capacity remains for the drone to return to the user, even taking into account the 5.1 km return distance in the case of mission three.

13.6. System level sensitivity analysis

In the section some of the fundamental assumptions are checked in order estimate their effect on the design.

Obstacle Avoidance One of the larger assumptions made is that the drone requires an obstacle avoidance to function. This assumption is borne out the thinking through edge cases. It could be possible that in almost all real-world cases the user has a clear view of the sky, such that the drone could take off and fly into the sky nearly vertically with few obstructions. If that is the case the drone could be made to be much lighter and cheaper, making it easier and more affordable for the user to get and bring along on hikes. Conversely, dynamic obstacles have been neglected. If dynamic obstacles turn out to be significant, the sensor selection and avoidance strategy may need to be adjusted, increasing both mass and cost.

Path Planning Many path planning algorithms were evaluated in this project, with the expectation that the drone would need to explore cluttered terrain in order to find a clear path into the open sky. This puts a lower bound on the computational power of the flight computer. If in the real world, like in the section above, the drone can reach the open sky easily a cheaper and lighter flight computer could be chosen and/or the companion computer could be omitted. On the other hand, path planning was proposed in the form of more large scale flight plans towards e.g. a location were secondary communication is available. This again puts lower bounds on the companion computers capabilities that need to be Incorporated. If the capabilities are exceeded, the companion computer selection needs to be revised or the strategy restricted to an appropriate extent.

Stability and Control Stability and control were evaluated without taking into account dynamic responses to disturbances such as gusts. Especially in obstacle avoidance, this could pose threats a cluttered environment. If the dynamic modes of the system turn out to be very chaotic and hard to control, characteristics such as the moments of inertia could be first candidates for change, involving the rearrangement of internal components or similar structural changes. The required combination of drivetrain and moment arm could also be affected. Lastly, the influence of the airfoil-shaped arms was not analysed for stability. In case these influence the stability characteristics dramatically against expectations, a redesign might be required.

Service Height The goal altitude increase of 2000m was set by a relatively rudimentary analysis and backed up by some more detailed statistical sampling of selected areas. It could be the case that moving a small amount horizontally could also allow the drone to make contact. This could reduce the requirements on the performance of the drivetrain significantly. On the other hand the areas analysed were few in number, thus it could be that there are locations within Europe where 2000m of altitude gain is insufficient. This could substantially increase the required battery capacity, and thus the weight of the drone.

Battery Technology A large design driver is the current state of battery technology. The drone designed is based on current market-ready batteries. In the future it is likely battery technology will improve substantially, making batteries more power-dense, cheaper and safer. This can improve the feasibility and performance of the design substantially, since the battery is the heaviest single component.

Frame Aerodynamics While the climb phase takes up a significant portion of the battery capacity, the loiter is by far the dominant part. It could be the case that if the frame is made lighter, at the cost of its aerodynamic shape, the total required battery capacity actually decreased. This is relatively unlikely due to the small amount of extra mass the aerodynamic improvements represent, but should still be analysed in future iterations.

Satellite communications The maximum time required to send a messaged is currently 20 minutes, but this is based on manufacturer data whose testing conditions are unknown. It could be that at altitude signal strength is strong enough that communication is near-instant. If this is the case the loiter requirement could be reduced, vastly decreasing the required battery capacity. It would also modify the optimisation target of the drivetrain analysis, perhaps allowing for the selection of a lighter and cheaper motor.

Legalities Perhaps the most uncertain assumption is that the legal framework to allow products like this will be in place in Europe by the time the product is ready for launch. If this is not the case then the sale of the product in most of its target market would likely be illegal. This would have a negative effect on the estimated return on investment.

14. Technical Budgets

This chapter shows the technical budgets that were introduced in section 4.2. The completed mass budget can be found in Table 14.1 and the completed cost budget can be found in Table 14.2. As can be seen in Table 14.1 and Table 14.2, the mass of the drone is over budget. The mass budget is over by approximately 17 percent. This would mean that the requirement on mass is not met. Given the limited time resources only one iteration for the complete design was performed. The cost budget shows that the total cost of the drone (€ 646) is below the budgeted value of € 700. For the components that were selected off-the-shelf it should be noted that the price was assumed to be 80% of the prices found at third party sources. This assumption was made as buying components in bulk quantities directly from the manufacturer tend to reduce the price of a single component. As the current design cost is dominated by the off-the-shelf components, this assumption has a significant influence on the total cost calculated. Also, the cost budget does not take into account other costs that influence the cost for the customer, for example the development cost or labour cost. Therefore more analysis is necessary to validate if the total cost for the end-user is below € 700. It is expected that the cost for the separate components of the drone should be reduced to meet the cost requirement. Therefore, the technical budgets also include updated values for the budgets assigned to every department. These budgets were based on the total mass or cost of a department and the possibilities to meet the new budgets. For example, the GNCS department went over the cost budget. It can be seen that the flight computer has a high cost. Other flight computers that were considered were less expensive. So it might be reasonable to iterate the flight computer trade-off to reduce the cost. For future design iterations the main focus should be on reducing cost and mass for the complete system as these are two driving requirements.

Table 14.1: Mass budget of current design

		Iteration 1	Iteration 2			Iteration 1	Iteration 2
Electronics	Power Distribution Board	6		GNCS	Flight Computer	9.1	
	Battery	163.7			Companion Computer	9.25	
	Wiring	9			Collsion Avoidance Sensors	35	
	Electronic Speed Controller	24			Other Sensors	1	
	Battery Management System	9.8			GNCS Total	54.35	
	Electronics Total	212,5			Margin (%)	-55.3	
	Margin (%)	-6.25			Budgeted	35	50
	Budgeted	200	190				
				Frame	Arms	45.6	
Communication	GNSS Module	5			Bulkhead	32.3	
	Primary Communication Module	36			Pod	55.3	
	Secondary Communication Module	8			Battery Cage	10.8	
	Communication Total	49			Electronic Stack Mount	10.0	
	Margin(%)	-63.3			Folding Mechanism	5.2	
	Budgeted	30	50		Frame Total	159.2	
					Margin (%)	-189.4	
Drivetrain	Propellers	26			Budgeted	55	110
	Motors	60.8					
	Drivetrain Total	86.8		Operations	Warning System	2.68	
	Margin (%)	21.1			Primary User Interface	19.96	
	Budgeted	110	80		Camera Module	1.1	
					Operations Total	23.74	
					Margin(%)	-18.7	
					Budgeted	20	10
				Total Mass		585.56	
				Total Margin (%)		-17.1	
				Total Mass Budgeted		450	490
				Budget Margin (%)		10	2
				Budgeted		500	500

Table 14.2: Cost budget of current design in euros

		Iteration 1	Iteration 2			Iteration 1	Iteration 2
Electronics	Power Distribution Board	6.02		**GNCS**	Flight Computer	144	
	Battery	20.00			Companion Computer	16.00	
	Wiring	4.00			Collsion Avoidance Sensors	28.96	
	Electronic Speed Controller	21.44			Other Sensors	1.15	
	Battery Management System	3.60			GNCS Total	190.11	
	Electronics Total	55.06			Margin (%)	-8.64	
	Margin (%)	-83.52			Budgeted	175	175
	Budgeted	30	60				
				Frame	Arms	41.52	
Communication	GNSS Module	4.30			Bulkhead	9.15	
	Primary Communication Module	164.90			Pod	3.40	
	Secondary Communication Module	9.27			Battery Cage	0.99	
	Communication Total	178.48			Electronic Stack Mount	7.00	
	Margin(%)	10.76			Folding Mechanism	12.60	
	Budgeted	200	180		Frame Total	74.66	
					Margin (%)	-148.87	
Operations	Warning System	4.25			Budgeted	30	60
	User Interface	9.22					
	Case	25.25		**Drivetrain**	Propellers	35	
	Charging Module	12.48			Motors	48.48	
	Camera Module	13.07			Drivetrain Total	83.48	
	Operations Total	64.27			Margin (%)	-4.35	
	Margin(%)	41.57			Budgeted	80	80
	Budgeted	110	70				

	Iteration 1	Iteration 2
Total Cost	646.06	
Total Margin (%)	7.71	
Total Cost Budgeted	625	625
Budget Margin (%)	10.71	10.71
Maximum Cost	700	700

15. Risk

During any phase of the design process, risk identification and mitigation is important. Problems may arise during the course of the design project if risks are not properly identified and managed in advance. In this section the technical risks related to the final design will be extensively handled. First, the preliminary risk map is shown and the process of identification and evaluation of the technical risks are explained. This will be followed by the explanation of the risk mitigation process resulting in a risk map after mitigation.

In order to evaluate the risk based on their impact and probability, a scale of five is used. A score of one means the lowest impact or probability, whereas a score of five being the highest. The risks will be divided into two main categories, namely risks relating to the operation of the drone and risks relating to the production of the drone. The operations risks category can be subdivided in risks related to electronics, aerodynamics, stability and control, structure and propulsion. The production risks category can be further subdivided in risks related to part manufacturing and risks related to assembly. The risk identifiers will be structured in the following way: Risk - Risk category - Number. In Table 15.1 an overview of the risk identifiers can be found.

Table 15.1: Structuring of risk identifiers

Category	Risk Identifier	Category	Risk Identifier
Assembly	R-AS-number	Part manufacturing	R-PM-number
Propulsion	R-PR-number	Aerodynamics	R-AE-number
Electronics	R-EL-number	Structure	R-ST-number
Performance	R-PE-number		

15.1. Technical Risk Analysis Before Mitigation

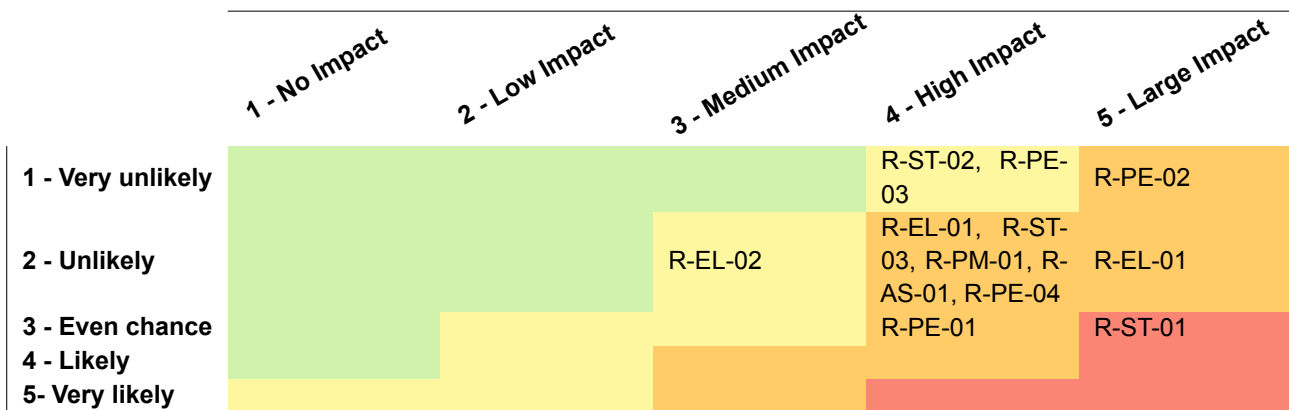The result from the risk identification and evaluation before mitigation can be found in Table 15.2

Table 15.2: Technical risk identification and analysis

Risk ID	Event	Probability (1 − 5)	Impact (1 − 5)	Description
R-PE-01	Damage to propeller	3	4	One of the four propellers of the drone might get damaged due to small projectiles like hail and since the drone should be able to operate in rough weather conditions, the probability is relatively high. When the rotors of the drone are being damaged, this might cause one or more propellers to break off. This might result in failure of the mission and thus has a huge impact.
R-PE-02	Network unavailability	1	5	An available network is crucial to be able to communicate with the emergency extraction services and for that reason, network unavailability has a huge impact on the mission success. The probability of network unavailability is low, since the drone will be equipped with an Iridium module, which has global coverage, and a cellular module as back up communication means.
R-PE-03	Black Box failure	1	4	The Black Box of the drone might fail due to moisture ingress. A high impact is given to this risk as failure of the Black Box will make critical mission data being lost for recovery.
R-PE-04	Sensor failure	2	4	Failure of the top sensor might result in failure of the mission since this sensor is needed to find an opening and allow the drone to climb. The vertical sensor placed at the bottom of the drone is less critical, since the drone will still be able to fly when this sensor fails. For the sensors placed in the horizontal direction, loss of a sensor is allowable as the drone will still be able to sense its surroundings with the remaining two sensors. However, this flight will be at reduced performance since the horizontal field of view of the LastHope drone will be decreased.
R-EL-01	Overheating of ESC	2	4	ESCs tend to easily get overheated if used above their rated capability. However, since the rated capability of each ESC is higher than the maximum current drawn by the motors from the ESCs, the probability is very low. The impact is high as overheating might result in a burned ESC which leads to the drone becoming inactive.
R-EL-02	Voltage spikes	2	3	The voltage of the battery might increase exponentially due to a huge current draw which will result in a power output from the battery which is not smooth. The probability of this risk is low as the current draw of the drone is relatively low and will probably not drain the battery.
R-ST-01	Arm breaking	3	5	The arms of the drone might break in high loading situations, such as a crash, as the arms of the drone are quite fragile. The drone will no longer be operational and will need to be repaired. This risk is related to the highest impact as a broken arm may lead to failure of the mission. A medium probability of 3 is given to this risk.
R-ST-02	Shell buckling	1	4	As a result of a crash, the shell of the drone might start to buckle. A high impact of 4 is given to this risk as the sensors might point in the wrong direction due to the buckling of the shell which can confuse the flight computer. The probability of this risk is low as the shell designed is very rigid which is further elaborated on in chapter 9.
R-ST-03	Hinge freeze	2	4	The occurrence of a hinge freeze could occur due to extended moisture ingress. The probability of this risk is low as it would only occur due to failure in the drone case, for example if the user forgets to put the drone back in the case after usage. The impact is high a frozen hinge renders the drone inoperable during an emergency.

R-EL-03	Power loss	2	5	Power losses could occur if electrical connections to the power supply are compromised and will most likely be caused by a crash of the drone leading to vibrations or water ingress. In case of a power loss, the drone will not be able to complete its mission resulting in the risk having a very high impact. A low probability of 2 is estimated for this risk.
R-PM-01	Sending wrong outline to injection moulding manufacturer	2	4	By sending the wrong outline of parts to the injection moulding manufacturer, the LastHope company would suffer a financial loss since many incorrect parts would be produced which could not be used in the final assembly. As the production of moulds for injection moulding are in general expensive, making the moulds with the wrong outline will result in a large loss of money.
R-AS-01	Improper assembly of the BMS to battery	2	4	Improper assembly of the BMS to the battery will result in inappropriate charge cycles of the battery as the BMS protects the cells of the battery from being overcharged or being overdischarged which will decrease the quality of the battery.

Based on the risks identified in Table 15.2, the risk map as shown in Table 15.3 could be made. As can be seen, four different risk levels, shown via the different colours, have been assigned to different combinations of impact and probability. Unacceptable risks which are represented by red risks must be mitigated. Orange risks are high risks which are still acceptable but close attention must be placed on their impact. Yellow risks represent moderate risks which are acceptable, but it should be noted that they should be kept track off. Finally, the green risks represent low risks which are mostly untracked as they are acceptable.

Table 15.3: Risk map before mitigation

	1 - No Impact	2 - Low Impact	3 - Medium Impact	4 - High Impact	5 - Large Impact
1 - Very unlikely				R-ST-02, R-PE-03	R-PE-02
2 - Unlikely			R-EL-02	R-EL-01, R-ST-03, R-PM-01, R-AS-01, R-PE-04	R-EL-01
3 - Even chance				R-PE-01	R-ST-01
4 - Likely					
5- Very likely					

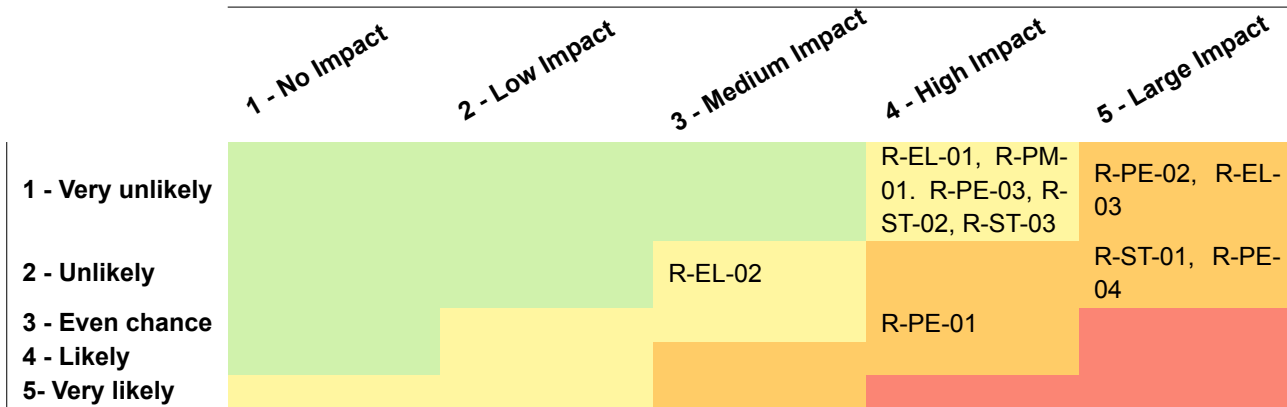## Technical Risk Analysis After Mitigation

A risk analysis performed and for each risk in the unacceptable (red) and high (orange) risk categories a mitigation strategy is formulated. This analysis can be found in Table 15.4.

Table 15.4: Mitigation analysis

Risk ID	Mitigation	Probability (1 – 5)	Impact (1 – 5)
R-PE-01	Propellers of a drone can be protected by using a ducted fan. The use of ducted fans has been considered during the design, but seemed to be unfeasible as including ducted fans would mean that the drone would not fit within the requirement **SYST-GENR-03** stating that the dimensions of the drone in storage mode shall not exceed 200 x 100 x 100 mm (length, width, height). For this reason, this risk could not be mitigated.	3 (3)	4 (4)
R-PE-02	The probability of this risk has already been decreased by having a secondary communication means available when the primary communication means is not able to sent signals. Further decreasing the probability of this risk is not feasible as including a third communication means the drone will likely not fit within the given budgets. On top of this, as the probability of this risk is already really low, this is not needed.	1 (1)	5 (5)
R-PE-04	The impact of the failure of one of the sensors can be decreased by adding more sensors to the drone such that a redundancy is applied. However, at this stage the cost budget does not allow for any extra sensors, so one should check during the post-DSE phase if it is possible to make some budget free to allow for extra sensors.	2 (2)	4 (4)
R-EL-01	In order to decrease the probability of the risk of an ESC overheating, it was decided to not place the ESCs near the battery as it might become hot. To even further decrease the probability of this risk, it was decided to investigate where in the arms cooling vents could be made to allow for aerodynamic cooling. However, this should be investigated in the post-DSE phase.	1 (2)	4 (4)
R-ST-01	Since the team was not able to characterise all loads during the final design phase, a high safety factor of 2.5 was used for the design of the arms to ensure reliability. For the post-DSE phase, it is decided that extensive testing should be carried out in order to characterise the loads such that the probability of arm failure can be decreased. As the drone will still not be able to fly if an arm breaks, the impact will stay the same. The drone will be provided with spare arms such that broken arms can be replaced in case of a crash.	2 (3)	5 (5)
R-ST-03	The risk of a hinge freezing can be mitigated by applying a viscous grease which will help protect the working components from rusting together and freezing the hinge. The viscous grease should be applied during the integration of the propulsion unit into the full drone and it should be inspected at the certification checks.	1 (2)	4 (4)
R-EL-03	The impact of a power loss can not be mitigated when it occurs, so all efforts should be made in order to make this minimise the probability of this risk. As the electronic connections have not been investigated during the final design phase, the team should design the connectors during the post-DSE phase such that they fit either correctly, or not at all, in order to exclude the possibility of hidden faults. All the connectors should be rated to the conditions it is expected to operate in	1 (2)	5 (5)
R-PM-01	The probability of sending the wrong outline to the injection moulding manufacturer could be minimalised by making extensive quality control schemes such that it will be checked by many people. This scheme should be made during the post-DSE phase.	1 (2)	4 (4)

The risk map after mitigation can be found in Table 15.5. It shows that some high risks (orange area) and unacceptable risks (red area) are moved to more tolerable areas. However, it should be noted that some of the high risks could not be mitigated at this point. On top of that, some mitigation strategies should be further investigated during the post-DSE phase.

	1 - No Impact	2 - Low Impact	3 - Medium Impact	4 - High Impact	5 - Large Impact
1 - Very unlikely				R-EL-01, R-PM-01. R-PE-03, R-ST-02, R-ST-03	R-PE-02, R-EL-03
2 - Unlikely			R-EL-02		R-ST-01, R-PE-04
3 - Even chance				R-PE-01	
4 - Likely					
5- Very likely					

16. RAMS characteristics

The Reliability, Availability, Maintainability and Safety characteristics of the concept are analysed in this chapter.

16.1. Reliability

The fact that the LastHope drone design uses components that have been demonstrated to work on other drones implies a certain level of reliability. However, the manufacturers do not provide reliability statistic and data on the reliability of their components. For the post-DSE phase, the team will make contact with the manufacturers of the chosen components to mention that the components will probably be bought in bulk and ask if they could provide the team with the reliability data of the components. Some measures has been taken in order to increase the reliability of designed components. For example for the design of the arms, a safety factor of 2.5 was chosen.

In order to get an estimate of the reliability of the subsystems of the drone, data is used from a commercial drone which provides the Mean Time Between Failures (MTBF) of its subsystems which is expressed in hours of activity. A higher MTBF result in a more reliable subsystem. As military drones usually use expensive materials and very advanced technology, it was chosen to use the data of a commercial drone instead of a military drone. Table 16.1 shows an overview of the MTBF data of several subsystems of a commercial drone. It can be seen that the power plant and the navigation system are the least reliable subsystems.

Table 16.1: MTBF's of subsystems of commercial drone[21]

Subsystem	MTBF (flight hours)
Ground control system	500,000.0
Mainframe	360,984.8
Power Plant	100,603.6
Navigation system	106,269.6
Electronic system	199,600.8
Payload	909,090.9

16.2. Availability

Drone availability

Every user who is going on an adventure with the drone stored in their backpack will be able to use the drone as soon as possible in case of an emergency. The steps needed to be taken by the user to let the drone fly are extract the LastHope case, position the case on the launching site, open the case, prepare the drone for take-off, press ON/OFF button, check the status of the drone, input necessary user information and press the button to commence the mission. On top of this, since the LastHope drone will be able to fly in all weather conditions, it will be highly available

Technological availability

As no very 'new' or developing technologies were used, the technology used in designing the drone was highly available. The fact that certain hardware and software will be bought for the drone from third parties also implies a level of availability. The current silicon chip shortage could in the future influence the availability of electronics such as the flight computer, companion computer, ESC and BMS. The sustainability tool Pharos seemed to be unavailable for the use of the team as a very expensive subscription should be paid if you want to use the website. However, after the team emailed with the company and explained the situation, they got free access to the website.

Material availability

The materials used are:

- Aluminium for the battery bracket
- Nylon PA12 for the arms
- Nylon PA12 for the bulkhead
- PETG for the shell

- PLA for the outer shell of the case
- TPU for the inner liner of the case
- Coir fiber impregnated with latex for the cushioning of the case

These materials are all common in the industry and for that reason highly available.

16.3. Maintainability

Maintenance activities influence the safety and availability of the drone. Less maintenance activities result in a higher availability of the drone. It is desired that the LastHope drone experiences as little maintenance as possible, but still ensuring safety and reliability. The maintenance will divided into three categories namely: certification checks, post-flight checks and pre-adventure checks.

Certification checks

Certification checks will be performed once per year as a maintenance check even if there is no damage reported. The whole drone will be checked internally and externally during these certification checks. This check will be performed to find some less obvious damages. Examples of components being checked during the certification checks are the motors, ESC's, electrical connections and hinge mechanism. Licensed service checkers such as distributors or staff members with authorities will perform the certification checks since these checks are more extensive. The cost of a certification check will be € 50 per year, comparable with an average APK check.

Post-flight checks

The drone should be checked by the user everytime after it has been used. This check is performed to find obvious damages and consists of looking for surface damages, checking the propellers, inspecting the outer seals, checking the battery, making sure all electronics are intact and taking a look at the structural integrity. The drone itself will perform checks as well. For example, it can check the state of the battery. Another important aspect of the post-flight checks is checking the balance on the SIM card which should be able to cover at least 250 MB of data to make sure the photos and videos can be sent during emergency. The user will be able to check and if necessary upgrade the balance on the site of the SIM card provider. The drone will be stored in the case until the next hike if there is no damage reported. Otherwise, the drone should be brought to a maintenance centre.

Pre-adventure checks

The drone should be checked if it still performs properly before the user would head out on an adventure. For this reason the same checks will be performed as during the post-flight checks. The user should be given a spare LastHope drone to use during his/her hike adventure if there are some damages reported as the damaged drone should be repaired in a maintenance centre.

16.4. Safety and redundancy of critical components

The overall performance of the drone can be improved as a result of applying redundancy of critical components which will increase the reliability of the design. Due to redundancy the drone will be able to continue

functioning in case of a system failure. The following safety critical functions were determined where if possible redundancy need to be applied: battery, propellers, drone arms, sensors, flight computer, power distribution board, communication means and electronic speed controller:

- **Battery**: To prevent the battery from operating outside safety conditions, the Tinytronics BMS 3S will be present in the design. On top of that, a battery cage is designed such that the battery can be suspended under the bulkhead. This battery cage is strong enough to transfer the accelerations the drone experiences to the battery.

- **Propellers**: Since toughness has been extensively considered during the propeller design, it is very probable that the propellers will survive most sudden impacts without breaking. However, the team was not able to quantify the limit of the impact the propellers would survive.

- **Drone arms**: Usually, the arms of the drone are fragile. On top of that, resulting from **STAK-SUST-01** stating that the drone shall be able to be repaired in a modular fashion, it was decided that the arms will be replaceable in easily in a practical manner namely by first removing the motor and removing the hinge screws. Then the ESC should be pulled out and put in the new arm. Finally, the motor should be attached to the new arm and two hinge screws should be replaced. As explained in chapter 7, two spare arms will be available in the case of the drone. The drone arms have been designed with a safety factor of 2.5.

- **Power Distribution Board**: It was decided to place the PDB on the underside of the bulkhead, between the battery and the bulkhead such that the PDB is protected by the battery cage.

- **Communication means**: The drone should be able to communicate with the emergency services in order to be able to perform the main objective of the LastHope drone, namely being able to rescue the user. A redundancy is applied by having a secondary communication method available as well, in case of the first communication method is not working. It was decided that the secondary communication means must not rely on satellite connection as this will increase the overall reliability of the communication subsystem and makes the drone being able to sent pictures and videos of the emergency situation via cellular connection as secondary communication means as further explained in chapter 12.

- **Electronic Speed Controller**: The ESC's are not placed nearby the battery as it might become very hot there which can result in one of the ESC's overheating if the motor is spinning at high rpm. In the post-DSE phase it will be determined where in the arms cooling vents should be made to allow for air-cooling of the ESC's. It should be noted that each ESC is rated for 40A maximum, but the drone will fly with a much lower ampere draw through each ESC so it is not likely than one of the ESC's overheats.

- **Sensors**: For the CAS sensors no redundancy is applied to the vertical sensors as this was not allowed by the given budgets. As three CAS sensors are placed facing the horizontal direction, a redundancy is applied as the drone is still able to confirm a clear path if one of them fails. However, it should be noted that the horizontal field of view decrease in the case of one of the horizontal CAS sensors failing.

- **Flight computer**: The IMU is one of the most important parts of the flight computer as without IMU the drone is not able to determine its attitude. For that reason a redundancy is applied by selecting a flight computer with two back up IMU's included.

17. Post-DSE Analysis

In this section all the steps to be performed after the end of the Design Synthesis Exercise are outlined. First the operational concepts and logistics that are to be set up are described. The a flow diagram of the coming steps is presented. After that market research is performed together with a cost breakdown analysis in order to form a foundation for the return on investment analysis.

17.1. Operations & Logistic Concept

In order to ensure that the system is accepted within the market for its intended use, an infrastructure is needed. The logistics start from the supplier and ends at the disposal. The supplier provides all the necessary information to the manufacturers where the drone is built, assembled and integrated. After which the batches produced are sent to the distribution center where it will be sent to authorised retailers. The distributors are also in communication with the satellite network in order to set a framework for the product to be integrated in the system. During which the retailers will have to go through training sessions to be well informed on the product.

This ensures that the retailer is certified and can use the product to its fullest extent. Moreover, they will also have access to replacement parts as this will be where the drones are stored, repaired and ready to be used.

Once the drone is passed on to the customer with the necessary information acquired, it will be stored the majority of its time. However, when the drone is deployed in the case of an emergency, the drone will carry its message and send the necessary information to the international emergency response coordinator. These already exist and contract their services out to other companies. The message is then relayed to the rescue operator where a SAR team is sent to rescue the user.

After the mission, the drone is retrieved and sent to the returns management where they will assess the condition of the drone. Depending on the re-usability of the drone, it will be either sent back to the authorised retailer where a more in depth inspection is performed or to the recyclers where the non-reusable parts are separated accordingly and sent to the disposal areas or kept for recycling. The schematic representation of the operations and logistics flow of the system is shown in figure 17.1.
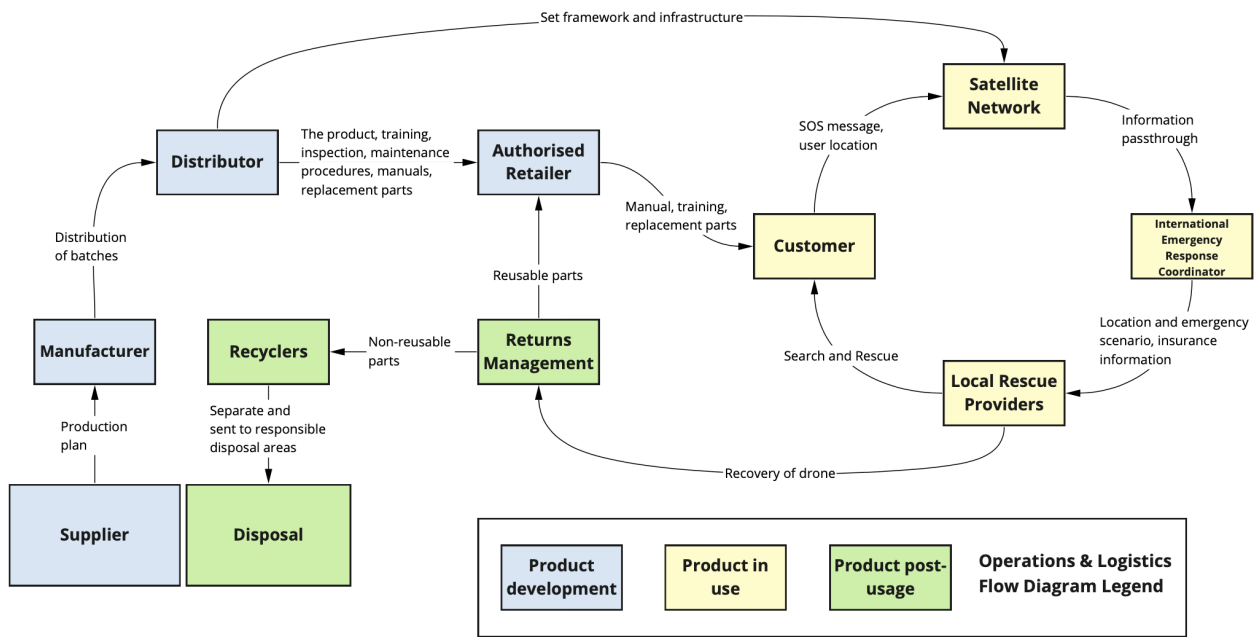

Figure 17.1: Operations & Logistics concept flow representation

17.2. Project Design & Development Logic

It is important to have an overview of the phase after completing the DSE. The project design and development logic indicates all the activities that would take place in order to place the product in the market. This further elaborates on what is shown in section 17.1 in the product development phase where the drone undergoes manufacturing, which is explained in detail in chapter 18, distributing and marketing. The plan shown in figure 17.2, depicts the plan to bring the drone to the market. The level of detail and specificity of the plan is limited due to the lack of factors of the design being currently unconstrained. It should be noted that building anticipation from the market and establishing relationships with industry partners will lead to the success of such product. Stakeholders which have direct and indirect impact are crucial to maintain involved in the project in order to benefit both parties. Partners that are involved in the project are shown in figure 17.1.
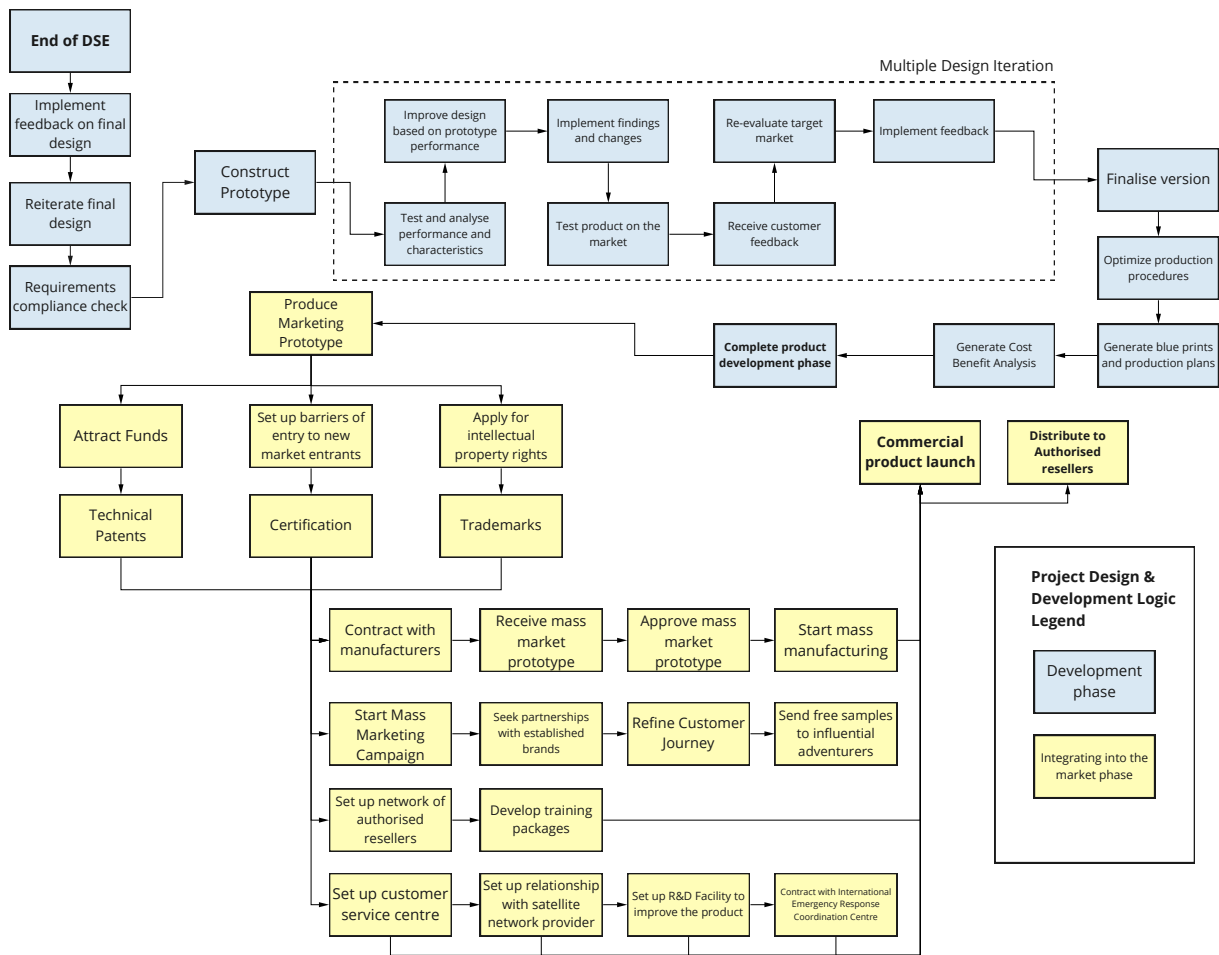
Figure 17.2: Project Design & Development Logic Diagram

17.3. Verification and Validation

During the detailed design phase verification and validation was performed mostly per subsystem. Verification was performed using the requirement compliance matrices for both system and subsystem requirements, these are found at the end of every subsystem chapter and in section 2.2. Furthermore for subsystems which produced code or design tools unit tests and debugging was performed in order to verify proper functioning of the tools. The performance analysis performed in section 13.5 may also provide a form of verification for the entire system which shows that the design is capable of performing its intended missions. Finally a small test was performed in order to validate the drivetrain tool in section 8.4.
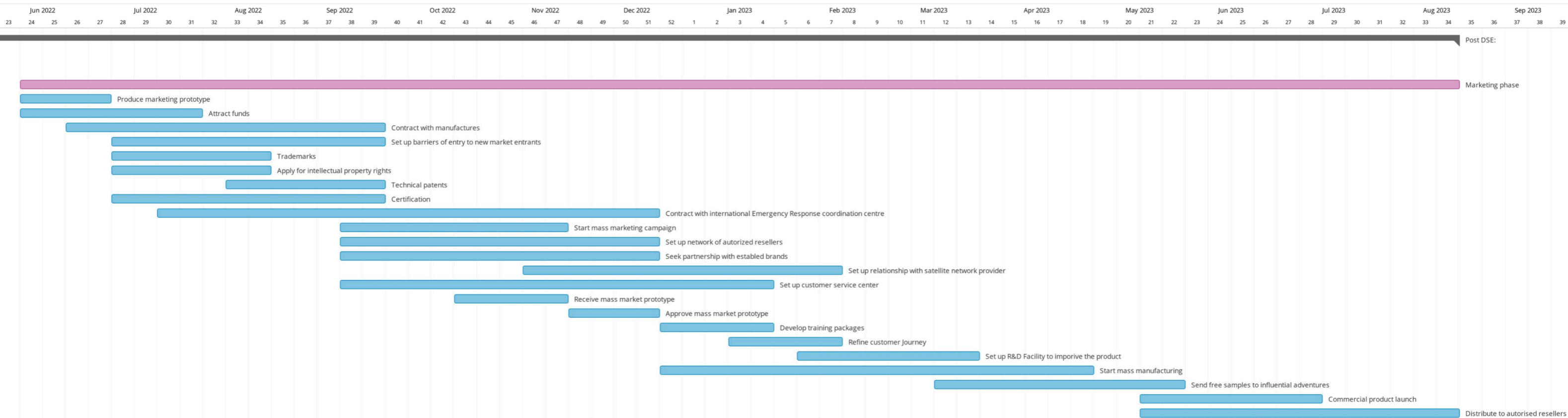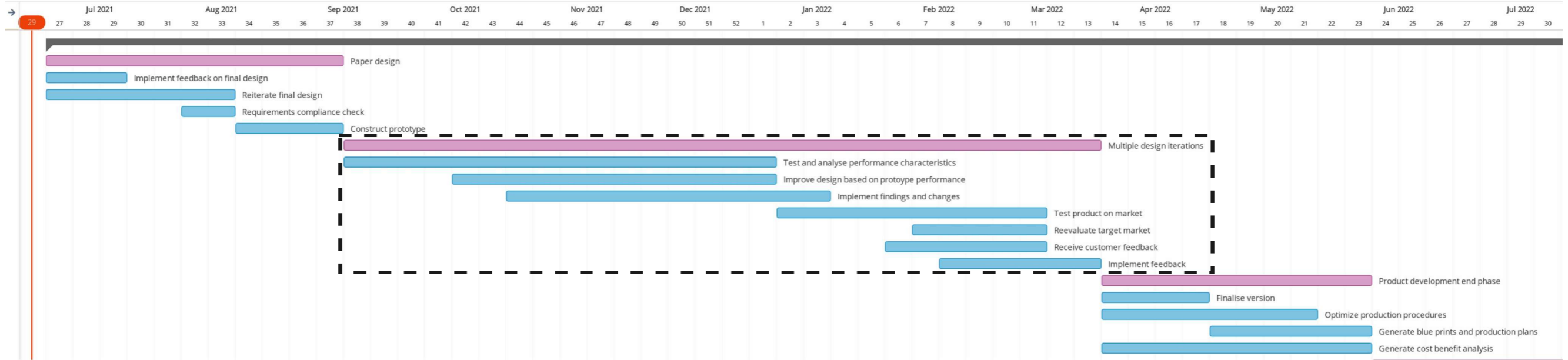
Although sufficient work has been done during this stage a plan for validation procedures should be set up for the Post-DSE phase. During the Post-DSE phase a prototype should be assembled which can be thoroughly tested. For off-the-shelf components the components themselves should not be tested as these are validated by the manufacturer, however their integration within the system should be thoroughly tested. This could be done by measuring the current draw of each component and ensuring this is sufficient and below the components limit. The implementation of software within the drone should be tested in order to debug any final bugs which may be present. Structural tests of the frame and container should also be performed as suggested in their respective chapters. Finally a flight test where different missions such as the ones presented in section 13.5 are performed by the drone. The performance may be checked in order to validate the entire system as a whole.

17.4. Project Gantt Chart

On the next page the Project Gantt Chart can be found. This presents the logical order of the Project Design & Development Logic in figure 17.2 combined with the estimated time required. The highlighted block indicates that multiple iterations of the sub tasks might be necessary to come to a final design of the drone.

DSE 2: Last Hope
Read-only view, generated on 29 Jun 2021

| Timeline | Jul 2021 | Aug 2021 | Sep 2021 | Oct 2021 | Nov 2021 | Dec 2021 | Jan 2022 | Feb 2022 | Mar 2022 | Apr 2022 | May 2022 | Jun 2022 | Jul 2022 |

Paper design
Implement feedback on final design
Reiterate final design
Requirements compliance check
Construct prototype
Multiple design iterations
Test and analyse performance characteristics
Improve design based on protoype performance
Implement findings and changes
Test product on market
Reevaluate target market
Receive customer feedback
Implement feedback
Product development end phase
Finalise version
Optimize production procedures
Generate blue prints and production plans
Generate cost benefit analysis

Instagantt

| Timeline | Jun 2022 | Jul 2022 | Aug 2022 | Sep 2022 | Oct 2022 | Nov 2022 | Dec 2022 | Jan 2023 | Feb 2023 | Mar 2023 | Apr 2023 | May 2023 | Jun 2023 | Jul 2023 | Aug 2023 | Sep 2023 |

Post DSE:

Marketing phase
Produce marketing prototype
Attract funds
Contract with manufactures
Set up barriers of entry to new market entrants
Trademarks
Apply for intellectual property rights
Technical patents
Certification
Contract with international Emergency Response coordination centre
Start mass marketing campaign
Set up network of autorized resellers
Seek partnership with establed brands
Set up relationship with satellite network provider
Set up customer service center
Receive mass market prototype
Approve mass market prototype
Develop training packages
Refine customer Journey
Set up R&D Facility to imporive the product
Start mass manufacturing
Send free samples to influential adventures
Commercial product launch
Distribute to autorised resellers

17.5. Market Analysis

As performed in the baseline report [1], the main market competitors consist of personal locator beacons (PLBs), satellite messengers, and satellite phones. PLBs can transmit your location via satellite but do not show more than your location and that you are having an emergency. Satellite messengers allow you to send messages using your phone via satellite. Satellite phones allow the user to place a call.

Looking at information on the market development for drones, personal locator beacons and satellite phones, it is clear that each of them are growing. The drone market in particular is growing quickly, with its compound annual growth rate (CAGR) being 57.5% for the coming years until 2028 globally[1]. The markets for PLB's and satellite phones are also growing, but not as substantially as drones with PLB's having a CAGR of 5.6%[2] and satellite phones having a CAGR of 4%[3]. Regarding the market sizes themselves, the size of the drone market is considerably larger compared to PLBs and satellite phones due to the fact that drones are being used for such a wide variety of applications across multiple industries. The drone market is estimated to reach $501.4 billion by 2028. The size of the markets for PLBs and satellite phones are smaller as stated, currently being $175.4 million and $5.262 billion as of last year.

As the proposed drone would overlap between these markets, it can be said that there is at least a potential segment for it to be sold in. Individual customers would consist of people that are either avid hikers who want to have an even more reliable option compared to other satellite-reliant options or drone enthusiasts who are also hikers. However, it should also be asked how many drone enthusiasts would purchase a drone that they could not fly themselves and would never see flown unless in an emergency situation. Therefore, the LastHope drone is more likely to be a competitor in the emergency equipment markets than the drone market. Similarly, if the drone can be successfully demonstrated to be more reliable than a PLB or satellite messenger in various emergency situations and geographies, then the customer base would be most likely made up of extreme hikers. It can also be assumed that many of these hikers probably already have some sort of emergency communication device and would not rely on cell phones, meaning that it is unlikely that they would buy a new device, unless it added a lot of value beyond their current option. Compared to existing options, the main value that would be added by the drone would be its added reliability to reach emergency services in areas or situations when satellites are for whatever reason unreachable from the user's positions. This will be a tough selling point to people as it is impossible to quantify how much more likely it is that they could gain connection with the satellite than when using one of the other options.

Another worthwhile point to bring up beyond the functionalities of the various options is their price. First off, it is worth mentioning that the market price of the drone in its current form is €772. This takes into account no profit margin, so either the drone will have to be made cheaper or the price will have to be raised to take a profit. For now, the current price will just be used. Existing PLB and satellite messenger options range from €100-500. It begs the question how many of these people would opt instead for a drone that costs potentially more than twice as expensive as upper range PLB's and satellite messengers and only has the limited functionality to send a message autonomously. The satellite messenger, for example, offers the functionality to send messages using your phone and would cost around half the drone. Resulting from this thought process, it is a better option to aim for larger deals with natural parks and adventure groups which frequently pass through areas where satellite line-of-sight is obstructed, than to go for individual consumers. This would enable a larger amount of drones to be sold in one go and could be used to demonstrate the effectiveness of the drone. If a park would rent these out to each visitor or a hiking group would have their members carry them, it would only be a matter of time before there would be a situation where it would be used. It is of course desired that the drone never be used, but having some cases where it would be used would go a long way to raise confidence in the product and help takeover a larger share of the market.

Taking all of this into account, an initial market volume should be specified. The market volume is a measure of the potential of the product in the market and is found using Equation 17.1[4] where the penetration rate is

[1]Global Drone Markethttps://www.globenewswire.com/news-release/2021/05/05/2223128/0/en/Commercial-Drone-Market-Size-Share-Trends-Analysis-Report-By-Product-By-Application-By-End-use-By-Region-And-Segment-Forecast html, [accessed on 21-06-21]

[2]PLB Markethttps://www.marketsandmarkets.com/Market-Reports/emergency-beacon-transmitter-market-93220519.html, [accessed on 21-06-21]

[3]Sat Phone Market Markethttps://www.globenewswire.com/news-release/2021/03/22/2197008/0/en/Global-Mobile-Satellite-Phone-Market-to-Garner-a-Revenue-of-5-262-1-Million-Growing-at-a-CAGR-of-4-0-during-2019-to-2027-185-html, [accessed on 21-06-21]

[4]Market Volume Explanation https://learn.marsdd.com/article/how-to-estimate-market-size-business-and-marketing-planning-for-sta [accessed on 22-06-21]

how much of the market would be accessible via the product.

$$\text{Market Vol.} = \text{\# Target Customers} * \text{Penetration rate} \tag{17.1}$$

Given that the average penetration rates for consumer products are 2-6%[5] and that the drone has an extremely specialised purpose, does not add massive added value compared to existing options and is not mandated via regulation, a penetration rate of 0.5% is selected for the time being. Even though the U.S. is not the target market at the moment given that the current version of the drone is only applicable for Europe, it can still be used to judge the number of target customers. In 2017, there were 560,566 registered PLB's in the U.S.[6]. If the European market is assumed to be of a similar size, then the market volume would be a potential 2800 customers for the drone. The market value[7] can then be found via Equation 17.2.

$$\text{Market value} = \text{Market volume} * \text{Price} \tag{17.2}$$

Given the market volume of 2800 customers and the drone's price of € 772, this would give a market value of a little over € 2 million. This smaller series is also beneficial as it is expected that the next version of the drone will come with many improvements and it is beneficial to keep the batch size smaller in the beginning in case there are any large unforeseen production problems. This would help save as much money as possible early on before profit has been made.

17.6. Cost Breakdown

Using the series of 2800 drones above, one can calculate what the cost breakdown would be to develop, produce, and operate the drone. The development cost would take into account the prototyping production and testing. To create the prototype, existing supply chains and additive manufacturing would be used to put the drone through multiple rounds of prototyping quickly.

The production can be broken down into two options depending on the initial investment received. If the initial investment received is sufficient, a large up-front amount can be put into making the moulds needed for the injection moulding of certain parts with these frames. This of course requires a large degree of confidence in the arms and that they would not require changes later on. These moulds range in the tens of thousands of euros but will bring down the marginal cost to produce each drone part greatly. For example, the injection mould for the drone's arm was found to cost € 28,286. If sufficient investment is not achieved to at buy the moulds and produce the needed number of arms, additive manufacturing can be used to create the parts, but it will cost more per part and it is likely fewer drones would be made after the initial investment. This has been further worked out in section 18.1.

Furthermore, if there is enough investment to make a large batch of the arms instead of a smaller amount, this also drives the cost down. Using the production of 2800 drones and correspondingly 16,800 arms as an example , an arm would cost € 1.53[8] to produce. If insufficient investment is achieved to make all 16,800 and say only 2,000 can be made, then each arm would cost € 3.52 to produce. Getting the larger investment to buy the injection moulds and also produce a larger batch of parts would lead to massive savings in the long term. Using the same example, if 16,800 arms can be made instead of 2,000, then 2 euros would be saved per drone leading to a saving of € 5,600. The savings become even more extreme for smaller batches of parts. If one can extend this to the other parts required for the drone, the savings would only grow.

For the specific components that are bought off-the-shelf such as electronics, it is expected that the cost for these will go down by 20%. This must be looked into further at a later stage to find the true decrease in cost. This will lead to a production cost per drone of € 646. A breakdown structure of the cost for the post-DSE phase is shown in figure 17.3.

---

[5]Lighter Capital Penetration Rate Explanation https://www.lightercapital.com/blog/what-is-market-penetration-strategy-definition-exam [accessed 22-06-21]

[6]NOAA PLB Registration https://www.noaa.gov/media-release/noaa-satellites-aid-in-rescue-of-275-lives-in-2017, [accessed on 22-06-21]

[7]Market Value Explanation https://learn.marsdd.com/article/how-to-estimate-market-size-business-and-marketing-planning-for-start [accessed on 22-06-21]

[8]Custom Part Net Injection Moulding Calculator https://www.custompartnet.com/estimate/injection-molding/, [accessed 22-06-21]
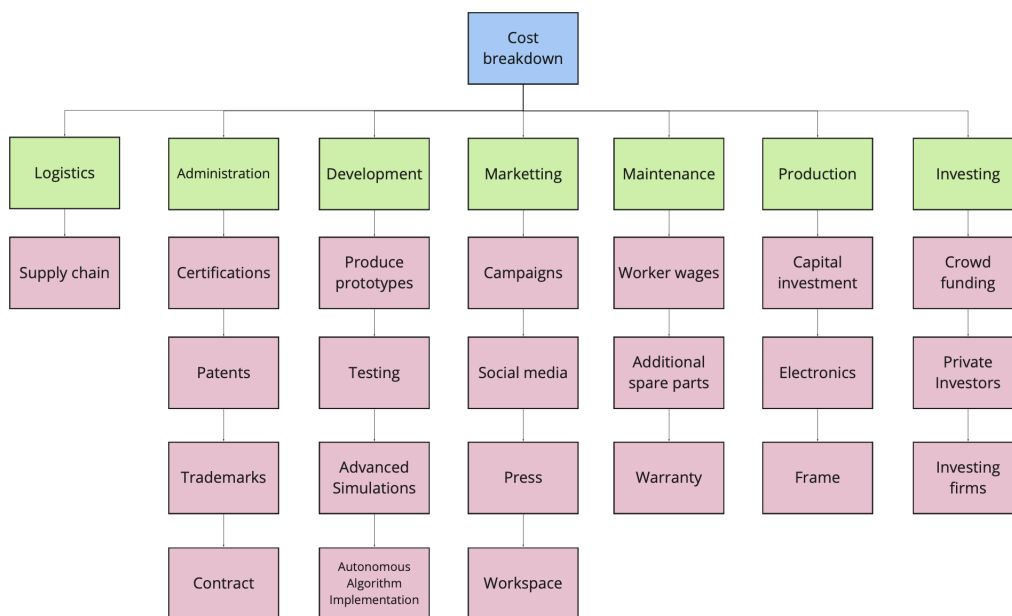
Figure 17.3: Cost Breakdown Post-DSE Structure

17.7. Return on Investment

The return on investment was found to be 4.7% after putting together the cost for development, production, and operating the drones for a period of one year. This is not likely to be enough to generate interest from investors as they could get a greater return of 7% with a lower risk from investing in an index fund[9]. As a result, it is recommended to raise the sale price of the drone to at least € 960 or find a way to decrease production costs further in order to raise the return on investment to 14%, which is likely to be more attractive for investors. It should be noted however that this does not take into account the needed profit margin to continue growing.

An additional reccomendation would be to look into crowd funding such as KickStarter[10] as the expectations from investors are removed. This would also help build a customer base after the first drones are delivered for future versions and build confidence in the product if successful. The assumptions for the return on investment can be found below and the cost breakdown is in Table 17.1.

- The number of drones sold was 2,800
- The development costs of the prototype and testing is € 30,000[11]
- The up-front production costs are the price of the injection moulds for the arm and bulkhead
- The cost to produce each drone takes into account a 20% reduction in the price of buying the electronics in bulk which leads to a cost per drone of € 646

- The operational cost is the € 13.6 per month for each drone to use the satellite network outlined in chapter 12
- Each user will be charged € 15 per month to account for administrative costs for arranging the satellite subscription
- The revenue assumes a consumer price of € 700 and the € 15 made per month for each of the 2,800 users

Table 17.1: Cost Breakdown and Return on Investment

Development Cost	€ 30,000
Starter Production Cost	∼€ 52,000
Drone Production Cost	€ 1,808,800
Operational Cost	€ 456,960
Total Cost	€ 2,347,760
Revenue	€ 2,464,000
Return on Investment	4.7%

[9]Average Return From Index Fund `https://finance.zacks.com/rate-return-index-fund-6679.html`, [accessed on 22-06-21]

[10]KickStarter `https://www.kickstarter.com/`, [accessed on 22-06-21]

[11]Product Development Cost `pacific-research.com/what-is-the-cost-of-product-development-prl/`, [accessed on 22-06-21]

Conclusion

To conclude, it is advised to find additional ways to add value in the drone which would make it more competitive with existing options. It is advised to find additional ways to decrease production costs and look into what profit margin would be required in the future to continue growing after the initial 2800 drones. If the price to produce the drone goes down substantially, the sale price of each drone can go down for future versions which would also make it more competitive with other options on the market. Although not elaborated on in this report, there are substantial legal obstacles regarding the autonomous nature of this drone which render it illegal in its current form. Navigating this would likely require years of negotiations with the right authorities to prove that the drone is safe to be flown without a pilot and would require additional funding to achieve the right certifications.

18. Production Plan

In this chapter the production of the drone is examined. First, using commercial quotes and estimates, detailed cost estimates for various parts are made. Then the manufacturing and assembly is analysis and a production timeline is generated.

18.1. Manufacturing Cost Estimates

In order to evaluate manufacturing costs and eventual ROI a manufacturing analysis was performed. This was also used to substantiate the design and material choices made in the design of the frame in section 9.4. For each part the most promising manufacturing methods were analysed and cost estimates were made for production scales ranging from 1 to 10,000 drones. Each material option was examined in terms of cost, but also in terms of its environmental impact, both in terms of its carbon emissions and possible hazards. The results from this analysis can be found in Table 18.1.

One striking result are the large up-front costs for injection moulding. The moulding costs were calculated using an industrial cost estimating tool[1]. The price for a mould of moderate complexity was found to be around 20.000 euros. The price increase between a moderate and a complex mould is on the order of magnitude of 50%. However at scale the fixed costs become an increasingly smaller part of the cost per component, that means that with scale the added cost of complexity decreases. For the arm, for example, the break-even series run between injection moulding and additive manufacturing is about 700 drones (4200 arms). But, for a complex mould this point is at about 880 drones (5280 arms). This relatively small change in production number could allow for more complex, but lighter and cheaper, parts.

18.2. Production Timeline

In anticipation of the market analysis, a production timeline is also desired. First the component parts of the drone were collated. From those logical sub-assemblies were created. Electrical components are tied as much as possible to their matching structural component in order to make assembly and integration as fast an simple as possible. Integration of the wiring harness is postpones to the last possible moment in order to prevent it being in the way for the assembly of other components, and to allow easy access for component-level quality assurance testing, if desired. The production flow diagram is chronologically arranged over a 14 week period and can be seen in figure 18.1. Manufacturing and ordering of parts is done in batches. Assembly, integration and testing is done on a continuous basis.

---

[1]Cost Estimator, `https://www.custompartnet.com/estimate/injection-molding/`, Accessed 17-06-2021

Table 18.1: Production Costs per part disaggregated by production method and series run

| Part	Production Option	Pharos hazards	Ecolizer	Number	Series Run				
					1	100	500	2,000	10,000
Arm	Inj. Moulding - Simple			Total Frame Cost	€ 1,749	€ 91.20	€ 55.06	€ 29.19	€ 19.29
	Material ABS	Moderate Hazard respiratory	251	Variable Costs	€ 3.68	€ 3.68	€ 1.56	€ 1.17	€ 1.06
				Fixed Costs	€ 21,613	€ 21,613	€ 21,613	€ 21,613	€ 21,613
				Per Arm	€ 3,606	€ 39.70	€ 8.77	€ 2.97	€ 1.42
				Per Drone	€ 21,635	€ 238.21	€ 52.61	€ 17.85	€ 8.54
	Inj. Moulding - Complex			Variable Costs	€ 265.00	€ 3.68	€ 1.56	€ 1.17	€ 1.06
	Material ABS	Moderate Hazard respiratory	251	Fixed Costs	€ 28,286	€ 28,286	€ 28,286	€ 28,286	€ 28,286
				Per Arm	€ 4,979	€ 50.82	€ 10.99	€ 3.52	€ 1.53
				Per Drone	€ 29,876	€ 305	€ 66	€ 21	€ 9
	SLS 3D Printing	Low confidence carcinogenic & persistence	773	Per Arm	€ 25.59	€ 9.53	€ 6.92	€ 6.92	€ 6.92
	Nylon PA12			Per drone	€ 153.54	€ 57.18	€ 41.52	€ 41.52	€ 41.52
				Total Per arm	€ 25.59	€ 9.53	€ 6.92	€ 2.97	€ 1.42
				Total	€ 153.54	€ 57.18	€ 41.52	€ 17.85	€ 8.54
Bulkhead	Inj. Moulding - Simple			Cost per part	€ 23,368	€ 234.40	€ 47.46	€ 12.41	€ 3.07
	Material ABS	Moderate Hazard respiratory	251	Variable Costs	€ 265.19	€ 3.37	€ 1.26	€ 0.86	€ 0.75
				Fixed Costs	€ 23,103	€ 23,103	€ 23,103	€ 23,103	€ 23,103
	SLS 3D Printing	Low confidence carcinogenic & persistence	773	Cost per part	€ 96.80	€ 17.56	€ 9.15	€ 9.15	€ 9.15
	Nylon PA12								
	Laser Cutting	Very high hazard with high confidence ecotoxicity	673	Cost per part	€ 27.53	€ 2.08	€ 1.64	€ 1.44	€ 1.39
	Aluminium AG3M								
				Total	€ 96.80	€ 17.56	€ 9.15	€ 9.15	€ 9.15
Pod top	Vacuforming			Cost per part	€ 611.23	€ 6.34	€ 1.45	€ 0.54	€ 0.29
	ABS	Moderate Hazard respiratory	251	Material costs	€ 0.23	€ 0.23	€ 0.23	€ 0.23	€ 0.23
	PETG	Low confidence persistence & carcinogenicity	135	Fixed Costs	€ 611.00	€ 611.00	€ 611.00	€ 611.00	€ 611.00
Pod bottom	Vacuforming			Cost per part	€ 858.23	€ 8.81	€ 1.95	€ 0.66	€ 0.32
	Material ABS	Moderate Hazard respiratory	251	Material costs	€ 0.23	€ 0.23	€ 0.23	€ 0.23	€ 0.23
	Material PETG	Low confidence persistence & carcinogenicity	135	Fixed Costs	€ 858.00	€ 858.00	€ 858.00	€ 858.00	€ 858.00
				Total	€ 1,469	€ 15.16	€ 3.40	€ 1.20	€ 0.61
Battery Cage	Laser Cutting			Cost per part	€ 28.92	€ 1.30	€ 0.99	€ 0.99	€ 0.99
	Material Aluminium AG3M	Very high hazard with high confidence ecotoxicity	673						
				Total	€ 28.92	€ 1.30	€ 0.99	€ 0.99	€ 0.99
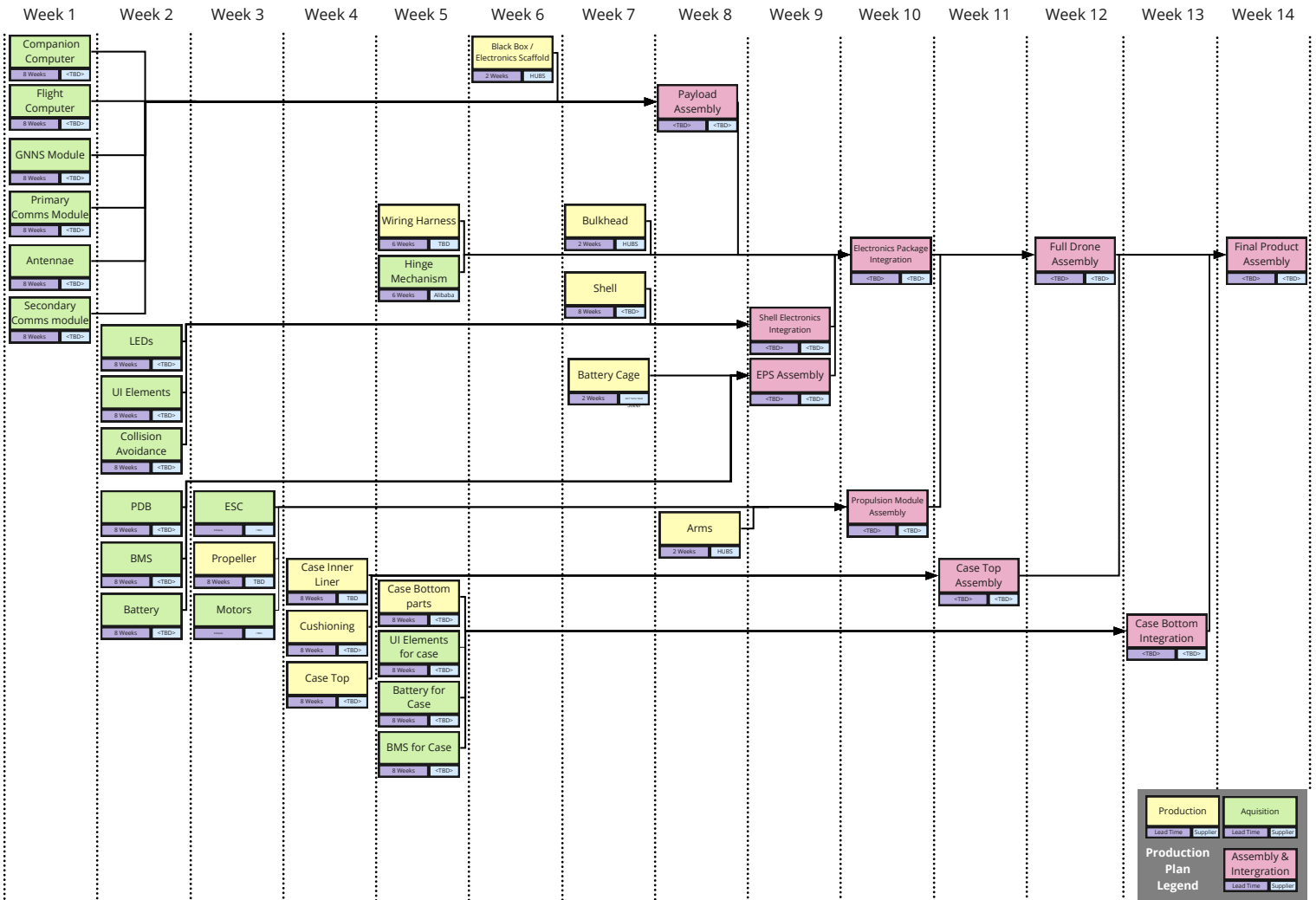
Figure 18.1: Proposed production flow diagram

19. Sustainability Approach

This chapter will outline how sustainability was incorporated in the design of the system and throughout various stages in the process and an outlook will be given for a proposed strategy in the future stages.

19.1. Concurrent Implementation

In the beginning of the early project stages, a strategy to commit to a sustainable culture within the design team was incorporated. Although on a small scale, the rules set in place at this stage were generally followed by the design team and sustainability was encouraged throughout all phases. The rules were meant for everyday implementation, small things that when added up contribute to a more sustainable overall culture within the design team. These were based on three pillars:

1. Environmental aspects
2. Social aspects
3. Economical aspects

These three pillars were considered not only for the organisational aspects and culturre of sustainability within the design team, but for the technical approach as well. The technical approach was fleshed out in the midterm phase, where more knowledge about the exact compositional possibilities of the design could enable the formation of a strategy incorporating the above three aspects into the final product and design process. A number of requirements were derived that tackled multiple aspects of the three pillar or triple bottom line approach. These range from toxicity aspects to operability and hazard considerations up until the inclusion of

more sustainable materials. Furthermore, it became clear that the the incorporation of external tools would yield the most practical approach to sustainability in terms of component and material selections with the resources available. The tools used where Pharos[1], the ecolizer tool[2] and the IdematLCA app [3]. these will be discussed in a separate section. Throughout the design process, recurring dedicated quality control was implemented with regards to sustainability, among other quality control on current general sub-system design progress, to ensure that the strategies laid out were suitable for the task at hand and implemented as intended.

19.2. Material Selection and Tool Implementation

In the end, the main way that sustainability was implemented into the design was through the material choices and the certification compliance of the off-the-shelf components. A more detailed outline of the incorporation of external tools, their description and additional considerations may be found in [2]. A brief overview will be given here for how sustainability was implemented in this phase of the design via the materials chosen and which tools ended up being used.

For material choices, there are three aspects besides the toxicity, which is evaluated using Pharos, and the Ecolizer score which are relevant. These three aspects are whether it is bio-based, recyclable, or 3D printable. Being bio-based means that it is a renewable material which does not rely on non-renewable substances to be produced. Recyclablility is important as it means products can be renewed at the end of their life cycle. Lastly, being 3D-printable means that consumers can 3D print replacement parts and avoid throwing the whole product away. Although it is nice if materials have all of these characteristics, it is often not the case. It is not evaluated in the report, but there are sometimes cases where materials which are bio-based but not recyclable end up costing more embodied energy to produce than non-renewable options which are recyclable. How successfully the materials are recaptured for recycling is also key, but not evaluated in this report. To provide an example, for the drone's container , only sustainable material options were considered for the outer shell, inner liner, and cushioning materials. The materials chosen for those were Polylactic Acid (PLA), Thermoplastic Polyurethane (TPU), and Coir Fibre. PLA and coir fibre are bio-based, whereas TPU is not. TPU is very good however as it is 3D printable and recyclable, whereas Coir fibre is not. Overall, these materials are deemed to be more sustainable than metal or non-bio-based fibre composites such as carbon fibre which could've been used otherwise.

Pharos

Pharos was used to evaluate toxicity requirements that were set-up not only to protect the user but also the wildlife and local ecosystem. A number of requirements were set up dedicated to toxicity that were based on the green screen score methods [4]. The design team would like to thank the Pharos team for extending the free membership for all teammembers over the duration of this project. The tool was applied within the following subsystem for material and component selection:

- Paint for visibility aspects in the operations department found in section 7.3
- All materials in structural department, as shown in Table 18.1

Ecolizer

The Ecolizer tool was used to establish a relative sustainability ranking of different material candidates. The tool was applied in the following subsytems:

- Propeller selection chapter 8
- All components in the structural department, shown in Table 18.1
- Outer shell of the case section 7.1

Idemat LCA App

The IdematLCA app allows for a first estimate of the sustainability impact of a certain material/component over its lifetime in the form of a simplified life cycle analysis similar to the Ecolizer tool., with a slightly different material/component catalogue. This tool was incorporated in case the Ecolizer tool did not provide all material candidates within its framework, however in the end it did not find any use, as the Ecolizer tool proofed sufficient.

---

[1]Pharos,`https://pharosproject.net/`, accessed: June 21st 2021

[2]Ecolizer,`https://www.ecolizer.be/`,accessed: June 21st 2021

[3]IdematLCA, `http://idematapp.com/about/`, accessed: June 21st 2021

[4]Green screen, `https://www.greenscreenchemicals.org/learn/greenscreen-list-translator`, accessed: June 21st 2021

19.3. Component Selection

For the component selection, it was difficult do establish sustainability parameters. Ideally, a thorough supply chain managment strategy should be implemented, such that sourcing and manufacturing partners can be chosen based on all three pillars: Environmental, social and economic sustainability. However it was quickly discovered that this is simply out of the scope of this project, therefore at least certified products and manufacturing partners should be chosen, if data can be obtained. The following certificates were incorporated;

- ISO 14001 certification for partners: Certifies the presence of an appropriate environmental sustainability management system within the company [5]
- RoHs directive: Restricts the use of hazardous materials not used within a given electrical component.[6]
- FLA: The Fair labour association was incorporated initially to ensure that the supply partners comply with fair and safe labour standards. It has been proven difficult however to find companies within the field of electronic suppliers.

19.4. Additional Metrics

Although of great importance, the material and component selection alone does not make the design sustainable. Some metrics may be relatively difficult to evaluate in a quantitative fashion, such as the following: Is the design modular? Is the design repairable? Can the design be made more safe for the operator? Therefore a number of requirements were set up to drive the design in a direction that takes these intangible aspects into account, additionally to tangible aspects such as toxicity. An example for the first two aspects is represented by the Electronic Speed Controller (ESC) trade-off as elaborated in section 11.3, in context of requirement **STAK-SUST-01**, which demands the drone to be repairable in a modular fashion. An integrated 4-in-1 solution was deemed inappropriate as modular maintainability would come into question, even though practically speaking it might yield benefits in terms of volume allocation. Multiple aspects were also woven into the design process without explicit requirements. These could be seemingly small aspects such the warning of the user prior to take off or the critical qualitative evaluation of rotor blade size and rotational speed in context of possible user injuries. Aspects such as these were brought up and addressed in weekly recurring quality control sessions regarding sustainability throughout the design process for each subsystem.

19.5. Post-DSE Phase

The main focus in terms of sustainability in the post DSE phase will lie with the following aspects:

- Sustainable supply management
- Further component analysis
- Active incorporation of sustainability program into the business model of the project

The first point is motivated by the fact that dedicated supply chain management is simply not possible with the resources at hand. Ideally, only partners are chosen that adhere to fair labour and environmental standards. Furthermore it is very difficult to estimate the cost impact of such a scheme, however companies such as Fairphone [7] prove that it is not impossible to strive for a product built on a supply chain respecting workers and environment. Therefore one of the key aspects of the post-DSE phase is the detailed analysis and choice of suppliers and manufacturers. The second point is rooted in the fact that while an effort was made to incorporate sustainability into the ongoing design process, a number of aspects were not considered: Can a more sustainable battery type be chosen with similar performance aspects? Can more durable materials be chosen and what is the expected impact of 3D printing on the sustainability footprint of the product. Questions such as these were limited by the resource constraints of this project, but can be fleshed out in the Post-DSE phase. Lastly, sustainability should be actively incorporated into the distribution model of the drone. Throughout the design a number of recyclable materials were chosen in order to leave the door open towards a more sustainable end of life phase of the product.

The container was given special attention with regards to a sustainable design philosophy, as it was expected that there would be less conflict with performance parameters as opposed to the drone itself. The outer shell material was selected in a trade off process incorporating the Ecolizer tool. The other materials chosen

---

[5]ISO 14001, `https://www.iso.org/iso-14001-environmental-management.html`, accessed: June 21st 2021

[6]RoHs,`https://ec.europa.eu/environment/topics/waste-and-recycling/rohs-directive_de`,accessed: June 21st 2021

[7]Fairphone,`https://www.fairphone.com/en/`, accessed: June 21st 2021

vary in recyclability and bio-based aspects, however all of them have at least one of these two characteristics. Furthermore, even thought the Ecolizer tool provides a lot of use-cases, a different tool had to be implemented to gather information about bio-based materials. For this task, Granta [8] was incorporated which provides more detail for a broader range of characterstics. With the given composition of the drone, the following strategy is supposed to further incorporate sustainability within the post-DSE phase:

- Establishment of maintenance program
- Establishment of recycling program
- Establishment of refurbishment program

The proposed strategy should ideally be tightly integrated: When a user brings in a broken system for maintenance after use, components such as the ones mentioned above that sustained damage may be integrated into a recycling program. This would most likely be outsourced and preferably the recycled material could be used for a new batch of the same components. There are two issues to tackle in this case: Can the performance with a recycled part be guaranteed and is it economically possible and viable. These aspects would need to be evaluated in such a proposal. Another proposal is a refurbishment program: For a broken system, some components might still be intact. If the user does not want to have it maintained and would rather buy a possibly new iteration of the system or due to the entailing cost of maintenance, the drone could essentially be bought back from them for a reasonable price. While it is difficult to argue refurbished components for a safety device simply due to questions on performance, individual components such as the flight computer, GNSS module or secondary communications module could be resold for a lower price, separately from the main system and for hobby users.

Even though these approaches are enticing, they require a detailed analysis to proceed. This would be one of the immideate next steps of the post DSE phase with regards to sustainability.

19.6. Conclusion

For the final design at hand, a range of measures were taken to ensure that the design is as sustainable as possible within the scope of this project. Sustainability was deemed to be not only a set of restraints that the design should be be aimed to comply with, but much more a set of attributes that should be strived for and woven into the concurrent design process. Even though this was the case, in order to ensure sustainability in the future, a number of steps outlined previously should be incorporated, outlined in section 19.5 to ensure that sustainability keeps its place for this design.

20. Summary and Conclusion

A detailed design has been made of this drone. It was found that it is possible to make a design that fulfils the design mission, but a number of uncertainties remain. Firstly, the given constraints of a maximum mass of 500 grams and maximum cost of 700 euros prove infeasible with the production numbers deemed realistic in this report. Secondly, with the current means available it is not possible to evaluate whether dynamic obstacle avoidance is possible and static obstacle avoidance, while somewhat less challenging, is still hard if not impossible to guarantee. This is because the scope of the sensor array is constrained severely by the cost and mass budgets.

Sensors The drone require sensors to aid autonomous flying. Different sensor principles were evaluated, LiDAR and ultrasonic were seen as most suitable. A market analysis found suitable options, turned them into packages. A five ultrasonic package won, however, this can only identify obstacle ranges and not exact location. The budget proved to be constraining.

Communications The communication's subsystem contains four modules, namely, primary communication, secondary communication, global navigation satellite system and the camera module. The primary communication module is used to establish connection with the satellite system with global coverage. The secondary communication module uses cellular signal to connect with the emergency services. This method is also used to send the additional user information, acquired from the camera module when taking off to assist the rescue team to locate the user. Lastly, the GNSS module uses four different satellite constellations to provide the emergency services with the user's coordinates and it's landing coordinates for drone recovery.

---

[8]Granta, https://www.ansys.com/products/materials/granta-edupack, accessed: 22.06.2021

Flight Computer In order to fly and navigate autonomously a flight computer and companion computer selected. Together they ensure stability and control and run the path-finding algorithm. Several path-finding algorithms are developed and analysed, but more time is required to make a sensible conclusion on them. Due to the inclusion of a more detailed dynamical model and potentially optical flow, the drone is expected to be able to operate in GNSS denied-environment, but the availability of GNSS would greatly increase the decision making and precision of the drone.

Drivetrain To optimise propulsive efficiency and save battery mass a propeller is designed to suit the mission. This propeller saves a considerable amount of energy compared to the available commercial standard. The propeller is coupled with an electric motor selected out of a database of over a thousand motors for highest efficiency.

Electrical Power System This consists of an ESC, PDB, BMS and battery. The selected ESC is cheap, small and rated higher than the operating current. This is good because the probability of overheating is lower. For the battery different chemistry types were analysed. No trade-off was done, as the design space was already sufficiently constrained. Mass was found to be the dominant parameter. A shortlist of BMS's that are compatible was made. All options considered were able to protect against short circuits. Because the identified options were the same size, the cheapest one was chosen. Due to trade-offs performed for the FC and the ESC, it was decided not to use a PDB included in the FC or ESC. An overview was made of compatible PDB's. There was only one PDB which was capable of safely delivering the maximum output current.

Frame A frame was designed in order to house and protect all the components. All the components of the frame are made out of non-toxic and recyclable materials. All components are designed with either a safe-life or fail-safe approach where applicable. The frame is tailored to achieve a balance between aerodynamic efficiency, weight and structural performance and reliability. It is designed to fold into a small space in order to make it as convenient as possible for the user to bring along on their adventures. For each component load cases were identified appropriate safety factors were defined. FEM was performed in order to evaluate each component. Over-designed components were made lighter and components that were too weak were redesigned. Aerodynamic analysis was performed in order to evaluate drag and gust performance of the drone. The C_D of the design is found to be 0.3.

Production A manufacturing analysis was made for manufacturing the frame components of the drone. A variety of production methods were analysed for a range of production numbers. At scale injection moulding can significantly reduce the cost of the frame, but it is likely not feasible at the projected production scale.

Sustainability has been woven into the design process and philosophy of this project. It was not only deemed a question of compliance, but an additional quality that this design provides. Materials and components were analysed with a number of external resources regarding sustainability. System elements such as the case and frame allowed for a more in-depth analysis and design strategy. For the future incorporation of sustainability, the possibilities of sustainable supply chain management and recycling/refurbishment opportunities need to be thoroughly investigated.

Risk An extensive risk analysis was performed resulting in a number of important design considerations. Due to weight constraints the risk of propeller breakage could not be mitigated completely. Also, more research is needed into the reliability of electrical connections.

Warning System The visibility approach and warning system consists of both active and passive measures. The active measures consist of 4 white LEDs and the inclusion of a buzzer. The 4 LEDs increase visibility during night time and the buzzer can be used as a locator device. For passive measures paint and reflectors are selected. The paint selected is a fluorescent yellow substance which increases visibility during dusk conditions. On the four drone arms reflective strips are placed for the same purpose.

Container A container can be designed which houses the drone, its spare parts and charging module. It can be made out of mostly bio-based and recyclable materials. It has been designed for the user to operate if they only have one hand available.

User Interface The user interface consists two interfaces, namely primary and secondary. The primary is situated on the drone where it contains one button, which turns on and deploys the drone, and a set of RGB light indicators, which are used to inform the user of the status of the drone such as diagnostics and battery level. The secondary user interface, which is located on the drone's case, is for scenarios where the user is lost or has more time available. The drone will also automatically take photos and videos while it climbs in order to provide the emergency services with additional information assisting the search and rescue. Last but not least, after locating the drone when the mission is complete, the recovery team will use the same button on the drone to deactivate the warning system.

21. Recommendations

This chapter discusses the most important recommendations for the future. These recommendations focus on decreasing the cost and mass of the drone and case. This is because the key requirement on the mass of the drone is not met. At this stage in the project it is not possible to put a number on the cost for the end-user. From the technical budgets it is clear that the current design would have a cost of at least €646. This only contains the price of producing or buying the different parts that make the current design. Therefore it is expected that the cost requirement might not be met with the current design.

21.1. Recommendations on Mass

- If additional computational capacity and time is available, the drivetrain design might be optimised more. A more efficient drivetrain design can result in a smaller battery. Having a smaller battery would reduce the mass of the design.
- If additional computational power and time is available, the frame and case design can be iterated to save mass. As some parts will be manufactured using additive manufacturing, reducing mass of these components will also reduce the cost of the components.
- It is recommended to research electronic components (battery, ESCs, sensors and motors) that are still in development. These newly developed components can have a lower mass.

21.2. Recommendations on Cost

- As stated in chapter 10, the flight computer selected has to be evaluated as the sensitivity analysis showed that a different and cheaper flight computer is also be suitable for the current design. This comes with the cost of an extra 10 grams.
- As stated in chapter 8, the material selection of the propeller has to be evaluated as the manufacturing cost was not included. More analysis is necessary in the manufacturing costs of beechwood propellers. Switching material can reduce the production cost of the propellers significantly.
- To decrease the cost, the inclusion of the spare parts should be reconsidered.
- It is recommended to research electronic components (battery, ESCs, sensors and motors) that are still in development. These newly developed components can have a lower cost.

21.3. Other Recommendations

- It is recommended to add additional functionalities to the drone to increase its market share.
- The current regulations on autonomous flight prevent the drone from being flown. It is recommended to approach the authorities and try to change the regulations.
- More research into communication means is necessary as the infrastructure for the secondary communication subsystem will not be supported anymore from 2025 onward.
- Further analysis is necessary on the development costs as it might show that the current values underestimate the actual costs. Having a good prediction of the development costs is of great importance to say if launching the drone on the market is attractive for investors.
- If it is not possible to further reduce the cost of the drone, the option to increase the cost for the end-user should be considered.

Bibliography

[1]   Group 02. *Baseline Report: LastHope - Drone to Call for Help*.

[2]   Group 02. *Midterm Report: LastHope - Drone to Call for Help*.

[3]   M.G. Mohammed et al. "Theory and Practice of the Hydrodynamic Redesign of Artificial Hellbender Habitat". In: *Herpetological Review* 47 (2016), pp. 586–591. URL: `https://www.researchgate.net/publication/317690978_Theory_and_Practice_of_the_Hydrodynamic_Redesign_of_Artificial_Hellbender_Habitat`.

[4]   W. Asker et al. "Object Tracking Using Vision on Raspberry Pi". In: *International Conference on Aerospace Sciences and Aviation Technology* 16 (May 2015), pp. 1–9. DOI: `10.21608/asat.2015.22940`.

[5]   M. Biczyski et al. "Multirotor Sizing Methodology with Flight Time Estimation". In: *Journal of Advanced Transportation* 2020 (2020), pp. 1–14.

[6]   S. Cakaj et al. "The Coverage Analysis for Low Earth Orbiting Satellites at Low Elevation". In: *International Journal of Advanced Computer Science and Applications* (). DOI: `10.14569/IJACSA.2014.050602`.

[7]   A. Cervone and B.T.C. Zandbergen. *Electrical Power Systems for Aerospace Vehicles*. Feb. 2017.

[8]   *CES EduPack Software*. Cambridge, UK, 2020.

[9]   Sony Energy Devices Corporation. *Sony VTC6 Datasheet*. 1st ed. June 2015.

[10] J.J. Corrigan and J.J. Schillings. *Empirical model for stall delay due to rotation*.

[11] G. Du and Q. Quan. "Controllability Analysis for Multirotor Helicopter Rotor Degradation and Failure". In: *Journal of Guidance, Control and Dynamocs* 38 (2015). DOI: `10.2514/1.G000731`.

[12] G. ÉCORCHARD, A. HEINRICH, and L . PŘEUČIL. "EGO-MOTION SENSOR FOR UNMANNED AERIAL VEHICLES BASED ON A SINGLE-BOARD COMPUTER". In: *Human-Centric Robotics* (Aug. 2017). DOI: `10.1142/9789813231047_0025`. URL: `http://dx.doi.org/10.1142/9789813231047_0025`.

[13] S. Erol. "A Comparative Study for Performance Analysis of Kinematic Multi-Constellation GNSS PPP in Dynamic Environment". In: *Marine Science and Engineering* (2020), p. 19.

[14] D. Ferreira et al. "Efficiency, quality, and environmental impacts: A comparative study of residential artificial lighting". In: *Energy Reports* 5 (2019), pp. 409–424. ISSN: 2352-4847. DOI: `https://doi.org/10.1016/j.egyr.2019.03.009`. URL: `https://www.sciencedirect.com/science/article/pii/S2352484718303652`.

[15] B. Ganesan, J.Valarmathi, and N. Dr. VPS. "Survey on UAV navigation in GPS denied environments". In: (Oct. 2016), pp. 198–204. DOI: `10.1109/SCOPES.2016.7955787`.

[16] K.E.T. Giljarhus. *Implementation of the Blade Element Momentum Theory for turbines and propellers in Python*. 2020. URL: `https://github.com/kegiljarhus/pyBEMT#readme` (visited on 06/10/2021).

[17] M. Irsigler et al. "Aspects of C-Band Satellite Navigation: Signal Propagation and Satellite Signal Tracking". In: (Jan. 2002).

[18] J.Yasin et al. "Unmanned Aerial Vehicles (UAVs): Collision Avoidance Systems and Approaches". In: *IEEE Access* 8 (June 2020), pp. 105139–105155. DOI: `10.1109/ACCESS.2020.3000064`.

[19] R. Leishman et al. "Quadrotors & Accelerometers: State Estimation with an Improved Dynamic Model". In: *Control Systems Magazine* 34 (Feb. 2014). DOI: `10.1109/MCS.2013.2287362`.

[20] R. MacNeill and D. Verstraete. "Blade element momentum theory extended to model low Reynolds number propeller performance". In: *The Aeronautical Journal* 121.1240 (). DOI: `10.1017/aer.2017.32`.

[21] E. Petritoli, F. Leccese, and L. Ciani. "Reliability and Maintenance Analysis of Unmanned Aerial Vehicles". In: 1 (Sept. 2018), p. 16. DOI: `10.3390/s18093171`.

[22] S. R. Pratt et al. "An Operational and Performance Overview of the IRIDIUM Low Earth Orbit Satellite System". In: *Commun. Surveys Tuts.* 2.2 (Apr. 1999), pp. 2–10. DOI: `10.1109/COMST.1999.5340513`. URL: `https://doi.org/10.1109/COMST.1999.5340513`.

[23] Q. Quan. *Introduction to Multicopter Design and Control*. 8th ed. Beijing, China: Springer, 2017.

[24] T.L. Saaty. *The Analytical Hierarchy Process*. 1st ed. McGraw Hill International, 1980.

[25] A. Sabatini and V. Genovese. "A Sensor Fusion Method for Tracking Vertical Velocity and Height Based on Inertial and Barometric Altimeter Measurements". In: *Sensors (Basel, Switzerland)* 14 (Aug. 2014), pp. 13324–47. DOI: `10.3390/s140813324`.

[26] M. Foad Samadi and M. Saif. "Integrated Battery Management System". In: (Dec. 2015), p. 22. DOI: `10.1007/978-3-319-15898-3_11`.

[27] H. Snel, R. Houwink, and J. Bosschers. *Sectional prediction of lift coefficients on rotating wind turbine blades in stall*. Dec. 1994.

[28] S. Urbanski. "Wildland fire emissions, carbon, and climate: Emission factors". In: *Forest Ecology and Management* 317 (2014), pp. 51–60.

[29]   L. Viterna and R. Corrigan. "Fixed pitch rotor performance of large horizontal axis wind turbines". In: *Large Horizontal-Axis Wind Turbines* -1 (Jan. 1982), pp. 69–85.

[30]   Q. Wang et al. "Thermal Runaway Caused Fire and Explosion of Lithium Ion Battery". In: *Journal of Power Sources* 208 (2012), pp. 210–224. ISSN: 0378-7753. DOI: `https://doi.org/10.1016/j.jpowsour.2012.02.038`. URL: `https://www.sciencedirect.com/science/article/pii/S0378775312003989`.

[31]   J. Winkel. "Modeling and Simulating GNSS Signal Structures and Receivers". PhD thesis. Nov. 2003.

[32]   C. Zammit and E. van Kampen. "Comparison between A* and RRT Algorithms for UAV Path Planning". In: *Proceedings of the 2018 AIAA Guidance, Navigation, and Control Conference* (2018). DOI: `https://doi.org/10.2514/6.2018-1846`.

[33]   H. Zhang et al. "A method for evaluating the wind disturbance rejection capability of a hybrid UAV in the quadrotor mode". In: *International Journal of Micro Air Vehicles* 11 (2019). DOI: `10.1177/1756829319869647`. URL: `https://doi.org/10.1177/1756829319869647`.